

ABSTRACT

Title of Document: COMPOUND SPECIFIC CARBON ISOTOPE
ANALYSIS FOR BIOMARKERS
ASSOCIATED WITH MARINE
METHANOTROPHY IN THE ARCTIC

Mara Ryan Dougherty,
Doctor of Philosophy, 2012

Directed By: Professor Alice C. Mignerey,
Department of Chemistry and Biochemistry

A large reservoir of methane exists in marine sediments. The fate of methane is of particular concern in the Arctic, a region that has already demonstrated sensitivity to climate change. The removal of this potent greenhouse gas from the carbon cycle is largely mediated by microorganisms. In methane bearing ocean sediments where sulfate penetrates the surface sediment, sulfate reducing bacteria (SRB) and archaeal methanotrophs are found and believed to act as a consortium in the anaerobic oxidation of methane (AOM). Despite efforts based on thermodynamic models, rate measurements, and $\delta^{13}\text{C}$ analysis of microbial biomarkers, the process by which methane is removed from anoxic sediments remains speculative.

Sediment samples were collected from the Beaufort Shelf, east of Point Barrow, AK as part of the Methane in the Arctic Shelf/Slope (MITAS) Expedition in 2009. Core PC13 from this cruise was selected for compound specific carbon isotope

analysis due the measured sulfate and methane concentrations. Stable carbon isotope analysis of the bacterial biomarkers selected specifically for known SRB phylotypes associated with AOM (i.e., i-C_{15:0}, ai-C_{15:0} and C_{16:1} fatty acid methyl esters) resulted in $\delta^{13}\text{C}$ values ranging from -27.8 to -25.3‰, strongly ¹³C-enriched relative to the biogenic methane in this core ($\delta^{13}\text{C}$ = -100.0 to -74.6‰). At AOM sites, the microbial community involved in the process should reflect the carbon isotopic signature of the methane in instances of methanotrophy. In PC13, the bacterial biomarkers were not ¹³C-depleted like the methane, suggesting the lack of sulfate dependent AOM. The measurement of sulfate reduction rates and phylogenetic investigations corroborated the result from biomarker analysis, that the primary pathway for methanotrophy at this site is not coupled to sulfate reduction.

Radiocarbon analyses of the bacterial biomarkers from PC13 were not utilized for the determination of methanotrophic pathways because the biomarkers targeted were for phylotypes whose dominant function at this site is not coupled to methanotrophy. However, the radiocarbon age of the bacterial markers may be useful in determining the sediment deposition rate at this site. For these biomarkers at 396 and 516 cm below the seafloor, the radiocarbon ages are 5805 and 5878 radiocarbon years, respectively. These ages result in an offset of 2500 radiocarbon years older relative to the shell fragments analyzed from the same depth. The biomarker age likely represents the older sediment delivered to the western Arctic via current systems, while the age of the shell fragments were deposited contemporaneously.

LAY ABSTRACT

A large reservoir of methane exists in marine sediments. The fate of methane is of particular concern in the Arctic, a region that has already demonstrated sensitivity to climate change. The removal of this potent greenhouse gas from the carbon cycle is largely mediated by microorganisms. In methane bearing ocean sediments where sulfate penetrates the surface sediment, sulfate reducing bacteria (SRB) and archaeal methanotrophs are found and believed to act as a consortium in the anaerobic oxidation of methane (AOM). Despite efforts based on thermodynamic models, rate measurements and stable carbon isotope analysis of microbial biomarkers, the process by which methane is removed from anoxic sediments remains speculative.

Sediment samples were collected from the Beaufort Shelf, east of Point Barrow, AK as part of the MITAS Expedition in 2009. Based on measured sulfate and methane concentrations, core PC13 from this cruise was selected for compound specific carbon isotope analysis of bacterial biomarkers that have been associated with known AOM sites. In PC13, the bacterial biomarkers were not ^{13}C -depleted like the methane, suggesting the lack of sulfate dependent AOM. The radiocarbon age of the bacterial biomarkers is younger than anticipated for sediments greater than four meters deep, confirmed by the analysis of shell fragments from PC13. The biomarker age likely represents the older sediment delivered to the western Arctic via current systems, while the age of the shell fragments reflects the time of deposition.

COMPOUND SPECIFIC CARBON ISOTOPE ANALYSIS FOR BIOMARKERS
ASSOCIATED WITH MARINE METHANOTROPHY IN THE ARCTIC

By

Mara Ryan Dougherty

Dissertation submitted to the Faculty of the Graduate School of the
University of Maryland, College Park, in partial fulfillment
of the requirements for the degree of
Doctor of Philosophy
2012

Advisory Committee:
Professor Alice C. Mignerey, Chair
Professor Philip DeShong
Professor John Ondov
Professor Neil Blough
Dr. Kenneth Grabowski
Professor Karen L. Prestegaaard

© Copyright by
Mara Ryan Dougherty
2012

Dedication

To Mom and Dad,

for always loving me and helping me become the person I am today.

And to Ryan,

for sharing your life with me and making me feel like I am home.

Acknowledgements

There was once a time when I thought this section of my dissertation would be my longest chapter. It is amazing how many people throughout my seven years of graduate school contributed to my work with love, patience, kindness, support and scientific expertise to help me navigate this project and make today possible. I know I will never be able to mention all of you here, but that does not make my gratitude for what you have given me any less.

I have been very fortunate to have two phenomenal advisors who have guided me through all my years in graduate school, Dr. Alice Mignerey, my advisor at the University of Maryland, College Park and Dr. Kenneth Grabowski at the Naval Research Laboratory in Washington, DC. Alice, thank you for being the kind of advisor who cares about her student's happiness first and allows us to forge our own path in research. Ken, I truly cannot thank you enough for your support on this project. You committed yourself to me and this project, even when the group at NRL shifted away from this work. I know it could not have been easy to split your time and efforts and I am forever grateful for your constant guidance and friendship throughout my time in graduate school.

To the members of Mignerey group past, present and honorary, you are such being a warm and welcoming group of people. You all make it a true pleasure to be a member of this group. Special thanks to Cassie Taylor and Lenny Demoranville, I would not have made it through the first few years without you. I also need to thank Maryann McDermott Jones for seeing the teacher in me and helping me to find the path I am so excited to continue on.

To all those at NRL who helped me with this work, you have been amazing and I owe you all many thanks. Becca Plummer, for your tireless work on the massive data set from the MITAS cruise and for answering every email I ever sent you, even if I was asking for the same data set for a sixth time because I could not remember the file name. Tom Boyd, for helping me to analyze the FAMES on the GC-IRMS and for fixing a broken instrument a number of times so I could do this analysis which became essential in understanding this data. Rick Coffin, for taking me as a graduate student on two research cruises, finding money in the budget to supply consumables for my project and for finding the funds so I could actually be a part of the research cruises. Leila Hamdan, I cannot thank you enough for all the help you have given me over the years. Thank you for trusting me and my thumbs as the shipboard pipette team, for helping me make sense of these unexpected results, for meeting with me every week for months on end, for reading my dissertation, and for saying the right thing just when I needed comfort, encouragement or congratulations.

Suni Shah, without you I may still be trying to get this project started. I do not know how I would have ever learned how to appropriately handle these samples for radiocarbon analysis if it had not been for you. Thank you for your guidance through every step of this project and for opening your home to me for my time at Woods Hole. A big thanks the wonderful scientists and support staff at WHOI for being so helpful and welcoming during my weeks at your lab. Thank you to Ann McNichol and Dr. William Jenkins, not only for awarding me the NOSAMS Graduate Student Internship, but also letting me come back for a second time to run

PC09 on the PCGC. Li Xu, thank you immensely for your instruction and never ending patience in the lab during my time at WHOI.

To my sisters, Casey and Brynn, thank you for loving and supporting me and trying to understand what this dissertation is actually about, you will never know how much this means to me. To my parents, Peggy and Patrick, the lesson I learned from my high school chemistry class has stuck with me through the years. No matter if I failed, you would be proud of me for simply trying. Knowing I had your constant love and support, no matter the outcome of this endeavor, enabled me to be successful. I am so lucky to have you both in my life.

To Ryan, I know for certain this whole process has been difficult you, but you went through it along side me without complaint. I cannot even begin to express how grateful I am to have you in my life. Thank you for feeding me, for taking care of Roscoe, for reading every terrible first draft and incomplete sentence, for telling me everyday of the long process that I could do it and for really believing it, even on my worst days. I love you. And to Roscoe, for always making me smile.

A fellow graduate student once referred to my project as “the little dissertation that could”. I truly believe this would never have been possible without all of you.

Thank you.

Table of Contents

Dedication	ii
Acknowledgements	iii
Table of Contents	vi
List of Tables	viii
List of Figures	ix
List of Abbreviations	xi
Chapter 1: Introduction	1
Chapter 2: Background	5
2.1 Methane and Methane Hydrates	5
2.2 Anaerobic Oxidation of Methane	11
2.3 Radiocarbon and Accelerator Mass Spectrometry	20
Chapter 3: Collection, Preparation and Analysis of Fatty Acid Methyl Esters (FAMES) for Stable Carbon Isotope Investigations	30
3.1 Sediment Collection, Sampling and Storage	30
3.2 Methods	32
3.2.1 <i>Geochemical Analysis</i>	32
3.2.2 <i>Total Lipid Extraction</i>	34
3.2.3 <i>Preparation of samples and GC-FID Analysis</i>	39
3.2.4 <i>GC-IRMS Analysis</i>	42
3.3 Results	43
3.3.1 <i>Geochemical Analysis</i>	43
3.3.2 <i>GC-FID Analysis for Abundance</i>	45
3.3.3 <i>GC-IRMS Analysis for FAMES Identification and $\delta^{13}C$</i>	49
Chapter 4: Stable Carbon and Radiocarbon Isotope Analysis of Bacterial Fatty Acid Methyl Esters (FAMES)	61
4.1 Introduction	61
4.2 Separation and Collection via Preparative Capillary Gas Chromatography (PCGC)	61
4.3 Results	67
4.3.1 <i>PCGC Isolation and Sample Collection</i>	67
4.3.2 <i>Estimation of Sample Collected</i>	70
4.3.3 <i>Radiocarbon Age and $\delta^{13}C$ of samples</i>	74
Chapter 5: Discussion	79
5.1 Lack of Support in Biomarkers for SRB Dependent Methanotrophy	79
5.2 Sedimentation Rates Estimated from Bacterial Biomarkers	86
5.3 Stable Carbon Isotope Analysis	94
5.4 Further Investigations	97

Chapter 6: Conclusion.....	100
Appendix 1: Assessment of a New Radiocarbon Technology for Compound Specific Radiocarbon Analysis	103
A1.1 Introduction.....	103
A1.2 Background.....	104
A1.3 Preparation of Gas Mixtures – Series 1	106
<i>A1.3.1 Dead CO₂</i>	110
<i>A1.3.2 Modern CO₂</i>	115
<i>A1.3.3 Analysis of Gas Mixtures</i>	118
A1.4 Modifications and Additional Gas Series Preparation.....	119
<i>A1.4.1 Modifications to the Distillation/Graphitization Apparatus</i>	119
<i>A1.4.2 Preparation of Gas Mixtures – Series 2</i>	120
<i>A1.4.3 Preparation of Gas Mixtures – Series 3</i>	121
A1.5 Large Volume Calibration Gases.....	123
A1.6 Discussion	131
<i>A1.6.1 ICOGS Requirements</i>	131
<i>A1.6.2 Preparation of Materials</i>	132
A1.7 Conclusions.....	135
Appendix 2: Total Lipid Extraction.....	137
Appendix 3: Sample Preparation at WHOI	145
Appendix 4: Matreya LLC – Bacterial acid methyl esters CP Mix.....	152
Appendix 5: Gas Chromatography Mass Spectrometry Data.....	153
Appendix 6: Isotope Ratio Mass Spectrometry Data.....	174
Works Cited	220

List of Tables

Table 2. 1. Biomarkers for archaea and sulfate reducing bacteria.....	18
Table 3. 1. Analyses, sample type and location for relevant measurements.	32
Table 3. 2. Calculated mass of dry sediment from porosity.	36
Table 3. 3. Fractions isolated from column chromatography.	40
Table 3. 4. PC09 GC-IRMS analysis.....	52
Table 3. 5. PC13 GC-IRMS analysis.....	53
Table 3. 6. Origin of FAMEs biomarkers.	54
Table 4. 1. Samples combined for radiocarbon analysis.	62
Table 4. 2. Designation, name and structure of isolated bacterial FAMEs.	63
Table 4. 3. Estimated mass of sample recovered ($\mu\text{g C}$).	73
Table 4. 4. Reported fraction modern, radiocarbon age, and $\delta^{13}\text{C}$ from analysis at NOSAMS.....	75
Table 5. 1. Bacterial FAME biomarkers $\delta^{13}\text{C}$ from various AOM sites.....	80
Table A1. 1. Designated areas on the distillation/graphitization apparatus for gas expansion.	116
Table A1. 2. Select samples from the prepared gas mixtures analyzed by the ICOGS system.	119
Table A1. 3. Results from the analysis of the near dead series at LLNL.	122
Table A1. 4. Composition of the prepared large volume gas bottles and the facility to which they were distributed.	126

List of Figures

Figure 2. 1. Methane contributions to the atmosphere from natural and anthropogenic sources.....	5
Figure 2. 2. Structures of methane hydrates.	8
Figure 2. 3. Methane hydrate from Gulf of Mexico cruise in 2007.....	9
Figure 2. 4. Diagram of potential syntrophic metabolism responsible for sulfate dependent AOM.....	15
Figure 2. 5. Two different AMS systems both used for radiocarbon analysis. (A) is the Naval Research Laboratory Trace Element AMS and (B) is the National Ocean Sciences AMS facility at Woods Hole Oceanographic Institute.	23
Figure 2. 6. Difference between AMS facility-reported uncertainty (σ_{AT}) and total propagated uncertainty ($\sigma_{\Delta lipid}$) plotted against total sample mass (m_T).	28
Figure 3. 1. Location of cores PC09 and PC13.....	31
Figure 3. 2. Sulfate concentrations and methane concentrations plotted with respect to the sediment sampling depth in centimeters below the seafloor for cores PC09 and PC13...	34
Figure 3. 3. Soxhlet extractor system for total lipid extraction.	37
Figure 3. 4. PC09 Sulfate and methane concentrations plotted relative to sediment sampling depth.....	44
Figure 3. 5. PC13 sulfate and methane concentrations plotted relative the depth of the sediment sample.....	45
Figure 3. 6. Chromatogram from GC-FID analysis of PC09 sample 113..	46
Figure 3. 7. Abundance of bacterial FAMES normalized to mass of dry sediment.....	48
Figure 3. 8. Chromatogram from GC-MS for PC09 sample 113.....	50
Figure 3. 9. Chromatogram for $\delta^{13}C$ analysis from the IRMS for PC09 sample 113. (A) shows the chromatogram as the ratio of $^{13}C/^{12}C$ and (B) shows the voltage in mV for the same sample.....	50
Figure 3. 10. Relative abundance normalized to $C_{18:0}$ and $\delta^{13}C$ for FAMES from PC09.	55
Figure 3. 11. Relative abundance normalized to $C_{18:0}$ and $\delta^{13}C$ for FAMES from PC13.	56
Figure 3. 12. $\delta^{13}C$ plotted relative to sediment depth for the FAMES grouped by chain length and even or odd numbered identification for PC13.	58
Figure 3. 13. $\delta^{13}C$ plotted relative to sediment depth for the FAMES grouped by chain length and even or odd numbered identification with geochemical parameters.....	59
Figure 4. 1. (A) is a schematic of the PCGC system. (B) is the 8-port PFC with 6 sample traps and one waste trap. (C) is the u-shaped traps for collecting the individual FAMES.	64
Figure 4. 2. GC-FID Chromatogram of PC09 sample 121	68
Figure 4. 3. (A) PCGC Chromatogram of PC09 sample 121 with the region for the bacterial FAMES boxed. (B) Boxed area from the top figure is enlarged and the bacterial FAMES are highlighted.....	69
Figure 4. 4. Post PCGC confirmation on the GC-FID.....	70
Figure 4. 5. FAMES Mix Standard for quantification on the PCGC.....	71
Figure 4. 6. FAMES Mix Standard for quantification on the GC-FID.....	71

Figure 4. 7. C _{17:0} FAME standard chromatogram from GC-FID with DB-23 GC column.	72
Figure 4. 8. $\delta^{13}\text{C}$ plotted versus depth for PC09 and PC13.	76
Figure 4. 9. Fraction modern (Fm) plotted versus depth for PC09 and PC13.	77
Figure 4. 10. Radiocarbon age plotted versus depth in PC09 and PC13.	78
Figure 5. 1. Abundance of bacterial phylotypes from PC13.	84
Figure 5. 2. Abundance of archaeal phylotypes from PC13.	85
Figure 5. 3. Map of the Arctic Ocean north of Russia and Alaska with Laptev Sea and Beaufort Sea.	88
Figure 5. 4. Map of the relevant piston coring sites from the MITAS Expedition, HOTRAX, and an additional site.	89
Figure 5. 5. Radiocarbon age plotted relative to depth for PC09, PC13, shell fragments collected from PC13 and HOTRAX cores.	90
Figure A1. 1. Graphitization units on the distillation/graphitization apparatus at NRL.	111
Figure A1. 2. Area of the distillation/graphitization apparatus where the two end member gases are connected.	112
Figure A1. 3. Picture of the area on the distillation/graphitization apparatus.	113
Figure A1. 4. The volume manipulator unit (VMU) on the distillation/graphitization apparatus at NRL.	114
Figure A1. 5. Pictures of the designated reservoirs on the distillation/graphitization apparatus.	117
Figure A1. 6. Calibration of optogalvanic signal compared ratios calculated based on pressures determined at NRL.	119
Figure A1. 7. Measured Fm at LLNL value plotted versus the predicted Fm calculated from measured pressures and AMS determined composition of end members.	123
Figure A1. 8. Depiction of the mixing process for preparing gas bottles.	125
Figure A1. 9. Initial measurement of the calibration gases by ICOGS system equipped with $^{13}\text{CO}_2$ laser.	126
Figure A1. 10. Residuals plotted versus a weighted average.	128
Figure A1. 11. Residuals plotted versus the ^{13}C measurement at WHOI.	129

List of Abbreviations

AMS	– Accelerator Mass Spectrometry
ANME	– Anaerobic methanotroph
AOM	– Anaerobic oxidation of methane
CFAMS	– Continuous flow accelerator mass spectrometry
CIS	– Cooled injection system
CSRA	– Compound Specific Radiocarbon Analysis
DCM	– Dichloromethane
DIC	– Dissolved inorganic carbon
DOC	– Dissolved organic carbon
DSS	– <i>Desulfosarcina/Desulfococcus</i>
EtOAc	– Ethyl acetate
FAMEs	– Fatty acid methyl esters
FAR	– Fourth Assessment Report
FID	– Flame ionization detector
Fm	– Fraction modern
GC	– Gas Chromatography/Chromatograph
GC-MS	– Gas chromatograph/mass spectrometer
GDW	– Gram dry weight
GWP	– Global warming potential
HOTRAX	– <i>Healy-Oden</i> trans-Arctic Expedition
HPLC	– High pressure liquid chromatograph/chromatography
ICOGS	– Intracavity Optogalvanic Spectroscopy

i.d. – Inner diameter

IPCC – Intergovernmental Panel on Climate Change

IRMS – Isotope ratio mass spectrometry/spectrometer

IUPAC – International Union of Pure and Applied Chemistry

LC-FAMES – Long chain fatty acid methyl esters

LN₂ – Liquid nitrogen

MeOH – Methanol

MITAS – Methane in the Arctic Shelf/Slope

MQU – Molar Quantification Unit

NIST – National Institute of Standards and Technology

NOSAMS – National Ocean Sciences Accelerator Mass Spectrometry

NRL – Naval Research Laboratory, Washington DC

o.d. – Outer diameter

OxI – Oxalic Acid I

OxII – Oxalic Acid II

PCGC – Preparative Capillary Gas Chromatography

PDB – Pee Dee Belemnite

‰ – Per mille, or one part per thousand

psi – Pounds per square inch

SC-FAMES – Short chain fatty acid methyl esters

SMTZ – Sulfate-methane transition zone

SR – Sulfate reduction

SRB – Sulfate reducing bacteria

SRR – Sulfate reduction rate

TIC – Total inorganic carbon

TLE – Total lipid extract

TOC – Total organic carbon

UHP – Ultra-high purity

USCGC – United States Coast Guard Cutter

VMU – Volume Manipulator Unit

VPDB – Vienna Pee Dee Belemnite

WHOI – Woods Hole Oceanographic Institute

Chapter 1: Introduction

The Intergovernmental Panel on Climate Change (IPCC) Fourth Assessment Report (FAR) defines greenhouse gases as “those gaseous constituents of the atmosphere, both natural and anthropogenic, that absorb and emit radiation at specific wavelengths within the spectrum of thermal infrared radiation emitted by the Earth’s surface, the atmosphere itself, and by clouds” (Solomon et al. 2007). It is these greenhouse gases that moderate the Earth’s temperature, retaining heat and radiating it back to the Earth’s surface in a process known as the greenhouse effect. Water vapor, carbon dioxide and methane are the most abundant greenhouse gases in the atmosphere, with carbon dioxide typically considered of greatest concern due to its increasing concentrations in the atmosphere, from post-industrial emissions. In 2010, CO₂ accounted for 83.6% of the United States greenhouse gas emissions (U.S. Environmental Protection Agency 2012). Despite the significant contribution CO₂ makes to the atmosphere, methane is a more potent greenhouse gas.

The global warming potential (GWP) of a greenhouse gas is defined relative to CO₂ and is reported over a particular timescale. The GWP of a particular gas is based on how well the gas can absorb thermal radiation over its lifetime in the atmosphere. According to the IPCC-FAR, methane’s global-warming potential is twenty-five times greater than carbon dioxide over a period of 100 years (Solomon et al. 2007). The IPCC reported atmospheric methane concentrations of 1774 ppb in 2005, approximately 2.5 times the estimated pre-industrial level of 715 ppb in 1750 (Solomon et al. 2007). The increased atmospheric methane concentrations coupled with methane’s GWP and

residence time in the atmosphere (approximately 12 years, Solomon et al. 2007) make methane a concern for climate change over the course of the next century.

A large reservoir of methane exists in marine sediments. The removal of this potent greenhouse gas from the carbon cycle is largely mediated by microorganisms. In methane bearing ocean sediments where sulfate penetrates the surface sediment, sulfate reducing bacteria (SRB) and methane oxidizing archaea are found and believed to act as a consortia in the removal of methane. However, the specific roles of the archaeal and bacterial partners and the flow of carbon and reduced species between them remains poorly understood, e.g., Nauhaus et al. (2002). Though Boetius et al. (2000) showed the microbial players are often clustered together, the SRB are not always present in association with the methane oxidizing archaea, e.g., Orphan et al. (2002), further complicating the anaerobic oxidation of methane (AOM) process. Efforts to address these questions using measured rates and stable carbon isotopic composition of bacterial and archaeal lipid biomarkers have yielded inconclusive results regarding the flow of carbon and intermediates in this consortia (Reeburgh 2007). Radiocarbon investigations can provide another dimension to the analysis of biomarkers by adding an age determination to the provenance. Coupling this radiocarbon analysis with the stable carbon isotopic signature can help to understand the source and environment of the species, the metabolism, and age of the reservoir providing the carbon. Determining the radiocarbon age of SRB biomarkers may elucidate the metabolic pathways of the microbial community and give insights into carbon cycling in ocean sediments.

This project employed compound specific carbon isotope analysis to determine if SRB were linked to methanotrophy in Arctic sediments. Specifically, a goal was to

identify both the origin and age of the methane source for bacterial phylotypes associated with anaerobic oxidation of methane (AOM), coupling radiocarbon with stable carbon isotope analysis. Sediment samples were collected from the Alaska Beaufort Shelf as part of the Methane In The Arctic Shelf/Slope (MITAS) in September 2009 targeting sites with methane hydrates. Core PC13 was identified for compound specific carbon isotope analysis of sulfate reducing bacterial biomarkers based on pore water and sediment profiles. These profiles indicated that both sulfate and methane concentrations reached a minimum concentration at 110 centimeters below the seafloor, known as the sulfate-methane transition zone (SMTZ), evidence attributed to AOM in marine environments (Martens and Berner 1974; Barnes and Goldberg 1976; Reeburgh 1976; Valentine 2002; Reeburgh 2007).

Target fatty acid methyl ester (FAME) biomarkers specific to SRB (sulfate reducing bacteria) were identified from previous work for marine sediments associated with AOM, specifically microbial mats and cold seeps – sites where the population responsible for the process would be abundant (Perry et al. 1979; Zhang et al. 2002; Elvert et al. 2003; Londry, Jahnke, and Des Marais 2004; Wegener et al. 2008; Aquilina et al. 2010). The bacterial biomarkers (i-C_{15:0}, ai-C_{15:0}, and C_{16:1}) were separated from the sediment and purified through a series of extractions and chromatographic techniques (Chapter 3). Subsequently, these individual target compounds were isolated and concentrated through Preparative Capillary Gas Chromatography (PCGC) in which 99% of the GC effluent can be collected based on retention times (Chapter 4). The collected compounds were combusted and prepared as targets for radiocarbon analysis using small sample Accelerator Mass Spectrometry (AMS) (Chapter 4).

Despite the prevalence of small sample AMS for radiocarbon measurements, this measurement on ultra-microscale samples (5-25 $\mu\text{g C}$) is difficult and labor intensive (Shah and Pearson 2007). Compound specific samples of individual biomarkers are likely to be limited in sample size and necessitate the availability of techniques capable of accurately measuring microgram quantities of carbon. To this end, collaborative efforts have been made to assess a novel technique for ^{14}C measurement, Intracavity Optogalvanic Spectroscopy (ICOGS), a system that has been developed at Rutgers University (Murnick, Dogru, and Ilkmen 2008) (Appendix 1). ICOGS has the potential to measure as small as 1- μg samples of carbon as CO_2 gas non-destructively (D. Murnick, personal communication) which eliminates the process blank associated with graphitization. It also allows for long measurement times to reduce background noise and therefore the measurement uncertainty. Although the ICOGS system was not at a point of stable operating conditions for compound specific radiocarbon measurements at the time of this analysis, the contributions to the ICOGS collaboration are shown in Appendix 1.

Chapter 2: Background

2.1 Methane and Methane Hydrates

There are a variety of sources for atmospheric methane, both natural (e.g., methanogens and wetlands) and anthropogenic emissions (e.g., livestock and natural gas industry). The contributions of the various sources of methane to the atmosphere are depicted in Fig. 2.1 based on reported values from the Intergovernmental Panel of Climate Change (IPCC) Fourth Assessment Report (Solomon et al. 2007).

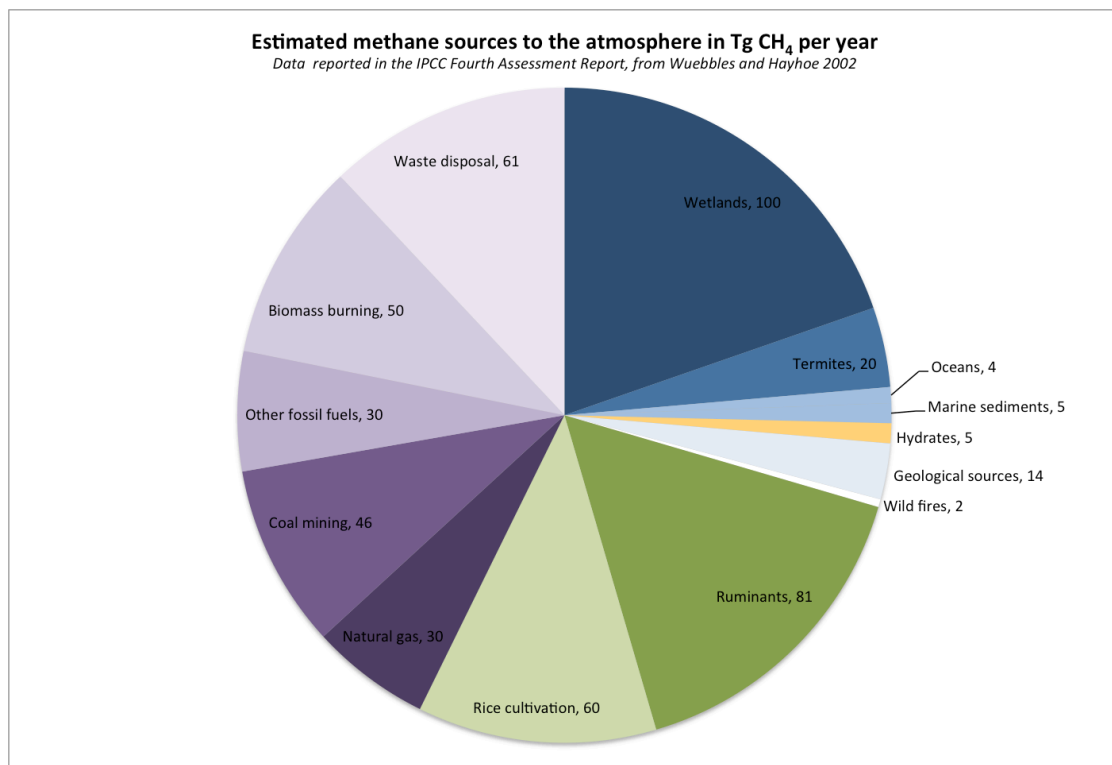


Figure 2. 1. Methane contributions to the atmosphere from natural and anthropogenic sources. Data from the IPCC Fourth Assessment Report (Solomon et al. 2007).

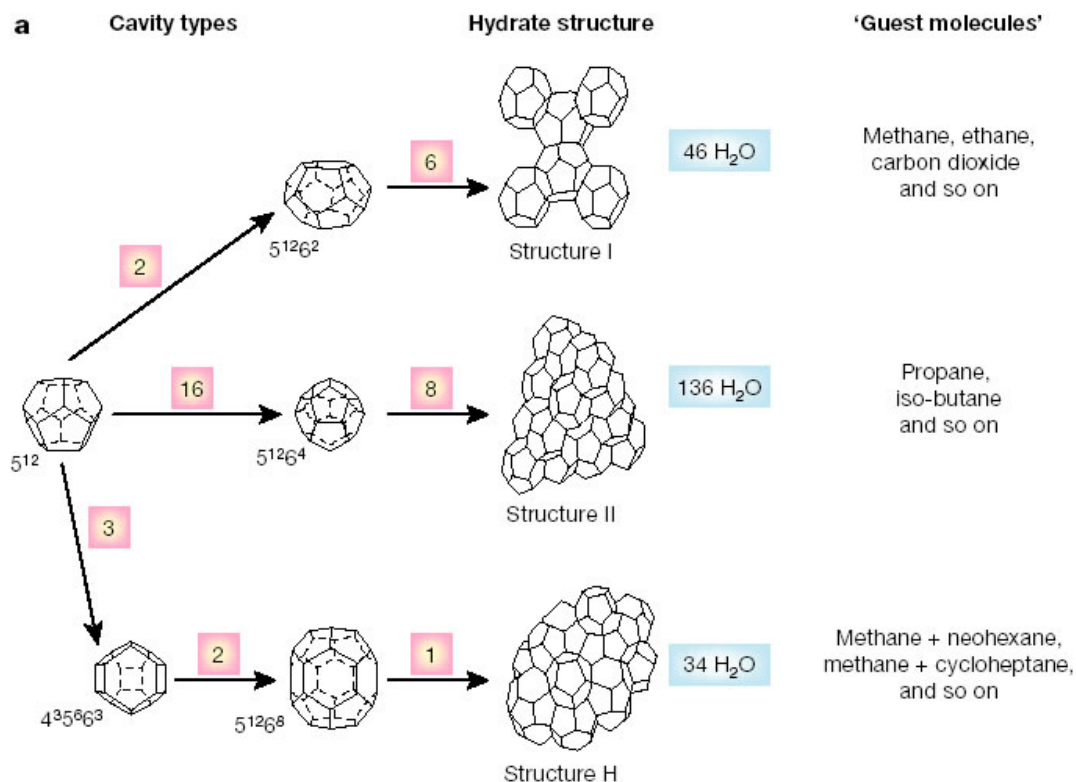
In the atmosphere, methane is removed through oxidation by a hydroxyl radical,



The methyl radical will then typically react further to form methyl hydroperoxide or formaldehyde, which can undergo photochemical decomposition to form carbon monoxide gas (Jardine 2004). The hydroxyl radical is formed in the troposphere from ozone and is responsible for the removal of a number of atmospheric pollutants (Wuebbles and Hayhoe 2002). Tropospheric oxidation of methane is the main pathway by which methane is removed from the carbon cycle accounting for approximately 90% of its removal, with minor sinks from stratospheric oxidation and soil uptake (Wuebbles and Hayhoe 2002; Jardine 2004).

Methane is produced in ocean sediments as part of the degradation of organic matter that occurs when detritus reaches the seafloor. There are generally two types of sediment methane sources, biogenic and thermogenic. Biogenic methane is derived from microbial activity in the sediment close to the seafloor. It is maintained as a stable end product in anoxic sediments at depths where sulfate, a more favorable electron acceptor with high concentrations in seawater, has been depleted. In sediments where the sulfate is exhausted, methane can accumulate. Where sulfate is present it can lead to the oxidation of methane. The horizon in the sediment where there is mutual depletion of methane and sulfate is known as the sulfate-methane transition zone (SMTZ). The depth of the SMTZ varies greatly in sediments worldwide depending on the organic material and methane availability (Valentine 2002). At much greater depths, thermogenic methane is produced from buried organic matter at high temperatures and pressures in a process called catagenesis. This methane can reach the seafloor through advection and/or diffusion.

Methane available in ocean sediments may be incorporated into ice-like lattice structures, trapping the gas in solids known as clathrates. Clathrates, also known as gas hydrates, form when certain temperature and pressure conditions are achieved (low temperature and high pressure conditional on sediment depth) and there is a sufficient supply of methane or other small molecule gases (e.g., ethane) to fill the cages and stabilize the hydrate (Judd et al. 2002; Bohrmann and Torres 2006). For example, the gas hydrate stability zone is shallower in the Arctic due to the lower bottom water temperatures (Bohrmann and Torres 2006). There are three possible structures for methane hydrates to form, designated structure I, structure II and structure H, as seen in Fig. 2.2 (Sloan 2003). Each cavity type is described by the number of sides for each shape that makes up a face of the cavity. For example, 5^{12} is a cavity with 12 faces and each face is a pentagon. The number in the red box designates the number of those particular cavities included in the overall hydrate structure (Sloan 2003). Each of the three structures has 5^{12} cavities in combinations with other cavities to form the overall hydrate structure. The blue box indicates the number of water molecules per unit cell for each of the three structures (Sloan 2003). The formation of a particular hydrate structure is dependent on the size of the gas molecule filling the cavity of the hydrogen bonded water molecules.



b

Hydrate crystal structure	I		II		H		
Cavity	Small	Large	Small	Large	Small	Medium	Large
Description	5 ¹²	5 ¹² 6 ²	5 ¹²	5 ¹² 6 ⁴	5 ¹²	4 ³ 5 ⁶ 6 ³	5 ¹² 6 ⁸
Number of cavities per unit cell	2	6	16	8	3	2	1
Average cavity radius (Å)	3.95	4.33	3.91	4.73	3.91 [†]	4.06 [†]	5.71 [†]
Coordination number*	20	24	20	28	20	20	36
Number of waters per unit cell	46		136		34		

*Number of oxygens at the periphery of each cavity.

[†]Estimates of structure H cavities from geometric models.

Figure 2. 2. Structures of methane hydrates (Sloan 2003). This figure can be found at the following URL: <http://www.nature.com/nature/journal/v426/n6964/images/nature02135-f1.2.jpg>

Methane hydrates are found worldwide in areas of permafrost and along continental shelves where conditions for stability (temperature, pressure and methane concentration) exist in the gas hydrate stability zone. The majority of methane hydrates are comprised of biogenic methane with some thermogenic methane hydrates found in the Gulf of Mexico and the Caspian Sea (Kvenvolden 1998). A gas clathrate retrieved

from marine sediment in the Gulf of Mexico by piston coring in 2007 is shown in Fig.

2.3. Stable carbon isotope values (designated $\delta^{13}\text{C}$) of methane gas are indicative of the methane source. Biogenic methane is typically isotopically lighter ranging from about -100 to -60‰ relative to the Pee Dee Belemnite (PDB) standard, which is set as the zero reference point for $\delta^{13}\text{C}$ measurements (Kvenvolden 1998). Gas hydrates formed with biogenic gas are comprised of mostly methane. Thermogenic methane hydrates have a $\delta^{13}\text{C}$ around -30‰ and contain longer chain hydrocarbon gases along with the methane (e.g., ethane and propane).



Figure 2. 3. Methane hydrate from Gulf of Mexico cruise in 2007. As the cores are pulled to the surface the pressure and temperature changes causing a destabilization of the methane hydrates.

Early calculations of the reservoir size of methane hydrates estimated that approximately 10,000 Gt was carbon trapped in methane hydrates, twice the estimate for carbon in all other fossil fuels combined (Kvenvolden 1988; MacDonald 1990). More recent estimates are based on a better understanding of methane hydrates and measured concentrations of hydrates at a number of field sites. These estimates range from 500 to 3000 Gt carbon in methane hydrates worldwide (Milkov 2004; Buffett and Archer 2004). The study of methane hydrates is an important field of research based on their potential

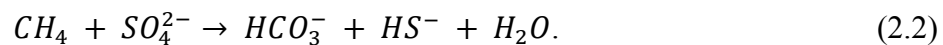
as an energy source (Kvenvolden 1998), though the decreased estimate of the reservoir size and the engineering challenges presented in the extraction of methane hydrates from the sediments, particularly in deep reservoirs, has lessened the relevance as purely a potential natural gas source. There is, however, a great interest in the potential implications the destabilization of methane hydrates could have on seafloor stability and the current climate. Structures supported by the seafloor, for example those that enable the extraction of oil from wells, are vulnerable to shifts in the seabed from methane clathrate destabilization beneath them. Additionally, large releases of methane from clathrates are hypothesized to be the cause of the Paleocene-Eocene thermal maximum, a period of rapid warming about 55 million years ago that led to the mass extinction of benthic foraminifera (Thomas et al. 2002; Dickens 2003; Archer 2007). Understanding the impact of methane release to geological events combined with the present understanding of methane hydrates can help to predict the impact methane hydrates may have on climate change in the future.

Seemingly small changes in temperature or pressure resulting from sedimentation, sea level change, and/or ocean warming, could be significant enough for the methane hydrates to destabilize and the gas trapped inside the clathrate to be released. This is especially of concern on the East Siberian Arctic shelf where the hydrate reservoir is shallow and there is already evidence of methane release to the atmosphere due to anthropogenic warming in the Arctic (Shakhova and Semiletov 2007; Shakhova et al. 2010). Amid current climate concerns, there has been a “doomsday” hypothesis that current ocean temperatures could warm to a large enough degree to cause a catastrophic release of methane from clathrates, triggering rapid warming amplified by other

greenhouse gases acting in a positive feedback loop, known as the “clathrate-gun hypothesis” (Kennett 2003). Modeling work done by Archer (2007) indicates the majority of the methane hydrate reservoir is isolated from the impact of global warming over the next 100 years. As sedimentation continually occurs, there is constant release of methane from clathrates. Methane concentrations in the atmosphere may spike, but the turnover rate of methane in the atmosphere is approximately twelve years. More prevalent concerns for methane hydrates are hazards for the oil industry and ocean drilling programs. Submarine landslides can be caused by the destabilization of methane hydrates and there is the potential link to methane hydrates to other marine hazards.

2.2 Anaerobic Oxidation of Methane

Despite the immense reservoir of methane in marine sediments and the large volume trapped as clathrates, methane from the seafloor is currently only a small contributor to atmospheric methane concentrations (Fig. 2.1). The vast majority of methane produced in ocean sediments never reaches the water column. Methane diffuses upwards and is depleted in the same sediment horizon as sulfate, which diffuses downward from its seawater source. This sediment horizon is known as the sulfate-methane transition zone (SMTZ) and is evidenced by pore water concentrations in anoxic sediments (Martens and Berner 1974; Reeburgh 1976; Barnes and Goldberg 1976). Based on the methane and sulfate concentrations, anaerobic oxidation of methane (AOM) was proposed responsible for the removal of methane from anoxic sediments by the net reaction,



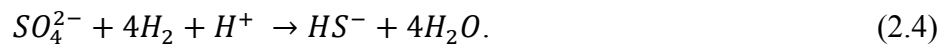
Sulfate reduction (SR) was proposed as an important process to AOM based on rate measurements in sediments. The processes of SR and methane oxidation in anoxic marine sediments were correlated to each other and supported by high rates of AOM in the sediment depths where SR is known to occur (Reeburgh 1980) and peak SR rates in the AOM zone (Devol and Ahmed 1981). Iversen and Jørgensen (1985) used ^{35}S and $^{14}\text{CH}_4$ -tracer techniques to measure methane oxidation and sulfate reduction. At the SMTZ, both processes reached a maximum providing further evidence linking SR to methane oxidation in anoxic marine sediments. Additionally, above and below the SMTZ the measured rates of AOM were insignificant compared to the rates observed at the horizon where the rates of both processes peaked (Iversen and Jørgensen 1985).

Inhibition experiments examined methane oxidation and sulfate reduction rates when known inhibitors of these processes were added to sediment samples (Alperin and Reeburgh 1985). The studies resulted in no inhibition of rates of methane oxidation when a known inhibitor of sulfate reduction, molybdate, was introduced. This work suggests an unknown organism or mechanism is responsible for the process of AOM, or perhaps that a partnership of a yet to be determined methane oxidizer and sulfate reducing bacteria (SRB) cooperate with hydrogen serving as an intermediate in the net oxidation of methane (Alperin and Reeburgh 1985).

Methane composed of the lighter isotopes of carbon and hydrogen is preferentially oxidized faster than heavier isotopes during the anaerobic oxidation of methane. This process leaves a pool of methane in the sediments that contains a greater $^{13}\text{C}/^{12}\text{C}$ at sediment depths where methane oxidation is prevalent, compared to the PDB standard. In sediments from the Skan Bay in Alaska, constant $\delta^{13}\text{C}$ values were

measured below 30 cm in depth, but a shift towards ^{13}C -enriched methane was observed at depths where methane concentrations were depleted (Alperin, Reeburgh, and Whiticar 1988). The fractionation of stable carbon isotopes will not be limited to the remaining carbon source pool, but will also occur during the uptake of methane as a microbe incorporates the carbon into its biomass.

Hoehler et al. (1994) combined field observations and laboratory experiments to propose the first mechanism, consistent with previous work in the field, for the net consumption of methane that coupled methane oxidation to SR. Even today, this work stands as the most widely accepted pathway by which methane is consumed in marine sediments (Knittel and Boetius 2009), but the process remains speculative. This theory proposes that methanogens produce hydrogen and carbon dioxide through “reverse methanogenesis” (Eq. 2.3) and sulfate reducers utilize the hydrogen as an electron donor (Eq. 2.4) (Hoehler et al. 1994; Valentine and Reeburgh 2000),



In these experiments, a low hydrogen concentration was necessary for AOM to occur. The use of the hydrogen by the sulfate reducers would maintain hydrogen concentration in sediments at a low level, making methane oxidation a thermodynamically favorable process, $\Delta G = -25 \text{ kJ mol}^{-1}$ (Hoehler et al. 1994; Hoehler et al. 1998; Valentine and Reeburgh 2000).

Despite the geochemical and thermodynamic evidence for the net anaerobic oxidation of methane, no syntrophic partner for SRB had been identified. Work done by Hinrichs et al. (1999) on sediments from a known methane seep in the Eel River Basin

presented evidence for a distinct group of archaea using methane as a carbon source in anaerobic conditions. Stable carbon isotope signatures for compounds identified as archaeal lipids were highly ^{13}C -depleted with methane as the only carbon source consistent with the values observed. The fractionation of the $\delta^{13}\text{C}$ likely occurred from the methane being utilized for biological processes (Hinrichs et al. 1999). Additionally, 16S rRNA phylogenetic analysis of the same samples from Eel River Basin identified a distinct group of archaea related to known methanogens. This work represents the first use of biomarkers, that is, compounds specific to a particular organism, in an attempt to solve the AOM mystery. Phylogenetic investigations continued using 16S rRNA sequencing in a variety of known AOM environments, identifying distinct anaerobic methanotrophs as ANME-1 and ANME-2 and SRB from the *Desulfosarcina/Desulfococcus* (DSS) groups (Hinrichs et al. 1999; Boetius et al. 2000; Orphan, House, et al. 2001).

Boetius et al. (2000) were the first to visually identify microbes responsible for AOM. Using fluorescence *in situ* hybridization with probes specific to archaea of known methanogens (from the Eel River Basin in Hinrichs et al. (1999) work) and SRB, aggregates of archaea were found to be surrounded by SRB (confirmed in Nauhaus et al. 2002). The clustered nature of the two microbial communities lends further support to the hypothesized two-step metabolic process for AOM because the intermediates can physically be shuttled between the groups shown in Fig. 2.4 (DeLong 2000). Direct coupling of sulfate reduction, as measured from the production of sulfide, to methane oxidation was observed in sediments with known communities of AOM microbes (Nauhaus et al. 2002). Early work had correlated the two processes due to the occurrence

of peak rates at the same depth in the SMTZ, but these more recent studies measured an increase in sulfate reduction when a greater concentration of methane was available in sediments with a large AOM population (Nauhaus et al. 2002; Valentine 2002; Knittel and Boetius 2009). Despite the evidence presented for the coupling of SR to the overall AOM process, none of the proposed intermediates for AOM (formate, hydrogen, acetate or methanol – all possible products of reverse methanogenesis) enhanced SR (Nauhaus et al. 2002; Valentine 2002).

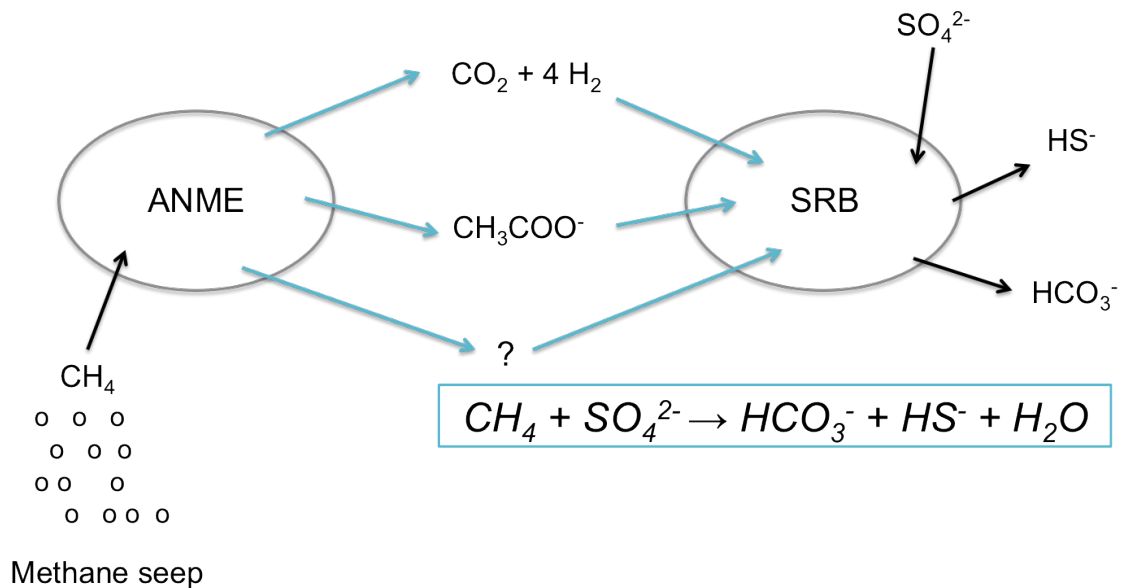


Figure 2. 4. Diagram of potential syntrophic metabolism responsible for sulfate dependent AOM. After Jørgensen and Kasten 2006.

Using fluorescence *in situ* hybridization with probes selected for ANME-2 and DSS coupled to secondary ion mass spectrometry, ¹³C-depleted isotopes were found in microbial cells – with methane being the only known source for the δ¹³C values (Orphan, House, et al. 2001; Orphan et al. 2002). This work confirmed that the ¹³C-depleted biomarkers were from organisms involved in AOM (Knittel and Boetius 2009) and ¹³C-depleted biomarkers are now considered evidence of the microbial players, both SRB and

methanotrophic archaea, involved in methane oxidation in anaerobic environments (Pancost et al. 2000; Elvert et al. 2000; Orphan, Hinrichs, et al. 2001; Orphan et al. 2002; Niemann and Elvert 2008).

There are many lines of converging evidence developed over the past thirty-five years supporting the net anaerobic oxidation of methane in marine sediments. Despite the progress made in the field, the metabolic pathways by which methane is removed from marine sediments is still speculative. Scientists have continued to use these historic indicators to identify sediments where AOM is occurring:

1. Methane and sulfate concentration profiles;
2. Rates of sulfate reduction and methane oxidation;
3. Depleted stable carbon isotope signatures.

More recent work has continued to investigate the microbial players responsible for AOM in anoxic sediments. Phylogenetic studies have continued to identify the active communities at the SMTZ. Three distinct groups of methanotrophic archaea have been identified in marine sediments associated with AOM: ANME-1, -2, and -3, with the ANME-2 group having sub-clades (Boetius et al. 2000; Orphan et al. 2002; Niemann et al. 2006; Knittel and Boetius 2010). These ANME groups are related to *Methanosarcinales* and *Methanomicrobiales*, but are distinct from each other (Boetius and Knittel 2010). All of the ANME groups identified are found in a variety of marine environments where net methane oxidation occurs. ANME-1 and -2 have been found in association with *Deltaproteobacteria* from the DSS group (Orphan, Hinrichs, et al. 2001; Knittel et al. 2003), while ANME-3 have a different bacterial partner related to the *Desulfobulbus* cluster (Niemann et al. 2006).

To date, no pure cultures of organisms from the microbial consortia responsible for AOM have been grown (Wegener et al. 2008; Holler et al. 2011). Investigations of the processes occurring in marine sediments associated with AOM have relied on the collection of sediments with an abundant microbial population, i.e., seep sites and microbial mats. In the absence of cultured samples, biomarkers that can be directly associated with the methanotrophic archaea and SRB from marine samples are used to elucidate the role of the consortia players.

Lipid biomarkers are of interest in organic biogeochemistry due to their diverse structures that can be linked to specific organismal sources. Additionally, lipids are amenable to chromatographic techniques allowing for separation of individual biomarkers from a complex sample matrix. Stable carbon isotope analysis of biomarkers (e.g., alkanes and fatty acids) can be used to identify specific sources contributing material to marine sediments, for example long chain fatty acids are widely thought to originate from C3 vascular plants (Hayes et al. 1990; Yunker et al. 2005). On a microbial level, the direct coupling of ^{13}C -depleted lipids to AOM communities at a number of sites allowed for the identification of target biomarkers for the microbial partners (Hinrichs et al. 1999; Orphan, House, et al. 2001; Orphan, Hinrichs, et al. 2001). Archaeal biomarkers are typically irregular isoprenoid hydrocarbons and SRB biomarkers are specific fatty acids, methylated for ease of separation (Pearson 2000; Ingalls and Pearson 2005). Table 2.1 shows examples of specific biomarkers of interest for both methanotrophic archaea and SRB.

Table 2. 1. Biomarkers for archaea and sulfate reducing bacteria.

Microbe	Biomarker	Reference
Archaea	Archaeol	(Pearson 2000; Ingalls and Pearson 2005)
	Hydroxyarchaeol	(Hinrichs et al. 1999)
	Crocetane	(Elvert, Suess, and Whiticar 1999; Thiel et al. 1999)
	Pentamethylicosane	(Pancost et al. 2000; Thiel et al. 2001)
	GDGTs	(Pancost, Hopmans, and Sinninghe Damsté 2001)
Bacteria	C15:0 iso and anteiso	(Zhang et al. 2002; Wegener et al. 2008; Aquilina et al. 2010)
	C16:1 various structures	(Elvert et al. 2003; Londry, Jahnke, and Des Marais 2004)
	C17:0 iso and anteiso	(Zhang et al. 2002; Aquilina et al. 2010)

The carbon available as source material for the microbial communities is limited to methane, sedimentary organic matter, dissolved organic carbon (DOC) and dissolved inorganic carbon (DIC), both from the pore water and sediments in marine sediments. If biomarkers for archaeal and bacterial players in the removal of methane from anoxic sediments can be isolated, their stable carbon isotopic signature should be indicative of the carbon incorporated into their biomass. The assimilation of carbon by organisms also results in the fractionation of ^{13}C relative to ^{12}C as compared to the source pool's isotopic signature. The ^{13}C -depleted stable carbon isotopes of lipid biomarkers have been considered conclusive evidence for the process of AOM, indicating the incorporation of ^{13}C -depleted methane into the biomass of the microbial community. Archaea are thought to oxidize the methane resulting in biomarkers more ^{13}C -depleted than the methane carbon source due to such fractionation (Hinrichs and Boetius 2002). The bacterial partners then use the products of methane oxidation as their primary autotrophic carbon source, reflected in a biomarker signature slightly more ^{13}C -enriched than the archaea (Hinrichs and Boetius 2002). Later work by Wegener et al. (2008) showed through ^{13}C -

labeling experiments the SRB incorporated carbon from labeled CO₂ into its biomass, not the labeled methane or methane derived intermediate substrates, e.g., formate or acetate. This result lends support to the theory of the consortia operating by shuttling electrons between the microbial players and the ¹³C-depleted signature for SRB results from an autotrophic uptake of methane derived DIC (Wegener et al. 2008; Knittel and Boetius 2009).

The specific roles of the archaeal and bacterial partners and the flow of carbon and reduced species between them remains poorly understood (Holler et al. 2011). Though Boetius et al. (2000) showed that the microbial players are often clustered together, the SRB are not always present in association with archaeal methanotrophs, further complicating understanding of the AOM process (Orphan et al. 2002). Additionally, AOM is typically studied in two unique marine environments – anoxic sediments where methane flux is controlled by molecular diffusion and seep sites, where phylogenetic studies have focused, due to the large microbial population resulting from high methane concentrations near the sediment-water interface. In fact, recent research suggests that at seep sites archaea may actually be producing ¹³C-depleted methane, not just oxidizing the methane present (Londry et al. 2008; Alperin and Hoehler 2009; Alperin and Hoehler 2010). Methane production by archaea does not discount the process of AOM, but ¹³C-depleted biomarkers should not be used as the sole line of evidence for methanotrophy. The processes controlling AOM in these distinct marine settings, as well as the specific players dominating the microbial population, may be vastly different and may not be representative of the processes occurring in the seafloor where the concentrations of methane are low by comparison to the methane rich locales.

Radiocarbon analysis of lipid biomarkers may provide more insights into the metabolism of the microbes in marine environments with net methane oxidation. Compound specific radiocarbon analysis (CSRA) gives information on the age of the carbon incorporated into the biomass, and therefore age and/or residence time of carbon in a source pool, adding another dimension to understanding microbial processes. CSRA for marine biogeochemistry requires precise measurement of small and often irreplaceable samples. Only very recently has the application of this technique been possible for AOM environments.

For further information regarding the progression of understanding the processes of AOM in marine sediments, the reader is referred to the following articles Valentine and Reeburgh 2000; Hinrichs and Boetius 2002; Reeburgh 2007; Knittel and Boetius 2009.

2.3 Radiocarbon and Accelerator Mass Spectrometry

Radiocarbon is one of three naturally occurring isotopes of carbon and has a natural abundance of 0.0000000001% (one part per trillion) in the atmosphere, while the stable carbon isotopes have abundances of 98.89% and 1.11% for ^{12}C and ^{13}C , respectively. Radiocarbon is generated in the atmosphere when cosmic rays react with N_2 molecules in the reaction



In the atmosphere, the radioisotope of carbon combines with oxygen to form $^{14}\text{CO}_2$ and mixes with the pool of CO_2 in the atmosphere.

Organisms take on the radiocarbon content of the food source they consume. Autotrophs directly use CO_2 as a carbon source while heterotrophs consume material that

has already incorporated CO₂ directly. Once an organism dies, the exchange of carbon with their environment ceases and the radioisotope decays. Radiocarbon, which has a half-life of 5730 years, beta decays by the reaction



The usefulness of natural decay processes and the long half-life of radiocarbon was seen by Libby, who used a Geiger counter that was able to distinguish natural radiocarbon decays from the background radiation as a means to determine the age of carbon containing substances (Taylor 2000). Decay counting continued to be the only means of radiocarbon determination for more than two decades, requiring large samples and long measurement times to observe enough decay events. Due to the natural abundance of radiocarbon, a 1-g sample of modern carbon would have 5×10^{10} atoms of ¹⁴C present. The amount of radiocarbon remaining in a sample after a certain period of time can be determined from the radioactive decay law in

$$N(t) = N(0)e^{-\lambda t}, \quad (2.7)$$

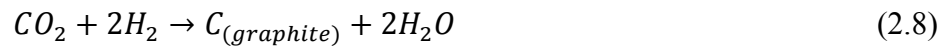
where N is the expected number of atoms at a given time t, N(0) is the initial number of ¹⁴C atoms present in the sample and $\lambda = \frac{\ln 2}{t_{1/2}}$ where the half-life ($t_{1/2}$) is 5730 years.

Using this equation, the number of ¹⁴C atoms that decay in a minute in one gram of carbon are approximately 13.8 atoms. With so few atoms decaying per minute, a large sample is required and measurement times are long. Accelerator mass spectrometry was developed in the late 1970's as a way to count the ¹⁴C atoms in a sample rather than waiting for the decay events.

Accelerator mass spectrometry (AMS) operates under common principles of mass spectrometry and has the same basic components: ion source, mass analyzer and detector.

However, unlike most other mass spectrometry techniques, negative ions are typically accelerated to high energies before they are analyzed. This technique is advantageous because of its high resolving power for isotopes and its ability to eliminate atomic and molecular isobars.

Material is prepared for radiocarbon analysis depending on the sample type (e.g., wood, carbonates, etc.). Different techniques are employed to remove possible contaminants and to prepare the sample for the conversion of carbon into carbon dioxide. The carbon dioxide is then reduced to graphite in the presence of a catalyst and hydrogen gas



The graphite is pressed into targets and loaded into a wheel for analysis. Graphite samples are sputtered by a cesium beam to produce negative carbon ions. A benefit of producing negative ^{14}C ions is the isobar ^{14}N does not produce stable negative ions. Therefore, a potential major interference does not affect radiocarbon measurements. From the source, the negative ions travel through an electrostatic analyzer (ESA) and a magnet before entering the accelerator as shown in Fig. 2.5.

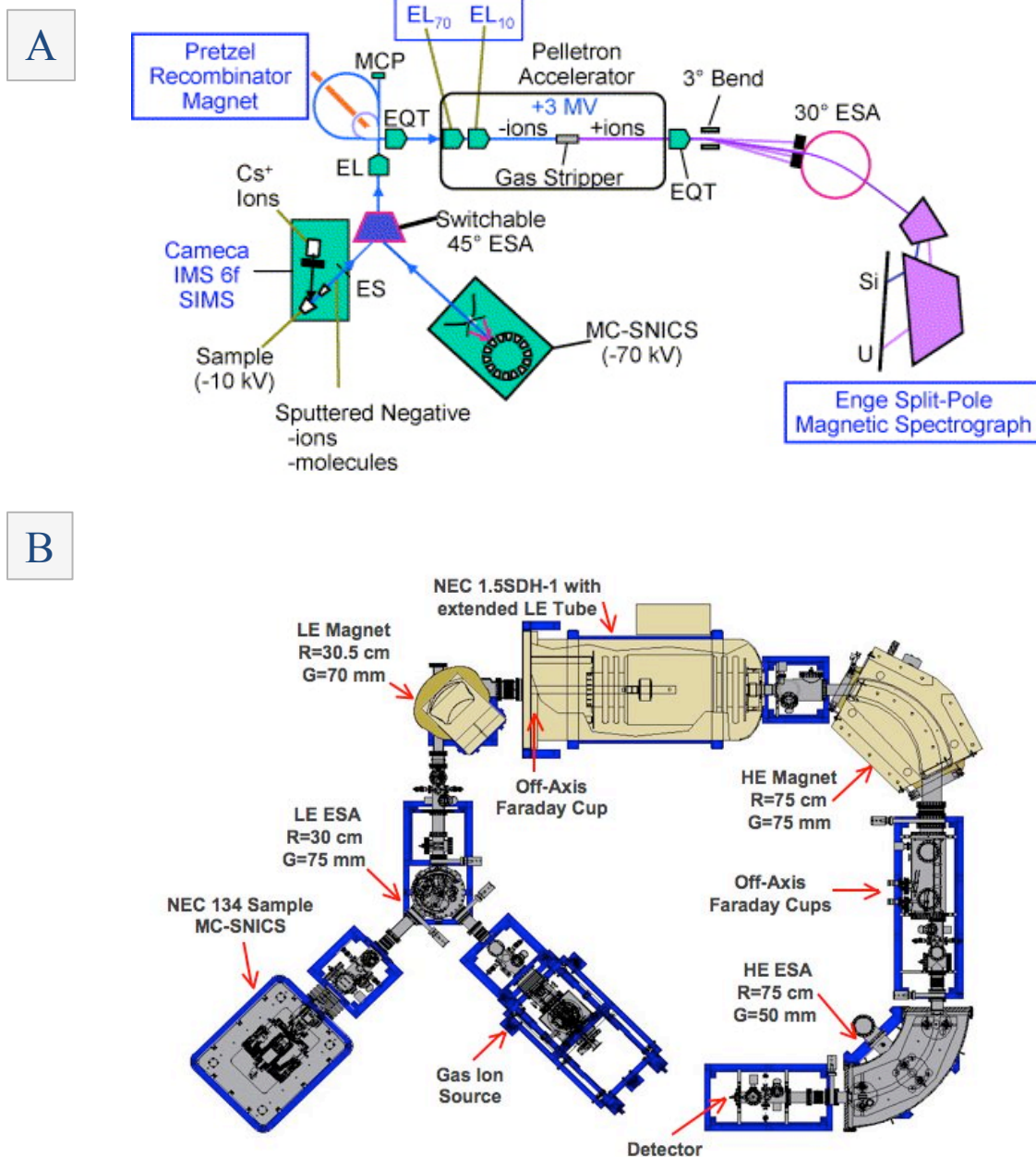


Figure 2. 5. Two different AMS systems both used for radiocarbon analysis. (A) is the Naval Research Laboratory Trace Element AMS and (B) is the National Ocean Sciences AMS facility at Woods Hole Oceanographic Institute. Both systems have the same basic components: ion source, low energy magnet, low energy ESA, Pelletron tandem accelerator, high energy magnet, high energy ESA, and detectors. (B) is from <http://www.who.edu/nosams/page.do?pid=40149&tid=282&cid=74873>.

Accelerated by the potential difference between ground and the central terminal, which at NOSAMS is at approximately +500 kV, the negative ions enter the electrostatic

accelerator, reach the terminal potential in the middle of the accelerator, and are stripped of electrons in a channel filled with argon gas. The now positive ions, in various charge states, are accelerated away from the positive canal toward ground potential. By stripping the negative ions in the tandem accelerator, molecular ion interferences (e.g., $^{13}\text{CH}^-$ and $^{12}\text{CH}_2^-$) are destroyed. Though the components of each system vary, the operating principles are the same. At the high energy end (post acceleration), the positive beam of ions passes through both a magnet and ESA selecting for the desired ions. The ^{12}C and ^{13}C isotopes are typically measured separately from the ^{14}C . At the ^{14}C detector, the exact ion determination is made using an energy detector situated for a particular mass to charge and energy to charge ratios. This enables the ions to be detected virtually free of all molecular interferences. The final detection step also distinguishes any isobars, which reach the detector with the same energy, based on their energy loss per length of travel (dE/dx), since the ions go through a thin foil placed in front of the energy detector. At NOSAMS, the ^{14}C ions are detected with a solid-state, silicon-surface-barrier detector (Roberts et al. 2003).

Coal blanks and oxalic acid standards are combusted and processed in a manner identical to the solid organic samples. The blanks serve as a means of estimating the contamination from the system associated with sample processing. The standards provide a baseline and correction factor incorporated in the reporting of ^{14}C data. Minze Stuiver and Henry A. Polach published a pivotal paper in 1977 that established standards by which to report radiocarbon data. Their work established 1950 as the date for modern carbon, a reference “time zero”. This chronological start point is associated with “1890 wood”. The radiocarbon signature of “1890 wood” was extrapolated based on natural

decay to 1950, and was chosen to eliminate influences from the industrial revolution and the testing of nuclear weapons occurring after 1890. The National Institute of Standards and Technology (NIST) standards, oxalic acid I (OxI) and oxalic acid II (OxII), are widely used as modern standards and their radiocarbon age determined based on the 1950 scale. A variety of corrections are included when determining the radiocarbon age, or fraction modern (Fm) carbon. Normalization for fractionation during sample generation and processing is based on the measured ratio $^{13}\text{C}/^{12}\text{C}$. All corrections and reporting of radiocarbon data are done according to the protocol established by Stuiver and Polach (1977).

AMS has far surpassed decay counting as an efficient and accurate means of detecting ^{14}C . AMS is able to directly count ^{14}C atoms present in a sample using tandem electrostatic accelerators instead of waiting for the nucleus to decay (Gove 2000). The effectiveness of this method is demonstrated by a high sensitivity to very low abundances, a small sample size requirement, and data collection occurring in a rapid time frame (Donahue 1995). Since its inception, scientists have continually pushed the boundaries of AMS, decreasing the sample size and increasing the throughput of samples for ^{14}C detection. When it was first introduced, 1 mg of carbon (mg C) was a standard sample size for AMS measurement. Modern systems routinely measure samples of 100 $\mu\text{g C}$.

Despite all the advances in AMS over more than 30 years of radiocarbon measurements, compound specific radiocarbon analysis is challenging. Eglinton et al. (1996) from the Woods Hole Oceanographic Institution National Ocean Sciences Accelerator Mass Spectrometry (WHOI-NOSAMS) facility applied the technique of

Preparative Capillary Gas Chromatography (PCGC) for the purposes of radiocarbon dating. Their efforts represented the first application of the high-resolution separation technique for radiocarbon analysis (Eglinton et al. 1996).

The PCGC repeatedly collects samples immediately following their separation using a gas chromatograph. A challenge faced when exploring this technique for compound specific separations is the necessity for high resolving power due to the complexity of the carbon pools where the samples originated. Continually collecting the same eluted fraction allows the user to gather enough material to convert to CO₂ for an AMS measurement. This is beneficial because once the peak has been selected for analysis; the instrument will repeatedly collect the fraction of interest.

PCGC makes it possible for radiocarbon analysis to be done on samples previously uninvestigated due to size limitations, like biomarkers. This tool is efficient at isolating pure fractions of semi-volatile compounds from complex sample sources (Zencak et al. 2007). Eglinton et al. (1996) successfully collected more than 250 µg C from repeat injections using PCGC in their initial efforts, and found reproducibility in retention times. Thus far, the application of CSRA techniques to understanding the biogeochemistry of AOM has been limited, at least in part, by the large sample size requirement (>100 µg C) of conventional AMS techniques. The development of methods to routinely measure microscale-sized samples (25-100 µg C) at NOSAMS enabled the first use of CSRA to understand microbial function (Gove 2000). However, the 25 µg C threshold may be unattainable for microbial biomarkers associated with AOM. The majority of radiocarbon measurements that have been applied to understanding modern microbial processes (Ingalls et al. 2006; Shah et al. 2008) have been in the ultra-

microscale size range (5-25 $\mu\text{g C}$). Preparation of these small samples and their measurement, however, is labor-intensive and anything but routine. Contamination of samples with modern carbon is always a concern for radiocarbon work, but as sample size decreases there is also a concern for diluting a small sample with dead carbon.

Techniques have been developed at a number of radiocarbon laboratories to address issues in the preparation and measurement of microscale carbon samples. As the size of the sample decreases, the amount of carbon atoms available for detection decreases and the overall beam intensity is reduced. Systems tuned specifically for the reduced beam rather than the standard 1 mg C produced beam can improve the AMS system for the microscale samples (Santos et al. 2007). Additionally, the measurement of size-matched small standards and blanks can account for machine-induced fractionation (Pearson et al. 2006; Santos et al. 2007).

A great portion of the error associated with measuring small samples can be attributed to sample processing techniques prior to AMS analysis. Shah and Pearson (2007) determined the blank contributed from each step in processing individual lipids from particulate organic carbon in the water column for CSRA (Ingalls et al. 2006; Shah and Pearson 2007). The different sources of error investigated were from isolation and purification of the lipids, combustion of the samples, and residual contaminants (i.e., vacuum lines, flame sealing quartz, and Pyrex tubes). AMS facilities report errors associated with graphitization and sample handling in addition to the machine counting statistics, but there are still blank contributions from procedures prior to AMS sample analysis that are not considered. Below 25 $\mu\text{g C}$, the error reported by AMS facilities is insignificant compared to the error introduced through sample preparation, particularly

the combustion process, which drastically increases as the sample size decreases, as shown in Fig. 2.6 (Ingalls et al. 2006; Shah and Pearson 2007).

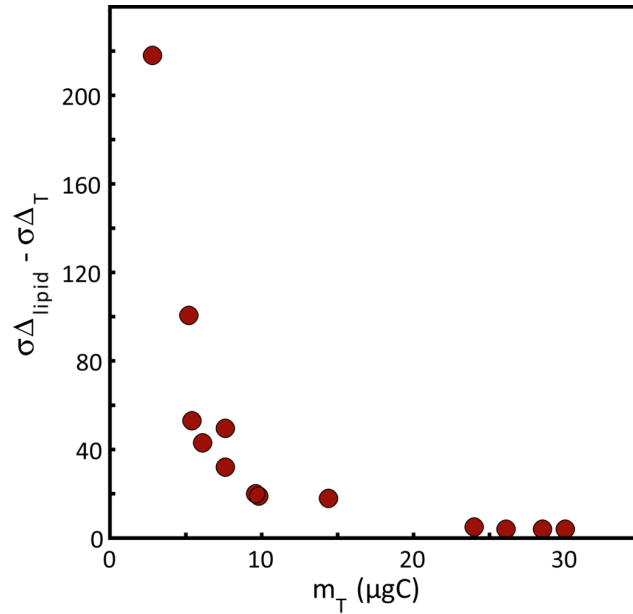


Figure 2. 6. Difference between AMS facility-reported uncertainty ($\sigma_{\Delta T}$) and total propagated uncertainty ($\sigma_{\Delta_{\text{lipid}}}$) plotted against total sample mass (m_T). The difference plotted on the y-axis is for propagated errors in $\Delta^{14}\text{C}$ measurements. Figure from Shah and Pearson (2007).

AMS requires sufficient sample size to produce a beam with a large enough intensity to result in reasonable counting statistics. While improvements to the system have reduced the minimum threshold for routine measurement from 1 mg C to 20 $\mu\text{g C}$, there is a limit to how small the current technologies will be able to measure. Dilution of samples with a filler of known isotopic composition is a possible technique, but suffers from a loss in precision (de Rooij, van der Plicht, and Meijer 2011). To improve small sample capabilities for radiocarbon analysis, new measurement techniques need to be developed or sample preparation methods need to be improved to eliminate contributions of sample processing to the overall blank. Intracavity optogalvanic spectroscopy

(ICOGS) and continuous flow accelerator mass spectrometry (CFAMS) have been proposed as two different technologies that may push the boundaries of the field.

A novel technique for ^{14}C measurement, ICOGS, has been developed at Rutgers University (Murnick, Dogru, and Ilkmen 2008). ICOGS is based on the optogalvanic effect, measuring the electrical response of a gas discharge to an optical perturbation provided by a $^{14}\text{CO}_2$ laser (Murnick, Dogru, and Ilkmen 2008; Murnick, Dogru, and Ilkmen 2010). ICOGS would eliminate the need for graphitization of CO_2 and associated blanks. Though the minimum threshold of carbon that can be measured as CO_2 gas is unknown, the gas is measured in a non-destructive manner, allowing for long measurement times to reduce background noise and thereby measurement uncertainty. Despite these advantages, the ICOGS instrument is not currently coupled to a combustion system, therefore the preparation of samples requires closed-tube combustion, a potentially large source of contaminant blank carbon for small samples (Shah and Pearson 2007). The gas chromatograph interface for CFAMS in development at NOSAMS is potentially capable of measuring small quantities of CO_2 gas directly. It has the advantage of eliminating the need for closed-tube combustion, but potentially will suffer from a lower signal to background noise ratio. Either technique would represent a huge milestone in the advancement of measurements for small sample radiocarbon analysis, but to date neither system has demonstrated the capability of routinely measuring small samples as well as the prevailing AMS systems.

Chapter 3: Collection, Preparation and Analysis of Fatty Acid Methyl Esters (FAMES) for Stable Carbon Isotope Investigations

3.1 Sediment Collection, Sampling and Storage

Samples were collected from the Beaufort Sea to the north and east of Barrow, AK in September 2009 as part of the Methane in the Arctic Shelf/Slope (MITAS) research cruise aboard the United States Coast Guard Cutter (USCGC) *Polar Sea*. Sample sites from the Beaufort Shelf were selected based on previous work in the region. Previous research cruises provided seismic data that indicated free gas was present in the sediments at both shelf and offshore slope sites. In addition, seismic data provided preliminary evidence of methane hydrates in deep subsurface sediments. The sediment samples were collected using a steel barreled piston corer with a 6.7-cm inner diameter (i.d.) polycarbonate liner (Hamdan et al. publication pending). Fourteen piston cores were collected and sampled on the MITAS Expedition, with four cores designated for compound specific carbon isotope analysis. Each core was subsampled at 20 – 70 cm intervals over the length of the core based on visual observations and physical indications (e.g., dark, sulfide containing sediment). A sediment plug was taken for methane analysis by drilling a hole in the liner and transferring a plug (3 mL) of sediment obtained in a syringe to a vial which was sealed on deck (Hamdan et al. 2011). On deck the core was split in half lengthwise using a core splitter. One half of the core, known as the “working half” was sub-sampled for various analyses, including: phylogenetic studies, porosity determination, carbon isotope analyses, and rate measurements for sulfate reduction and methane oxidation. Rhizon type pore-water extractors were used to

vacuum extract pore water from the other half of the core (Dickens et al. 2007) at intervals corresponding to sediment sampling. This half of the core was used for geological analyses and collection of shell fragments for dating the core, then this half was archived. The cores of interest to this work, PC09 and PC13, were approximately 4 m and 5.5 m in length, respectively. Their locations are shown in Fig. 3.1 in relation to Point Barrow, AK.

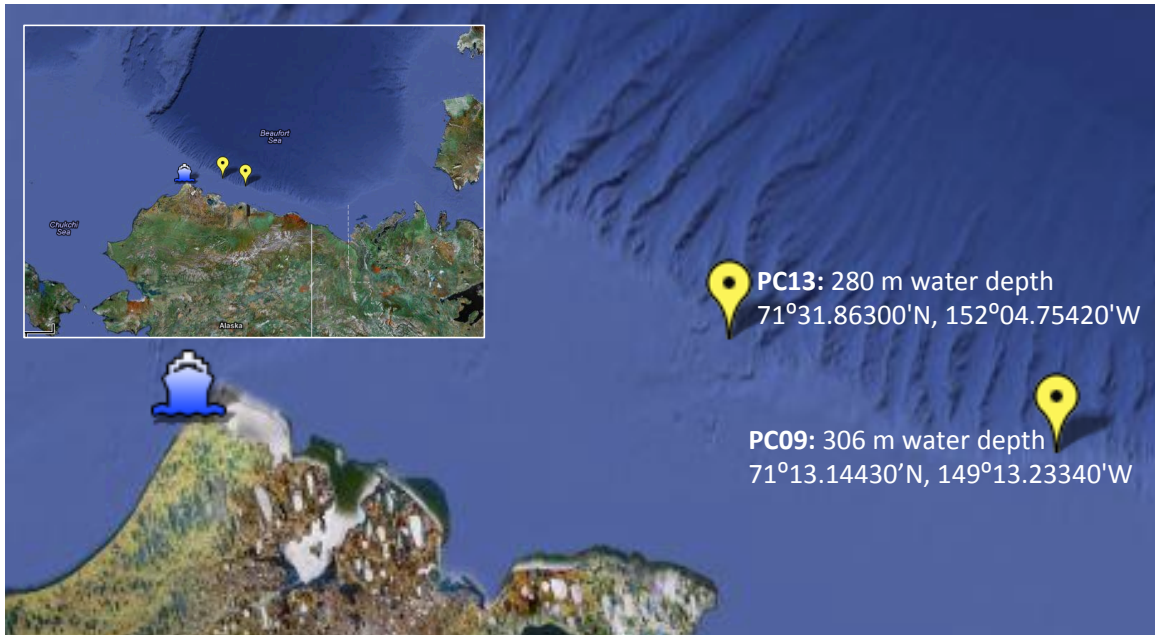


Figure 3. 1. Location of cores PC09 and PC13, the two cores selected for analysis in this study. The water depth for sampling, as well as the coordinates, are indicated at each site. Mapped using <https://maps.google.com>.

Both piston coring locations were east of Point Barrow, AK along the same isobath at the shelf break near the Beaufort Sea. Cores were selected for compound specific carbon isotope analysis based on methane concentrations measured shipboard and the indication of H₂S from a strong odor when the core was brought on deck. From the fourteen total piston cores collected as part of the MITAS Expedition, sediment subsamples were collected for compound specific investigations from four cores at intervals

consistent with sampling for geochemical analysis. Shipboard analyses determined the concentrations of both sulfate and methane. Stable carbon isotopes for geochemical parameters (e.g., dissolved inorganic carbon (DIC), total inorganic carbon (TIC), dissolved organic carbon (DOC), total organic carbon (TOC)) and porosity via gravimetric analysis were determined later at the Naval Research Laboratory (NRL). The sediment samples were transferred to lidded glass jars on deck and held at -80°C until total lipid extraction at the University of Maryland, College Park. Table 3.1 presents a summary of some of the geochemical analyses carried out as part of the MITAS Expedition that proved useful in the interpretation of compound specific carbon isotope data.

Table 3. 1. Analyses, sample type and location for relevant measurements.

Analysis	Sample Type	Location for Analysis
[CH ₄]*	Sediment plug/headspace analysis	Shipboard
[SO ₄ ²⁻]*	Pore Water	Shipboard
Porosity*	Sediment	NRL
δ ¹³ C methane*	Sediment plug/headspace analysis	NRL
[DIC], δ ¹³ C DIC	Pore water	NRL
[DOC], δ ¹³ C DOC	Pore water	NRL
[TIC], δ ¹³ C TIC	Sediment	NRL
[TOC] δ ¹³ C TOC	Sediment	NRL
Total lipid extraction*	Sediment	UMD
Biomarker Analysis*	TLE	NOSAMS, NRL

The () represents analyses essential to the interpretation of this dataset and are described within this chapter. The other analyses were carried out by collaborators on the MITAS Expedition and proved useful in the interpretation of this data set.*

3.2 Methods

3.2.1 Geochemical Analysis

The methane concentration was determined using a headspace technique from sediment plugs referenced to a known standard gas on a Shimadzu 14-A gas

chromatograph (GC) with a flame ionization detector (FID) and Hayesp-Q 80/100 column (Coffin et al. 2008; Hamdan et al. 2008). Sulfate concentrations were measured from pore water samples using a Dionex DX-120 ion chromatograph with a 4-mm AS-9HC column (Paull et al. 2005; Hamdan et al. 2011). The porosity of the sediment was determined by gravimetric analysis. The sediment was thawed and weighed, then baked overnight at 50 °C. The sediments were then weighed again to determine the sediment dry weight less the water content (Coffin et al. 2008) and hence the porosity according to

$$\text{porosity} = \frac{\frac{\text{sediment wet mass} - \text{sediment dry mass}}{\text{seawater density}}}{\frac{\text{sediment wet mass} - \text{sediment dry mass}}{\text{seawater density}} + \frac{\text{sediment dry mass}}{\text{sediment density}}}, \quad (3.1)$$

where the density of seawater is assumed to be 1.035 g mL⁻¹ and the density of sediment is estimated at 2.5 g mL⁻¹.

The stable carbon isotope composition ($\delta^{13}\text{C}$) of methane was analyzed with a Thermo Trace Gas Chromatograph (GC) interfaced via a GC-C III combustion unit to a Delta Plus XP isotope ratio mass spectrometer (IRMS) (Plummer, Pohlman, and Coffin 2005). Samples were injected into a stream of helium, cryogenically concentrated using a 3-cm section of a 0.32-mm i.d. Porapak-Q column, then rapidly desorbed onto a GC column (Plummer, Pohlman, and Coffin 2005). The methane was desorbed at 150 °C and separated on a 25-m, 0.32-mm i.d. Porapak-Q column at -10 °C with a flow rate of 1.6 mL per minute. The measured $\delta^{13}\text{C}$ signatures were standardized to a CO₂ reference gas, that had been standardized with NIST RM 8560 – a petroleum natural gas standard with a value of -44.84‰ relative to VPDB (Vienna Pee Dee Belemnite) (Plummer, Pohlman, and Coffin 2005).

3.2.2 Total Lipid Extraction

Sediment samples were stored at -80 °C in freezers at NRL until Soxhlet extraction. Of the four piston cores sampled for compound specific carbon isotope analysis (PC09, PC10, PC11 and PC13), cores PC13 and PC09 were selected for analysis. Horizons for Soxhlet extraction were selected based on the determined sulfate-methane transition zone (SMTZ) from measured sulfate and methane concentrations in PC13 as shown in Fig. 3.2. Core PC09 was identified as a reference core based on a low, almost negligible methane concentration for the whole depth of the core (Fig. 3.2) and the sulfate-methane transition zone (SMTZ) was beyond the depth of the core.

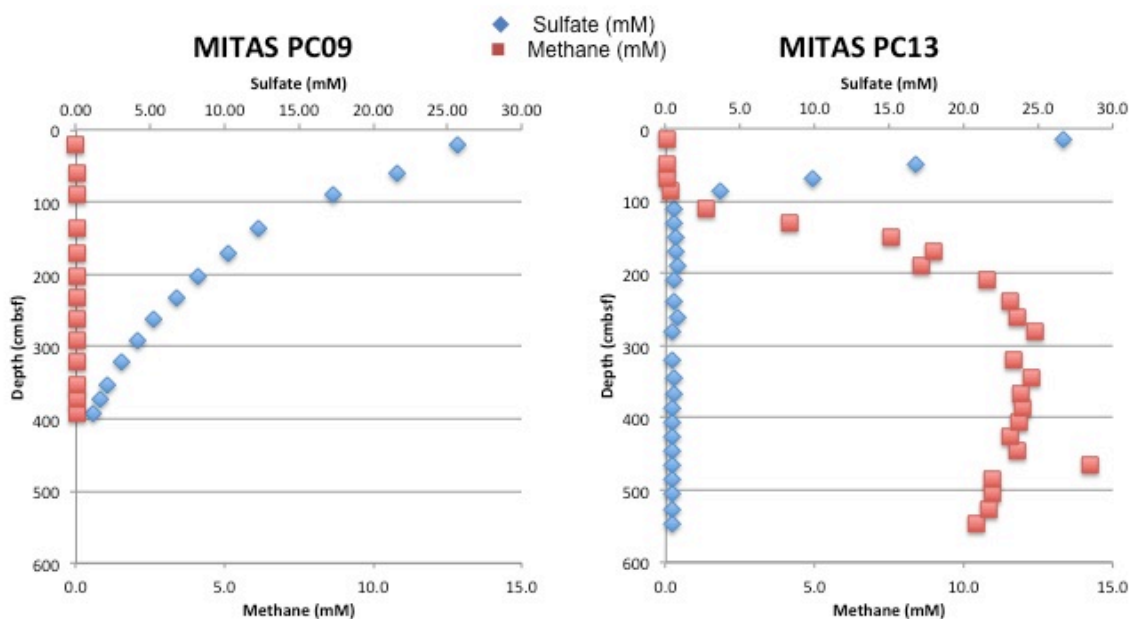


Figure 3. 2. Sulfate concentrations (blue) and methane concentrations (red) plotted with respect to the sediment sampling depth in centimeters below the seafloor (cmbsf) for cores PC09 and PC13 (Coffin et al. 2011).

Sediment was transferred from NRL to the University of Maryland, College Park on the day the extraction began. A baked (at 450 °C for 6 hours to combust residual hydrocarbons) piece of aluminum foil was used as a clean surface to transfer the sediment

from the jars used for sample collection to pre-weighed and combusted extractor thimbles (Quark Glass: Large 45 x 130 mm, medium porosity). Each sediment interval was divided between two thimbles and carried out as simultaneous extractions, later combined into a single sample.

The mass of sediment transferred to each extractor thimble was determined from the porosity of each sample. Since the sediment samples were taken from the working half of the core, the samples still contained pore water. To account for this added mass component, the measured porosity was used to calculate the sediment dry mass by the rearrangement of Eq. 3.1 to get

$$\text{sediment dry mass} = \frac{\text{sediment wet mass} \cdot (1 - \text{porosity})}{1 - \text{porosity} + \frac{\text{porosity} \cdot \text{seawater } \rho}{\text{sediment } \rho}} \quad (3.2)$$

Table 3.2 reports the results of this analysis for each sample in PC09 and PC13.

Italicized data were taken at intervals between geochemical analyses (the sample number ends with a “.5”), so the sediment depth and porosity are estimations made by taking the average of the sample above and below its numbered value.

Table 3. 2. Calculated mass of dry sediment from porosity.

Piston Core	Sample #	Sediment Depth (cmbsf)	Mass Sediment (g)	Porosity	Estimated "gram dry weight" Sediment
PC09	111	392	135.95	0.6607	75.270
	112	372	147.65	0.6403	85.005
	113	352	162.25	0.6434	92.875
	114	322	83.75	0.6707	45.437
	118.5	187	183.4	0.6661	100.454
	119	172	198.4	0.6644	109.034
	119.5	154.5	196.1	0.6631	108.053
	121	90	160.7	0.669	87.491
	122	60	142.05	0.6856	74.653
	123	20	80.35	0.6973	41.127
PC 13	188	546	72.65	0.6599	40.287
	188.5	536	124.4	0.6574	69.333
	189	526	99.15	0.6548	55.537
	191	486	130.25	0.6617	71.971
	193	446	151.8	0.6623	83.778
	194	426	101.05	0.6538	56.711
	196	386	95.3	0.6446	54.430
	197	366	149.8	0.6279	88.190
	202	240	79.4	0.6336	46.273
	203	210	58.3	0.6593	32.368
	204	190	115	0.7383	53.045
	208	110	135.9	0.6508	76.712
	210	70	78.55	0.6851	41.327
	211	50	133.15	0.6735	71.818

The total lipid extraction protocol was a modified Soxhlet extraction procedure from *Lipid Analysis in Marine Particles and Sediment Samples: A Laboratory Handbook* (Wakeham and Pearse 2004). The total lipid extraction was carried out using the large Soxhlet extractor shown in Fig. 3.3, after being baked and rinsed with methanol (MeOH), then dichloromethane (DCM). The extractor thimble was transferred to the Soxhlet extractor using large previously baked and rinsed tweezers. A 9:1 mixture of DCM:MeOH (GC² Honeywell Burdick & Jackson ®) was gently poured onto the sediment in the extractor thimble. Enough solvent was added to allow the Soxhlet

extractor to siphon at least twice through (a total solvent volume of 350 mL). Following a 48-hour extraction, the solvent ratio was changed to increase the polarity with a 2:1 DCM:MeOH ratio (a total solvent volume of 375 mL) for a 24-hour extraction.

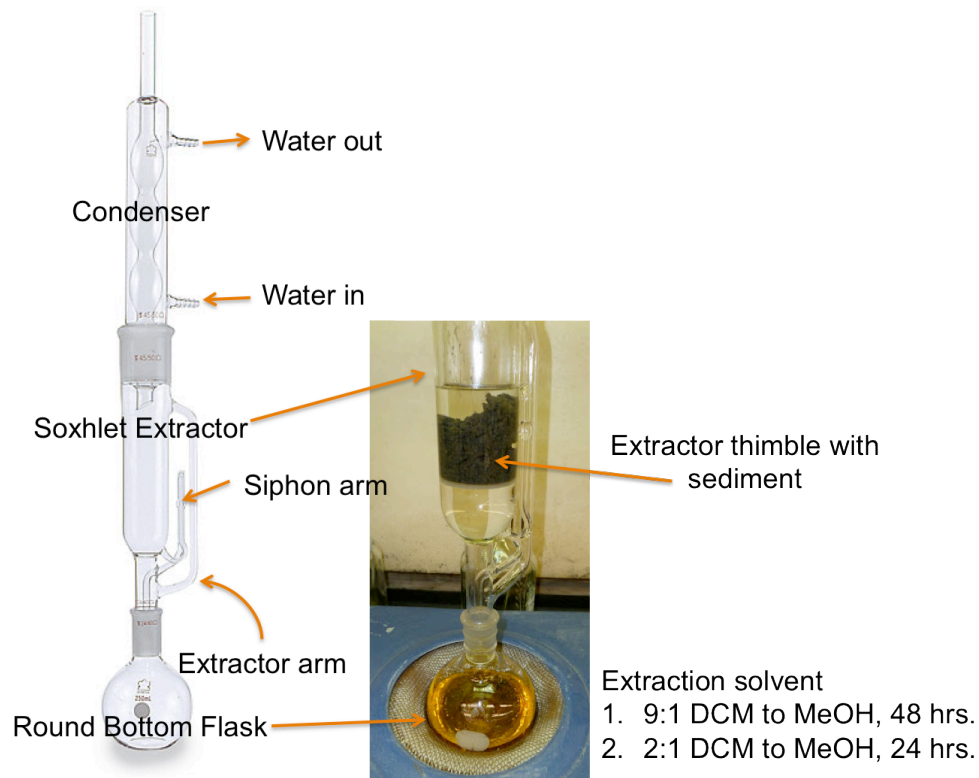


Figure 3. 3. Soxhlet extractor system for total lipid extraction. Soxhlet figure after http://static.coleparmer.com/large_images/9903710.jpg.

Once the extraction had completed and no more color was present in the solvents in contact with the sediment samples, the extracts were washed according to the protocol in *Lipid Analysis in Marine Particles and Sediment Samples: A Laboratory Handbook* (Wakeham and Pearse 2004). The two different polarity extractions for each Soxhlet apparatus were combined into a single 1-L separatory funnel and washed using a 5% NaCl solution 1:1 with methanol solvent (160 mL of 5% NaCl solution) to form two phases. The organic layer was drained and the remaining aqueous phase was washed

with DCM, drained and repeated. The aqueous phase was discarded and the organic layer was washed again with 5% NaCl at 1/3 the volume of the organic phase. The organic phase was drained into a turbovap flask and evaporated under a stream of ultra-high purity nitrogen gas (UHP N₂) to approximately 1 mL. Total lipid extracts were transferred using a Pasteur pipette to a 20-mL vial with a Teflon lined cap. The turbovap flask was rinsed twice with DCM, then twice with MeOH, each time transferring the contents of the wash to the sample vial. The total lipid extracts from the same sediment horizon were combined at this step in the process. Sodium sulfate was added to the vial to remove any remaining water and the samples were stored at 4 °C until transported to Woods Hole Oceanographic Institute (WHOI).

Total lipid extracts (TLEs) were transported to WHOI for sample processing and analysis as part of the National Ocean Sciences Accelerator Mass Spectrometry (NOSAMS) Graduate Student Internship Program. The methods used were followed from protocols described by Dr. Li Xu, a research specialist at WHOI (similar to (Ohkouchi, Eglinton, and Hayes 2003; Elvert et al. 2003)). The TLEs were transferred to a 20-mL vial through a Pasteur pipette with quartz wool to remove the drying agent (Na₂SO₄) from the samples. Samples were dried under a stream of UHP N₂ gas while heated gently in a heat block set to approximately 50 °C. Once the solvent was dried off, the TLEs were saponified in 0.5 M KOH solution prepared in 4:1 MeOH:H₂O for 2 hours at 80 °C.

The saponified sample was then separated into two fractions, neutrals and acids. The neutral lipids were obtained from the saponified solution by extracting three times with hexane and washing the neutral fractions with Milli-Q water twice. Sodium sulfate

was added to the neutral fraction and it was stored in the refrigerator for archaeal biomarker analysis at a later date. Fatty acids were collected when the remaining aqueous sample was acidified with 1:1 HCl:H₂O (acidity determined from pH paper), extracted from the organic layer in the vial three times with 4:1 hexane:DCM, and washed twice with Milli-Q water (discarding the aqueous layer). The sample was allowed to rest overnight with a drying agent to remove any remaining water. The drying agent was removed by transferring the sample into a combusted vial through a Pasteur pipette filled with quartz wool. The acid fraction was evaporated with UHP N₂ and then transferred to a 4-mL vial. The original sample vial was washed three times with DCM and transferred to the 4-mL vial to ensure the complete transfer of the acidified fatty acid sample. The sample was again dried to remove solvents and reacted for 3 to 9 hours at 50 °C with MeOH of a known isotopic composition to create fatty acid methyl esters (FAMES), a necessary step to increase the volatility of the fatty acids and improve separation via chromatographic techniques (Liu 1994). The FAMES were extracted with 10% ethyl acetate in hexane three times and the organic fraction was washed twice with Milli-Q water. A drying agent (Na₂SO₄) was added to dry the remaining water and the samples were stored in the refrigerator overnight.

3.2.3 Preparation of samples and GC-FID Analysis

Each sample that was dried overnight was then transferred to a 4-mL vial through a Pasteur pipette filled with quartz wool to remove the Na₂SO₄. The drying agent and vial were washed with DCM to ensure the entire FAMES sample was transferred. The sample was evaporated under a stream of UHP N₂ to remove the solvent and a nonpolar solvent, hexane, was added to the sample vial. The FAMES were separated into three

compound class fractions using the solvents described in Table 3.3, each 4 mL, via column chromatography (preparation of column described in full procedure included as Appendix 3).

Table 3. 3. Fractions isolated from column chromatography.

Fraction	Solvent	Collected
F1	Hexane	Alkanes
F2	5% ethyl acetate in hexane	FAMEs
F3	1:4 ethyl acetate:DCM	Hydroxy FAMEs

Each fraction was evaporated under a gentle stream of UHP N₂, transferred to a 2-mL GC vial with hexane, brought up to a final volume of 1 mL and analyzed on an Agilent 6890 GC-FID equipped with an autosampler and a Zebron ZB-5 30 m x 0.25 mm x .25 µm column. The GC-FID was run in splitless mode with the oven initially at 60 °C ramped to 120 °C at a rate of 20 °C min⁻¹, followed by a 4 °C min⁻¹ ramp until the oven temperature reached 320 °C and held there for 10 minutes.

Bacterial biomarkers of interest were identified by comparison to a FAMEs standard, Matreya LLC – Bacterial acid methyl esters CP Mix (see Appendix 4). FAMEs are named according to the International Union of Pure and Applied Chemistry (IUPAC) system of naming. Saturated FAMEs are specified with the number of carbon atoms identified before the colon and a “0” after the colon to indicate the number of double bonds present (e.g., C_{18:0}). Unsaturated FAMEs have the number of double bonds specified after the colon (e.g., C_{16:1} has one double bond, though the location is not specified) and branched FAMEs identify the branch point of the methyl designating the carbon with iso (i- designating branch point is on the carbon atom one from the end) or anteiso (ai- designating the branch point is on the carbon atom two from the end).

Following GC-FID analysis, samples collected in Fraction 2 (FAMES) for PC13 were combined for analysis based on the estimated amount of carbon present for each biomarker of interest from the peak area on the GC-FID and the analysis of a standard (combinations shown in Table 4.1). Samples were not combined prior to the GC-FID analysis in an effort to maintain a high sample resolution for the entire core, but sample size requirements necessitated combining adjacent sediment horizons. The FAMES fractions for samples were combined to target horizons in relation to the SMTZ: above, directly at, below, and two or more meters below the SMTZ. Targeting these regions with respect to the SMTZ ensured enough carbon was present in each sample for compound specific radiocarbon analysis and a $\delta^{13}\text{C}$ split. The methods for the use of the preparative capillary gas chromatography (PCGC) and radiocarbon analysis are described in Chap. 4. Upon collection of three target biomarkers via PCGC, the remaining sample isolated in Trap 0 (refer to Sec. 4.2.1 for description) was reserved for stable carbon isotope analysis at NRL.

An aliquot of each sample from PC09 FAMES fraction was transferred to a new GC vial and hexane was added to reach a total sample volume of 1 mL. The sample was then transported to NRL for analysis on the GC-isotope ratio mass spectrometer (IRMS). The remainder of each sample was retained at WHOI for later combination, separation and concentration on the PCGC. In total, four sample combinations from PC13 and nine original FAMES samples from PC09 (all excluding sample 121, see Table 3.2) were analyzed via GC-IRMS.

3.2.4 GC-IRMS Analysis

At NRL, tetracosane of known isotopic composition ($\delta^{13}\text{C} = -31.548\text{‰}$ referenced to NBS 22 standard at $\delta^{13}\text{C} = -30.031\text{‰}$) was added to each sample as an internal analytical standard to account for chromatographic effects on isotope ratios. The samples were injected into a Hewlett Packard 6890 GC for separation on a 60-m x 0.25-mm x 1- μm Hewlett Packard HP-5, 5% Phenyl Methyl Siloxane column. The GC was run in splitless mode with the oven initially at 150 °C ramped to 250 °C at a rate of 4 °C min⁻¹ and held for 10 minutes, followed by an 8 °C min⁻¹ ramp until the oven temperature reached 305 °C and was held for 10.50 minutes. The gas stream from the GC column was split, with 80% of the flow directed through a Finnigan MAT combustion interface to a Finnigan MAT Delta S IRMS (Boyd et al. 2006). The remaining flow was directed to an HP 5973 quadrupole mass spectrometer (MS) for identification of individual FAMES. Reference gas samples ($\delta^{13}\text{C}_{\text{VPDB}} = -45.01\text{‰}$) were injected into the source area of the IRMS in triplicate before and after sample introduction (Boyd et al. 2006). Specific FAMES (with retention times in the range of C_{15:0} to C_{20:0}) were identified through the use of the bacterial acid methyl esters standard (Appendix 4). Compounds eluting with retention times after C_{20:0}, referred to as the long chain FAMES (LC-FAMES), were tentatively identified using the NIST05.a.L mass spectral database associated with the Agilent software. All peak identifications were manually correlated to $\delta^{13}\text{C}$ values from the IRMS using the bacterial acid methyl esters standard. An offset of 80 seconds between the coupled systems was determined based on the analysis of the bacterial standard, up to and including C_{20:0}. The $\delta^{13}\text{C}$ values were calculated as

$$\delta^{13}\text{C} = \left[\frac{R_s}{R_{std}} - 1 \right] 1000(\text{‰}), \quad (3.3)$$

where R_s and R_{std} are the $^{13}\text{C}/^{12}\text{C}$ ratio of the sample and standard, respectively. Samples were referenced against CO_2 calibrated to VPDB. Voltages below 250 mV and above 10,000 mV were discarded and each sample was measured in triplicate. Each run was corrected for chromatographic conditions relative to the tetracosane

$$\delta^{13}\text{C}_{corrected} = \delta^{13}\text{C}_{measured} + \delta^{13}\text{C}_{true\ tetracosane} - \delta^{13}\text{C}_{measured\ tetracosane} , \quad (3.4)$$

where $\delta^{13}\text{C}_{measured}$ is the value reported from the IRMS, $\delta^{13}\text{C}_{measured\ tetracosane}$ is the value measured for the added tetracosane for each run of the sample, and $\delta^{13}\text{C}_{true\ tetracosane}$ is the known value of tetracosane, -31.548‰.

3.3 Results

3.3.1 Geochemical Analysis

Sulfate and methane concentrations for each sample were used to select cores for compound specific carbon isotope analysis (Coffin et al. 2011). Core PC09 was selected as a reference core due to its low methane concentration, less than 3.5×10^{-3} mM, for the depth of the core, and the SMTZ was beyond the length of the core collected, shown in Fig. 3.4. An additional factor in the selection of PC09 as a reference was that a collaborator on the MITAS Expedition measured the sulfate reduction rates, an important indicator of sulfate reduction coupled to anaerobic oxidation of methane, for sediment samples from both PC09 and PC13. Due to time and sample size constraints, the reported sulfate and methane concentrations are from a single measurement at each sediment depth.

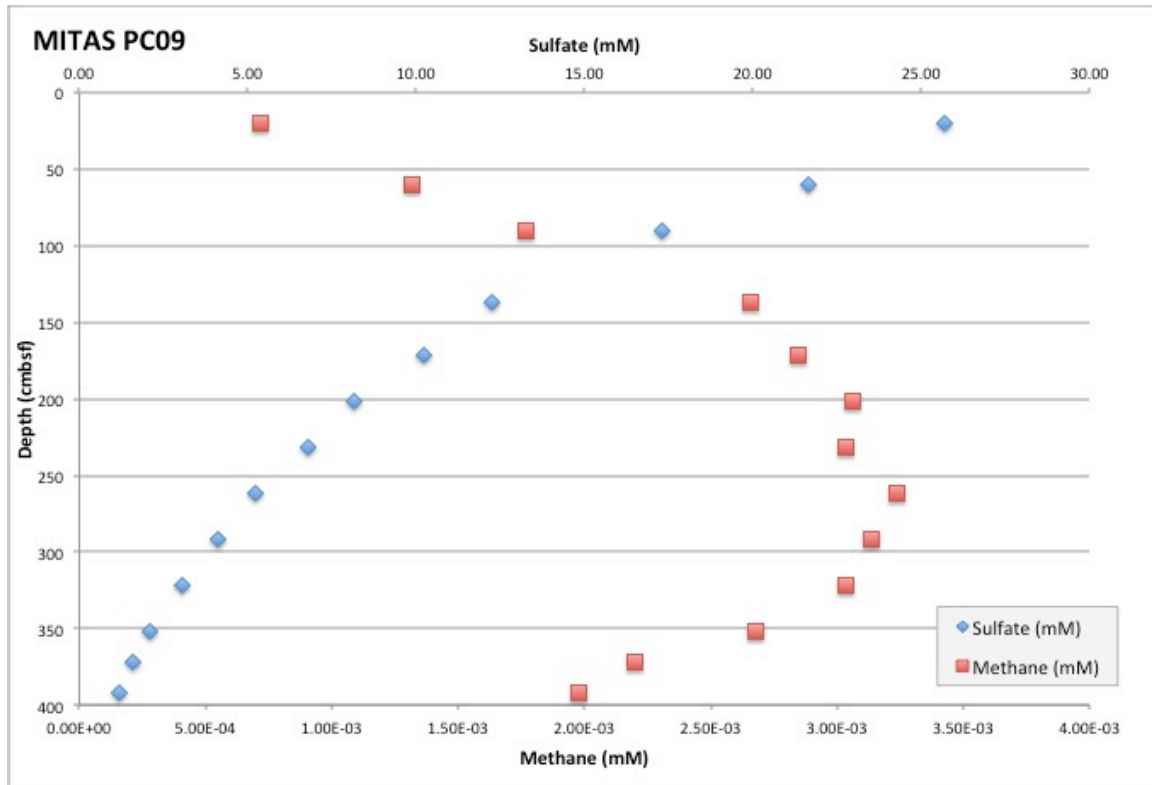


Figure 3. 4. PC09 Sulfate and methane concentrations plotted relative to sediment sampling depth in cmbsf (Coffin et al. 2011).

In PC13, sulfate concentrations were elevated at the sediment water interface (26.7 mM) and reduced to 0.5 mM at 110 cmbsf (centimeters below the seafloor). Concentrations just above the limit of detection were observed in the remainder of the core below the SMTZ. Methane concentrations were low at the top of the core and increased to approximately 10 mM at approximately 200 cmbsf. The concentrations stayed elevated at greater than 10 mM for the remainder of the core, 200 - 550 cmbsf. Based on the sulfate/methane concentration profiles shown in Fig. 3.5, both sulfate and methane approached a minimum concentration at approximately 110 cmbsf, the SMTZ.

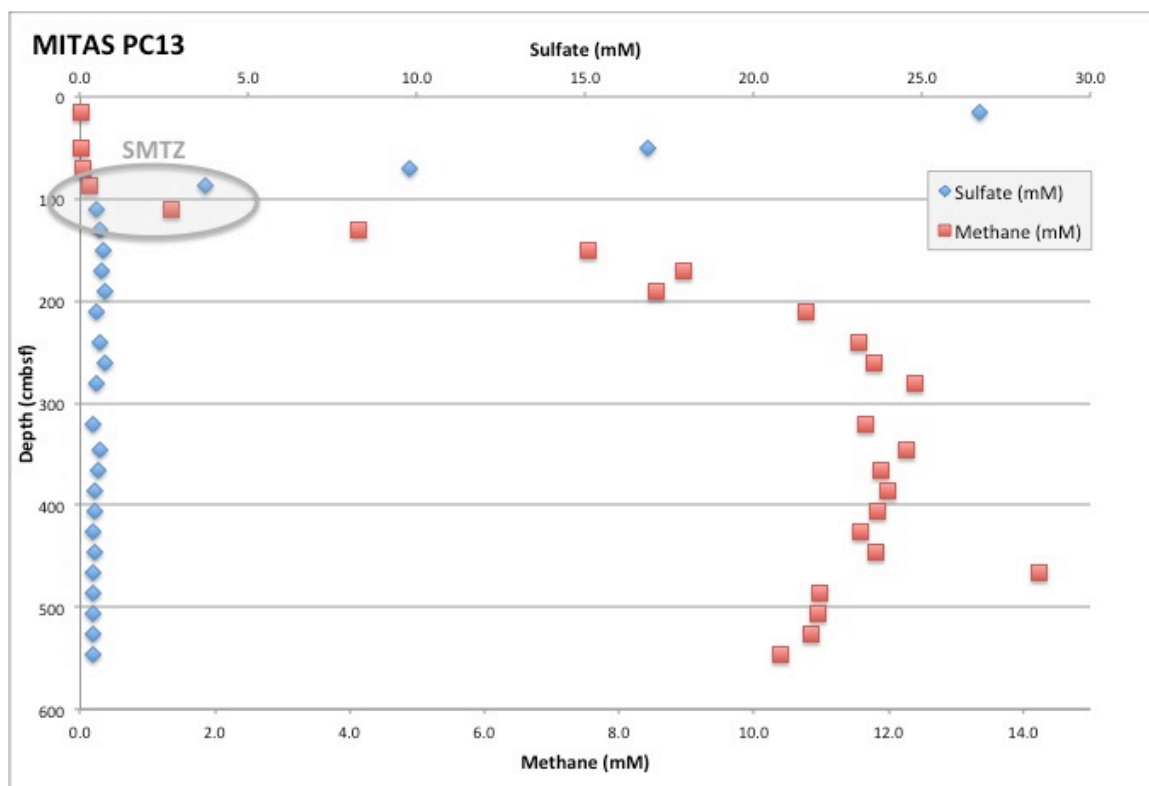


Figure 3. 5. PC13 sulfate and methane concentrations plotted relative the depth of the sediment sample (Coffin et al. 2011).

3.3.2 GC-FID Analysis for Abundance

The mass of the carbon obtained for each biomarker was calculated based on the peak areas from the GC-FID shown in Fig. 3.6 and the analysis of a $C_{17:0}$ standard ($20 \mu\text{g C mL}^{-1}$, peak area approximately 200), but the absolute abundances of the biomarkers are not well determined from the single trial on the GC-FID because the Agilent split/splitless injector has a high variability upon repeat injections (L. Xu, internal laboratory investigations at NOSAMS). Due to this uncertainty, the comparison for each sediment sample should be seen as a relative, not absolute abundance.

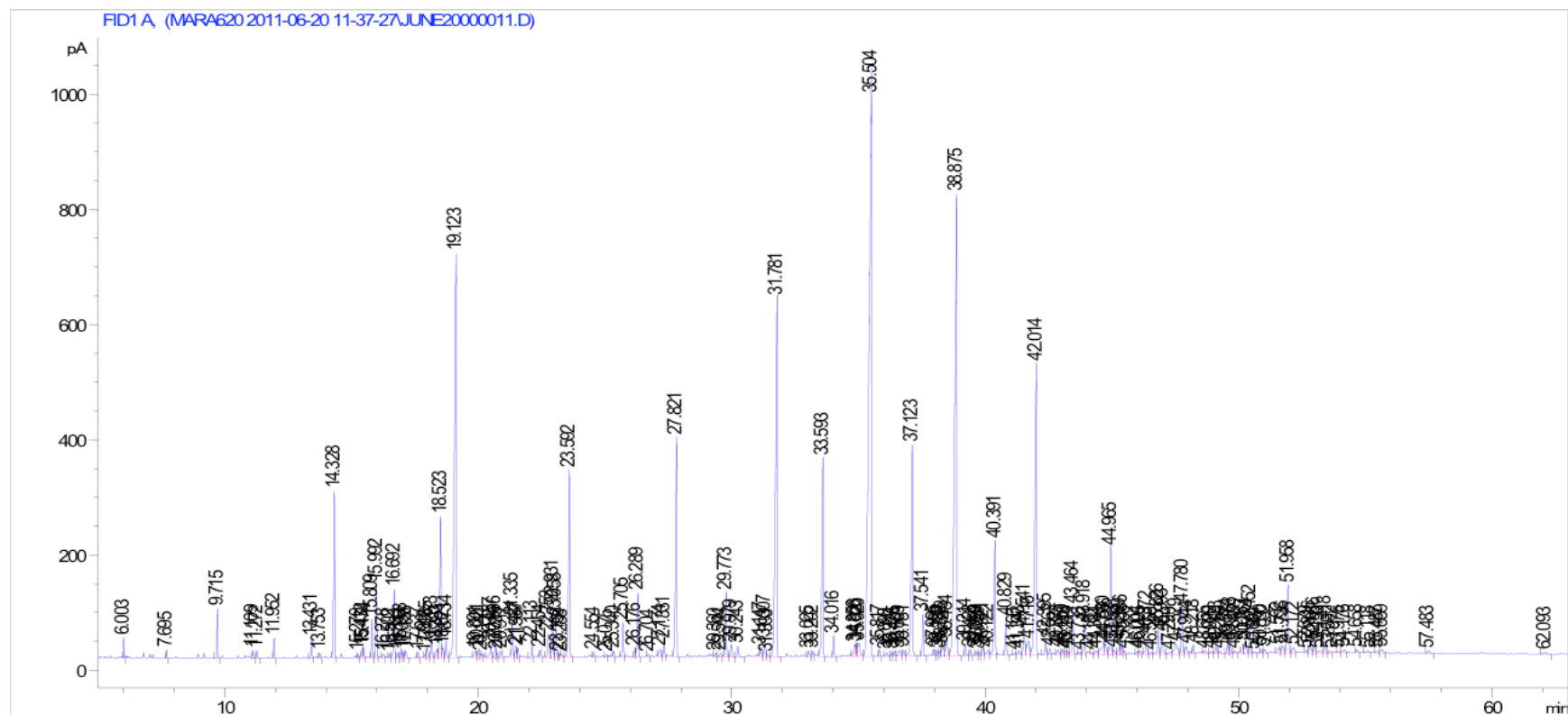


Figure 3. 6. Chromatogram from GC-FID analysis of PC09 sample 113. The x-axis is retention time in minutes and the y-axis is relative abundance.

The abundances of the i-C_{15:0}, ai-C_{15:0}, C_{16:1} (only the isomer with the greatest abundance), i-C_{17:0} and ai-C_{17:0} are shown in Fig. 3.7, normalized to weight of the dry sediment in grams (GDW). Sample 188 (546 cmbsf) from PC13 shows an extremely high relative abundance for C_{16:1} compared to the other four biomarkers and any other depth in both cores. A second representation with the C_{16:1} biomarker eliminated from the data set for each sample is included as Fig. 3.7B. With the exception of C_{16:1} from sample 188, none of the FAMES seem to be particularly abundant at any depth. In fact, the sample designated as the SMTZ (sample 208 from PC13) resulted in less abundance of the bacterial biomarkers compared to samples at both above and below the SMTZ. The C_{17:0} biomarkers are not confirmed as to which peak corresponds to the iso- versus the anteiso- configurations because both isomers were not present in the bacterial FAMES standard. The normalized abundance for the C_{17:0} FAMES is less than 0.1 ng C per GDW sediment with the majority of samples exhibiting abundances less than or nearly equal to 0.05 ng C per GDW sediment (Fig. 3.7B). The remaining C_{17:0} peaks are not shown in Fig. 3.7 because they resulted in small peak areas that were not integrated based on the data analysis parameters in the Agilent GC software.

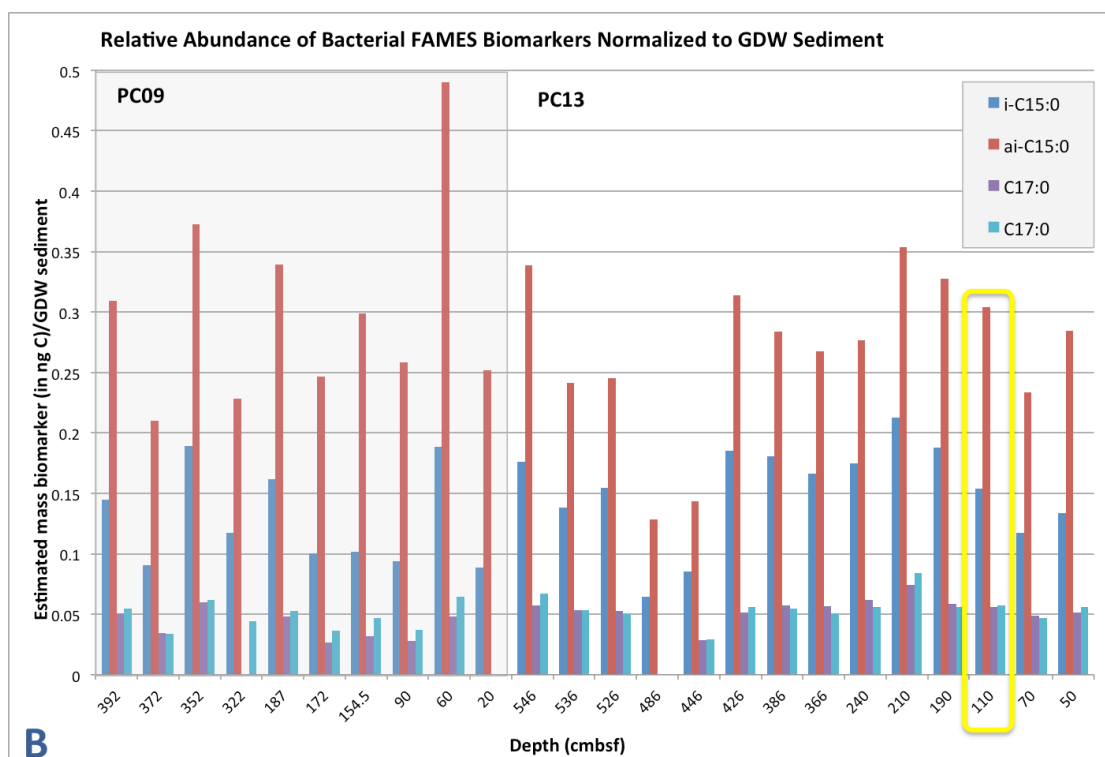
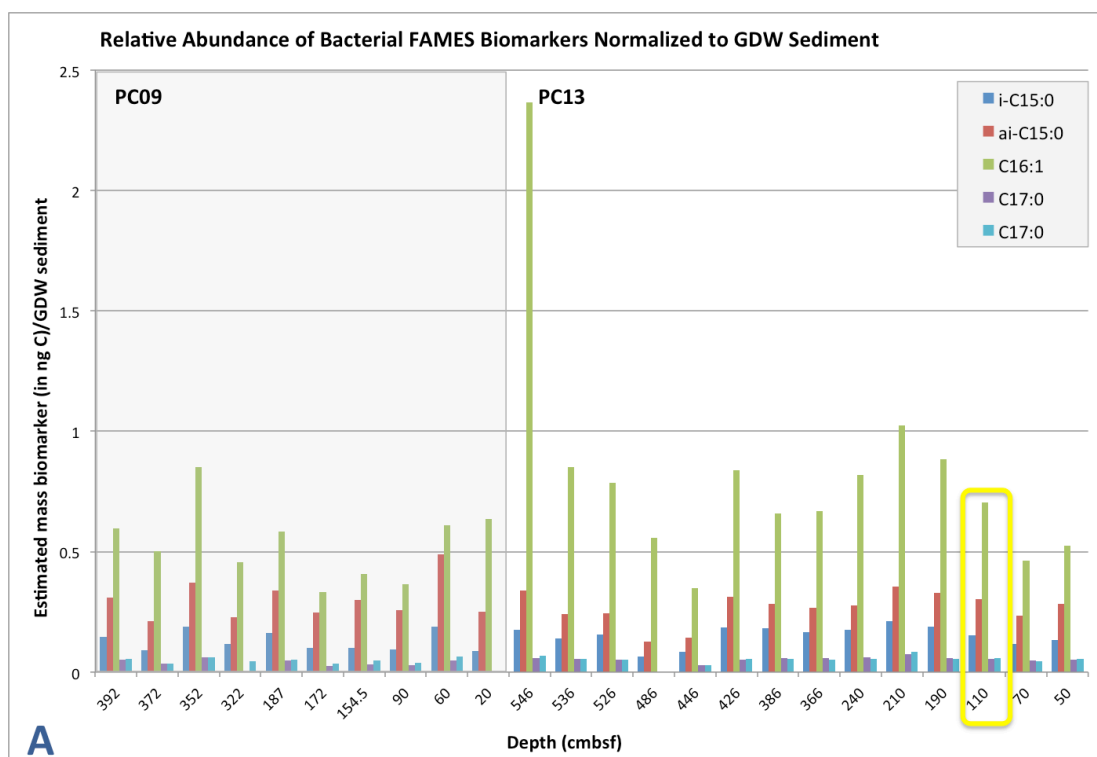


Figure 3. 7. Abundance of bacterial FAMES normalized to mass of dry sediment. The x-axis designates the depth of each sample. (A) shows the five biomarkers of interest, while (B) only shows iso- and anteiso- $C_{15:0}$ and iso- and anteiso- $C_{17:0}$. The yellow box indicates the sample from PC13 at the SMTZ, sample 208 at 110 cmbsf.

3.3.3 GC-IRMS Analysis for FAMES Identification and $\delta^{13}C$

In an attempt to identify other potential biomarkers associated with different bacterial species capable of sulfate reduction not targeted by the selected branched and unsaturated FAMES (Orcutt et al. 2005), stable carbon isotopes for the residual FAMES fraction were analyzed at NRL via GC-IRMS. For PC09, the aliquot of the FAMES fraction in hexane was analyzed and for PC13 the combined fractions from Trap 0 from the separation on the PCGC were analyzed and representative chromatograms are shown in Fig. 3.8 and 3.9. Samples from the two cores were processed differently due to the availability of the PCGC system at NOSAMS.

Definitive peak identification was made for C_{15:0} through C_{20:0} using the bacterial standard, while the remaining peaks were tentatively identified through the use of the GC-MS library, NIST05a.L. The results of these analyses are given in Tables 3.4 and 3.5, with the identified saturated FAMES designated by the length of the carbon chain and the remainder of the peaks given a “Peak ID” correlating to the order in which they eluted off the column. Those peaks without consistent identification from every depth in the core, based on retention time, are in italicized text and marked (*). Peaks that had a quality match of less than 70 (on a scale of 0 to 100) for the peak identification from the NIST05a.L database for all three trials of the triplicate analyses were eliminated from the data set. For PC13, the peak needed to appear in two of the three trials to be included in the data set. The same identification for multiple peaks near the abundant saturated FAMES, likely caused by the GC-MS integration parameters separately integrating a shoulder of the more abundant peak (e.g., in Table 3.5 C_{24:0} and Peak 29 both identified as tetracosanoic acid, methyl ester). The peaks resulting from different sediment depths

were correlated to one another based on retention time to further confirm the correct identification for each FAME. The compound identities were correlated to the $\delta^{13}\text{C}$ signatures using the bacterial FAMES standard based on retention times.

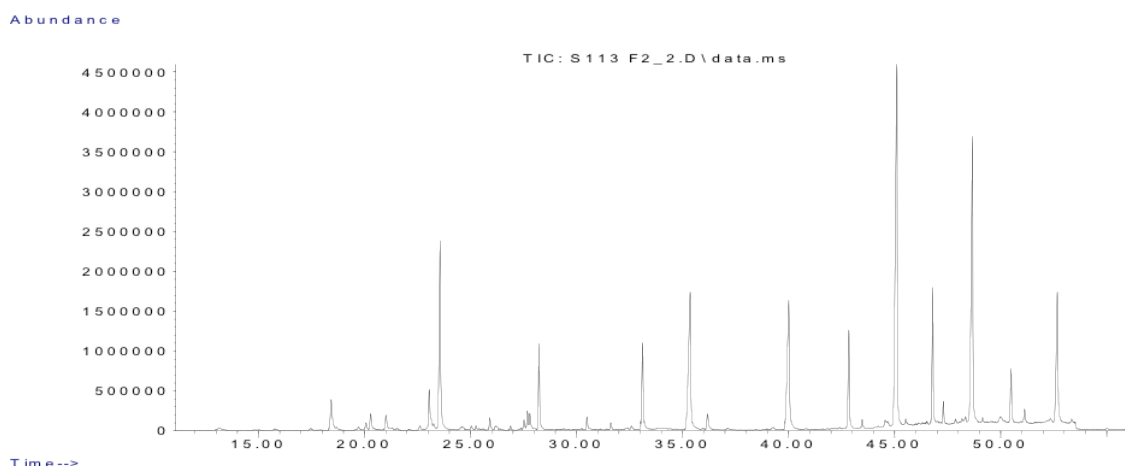


Figure 3. 8. Chromatogram from GC-MS for PC09 sample 113. The x-axis is retention time in minutes and the y-axis is relative abundance

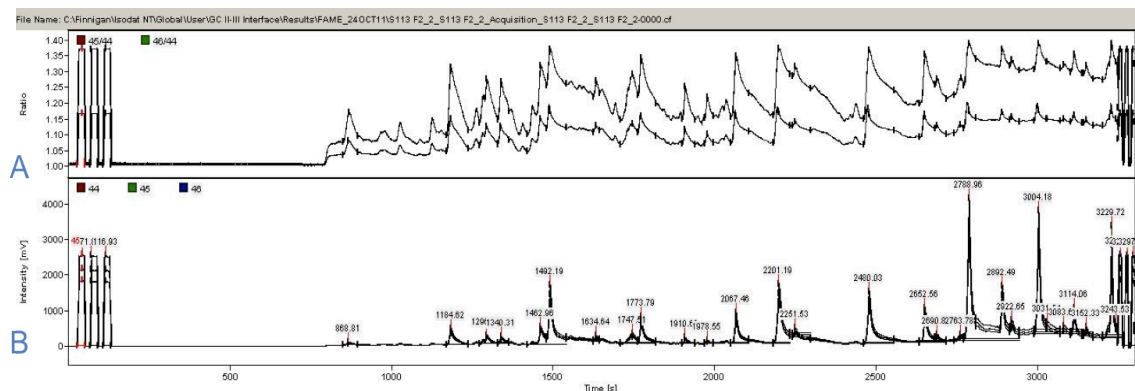


Figure 3. 9. Chromatogram for $\delta^{13}\text{C}$ analysis from the IRMS for PC09 sample 113. (A) shows the chromatogram as the ratio of $^{13}\text{C}/^{12}\text{C}$ and (B) shows the voltage in mV for the same sample.

A correction to account for the chromatographic conditions in the IRMS was applied for each run based on the resulting $\delta^{13}\text{C}$ for the internal standard, tetracosane, shown in Eq. 3.4. An additional $\delta^{13}\text{C}$ correction was applied to account for the methyl

group added to the fatty acid chain during the methylation step (Sec. 3.2.2). This applied correction is

$$\delta^{13}C_{FAME} = [(N + 1) \times \delta^{13}C_{measured} - \delta^{13}C_{MeOH}] / N, \quad (3.5)$$

where $\delta^{13}C_{measured}$ is the average value calculated from the corrected results obtained from the IRMS (after the tetracosane correction was applied), $\delta^{13}C_{MeOH}$ is the known isotopic composition ($\delta^{13}C_{MeOH} = -37.28\text{‰}$) and N is the number of carbon atoms in the fatty acid prior to methylation (Pearson 2000). The $\delta^{13}C$ values reported in Tables 3.4 and 3.5 are the average value for three triplicate analyses corrected for the methylation step and chromatographic conditions on the IRMS.

Table 3. 4. PC09 GC-IRMS analysis.

Peak ID	Compound Identification	111			112			113			114		
		Avg Retention Time (min)	Relative Abundance Normalized to C _{18:0}	δ ¹³ C	Avg Retention Time (min)	Relative Abundance Normalized to C _{18:0}	δ ¹³ C	Avg Retention Time (min)	Relative Abundance Normalized to C _{18:0}	δ ¹³ C	Avg Retention Time (min)	Relative Abundance Normalized to C _{18:0}	δ ¹³ C
1	Methyl tetradecanoate	18.430	0.570		18.417	0.549		18.421	0.594		18.414	0.554	
2	Methyl 9-methyltetradecanoate*	20.295	0.237		20.280	0.231		20.284	0.242				
C15:0	Pentadecanoic acid, methyl ester	21.017	0.198		21.004	0.185		21.008	0.226				
4	9-Hexadecenoic acid, methyl ester, (Z)-*	23.053	0.470		23.043	0.548		23.049	0.593	-26.840	23.038	0.542	
C16:0	Hexadecanoic acid, methyl ester	23.560	2.984	-26.859	23.542	2.832	-26.540	23.558	2.876	-26.135	23.518	2.919	-26.169
C17:0	Heptadecanoic acid, methyl ester	25.915	0.164		25.908	0.151		25.910	0.166				
7	Hexadecanoic acid, 3,7,11,15-tetramethyl-, methyl ester*							27.522	0.137				
8	9-Octadecenoic acid, methyl ester, (E)-*	27.681	0.198		27.674	0.209		27.675	0.227				
9	11-Octadecenoic acid, methyl ester*	27.805	0.207		27.794	0.221		27.795	0.222				
C18:0	Octadecanoic acid, methyl ester	28.234	1.000	-31.332	28.223	1.000	-28.705	28.229	1.000	-29.795	28.208	1.000	
C19:0	Nonadecanoic acid, methyl ester	30.495	0.135		30.488	0.126		30.488	0.138				
C20:0	Eicosanoic acid, methyl ester	33.118	1.330	-31.608	33.104	1.257	-30.251	33.116	1.329	-30.174	33.080	1.211	
Tetracosane	Tetracosane	35.441	6.924		35.400	6.305		35.360	3.371		35.397	14.554	
C21:0	Heneicosanoic acid, methyl ester	36.197	0.258	-35.817	36.183	0.256	-35.842	36.179	0.275				
C22:0	Docosanoic acid, methyl ester	39.996	2.879	-32.401	39.976	2.868	-31.436	40.003	3.027	-31.274	39.919	2.872	-33.725
C23:0	Tricosanoic acid, methyl ester	42.842	1.266	-33.698	42.832	1.317	-33.005	42.843	1.359	-32.832	42.804	1.470	-31.994
17	Heptacosane*	44.075	0.115		43.474	0.164		43.472	0.114				
C24:0	Tetracosanoic acid, methyl ester	45.100	7.019		45.080	6.916	-30.465	45.107	7.271	-29.205	45.031	7.993	
19	Pentacosanoic acid, methyl ester	46.805	1.606	-31.067	46.792	1.521	-31.321	46.802	1.557	-31.852	46.768	1.774	-32.337
20	Docosanedioic acid, dimethyl ester	47.306	0.214	-32.125	47.299	0.259		47.301	0.235	-28.111			
C26:0	Hexacosanoic acid, methyl ester	48.676	5.615	-30.491	48.650	4.898	-30.075	48.673	5.142	-29.819	48.605	5.651	-30.365
C27:0	Heptacosanoic acid, methyl ester*	50.503	0.842	-30.698	50.489	0.687	-34.637	50.493	0.716	-34.442	50.466	0.815	

Peak ID	Compound Identification	118.5			119			119.5			122		
		Avg Retention Time (min)	Relative Abundance Normalized to C _{18:0}	δ ¹³ C	Avg Retention Time (min)	Relative Abundance Normalized to C _{18:0}	δ ¹³ C	Avg Retention Time (min)	Relative Abundance Normalized to C _{18:0}	δ ¹³ C	Avg Retention Time (min)	Relative Abundance Normalized to C _{18:0}	δ ¹³ C
1	Methyl tetradecanoate	18.417	0.541		18.414	0.544		18.418	0.570		18.420	0.547	
2	Methyl 9-methyltetradecanoate*	20.280	0.268		20.275	0.331		20.283	0.387		20.281	0.423	
C15:0	Pentadecanoic acid, methyl ester	21.006	0.149										
4	9-Hexadecenoic acid, methyl ester, (Z)-*	23.042	0.519	-27.113	23.038	0.524		23.040	0.583		23.041	0.603	
C16:0	Hexadecanoic acid, methyl ester	23.547	2.901	-26.283	23.535	2.892	-27.116	23.537	3.186	-26.655	23.535	2.921	-26.684
C17:0	Heptadecanoic acid, methyl ester	25.904	0.159		25.903	0.169							
7	Hexadecanoic acid, 3,7,11,15-tetramethyl-, methyl ester*												
8	9-Octadecenoic acid, methyl ester, (E)-*	27.668	0.203		27.667	0.233		27.669	0.272		27.667	0.301	
9	11-Octadecenoic acid, methyl ester*	27.790	0.214		27.789	0.218		27.791	0.267		27.789	0.302	
C18:0	Octadecanoic acid, methyl ester	28.221	1.000	-30.821	28.216	1.000	-30.178	28.214	1.000	-29.584	28.214	1.000	-30.131
C19:0	Nonadecanoic acid, methyl ester	30.484	0.131		30.481	0.148		30.483	0.150				
C20:0	Eicosanoic acid, methyl ester	33.102	1.265	-29.837	33.091	1.205	-30.835	33.087	1.236	-30.623	33.085	1.184	-30.784
Tetracosane	Tetracosane	35.348	3.692		35.429	9.196		35.356	6.110		35.364	6.165	
C21:0	Heneicosanoic acid, methyl ester	36.165	0.253		36.178	0.281	-38.548	36.166	0.284		36.162	0.245	
C22:0	Docosanoic acid, methyl ester	39.968	2.679	-32.200	39.956	2.798	-31.023	39.944	2.823	-34.419	39.940	2.582	-33.830
C23:0	Tricosanoic acid, methyl ester	42.822	1.175	-32.882	42.819	1.390	-36.518	42.813	1.387	-33.252	42.809	1.225	-33.976
17	Heptacosane*				43.465	0.185		43.465	0.206				
C24:0	Tetracosanoic acid, methyl ester	45.074	6.128	-30.180	45.065	6.919	-31.518	45.058	7.184	-30.254	45.054	6.516	-31.425
19	Pentacosanoic acid, methyl ester	46.784	1.322	-32.183	46.780	1.562	-34.620	46.778	1.644	-32.412	46.776	1.450	-32.002
20	Docosanedioic acid, dimethyl ester	47.291	0.213		47.292	0.341	-31.120	47.290	0.384		47.285	0.180	
C26:0	Hexacosanoic acid, methyl ester	48.640	4.206	-30.567	48.632	4.780	-30.628	48.630	5.398	-31.152	48.624	4.795	-30.664
C27:0	Heptacosanoic acid, methyl ester*	50.477	0.594	-34.398	50.474	0.673	-32.246	50.472	0.778	-33.051	50.470	0.702	-34.258

Table 3. 5. PC13 GC-IRMS analysis. The C1, C2 and C3 designation are the identification codes assigned to each combination of sediment horizons (see Table 4.1).

Peak ID	Compound Identification	C1			C2			C3		
		Avg Retention Time (min)	Relative Abundance Normalized to C _{18:0}	$\delta^{13}\text{C}$	Avg Retention Time (min)	Relative Abundance Normalized to C _{18:0}	$\delta^{13}\text{C}$	Avg Retention Time (min)	Relative Abundance Normalized to C _{18:0}	$\delta^{13}\text{C}$
1	Methyl tetradecanoate	18.429	0.358	-24.836	18.506	0.363	-23.801	18.519	0.368	-24.763
2	Tridecanoic acid, 12-methyl-, methyl ester*				18.697	0.041		18.715	0.039	
3	Tridecanoic acid, 4,8,12-trimethyl-, methyl ester*				19.777	0.038		19.790	0.046	
C15:0	Pentadecanoic acid, methyl ester	21.007	0.169	-24.276	21.057	0.165	-23.378	21.074	0.160	-25.485
5	Pentadecanoic acid, 14-methyl-, methyl ester	22.594	0.037		22.638	0.043	-27.215	22.651	0.068	-26.647
C16:0	Hexadecanoic acid, methyl ester*	23.613	2.407	-26.679	23.684	2.041	-25.610	23.722	2.233	-26.257
7	Hexadecanoic acid, 14-methyl-, methyl ester	25.027	0.052	-24.815	25.052	0.047		25.069	0.072	-24.271
8	Hexadecanoic acid, 14-methyl-, methyl ester	25.242	0.033		25.268	0.032		25.286	0.053	
C17:0	Heptadecanoic acid, methyl ester	25.901	0.159	-21.465	25.931	0.139	-22.658	25.951	0.183	-24.936
10	Heptadecanoic acid, 16-methyl-, methyl ester*				27.382	0.029		27.393	0.044	
11	Hexadecanoic acid, 3,7,11,15-tetramethyl-, methyl ester	27.513	0.097		27.544	0.106		27.567	0.138	
12	9-Octadecenoic acid, methyl ester, (E)-	27.667	0.153	-25.431	27.702	0.198	-21.290	27.729	0.258	-24.223
13	9-Octadecenoic acid, methyl ester, (E)-*	27.791	0.182		27.815	0.157		27.839	0.211	
C18:0	Octadecanoic acid, methyl ester	28.258	1.000	-29.476	28.310	1.000	-27.441	28.332	1.000	-27.624
C19:0	Nonadecanoic acid, methyl ester	30.477	0.123	-28.494	30.497	0.120	-23.129	30.523	0.170	-25.757
16	5,8,11,14,17-Eicosapentaenoic acid, methyl ester, (all-Z)-*				31.617	0.067	-22.363	31.646	0.106	-23.660
17	11-Eicosenoic acid, methyl ester				32.589	0.039	-23.440	32.608	0.052	
C20:0	Eicosanoic acid, methyl ester	33.158	1.307	-30.323	33.199	0.988	-29.831	33.240	1.151	-29.920
Tetracosane	Tetracosane	35.488	3.266		35.466	1.541		35.652	2.868	
C21:0	Heneicosanoic acid, methyl ester	36.202	0.300	-31.347	36.220	0.223	-29.381	36.315	0.318	-29.854
21	Octadecanedioic acid, dimethyl ester	37.107	0.078	-18.057	37.123	0.052	-14.010	37.190	0.114	-25.626
22	13-Docosenoic acid, methyl ester, (Z)-*				39.248	0.052		39.276	0.069	
C22:0	Docosanoic acid, methyl ester	40.095	2.780	-31.381	40.153	1.966	-30.578	40.228	2.168	-30.678
C23:0	Tricosanoic acid, methyl ester	42.874	1.192	-32.722	42.905	0.840	-31.242	42.964	1.154	-32.747
25	Eicosanebioic acid, dimethyl ester*				43.479	0.105	-25.601	43.524	0.208	-29.523
26	15-Tetracosenoic acid, methyl ester	44.564	0.067	-26.672	44.582	0.170		44.597	0.091	
27	15-Tetracosenoic acid, methyl ester	44.627	0.038		44.678	0.068		44.644	0.112	
C24:0	Tetracosanoic acid, methyl ester	45.204	5.549	-29.810	45.243	3.737		45.317	4.310	
29	Tetracosanoic acid, methyl ester*	45.532	0.113		45.478	0.034		45.508	0.040	
30	Hencosanedioic acid, dimethyl ester*				45.552	0.101		45.593	0.090	
31	Pentacosanoic acid, methyl ester*				46.116	0.020		46.134	0.023	
C25:0	Pentacosanoic acid, methyl ester*	46.835	1.416	-27.536	46.857	0.963	-27.363	46.906	1.258	-29.305
33	Docosanedioic acid, dimethyl ester	47.298	0.211	-25.922	47.318	0.173	-26.456	47.382	0.428	-29.245
34	Hexacosanoic acid, methyl ester*	47.871	0.062		47.872	0.059		47.895	0.050	
35	2-Heptacosanone	48.338	0.117		48.352	0.099		48.359	0.091	
C26:0	Hexacosanoic acid, methyl ester	48.761	4.294	-28.621	48.798	2.836		48.864	3.278	-26.946
37	Hexacosanoic acid, methyl ester*	49.946	0.155	-28.874	49.993	0.122	-31.543	50.000	0.055	-30.754
C27:0	Heptacosanoic acid, methyl ester*	50.514	0.685	-29.379	50.538	0.462	-30.404	50.585	0.590	-30.845

The FAMES are grouped based on carbon chain length and even/odd carbon number. These designations are often used as markers to determine the origin of sedimentary material contributing to marine sediments. These common designations are reported in Table 3.6.

Table 3. 6. Origin of FAMES biomarkers.

Group	Compounds	Source
Short chain odd-numbered	C ₁₅ , C ₁₇ , C ₁₉	Bacteria
Short chain even-numbered	C ₁₄ , C ₁₆ , C ₁₈ , C ₂₀ *	Ubiquitous - Marine
Long chain even-numbered	C ₂₂ *, C ₂₄ , C ₂₆ , C ₂₈	Terrestrial - C3 Vascular Plants
Long chain odd-numbered	C ₂₁ , C ₂₃ , C ₂₅ , C ₂₇	Undetermined

Note the () indicate those compounds are not typically considered in discussions from those groupings of FAMES.*

Figures 3.10 and 3.11 have the abundance of each peak normalized to C_{18:0} from Tables 3.4 and 3.5, respectively, plotted as columns, with the $\delta^{13}\text{C}$ for each corresponding peak plotted on a secondary y-axis as circles. Each color represents a different sediment horizon and the labels on the x-axis correspond to the “Peak ID” from Tables 3.4 and 3.5. The error on the $\delta^{13}\text{C}$ values is the standard deviation from the average of triplicate measurements for each sample. The standard deviation for the relative abundance was also calculated, but not reported here.

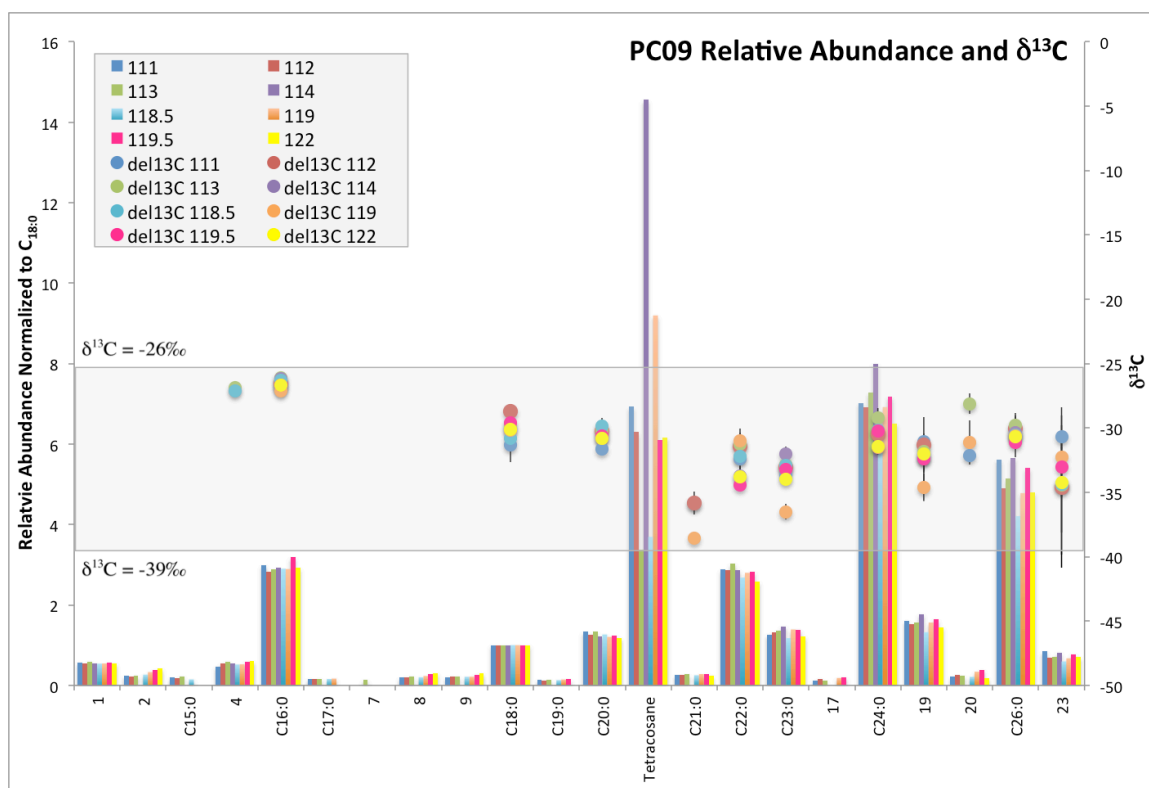


Figure 3. 10. Relative abundance normalized to $C_{18:0}$ (left axis) and $\delta^{13}C$ (right axis) for FAMES from PC09. The relative abundance normalized to $C_{18:0}$, is plotted as columns on the primary y-axis and the $\delta^{13}C$ value as circles on the secondary y-axis. Each sample depth is presented as a different color. The error on each $\delta^{13}C$ value is the standard deviation for the average of three triplicate analyses.

In general, the abundance of the even-numbered carbon chains is greater than odd-numbered carbon chains (Fig. 3.10). In PC09, there was not a sufficient signal from many of the samples to measure the $\delta^{13}C$ because the samples were analyzed as individual sediment depths, not combinations of adjacent horizons, and less than 25% of the peaks were eliminated from the data set based on the established quality match criteria. No results are available for any of the odd-numbered short chain FAMES (SC-FAMES $C_{15:0}$, $C_{17:0}$ and $C_{19:0}$) in PC09. The $\delta^{13}C$ values for the measurable individual FAMES ranged from -38.49 to -26.79‰, with the most ^{13}C -enriched contributions from the even-numbered SC-FAMES ($C_{16:0}$ and $C_{18:0}$). These tend to be the most ubiquitous of

the FAMES in marine sediments (Volkman et al. 1998). In general, long chain FAMES (LC-FAMES, carbon chain greater than 20 carbon atoms) at all depths are more ^{13}C -depleted than -30‰ in PC09, with the exception of individual FAMES from sample 113 ($\text{C}_{24:0}$, $\text{C}_{26:0}$, and peak 20 identified as docosanedioic acid, dimethyl ester).

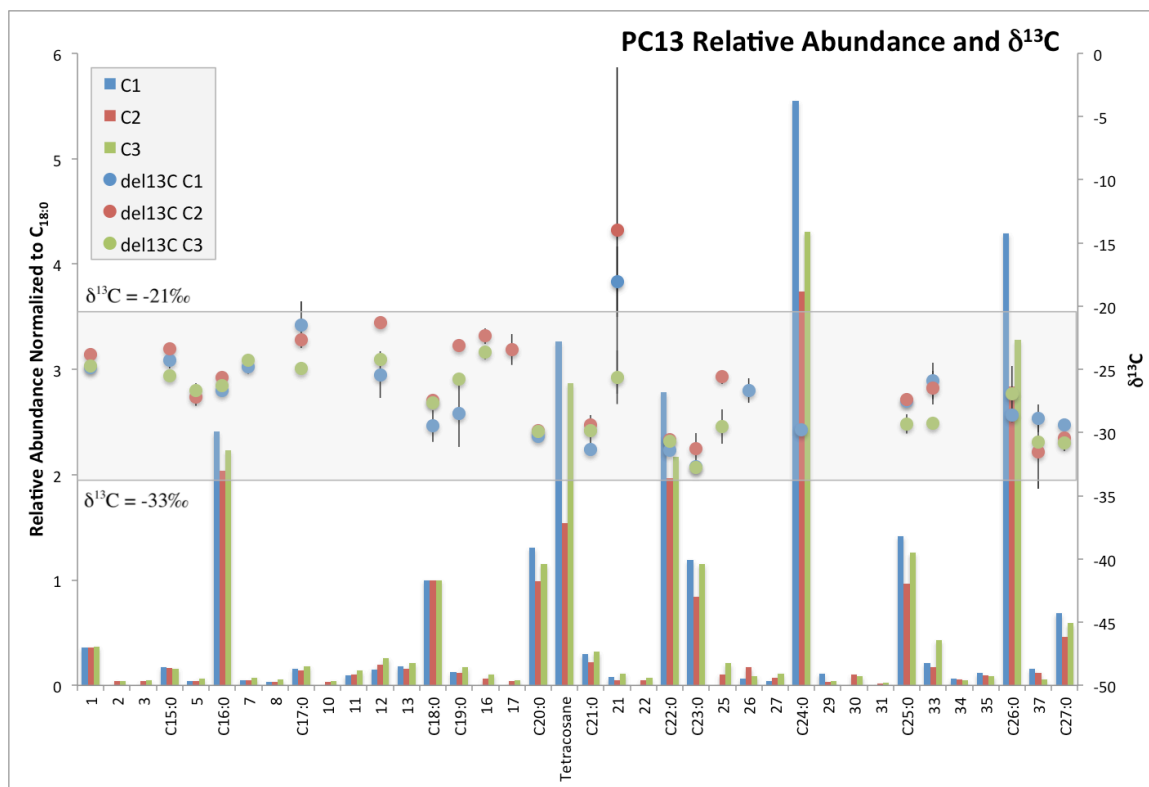


Figure 3. 11. Relative abundance normalized to $\text{C}_{18:0}$ (left axis) and $\delta^{13}\text{C}$ (right axis) for FAMES from PC13. The relative abundance normalized to $\text{C}_{18:0}$, is plotted as columns on the primary y-axis and the $\delta^{13}\text{C}$ value as circles on the secondary y-axis. Each sample depth is presented as a different color. The error on each $\delta^{13}\text{C}$ value is the standard deviation for the average of three triplicate analyses.

The results from GC-IRMS analysis for PC13 resulted in a significantly larger number of peaks compared to PC09 in addition to the saturated FAMES. The samples from adjacent depths in PC13 were combined together and run on the PCGC prior to analysis via GC-IRMS. The increased sample concentration resulted in more complex spectra. Represented in Fig. 3.11 are only the peaks common in two out of the three

sample depths from the GC-MS run when the retention times for the three samples were correlated. Previously eliminated from each sample data set were any peaks that did not have a library quality match greater than 70% for at least one of the three trials, eliminating close to 50% of the peaks from PC13. All the eliminated peaks had low peak areas and the majority did not have enough signal for an isotope ratio measurement (voltage less than 250 mV), but the full data set is shown in Appendix 5 and 6. Two of the FAMES ($C_{24:0}$ and $C_{26:0}$) from two trials oversaturated the detector (voltages greater than 10,000 mV) when analyzed on the IRMS portion of the instrument and therefore the $\delta^{13}C$ signature for these peaks could not be ascertained.

Overall, FAME compounds from PC13 are more ^{13}C -enriched (-33 to -21‰) than the analyzed FAMES from PC09 (-39 to -26‰). In PC13, the SC-FAMES are more ^{13}C -enriched than the LC-FAMES, similar to PC09. More variability in the $\delta^{13}C$ values for PC13 made it difficult to identify trends in isotopic composition and carbon chain type for pinpointing biomarker contributions. To assess groups of compounds with potential for origin identification, the FAMES were binned according to chain length (short or long) and number of carbon atoms in the chain (odd versus even). The average $\delta^{13}C$ value for each group of FAMES is plotted relative to sediment depth for PC13 in Fig. 3.12, with the error bars representing the standard deviation on this calculated average.

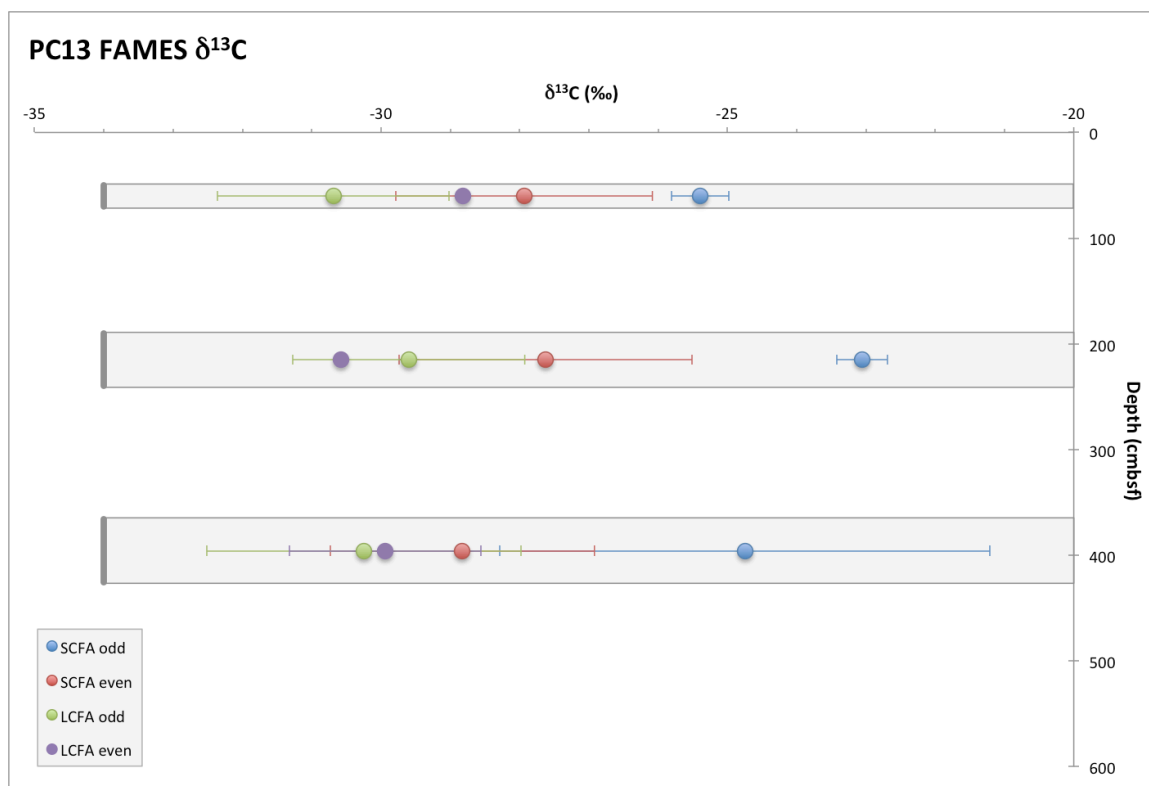


Figure 3. 12. $\delta^{13}\text{C}$ plotted relative to sediment depth for the FAMES grouped by chain length and even or odd numbered identification for PC13. Short chain FAMES are designated "SCFA" and long chain FAMES are designated "LCFA". The error bars on the values are the standard deviations of the calculated average for each biomarker group and the depth span is shown as a gray box for each sample.

In regards to the correlation to depth, none of the groups differ from among the three individual depths by more than 2.5‰, with SC-FAMES being the most variable with depth. The odd-numbered SC-FAMES are the most ^{13}C -enriched of all the classes of FAMES.

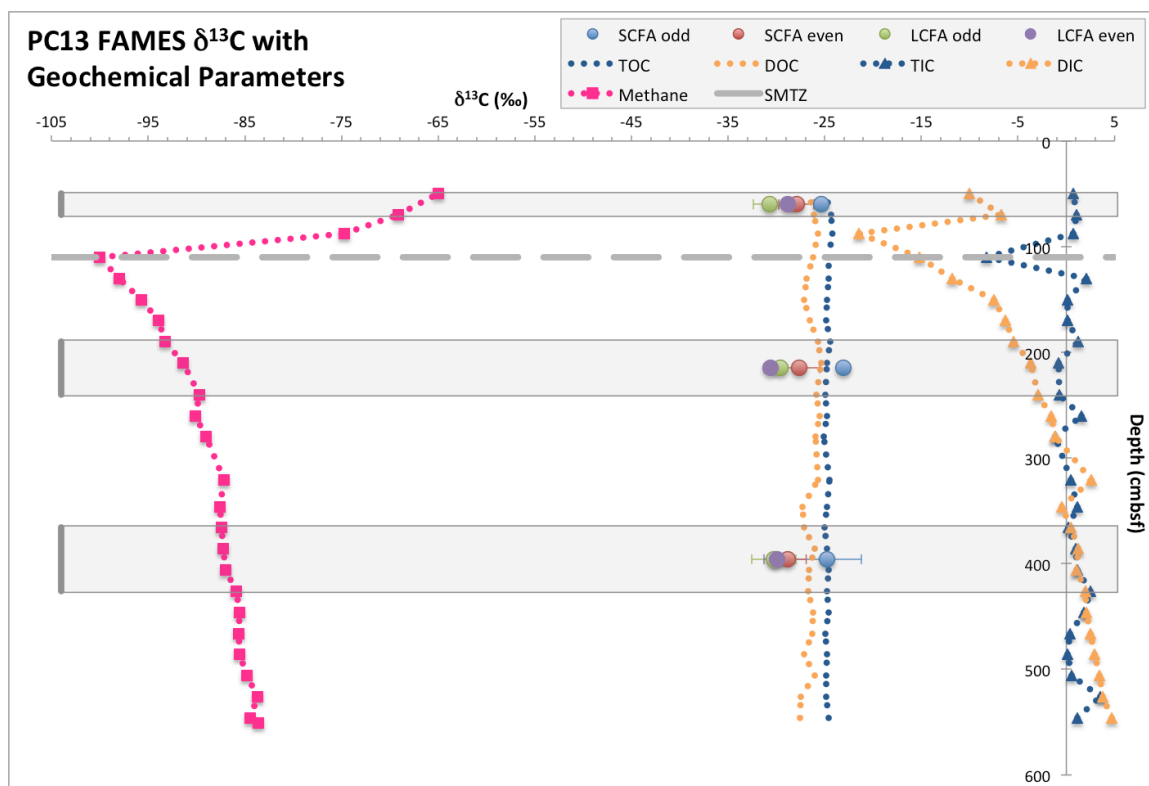


Figure 3. 13. $\delta^{13}\text{C}$ plotted relative to sediment depth for the FAMES grouped by chain length and even or odd numbered identification. Short chain FAMES are designated “SCFA” and long chain FAMES are designated “LCFA”. Included are the $\delta^{13}\text{C}$ values for other geochemical parameters: TOC, DOC, TIC, DIC, and methane (plotted with dashed lines). The geochemical parameters are plotted for the individual sample depths, while the biomarker groups are the combined samples covering the span of depth in the gray box. The error bars are the standard deviations of the calculated average for each biomarker group.

The geochemical parameters analyzed for $\delta^{13}\text{C}$ as part of the MITAS Expedition: DIC, TIC, DOC, DIC and methane (see Table 3.1), are plotted relative to the depth of sample. In Fig. 3.13, each of the geochemical parameters was measured twice (sample volume permitting) and standards were run every tenth sample to ensure the error was low, but are not reported here. The $\delta^{13}\text{C}$ for methane from PC13 ranged from -100.0‰ to -74.6‰ at the proposed SMTZ and below, respectively (Fig. 3.13) (Coffin et al. 2011). Methane $\delta^{13}\text{C}$ values near the top of the core ($\delta^{13}\text{C} \sim -67.1\text{‰}$) are likely reflective of atmospheric methane contributions. The $\delta^{13}\text{C}$ signature of the methane and the lack of

longer chain hydrocarbons is characteristic of a biogenic methane source. Both inorganic carbon parameters (DIC and TIC) show methane contributions to the inorganic carbon pool, with all three data sets exhibiting a $\delta^{13}\text{C}$ -depleted signature at the SMTZ. None of the groups of FAMES exhibit this depletion at the SMTZ, but rather maintain a relatively consistent $\delta^{13}\text{C}$ isotopic signature with depth, similar to the organic carbon pools, DOC and TOC. Both classifications of LC-FAMES are more ^{13}C -depleted than the SC-FAMES.

Chapter 4: Stable Carbon and Radiocarbon Isotope Analysis of Bacterial Fatty Acid Methyl Esters (FAMES)

4.1 Introduction

In addition to stable carbon isotope analysis for individual compounds from the entire fatty acid methyl esters (FAMES) fraction (Chap. 3), select compounds identified as biomarkers for sulfate reducing bacteria (SRB) associated with anaerobic methanotrophy in marine sediments were analyzed. These target compounds were isolated from the FAMES fraction and concentrated using a chromatographic technique known as preparative capillary gas chromatography. These biomarkers were separated from the FAMES fraction for both radiocarbon and stable carbon isotope analysis, while the remainder of the FAMES remained intact for analysis via GC-IRMS (Chap. 3).

4.2 Separation and Collection via Preparative Capillary Gas Chromatography (PCGC)

Sediment samples from adjacent horizons were combined prior to preparative capillary gas chromatography (PCGC). The integration of various samples was guided by observations of the SMTZ depth. In PC13, the FAMES fraction at the SMTZ was left as a single sample while FAMES extracted from depths above, below and two meters below the SMTZ were combined (Fig. 3.5). Without a defined SMTZ for the depth of the core, PC09 samples were combined to target depths in the core in relation to the SMTZ from PC13 (Fig. 3.4). The reason for combining adjacent fractions was twofold.

First, this was done to maximize the amount of carbon isolated for each sample to ensure there was more than 25 μg of carbon ($\mu\text{g C}$) present in the sample for a standard small sample radiocarbon measurement with a $\delta^{13}\text{C}$ split analyzed on a separate mass spectrometer. Secondly, to limit the number of radiocarbon measurements for both time and cost considerations in accordance with the National Ocean Sciences Accelerator Mass Spectrometer (NOSAMS) Graduate Student Internship, which funded the preparation and analysis of these samples.

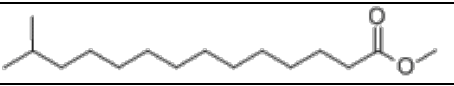
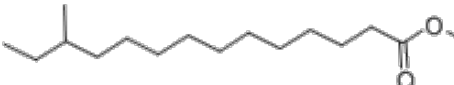
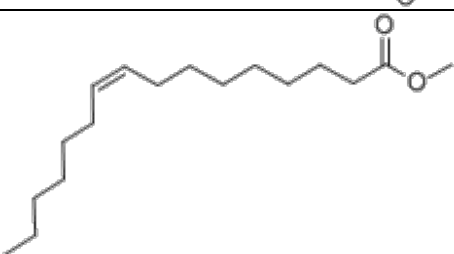
The combined samples are listed in Table 4.1 with the depth reported as the midpoint in the span of the sample depths. The samples analyzed on the GC-FID (see Chap. 3 for the sample preparation up to this point) were combined (as shown in Table 4.1) by transferring each individual sample (approximately 1 mL) from the 2-mL GC vial to a common 4-mL vial previously baked (at 450 °C for 6 hours) and rinsed with hexane using a baked Pasteur pipette. Each GC vial was washed three times with hexane and the washes were transferred to the common 4-mL vial. This new combined sample was dried under a stream of ultra-high purity nitrogen gas (UHP N_2) to reduce the volume, then transferred to a 250- μL GC vial insert for separation and collection on the PCGC.

Table 4. 1. Samples combined for radiocarbon analysis.

Core	Sample ID	Sample Number	Depth (cmbsf)
PC09	C7	111, 112, 113, 114	357
	C6	118.5, 119, 119.5	170.75
	S121	121	90
	C5	122, 123	40
PC13	C4	188, 188.5, 189, 191	516
	C1	194, 196, 197	396
	C2	202, 203, 204	215
	S208	208	110
	C3	210, 211	60

Target compounds were selected based on available literature identifying bacterial biomarkers and identified through the use of a standard, Matreya LLC - Bacterial acid methyl esters CP mix (see Appendix 4), on both the GC-FID and PCGC. Bacterial FAMES (i-C_{15:0}, ai-C_{15:0}, and C_{16:1}, see Table 4.2) were selected as biomarkers for collection via PCGC (Zhang et al. 2002; Elvert et al. 2003; Londry, Jahnke, and Des Marais 2004; Wegener et al. 2008; Aquilina et al. 2010). Other branched FAMES (i-C_{17:0} and ai-C_{17:0}) thought to be representative of SRB (Zhang et al. 2002; Aquilina et al. 2010) were tentatively identified using the bacterial standard, but not collected with the PCGC because peak areas were typically tens times less than those of C_{16:1} from the GC-FID and were often times indistinguishable from the baseline on a test run of each sample on the PCGC.

Table 4. 2. Designation, name and structure of isolated bacterial FAMES.

Designation	Name	Structure
iso-C _{15:0}	Methyl 13-methyltetradecanoate	
anteiso-C _{15:0}	Methyl 12-methyltetradecanoate	
C _{16:1}	Methyl cis-9-hexadecenoate* *Note this is just one example with a specified location of the double bond	

Note: All images taken from Chemical Book <http://www.chemicalbook.com>

The PCGC system at NOSAMS is shown in Fig. 4.1. The system consists of an Agilent 6890 GC with a flame ionization detector (FID) equipped with a Hewlett Packard 7683 Series Injector. The GC is integrated with a Gerstel cooled injection system (CIS), a zero-dead-volume effluent splitter, and a cryogenic preparative fraction collector (PFC

shown in Fig. 4.1B). The PFC has six u-shaped sample collection traps and one waste trap to collect the remaining effluent (Fig. 4.1C). The trap switching times are 0.01 minutes to allow for the collection of a single compound when the compounds elute off the column in rapid succession. The PFC is heated to ensure sample material flows to the trap and is not retained in the PFC.

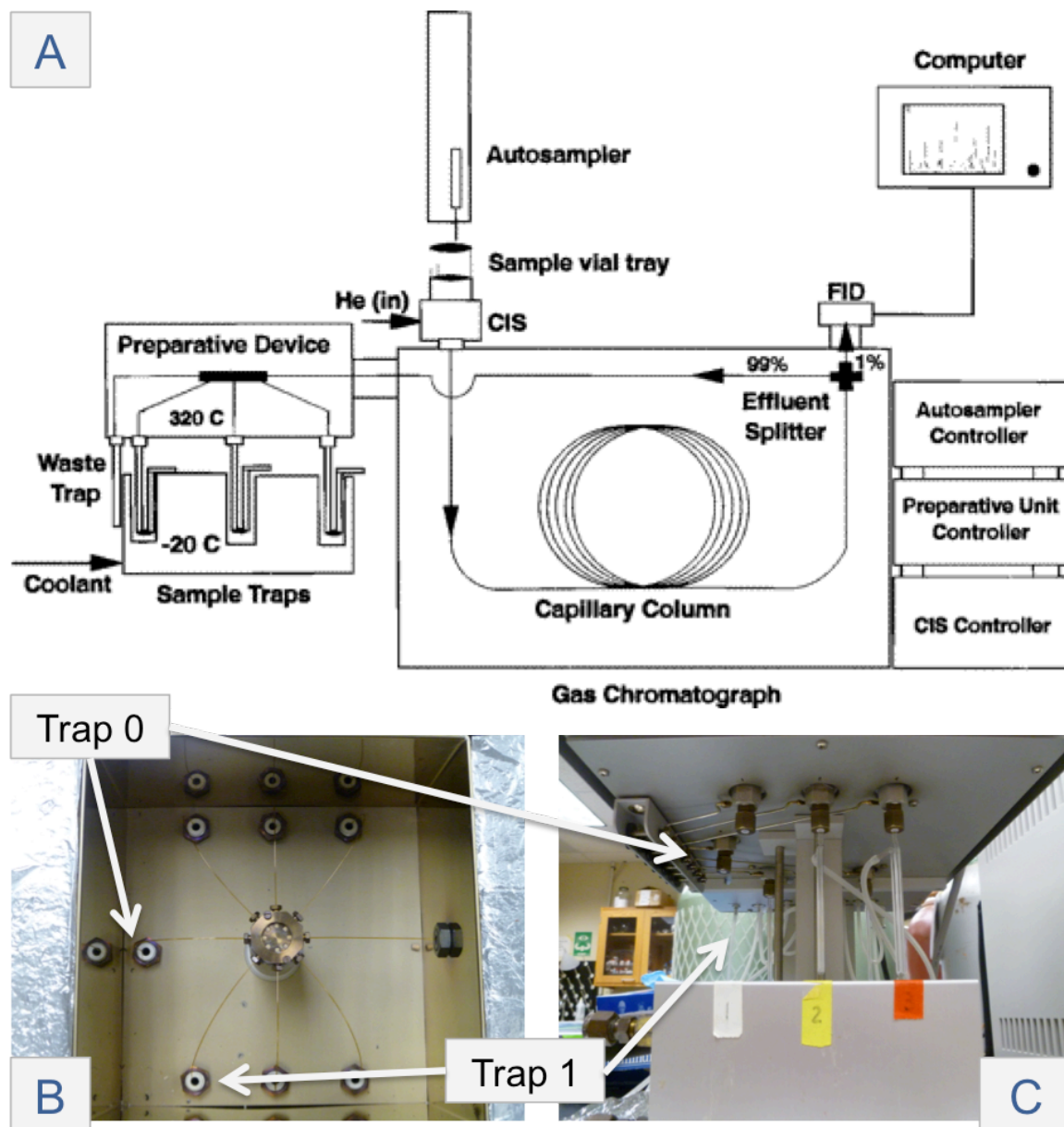


Figure 4. 1. (A) is a schematic of the PCGC system. (B) is the 8-port PFC with 6 sample traps and one waste trap. (C) is the u-shaped traps for collecting the individual FAMES.

The PFC was set to collect all three bacterial biomarkers in a single trap (Trap 1), in an effort to collect greater than 25 $\mu\text{g C}$ for radiocarbon analysis. A test run of each individual sample was analyzed on the PCGC to select windows for trapping the target compounds. These trapping windows were monitored and adjusted as necessary to accommodate any drift over repeat injections. The concentration of the sample and the number of injections was not standardized in an effort to collect all i-C_{15:0}, ai-C_{15:0}, and C_{16:1} present from a single sediment interval. Additionally, the waste trap from the sample injector was replaced with a clean and combusted 4-mL sample vial for each sample and rinsed with hexane and transferred back to the GC vial for continued injections on the PCGC as a means to maximize the amount of carbon collected.

The analyte was injected into the CIS of the PCGC equipped with a 30-m x 0.53-mm x 1- μm DB-Waxetr column at a rate of 9.0 mL min⁻¹. The initial oven temperature was held at 50 °C for 2 minutes followed by a 20 °C min⁻¹ ramp to a temperature of 110 °C, then a second ramp of 4 °C min⁻¹ to 220 °C. The temperature of the oven was increased again to 320 °C at a rate of 20 °C min⁻¹ and held for 9 minutes. Injection volumes varied from 1 to 4 μL with a total of 40 to 100 injections per sample. Once the entire sample was collected, Trap 1 was removed from the PFC and the contents of the u-shaped trap were transferred to a backed, pre-weighted vial rinsing with 200-300 μL hexane five times. The total volume of the sample collected was determined by measuring the mass of the liquid collected from the five washes and the known density of hexane (0.6548 g mL⁻¹). A 50- μL aliquot from Trap 1 was transferred to a GC insert and analyzed on the GC-FID to confirm the collection of i-C_{15:0}, ai-C_{15:0}, and C_{16:1}, then the contents of the GC insert were transferred back to the 4-mL sample vial. Trap 0 was

rinsed into a second 4-mL vial using dichloromethane (DCM) or hexane and retained for analysis on the GC-IRMS at NRL (as discussed in Chap. 3).

The column bleed (breakdown of the stationary phase in the GC column) was removed from the sample with column chromatography collecting three fractions, with the biomarkers retained in Fraction 2. The column was washed with hexane and the contents of Trap 1 were transferred to the column, washing the sample with 1.5 mL 1:1 DCM:pentane. Fraction 2 was collected with 4.5 mL 1:1 DCM:pentane and Fraction 3 was eluted from the column with DCM. Fraction 1 and Fraction 3 were analyzed on the GC-FID to confirm none of the desired biomarkers were washed into one of those fractions. Some of the solvent was removed under a stream of UHP N₂ and the sample was transferred to a baked quartz tube. The solvent was completely evaporated and copper oxide, as well as silver was added to the quartz tube. The sample was evacuated on the graphitization apparatus at NOSAMS, sealed with an acetylene torch, and combusted at a high temperature to convert the sample to carbon dioxide gas (Eglinton et al. 1996). Graphitization preparation for samples, blanks and standards containing less than 100 µg C is described in references Pearson et al. 1998 and Gagnon et al. 2000. Samples were analyzed at NOSAMS according to the standard protocols in operation there (please refer to the NOSAMS website <http://www.whoi.edu/nosams/page.do?pid=40146> and the “NOSAMS General Statement of ¹⁴C Procedures” for details on this analysis).

4.3 Results

4.3.1 PCGC Isolation and Sample Collection

A representative chromatogram at each step of analysis is shown for PC09 sample 121. Figure 4.2 shows the full chromatogram obtained on the GC-FID of the FAMES fraction (system conditions described in Chap. 3). The bacterial biomarkers of interest are marked on the figure, identified through the use of the bacterial standard under the same chromatographic conditions. Sample 121 was next analyzed on the PCGC. Because this sediment horizon was selected to correlate to the SMTZ in PC13, this sample was not combined with any other horizons resulting in the full chromatogram shown in Fig. 4.3A and a close up of the region corresponding to the target biomarkers shown in Fig. 4.3B. Following separation, isolation and concentration on the PCGC, the collected sample was analyzed on the GC-FID to confirm the collection of the target biomarkers as shown in Fig. 4.4. The non-integrated peaks before and after the C_{16:1} are likely other C_{16:1} isomers with a different location of the double bond that did not resolve as individual peaks on the PCGC, but rather appeared as shoulders of the main peak (see Fig. 4.3B at a retention time of approximately 34.2 minutes).

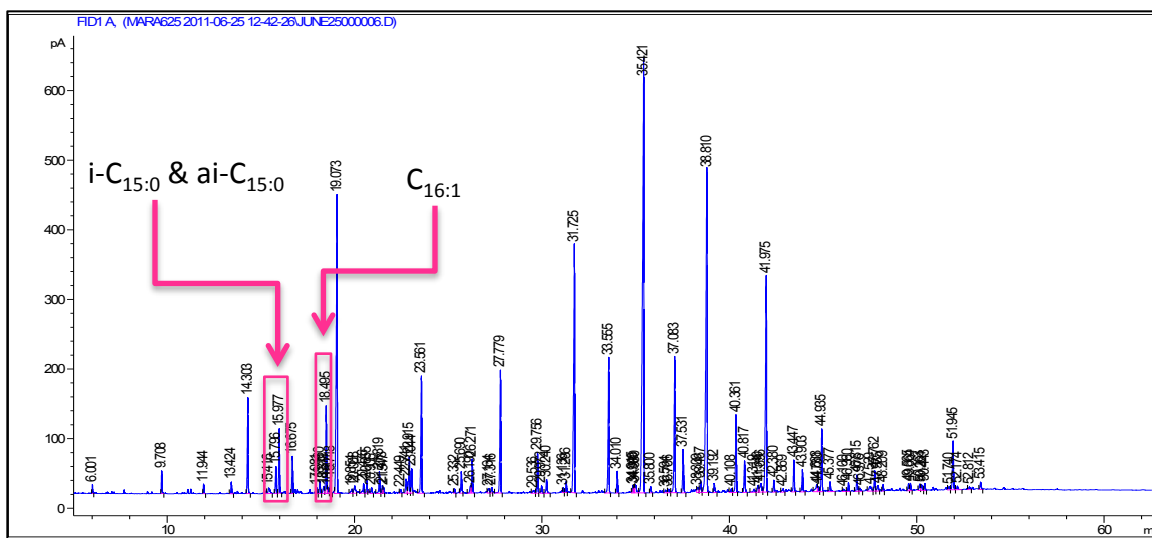


Figure 4. 2. GC-FID Chromatogram of PC09 sample 121 with the bacterial FAMES highlighted.

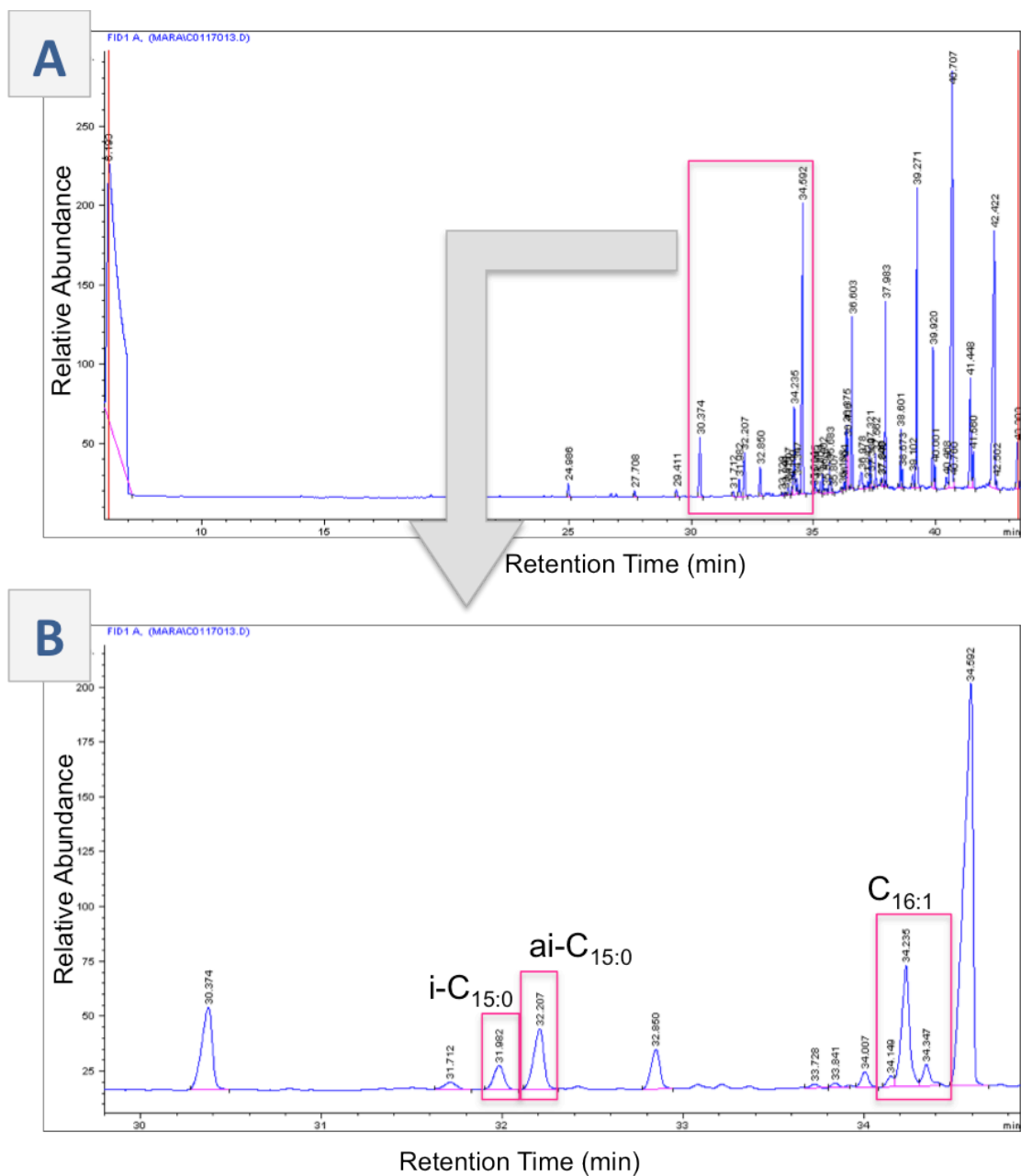


Figure 4. 3. (A) PCGC Chromatogram of PC09 sample 121 with the region for the bacterial FAMES boxed. (B) Boxed area from the top figure is enlarged and the bacterial FAMES are highlighted.

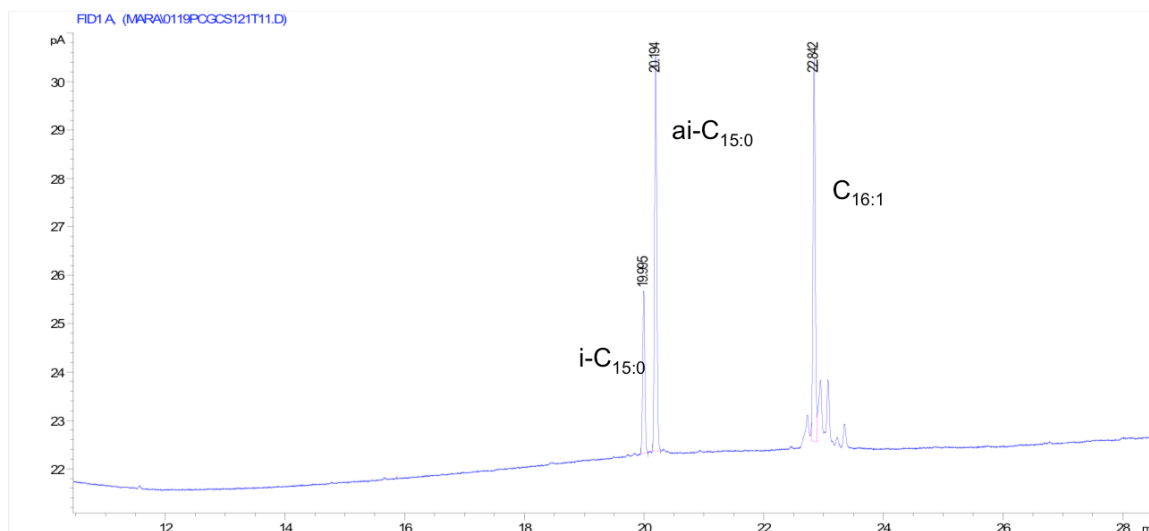


Figure 4. 4. Post PCGC confirmation on the GC-FID.

4.3.2 Estimation of Sample Collected

The amount of carbon collected for analysis via AMS was estimated based on the peak areas observed in chromatograms from the two different GC systems, PCGC and GC-FID, and the analysis of a quantification standard on each system. From the PCGC, the amount of carbon collected for each individual FAME was determined as the sum of all the peak areas from each run on the PCGC (between 40 and 100 runs). This total peak area for each biomarker was useful in the determination of the contribution each compound made to the sample analyzed by AMS, and estimating the amount of carbon that should be isolated if the trapping efficiency was 100%. On the GC-FID, the peak areas from a single injection and the total volume of the sample collected from the u-shaped trap were used to estimate the amount of carbon collected for combustion to CO₂ and analysis via AMS.

For PC09, a standard prepared from four FAMES (C_{15:0}, C_{16:0}, C_{17:0}, and C_{20:0}, referred to as “FAMES Mix Standard”) with known concentration and volume was analyzed on the PCGC, shown in Fig. 4.5. A second less concentrated FAMES Mix

Standard comprised of the same compounds was prepared and analyzed on the GC-FID (following methods described in Section 3.2.1) is shown in Fig. 4.6, to quantify the amount of carbon collected from the u-shaped trap since the efficiency of trapping and recovery is not 100%, but reported to be greater than 80% (Eglinton et al. 1996).

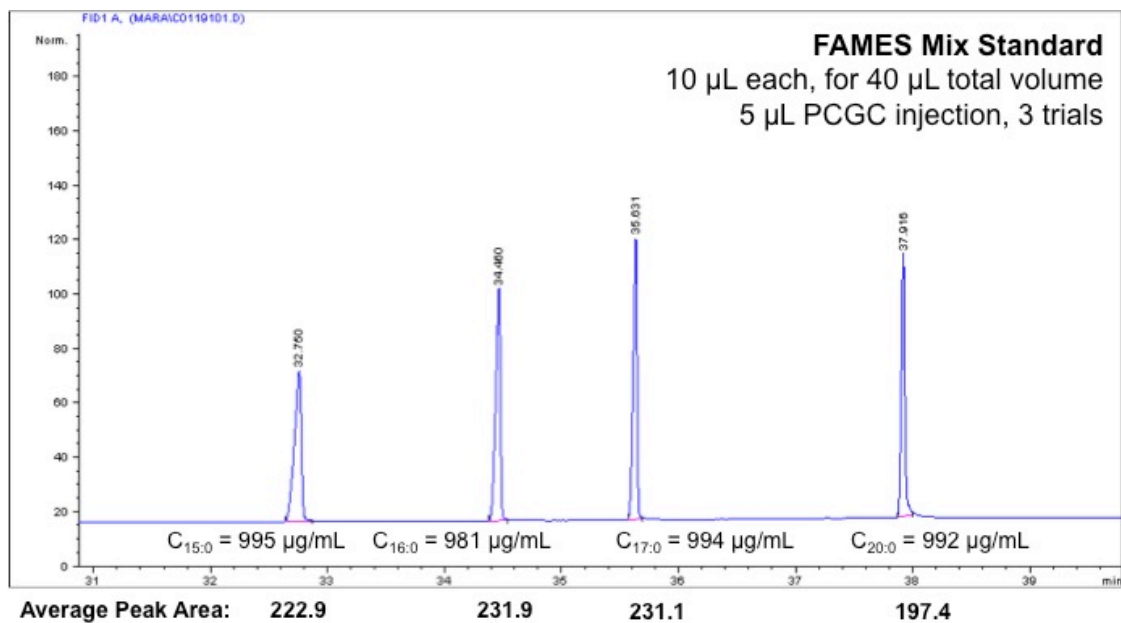


Figure 4. 5. FAMES Mix Standard for quantification on the PCGC.

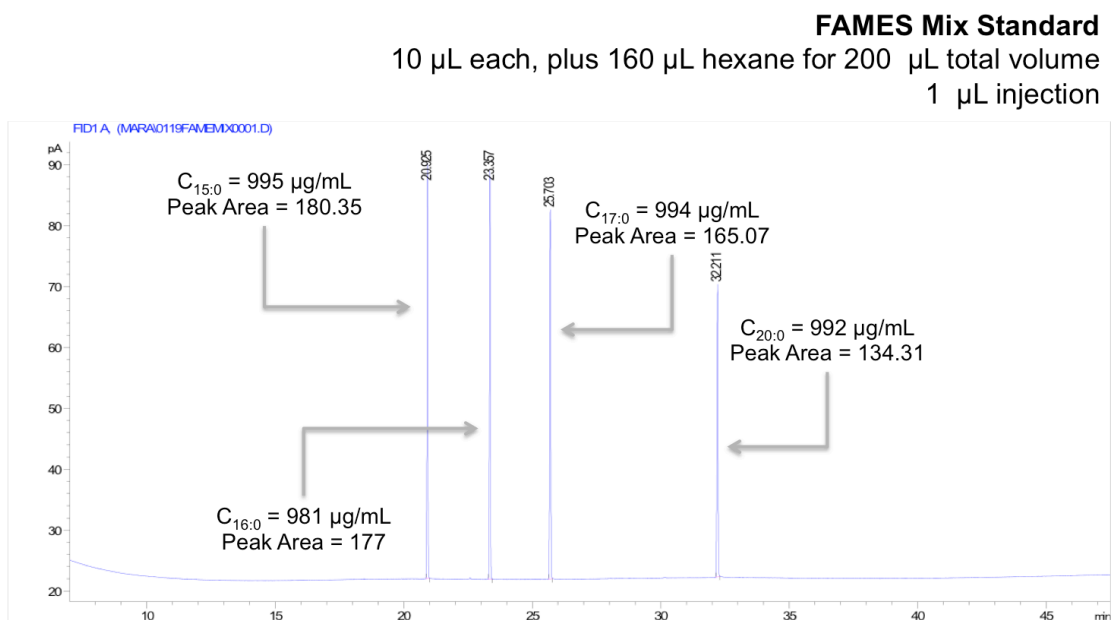


Figure 4. 6. FAMES Mix Standard for quantification on the GC-FID.

The FAMES Mix Standard was analyzed three times on the PCGC and the average peak area for each FAME is given in Fig. 4.5. Because there were four individual FAMES of known concentration in the FAMES Mix Standard for quantification, any individual peak can be used for quantification, but each one results in a slightly different result. Therefore, the low and high estimation are both reported in Table 4.3 to identify the possible range of values. For PC13, the same FAMES Mix Standard was used for correlation of PCGC results. An alternative standard, C_{17:0} FAME at 19.98 µg C mL⁻¹, was used in the quantification of the post PCGC collection on the GC-FID because the column was changed prior to analysis to a J&W DB-23 column (60-m x .25-mm x 25-µm and a maximum oven temperature of 250 °C). The results of each standard are shown in Fig. 4.5, 4.6 and 4.7 and the quantification is reported in Table 4.3.

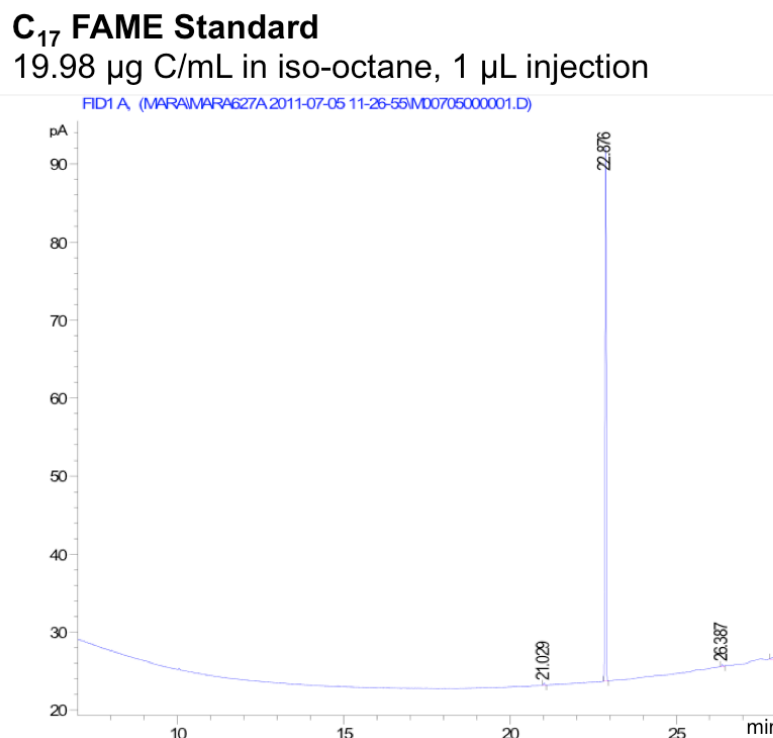


Figure 4. 7. C_{17:0} FAME standard chromatogram from GC-FID with DB-23 GC column.

Neither estimation technique (PCGC or GC-FID) is expected to accurately determine the exact amount of carbon in the collected samples. The CIS is more reproducible than the injector on the GC-FID, but the PCGC estimation is closer to an ideal amount of collected sample, not what is actually recovered. There is the added uncertainty of the unresolved C_{16:1} peaks contributing carbon atoms to the sample, as seen on the chromatogram from the GC-FID (Fig. 4.4), but the peak areas are not integrated for every run on the PCGC and therefore not incorporated in the total peak area from the PCGC. However, these calculations serve as an approximation of mass of carbon in each sample (reported in Table 4.3) and were used to determine the necessary sample preparation techniques at NOSAMS (standard small sample preparation versus new ultra-microscale techniques).

Table 4. 3. Estimated mass of sample recovered (µg C).

			Estimated mass collected (µg C) from PCGC		Estimated mass collected (µg C) from GC-FID		
Sample	Depth (cmbsf)	Volume of Collected Sample (mL)	Low	High	DB-23	Low	High
C7	357	1.20	87.53	103.97	-	63.45	84.94
C6	170.75	1.85	123.92	147.19	-	66.77	89.39
121	90	1.03	28.13	33.41	-	14.50	19.41
C5	40	1.23	65.95	78.33	-	38.98	52.19
C4	516	1.91	97.53	115.85	100.54	-	-
C1	396	1.86	61.75	73.34	62.41	-	-
C2	215	1.69	84.87	100.81	100.25	-	-
208	110	1.93	35.02	41.60	33.95	-	-
C3	60	1.71	46.89	55.69	52.65	-	-

4.3.3 Radiocarbon Age and $\delta^{13}\text{C}$ of samples

Stable carbon and radiocarbon isotopes for the bacterial FAMES collected via PCGC were analyzed by NOSAMS for nine total samples are reported in Table 4.4.

NOSAMS calculates the fraction modern in a sample by

$$Fm = \frac{(S-B)}{(M-B)}, \quad (4.1)$$

where all are $^{14}\text{C}/^{12}\text{C}$ ratios and S is sample, B is blank, and M is modern. Modern is defined as 95% Oxalic Acid I from the year 1950 normalized to $\delta^{13}\text{C}$ standard. Natural fractionation processes that occur due to the preferential uptake of lighter carbon isotopes based on mass are accounted for using $^{13}\text{C}/^{12}\text{C}$ ratio measured on a separate mass spectrometer, relative to the Vienna Pee Dee Belemnite standard (VPDB). Based on the mass, the assumption is $^{14}\text{C}/^{12}\text{C}$ fractionation is twice that of $^{13}\text{C}/^{12}\text{C}$. The correction for the fractionation based on the ^{13}C normalized to -25‰ is

$$Fm_{\delta^{13}\text{C}} = Fm \times \left[\frac{(1-25/1000)}{(1+\delta^{13}\text{C}/1000)} \right]^2. \quad (4.2)$$

These reported values were corrected for the methanol of known isotopic composition ($\delta^{13}\text{C} = -37.28\text{‰}$ and $Fm = 0.0028$) used in the methylation step, converting the fatty acids to FAMES (Pearson 2000). The correction for $\delta^{13}\text{C}$ is

$$\delta^{13}\text{C}_{FAME} = [(N + 1) \times \delta^{13}\text{C}_{measured} - \delta^{13}\text{C}_{MeOH}] / N, \quad (4.3)$$

where $\delta^{13}\text{C}_{measured}$ is the value reported from NOSAMS analysis, $\delta^{13}\text{C}_{MeOH}$ is the known isotopic composition ($\delta^{13}\text{C}_{MeOH} = -37.28\text{‰}$) and N is the number of carbon atoms in the fatty acid prior to methylation. The samples analyzed were a combination of three bacterial FAMES. The N in the fatty acid chain was determined as a weighted value based on the total peak area collected as a summation from every PCGC run for each

sample, resulting in a value between 15 and 16. The fraction modern was corrected using the same equation replacing $\delta^{13}\text{C}$ with Fm

$$Fm_{FAME} = [(N + 1) \times Fm_{measured} - Fm_{MeOH}] / N, \quad (4.4)$$

where $Fm_{measured}$ is the reported value from NOSAMS, the Fm_{MeOH} is 0.0028 and the N is the number of carbon atoms as determined for Equation 4.3. The radiocarbon age was determined from the Fm_{FAME}

$$\text{Radiocarbon Age} = -8033 \times \ln(Fm_{FAME}), \quad (4.5)$$

where 8033 is based on the Libby half-life for radiocarbon (5568 years).

Table 4. 4. Reported fraction modern, radiocarbon age, and $\delta^{13}\text{C}$ from analysis at NOSAMS.

Core	Sample ID	Depth (cmbsf)	Fraction Modern (Fm)	Fm Error	Radiocarbon Age	Age Error	$\delta^{13}\text{C}$ (‰)
PC09	C7	357	0.52063	0.0058	5243	95	-27.085
	C6	170.75	0.58476	0.0042	4310	60	-28.893
	121	90	0.64896	0.01	3473	130	-28.691
	C5	40	0.73108	0.0067	2516	80	-27.787
PC13	C4	516	0.48110	0.0049	5878	90	-25.453
	C1	396	0.48547	0.0059	5805	100	-25.586
	C2	215	0.56339	0.0068	4609	100	-25.321
	208	110	0.62406	0.0108	3788	150	-27.832
	C3	60	0.63144	0.009	3693	120	-27.191

The $\delta^{13}\text{C}$ results from both PC09 and PC13 are correlated to the sediment depth for each sample are shown in Fig. 4.8. The stable carbon isotopes are measured of a separate mass spectrometer at NOSAMS. The error on this measurement is not reported, but the uncertainty is approximately 0.1‰ (<http://www.whoi.edu/nosams/page.do?pid=40146>). In general, samples from PC09 are more ^{13}C -depleted (a more negative $\delta^{13}\text{C}$) than the samples in PC13, with this difference increasing with depth. Both cores follow a similar pattern of greatest ^{13}C -depletion at the

PC13 designated SMTZ sample depth of 110 cmbsf (208 and 121 for cores PC13 and PC09, respectively).

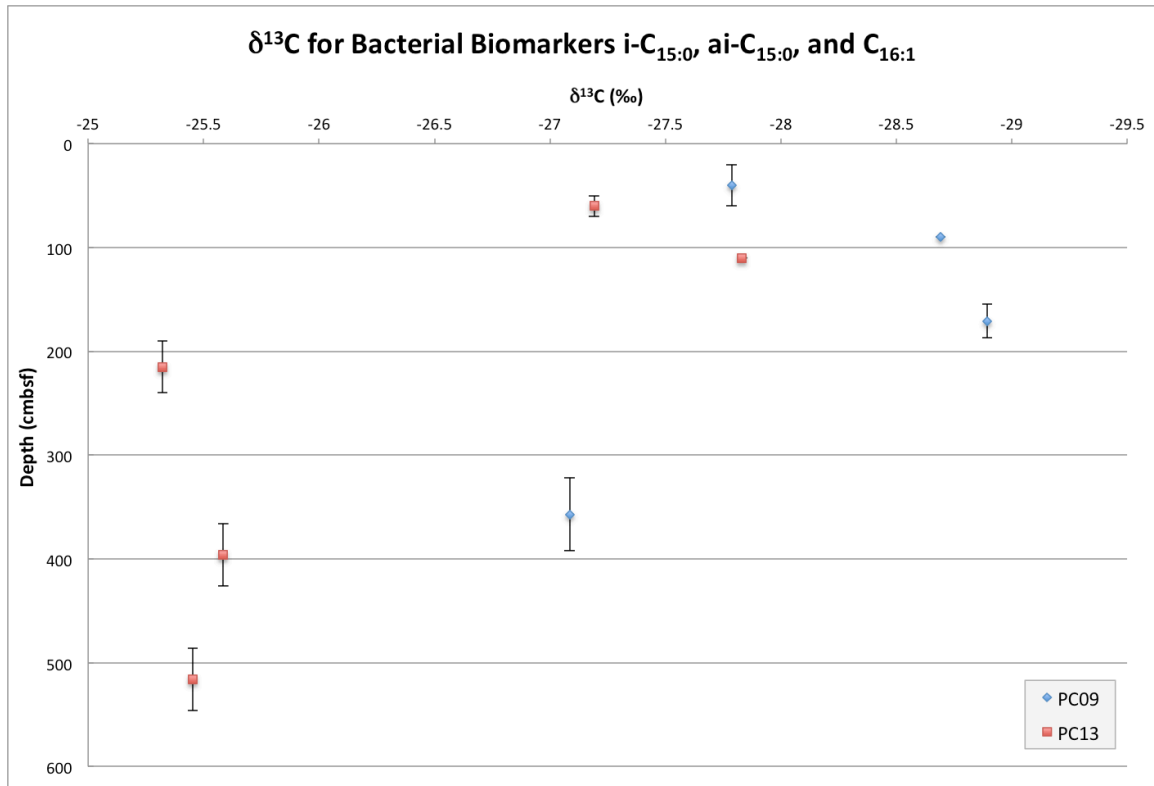


Figure 4. 8. $\delta^{13}\text{C}$ plotted versus depth for PC09 (blue) and PC13 (red). Note the bars in the direction of the y-axis represent the span of the depth in the sediment core for samples composed of multiple sediment horizons, not the error in the depth measurement. The error bars for the stable carbon isotope measurement are smaller than the designated markers at 0.1‰.

Fraction modern is plotted for each sample relative to depth in Fig. 4.9 and radiocarbon age is plotted relative to depth in Fig. 4.10. For both PC09 and PC13, the fraction modern, that is, the deviation from radiocarbon defined “modern”, decreases with increasing sample depth. This result is consistent with marine sediments, the deeper material has been at the site longer, so the radiocarbon present has decayed more over time. There is no apparent trend at the SMTZ in the fraction modern results. The radiocarbon age of at the deepest sediment from PC13 is approximately 5900 radiocarbon

years at 516 cmbsf and from PC09 is approximately 5250 radiocarbon years at 357 cmbsf (Fig. 4.10).

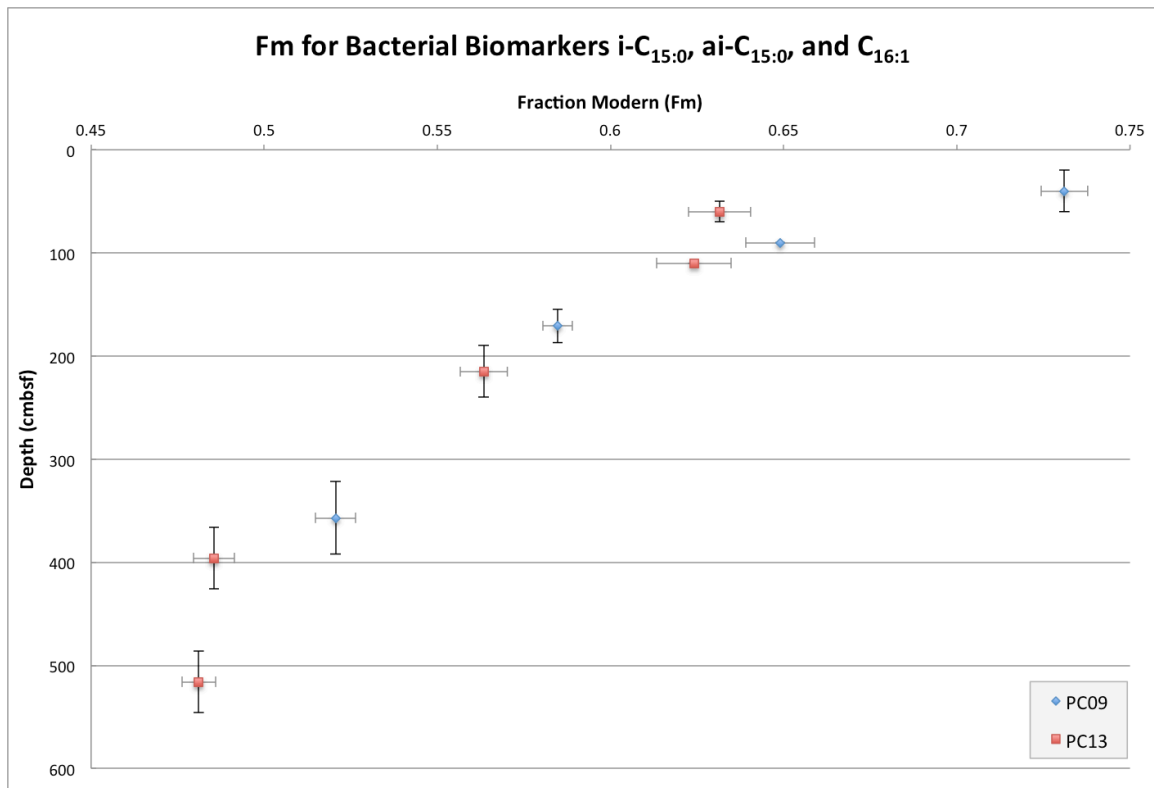


Figure 4. 9. Fraction modern (Fm) plotted versus depth for PC09 (blue) and PC13 (red). Note the bars in the direction of the y-axis represent the span of the depth in the sediment core for samples composed of multiple sediment horizons, not the error in the depth measurement. The error on the fraction modern as reported by NOSAMS is in gray.

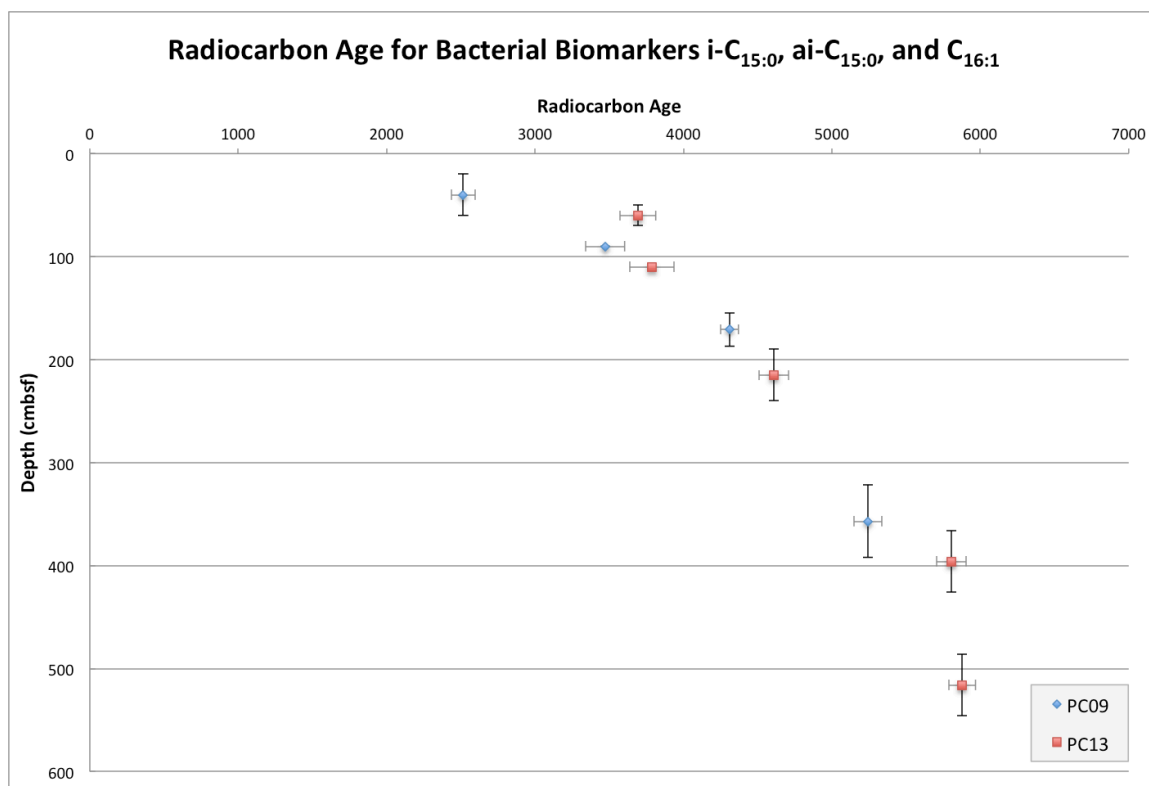


Figure 4. 10. Radiocarbon age plotted versus depth in PC09 (blue) and PC13 (red). Note the bars in the direction of the y-axis represent the span of the depth in the sediment core for samples composed of multiple sediment horizons, not the error in the depth measurement. The error on the radiocarbon age as reported by NOSAMS is in gray.

Chapter 5: Discussion

5.1 Lack of Support in Biomarkers for SRB Dependent Methanotrophy

Coupling radiocarbon analysis of bacterial biomarkers with stable carbon isotope analysis was an objective of the MITAS Expedition. Specifically, a goal was to identify both the origin and age of the methane source for bacterial phylotypes associated with anaerobic oxidation of methane (AOM). A phylotype is a biological classification based on the evolutionary relationship of one organism to other organisms. In marine environments, methane can have thermogenic, biogenic or mixed origins. Core PC13 was identified for compound specific carbon isotope analysis of sulfate reducing bacterial biomarkers based on pore water and sediment concentration profiles. These profiles indicated that both sulfate and methane concentrations reached a minimum concentration at 110 centimeters below the seafloor (cmbsf), known as the sulfate-methane transition zone (SMTZ), evidence attributed to AOM in marine environments (Martens and Berner 1974; Barnes and Goldberg 1976; Reeburgh 1976; Valentine 2002; Reeburgh 2007).

Target fatty acid methyl ester (FAME) biomarkers specific to sulfate reducing bacteria (SRB) were identified from previous work for marine sediments associated with AOM, specifically microbial mats and cold seeps – sites where the population responsible for the process would be abundant (Perry et al. 1979; Zhang et al. 2002; Elvert et al. 2003; Londry, Jahnke, and Des Marais 2004; Wegener et al. 2008; Aquilina et al. 2010). The bacterial biomarkers (i-C_{15:0}, ai-C_{15:0}, and C_{16:1}) were collected together for each sediment horizon (described in Sec. 4.2).

The average $\delta^{13}\text{C}$ values for i-C_{15:0}, ai-C_{15:0} and the range for isomers of C_{16:1} for sites associated with AOM reported for microbial mats and methane seeps are presented in Table 5.1 (Elvert et al. 2003; Orphan, House, et al. 2001; Hinrichs et al. 2000). The process by which methane is removed from the seafloor is not well understood (see the Chap. 2 and the references therein), but the ^{13}C -depleted isotopic compositions are thought to be indicative of the incorporation of ^{13}C -depleted methane carbon into bacterial biomass.

Table 5. 1. Bacterial FAME biomarkers $\delta^{13}\text{C}$ from various AOM sites.

Site Type	Biomarker	$\delta^{13}\text{C}$ (‰)	Reference
Microbial mat, Hydrate Ridge (Oregon)	i-C _{15:0}	-70	(Elvert et al. 2003)
	ai-C _{15:0}	-73	
	C _{16:1}	-90 to -50	
Methane seep, Eel River Basin (California)	i-C _{15:0}	-51.3	(Orphan, House, et al. 2001)
	ai-C _{15:0}	-51.9	
	C _{16:1}	-76.1 to -62.8	
Methane seep, Santa Barbara Basin (California)	i-C _{15:0}	-56	(Hinrichs et al. 2000)
	ai-C _{15:0}	-58	
	C _{16:1}	-103 to -22	

Evidence for incorporation of labeled $^{13}\text{CH}_4$ into bacterial biomarkers (e.g., i-C_{15:0} and ai-C_{15:0}) was reported in incubation studies of microbial mat samples from the Black Sea with evidence of high AOM activity (Michaelis et al. 2002; Blumenberg et al. 2004; Blumenberg et al. 2005). Wegener et al. (2008) compared the uptake of labeled $^{13}\text{CH}_4$ versus $^{13}\text{CO}_2$ in prokaryotic communities involved in AOM from three different methane seep sites. That study strongly suggests that SRBs involved in sulfate dependent AOM may utilize autotrophic metabolic pathways that rely on incorporation of dissolved inorganic carbon produced as a result of AOM rather than direct incorporation of methane or methane derived organic intermediates (e.g., formate, acetate). This confirmed results from a previous investigation that coupled methane oxidation to sulfate

reduction (as measured from sulfide production) with no apparent increase in the rate of AOM when possible intermediate substrates were available (Nauhaus et al. 2002). AOM derived dissolved inorganic carbon may be the origin of the $\delta^{13}\text{C}$ isotopic signature observed for the bacterial biomarkers, including i-C_{15:0}, ai-C_{15:0} and isomers of C_{16:1} with the consortium operating through the shuttling of electrons within the community (Nauhaus et al. 2002; Wegener et al. 2008; Knittel and Boetius 2009), but this is only one of the proposed pathways for AOM in marine environments.

To date, the mechanism by which sulfate dependent AOM occurs in marine sediments is still much debated, but if methane derived carbon is assimilated by the microbial community, the incorporation of this carbon should be reflected in the stable carbon isotope signature of the bacterial lipids. In PC13, the value of $\delta^{13}\text{C}$ for methane is reported as -100.0 to -74.6‰ (see Fig. 3.12). Stable carbon isotope analysis of bacterial biomarkers isolated from Arctic sediment in PC13 at NOSAMS (reported in Table 4.4) provided $\delta^{13}\text{C}$ values ranging from -27.8 to -25.3‰. Although there is a slight ^{13}C -depletion at the SMTZ (sample 208 at 110 cmbsf) relative to the other depths from PC13, as shown in Fig. 4.8, such depletion is not definitive evidence of a methane derived carbon as the primary substrate for the microorganisms associated with these biomarkers. The ^{13}C -enriched isotopic signature of the biomarkers compared to the ^{13}C -depleted methane coupled with the high concentration of methane at this site provides evidence that the biomass of targeted bacterial compounds is not derived from a methane carbon source.

It is unlikely the biomarkers selected were not representative of the SRB. Even-numbered saturated fatty acids (i.e., C_{16:0} and C_{18:0}) are ubiquitous in marine sediments

and lack specificity, but branched fatty acids (e.g., i-C_{15:0}, ai-C_{15:0}) can be attributed to specific species of bacteria (Kaneda 1991). Many previous works from sediments associated with AOM have identified i-C_{15:0}, ai-C_{15:0} and isomers of C_{16:1} as biomarkers for SRB associated with AOM (see Table 2.1). Collaborative work based on phylogenetic probing of the sites and measured sulfate reduction rates, coupled with the lack of a depleted methane influenced $\delta^{13}\text{C}$ signature for SRB biomarkers make a strong case for the observed methanotrophy occurring by a yet unidentified pathway not tied directly to sulfate reduction. The $\delta^{13}\text{C}$ -enriched isotopic signature of the bacterial biomarkers relative to the methane present at the SMTZ in PC13 may be indicative of methanotrophy not facilitated by an archaeal methanotroph (ANME) and SRB consortia identified in previous phylogenetic studies for AOM (Orphan, Hinrichs, et al. 2001; Knittel et al. 2003).

Three lines of investigation are typically used to indicate sulfate dependent AOM:

1. Methane and sulfate concentration profiles indicating a well defined SMTZ;
2. Sulfate reduction and methane oxidation have co-occurring rate maximum;
3. The ^{13}C -depleted stable carbon isotope signatures of biomarkers associated with ANME and SRB species.

The measured sulfate and methane concentrations resulted in what seemed to be a well-defined SMTZ at approximately 110 cmbsf in PC13, shown in Fig. 3.5. Despite the SMTZ, other corroborating evidence for sulfate dependent AOM is not present for PC13. None of the bacterial biomarker abundances are more concentrated at the SMTZ

compared to other sediment depths in the cores (Fig. 3.5 and 3.6), which would be expected if the SRB was the dominant and active community at the SMTZ depth (as observed by Elvert et al. 2003 at a microbial mat site). The sulfate reduction rates from radiolabelled measurements taken shipboard are uncharacteristic of a typical AOM site, reaching maximum rates at 210 cmbsf, not at the top of the core where the sulfate concentration is highest or at the SMTZ (Treude et al. 2012). Typical sediment cores associated with sulfate dependent AOM will present enrichment in ANME and SRBs from the *Deltaproteobacteria* class compared to other species at the SMTZ (Knittel et al. 2003; Lösekann et al. 2007). However, PC13 does not exhibit this pattern as shown in Fig. 5.1 and 5.2 (L. Hamdan, in preparation). The *Deltaproteobacteria*, specifically members of the order *Desulfobacteriales* have been frequently observed as participants in sulfate dependent AOM and in close association with the ANME. The *Desulfobacteriales* are often concentrated at the SMTZ in methane charged sediments (Hamdan et al. 2011). During this investigation however, the *Desulfobacteriales* were minimally abundant at the SMTZ (Fig. 5.1), and notably, ANME were not observed (Fig. 5.2).

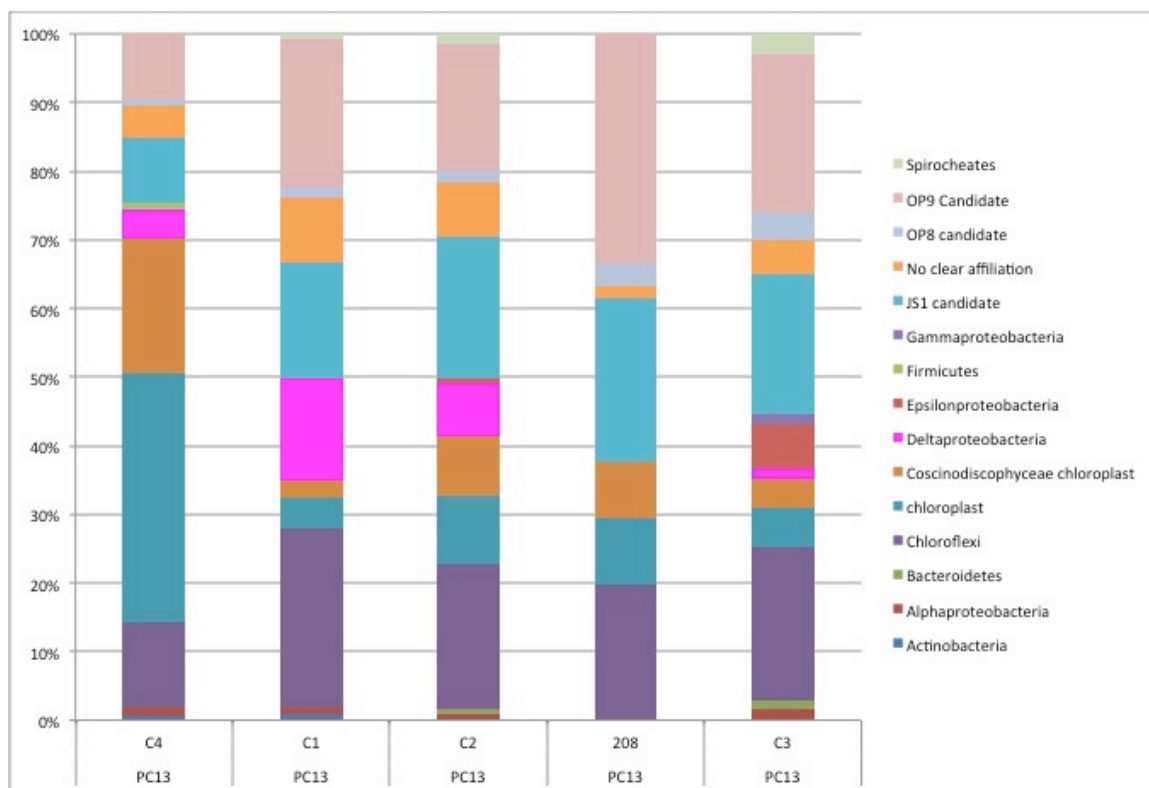


Figure 5. 1. Abundance of bacterial phylotypes from PC13. Data from L. Hamdan at the Naval Research Laboratory, Washington, DC.

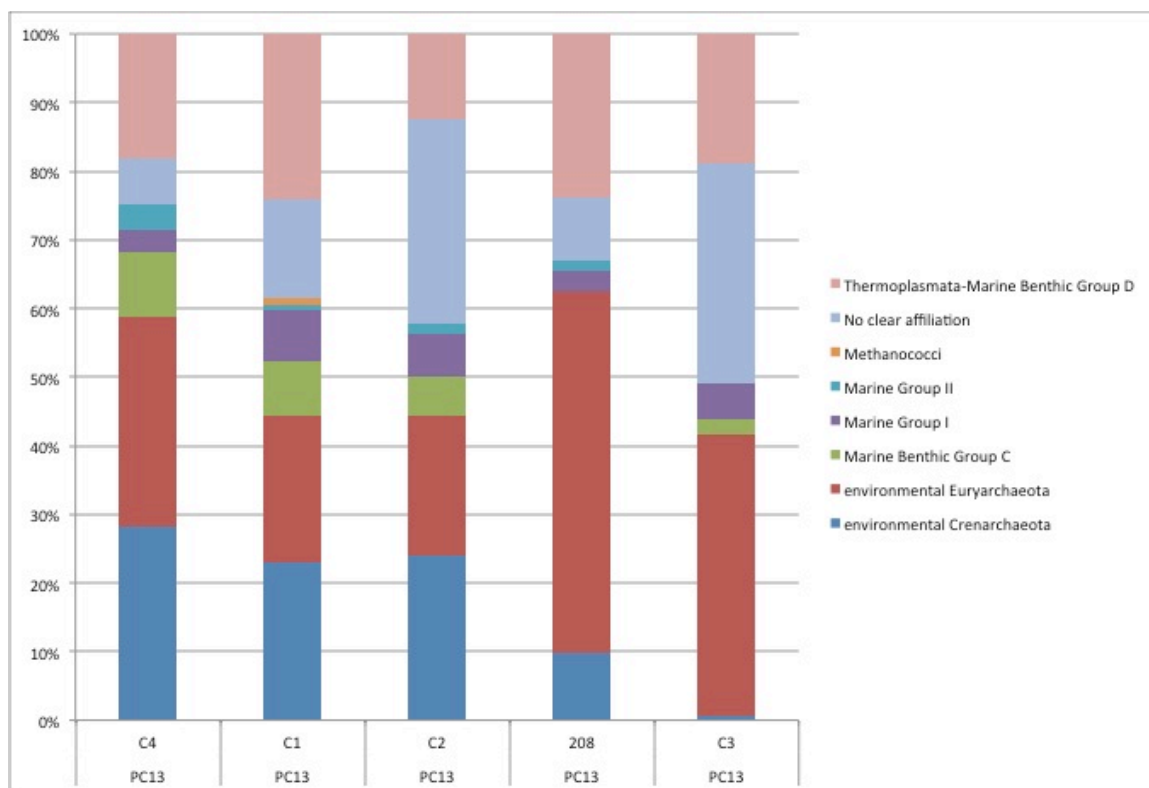


Figure 5. 2. Abundance of archaeal phylotypes from PC13. Data from L. Hamdan at the Naval Research Laboratory, Washington, DC.

Based on the evidence presented for PC13 here and from rate measurements made by collaborators, AOM is not significantly correlated to sulfate reduction. Stable carbon isotope signatures of known SRB biomarkers are ^{13}C -enriched in comparison to the methane signature at this site and do not experience a depletion at the SMTZ like the inorganic carbon (see Fig. 3.12). This $\delta^{13}\text{C}$ -enriched isotopic signature cannot be explained with methane derived carbon as the predominant contribution for incorporation in the isolated bacterial FAMES. This result is supported by rate measurements which indicate that methane oxidation and sulfate reduction are decoupled in PC13 and the lack of phylogenetic data identifying the typical communities found in association with sulfate dependent AOM.

5.2 Sedimentation Rates Estimated from Bacterial Biomarkers

Radiocarbon analysis of bulk total organic carbon (TOC) is not necessarily reflective of the actual sediment age in marine environments due to the presence of organic matter of both marine and terrestrial origin with unknown ages (Eglinton et al. 1997; Uchida et al. 2001; Uchida et al. 2005). Terrestrial organic matter ages on land before it is transported to the ocean, resulting in unclear depositional age of material which often has unknown origin and age (i.e., plant material versus eroded rock and soil). Knowing the approximate time the sediment was deposited and the sedimentation rate at a particular site can provide age context for analyses of a sediment cores and may provide a geological framework for understanding anomalies observed.

As part of the MITAS cruise, an attempt was made to “date” cores using shell fragments, but material was not collected at sufficient resolution to provide an age context for PC09 and PC13. Two shell fragments collected from PC13 at 433 and 578.5 cmbsf suggest a high sedimentation rate of approximately 430 cm kyr^{-1} based on calendar age determinations from measurements at NOSAMS. Average sedimentation rates throughout the Arctic Ocean are low at approximately 1 cm kyr^{-1} (Darby, Bischof, and Jones 1997; Darby, Polyak, and Bauch 2006), but increase on the continental shelf to a few cm per thousand years (Darby, Polyak, and Bauch 2006). Previous works from the Arctic suggest the sedimentation rate measured for PC13 is anomalously high compared to the reported averages in the Arctic region.

The primary contribution to sediment on the continental shelf in the Arctic is thought to be riverine deposition. The contribution of material released from sea ice melt

is significant off the shelf where sedimentation rates are low, but its influence along the Arctic shelf is not well understood (Darby et al. 2009). To date, carbon isotope work in the western Arctic has been limited and the majority of research has focused on determining the origin of organic carbon contributions to marine sediments, particularly sources of terrestrial inputs from river systems (Goñi et al. 2005; Yunker et al. 2005; Drenzek et al. 2007; Belicka and Harvey 2009).

The Mackenzie River is the primary source of sediment to the Beaufort shelf in Alaska and Canada (Hill et al. 1991). At the Mackenzie River delta, sedimentation rates range from 300 – 800 cm kyr⁻¹ and on the Mackenzie shelf are reported to be highly variably from 10 – 1000 cm kyr⁻¹ (Macdonald et al. 1998). However, the Mackenzie River is located approximately 750 km to the east of the sites targeted during this investigation. In the Arctic, plumes from the Mackenzie River would travel eastward due to the Coriolis effect, not contributing sediment to the coring sites under investigation (Pelletier 1975). Investigations in sedimentation along the continental margin of the Laptev Sea, shown relative to the Beaufort Sea in Fig. 5.3, reported sedimentation rates ranging from 13 – 164 cm kyr⁻¹ and two peak rates of 822 and 1152 cm kyr⁻¹ in sediments close to 10,000 years old. The high rates were linked to increased river inputs and coastal erosion occurring during a period of sea-level rise (Stein and Fahl 2000).

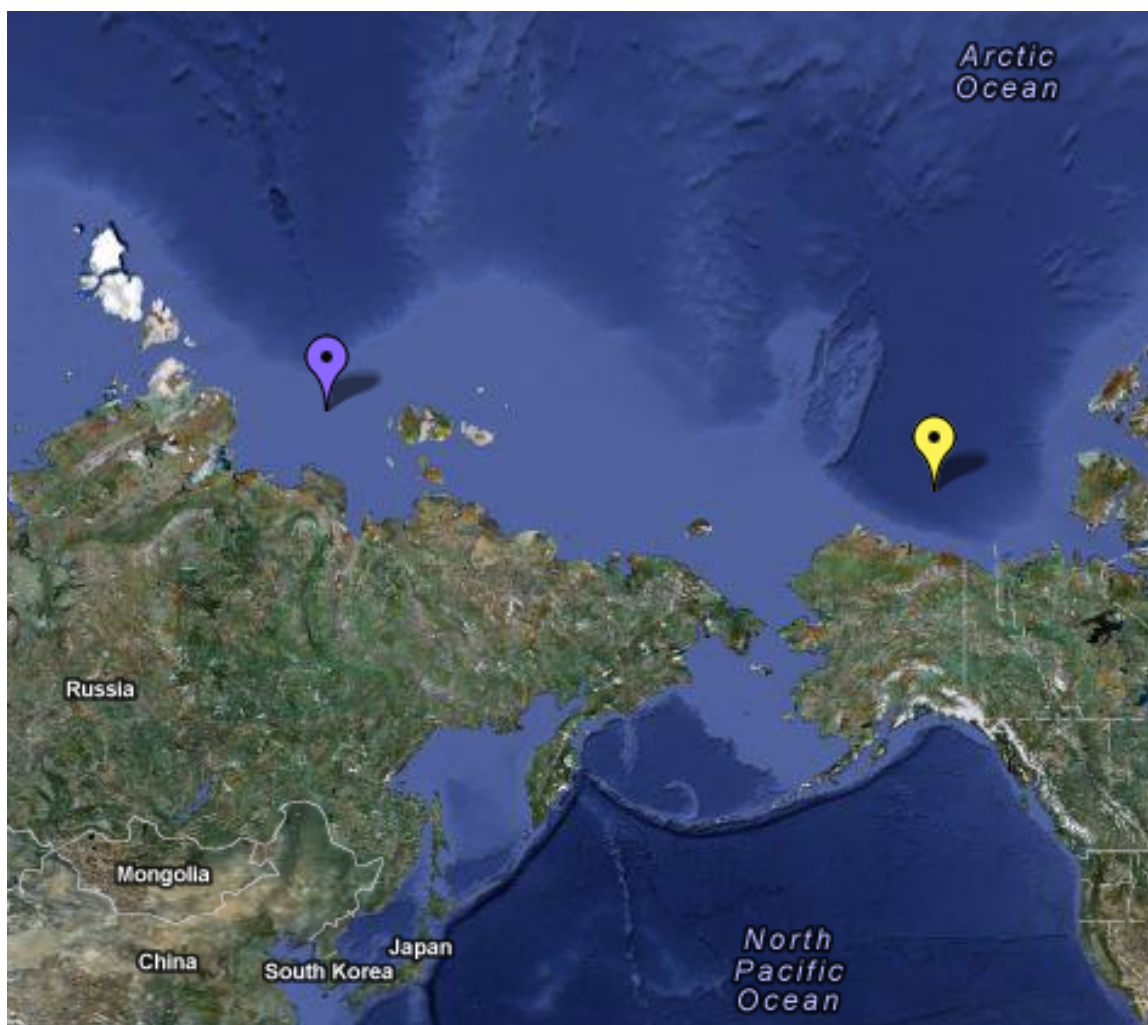


Figure 5. 3. Map of the Arctic Ocean north of Russia and Alaska with Laptev Sea (purple) and Beaufort Sea (yellow). Mapped using <https://maps.google.com>.

The radiocarbon age of the isolated bacterial biomarkers (i.e., i-C_{15:0}, ai-C_{15:0} and isomers of C_{16:1}) for PC09 and PC13 was measured. At a site with sulfate dependent AOM, it is hypothesized that the bacterial biomarkers will reflect the $\Delta^{14}\text{C}$ signature of the source methane, much like the $\delta^{13}\text{C}$, particularly at the SMTZ. The radiocarbon ages for PC09 and PC13 bacterial biomarkers are plotted relative to sediment depth in Fig. 5.5. Also included from the MITAS cruise are two shell fragments collected from PC13 and dated at NOSAMS (Rose et al. 2009), the best measurement of the “true” radiocarbon age of sediment at those depths for PC13. Reported radiocarbon ages from the dating of

shells from three additional sites located on the Beaufort Shelf are shown in Fig. 5.4. These cores were obtained on the *Healy-Oden* Trans-Arctic Expedition (HOTRAX), which collected twenty-nine piston cores along a transect across the Arctic Ocean (Darby, Jakobsson, and Polyak 2005), and are shown with a third piston core from another Arctic mission (Darby et al. 2009) in Figure 5.5 as dashed lines. Cores PC09 and PC13 are further east along on the Beaufort Shelf from HLY501-JPC05 and HLY203-JPC16, while HLY501-JPC08 is in Barrow Canyon.



Figure 5. 4. Map of the relevant piston coring sites from the MITAS Expedition (in yellow), HOTRAX (in pink), and an additional site investigated in Darby et al. (2009) (in teal). Mapped using <https://maps.google.com>.

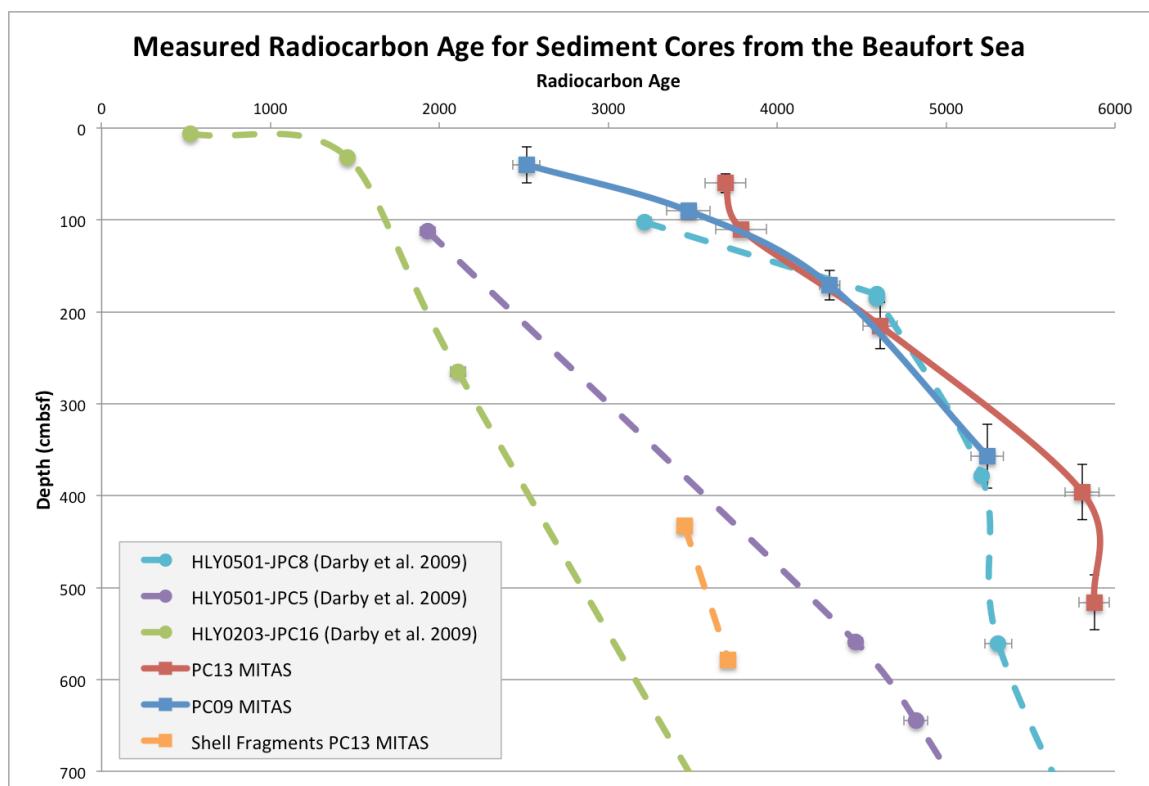


Figure 5.5. Radiocarbon age plotted relative to depth for PC09, PC13, shell fragments collected from PC13 and reported cores from Darby et al. (2009). Dashed lines represent a radiocarbon age from the dating of shells and shell fragments, while the solid lines are from bacterial biomarkers. Square markers are data collected from the MITAS Expedition, while circle markers are values reported in Darby et al. (2009). Note the bars in the direction of the y-axis represent the span of the depth in the sediment core for samples composed of multiple sediment horizons, not the error in the depth measurement. The error on the radiocarbon age as reported by NOSAMS and Darby et al. (2009) is in gray.

Results from the radiocarbon analysis of bacterial biomarkers were not useful to constraining carbon pathways between microbial species at this site because the microorganisms typically associated with sulfate dependent AOM were not abundant in PC13 and are not the candidate phylotypes responsible for methanotrophy at this site. The dating of shells from the MITAS Expedition falls within the range of radiocarbon ages interpolated in Fig. 5.5 at the same sediment depths for samples from Darby et al. (2009). All measured ages corresponded to a younger radiocarbon age than anticipated for this sediment depth based on previous investigations in the Arctic (Stein and Fahl 2000) and reported radiocarbon ages from the National Oceans and Atmospheric

Sciences National Geophysical Data Center

(<http://www.ngdc.noaa.gov/mgg/geology/data/0199/01995006/01995006.txt>). The radiocarbon age of the bacterial biomarkers from PC09 and PC13 seem to be reflective of this young sediment age as well. There is a sharp break in the curve at 400 cmbsf. This sharp break is likely indicative of rapid sedimentation for depths greater than 400 cmbsf because the bacterial biomarkers did not age significantly prior to deposition. Work done in the same region west of Point Barrow, AK (Darby, Jakobsson, and Polyak 2005; Darby et al. 2009) suggest a high sediment deposition rate with a peak rate greater than 1100 cm kyr^{-1} at 561 cmbsf at one location. These rates are thought to be controlled by the complex current flow along the Alaska Beaufort Shelf and specifically in Barrow Canyon.

Current influences on the Alaska Beaufort Shelf are likely the major contributing factor to the high sedimentation in this area, as was previously observed by others (Darby et al. 2009; Faux, Belicka, and Harvey 2011). The current flow northward, through the Bering Strait, increases in rate as it passes through the more constricted area (Coachman, Aagaard, and Tripp 1975). The flow rates measured in this region typically range from $5 - 20 \text{ cm s}^{-1}$, but can reach velocities up to 100 cm s^{-1} , speeds capable of carrying sediment particles (Darby et al. 2009). The PC09 and PC13 cores had a uniform composition of mostly silt and clay, with only some sand contributions for the depth of the cores, a similar composition described for HLY203-JPC16, HLY501-JPC5 and -JPC8 (Rose et al. 2009; Darby et al. 2009). The high sediment deposition rates estimated here are likely indicative of current transport followed by deposition of material, as was previously observed by others (Darby et al. 2009; Faux, Belicka, and Harvey 2011).

The best technique for determining the age of marine sediment, and by extension the sedimentation rate, is the radiocarbon dating of foraminifera. However, the same sample size requirements that plague compound specific radiocarbon studies are of concern when collecting enough foraminifera from a single sediment horizon to accurately “date” a core. An alternative approach of using molecular biomarkers, specifically alkenones, is gaining prevalence in paleoclimate studies coupled with sea surface temperature determinations in the absence of abundant foraminifera (Sachs et al. 2000; Uchida et al. 2005). But studies have shown there is an offset between the alkenone and foraminifera ages, as a result of processes occurring at the sediment water interface (Ohkouchi et al. 2002; Mollenhauer et al. 2003), that need to be taken into account.

Due to the lack of AOM coupled to sulfate reduction in PC13, it is anticipated these bacterial biomarkers may be representative of algal or bacterial marine production at the site where the sediment originates rather than reflective of methane derived carbon. Short chain FAMES (SC-FAMES) are typically biomarkers attributed to marine sources and are not identified as representative of terrestrial inputs or TOC. The marine, meaning produced within the coastal ocean environment, influence of the SC-FAMES, excluding the ubiquitous saturated even-numbered fatty acids C_{16:0} and C_{18:0}, correlates well with radiocarbon ages for alkenones provided in a study by Uchida et al. 2005, and therefore may be useful as a sediment age proxy.

The radiocarbon age of the bacterial biomarkers present in the sediment from this current work is attributed to marine sources. However, there is a significant offset of approximately 2500 radiocarbon years between the bacterial biomarkers for PC13 and the

two collected shell fragments at approximately 400 – 600 cmbsf in the core. A logical explanation is the sediment contribution's aging prior to deposition on the shelf sites, with the younger shell fragments likely being deposited contemporaneously at the site. For these bacterial markers to be appropriate for use as a chronology tool, they must be consistent over large time scales and uninfluenced by minor changes in sediment contributions. The proposed mixing of the sediment prior to deposition at these sites on the Beaufort Shelf is likely contributing to the overall similarities in deposition observed between the MITAS cores and the HLY501-JPC8, but there are obvious discrepancies at certain depths. The biomarkers in PC13 appear to represent a different deposition rate at the top of the core between 60 and 110 cmbsf than the other cores in this region (Fig. 5.4).

The absolute age of the sediment may not be indicated by the radiocarbon age of the bacterial biomarkers, but it may be possible to infer the sedimentation rate from these compounds after taking into account the initial offset due to sediment transport. Such information in the absence of abundant foraminifera to date an entire core is beneficial to understanding the processes occurring at a specific site. In fact, radiocarbon determination of the bacterial biomarkers and the rapid sedimentation rates inferred from the radiocarbon ages, has already provided insights to explain the occurrence of anomalously high concentration diatom phylotypes concomitant with the depths where rapid sedimentation was observed in PC13 between 400 and 600 cm deep (L. Hamdan, personal communication).

5.3 Stable Carbon Isotope Analysis

This work was part of a larger objective from the MITAS cruise, to elucidate the metabolic pathway for methane metabolism through radiocarbon analysis of biomarkers for archaea and bacteria commonly associated with AOM. The work presented in this thesis was to contribute an understanding of the role SRB played in AOM. Coupling the data to the archaeal biomarkers may have elucidated the role of methane in the metabolic budgets for various members of the microbial community at sites investigated in this study. Samples from both PC9 and PC13 were analyzed via GC-IRMS to determine if any FAMES other than $i\text{-C}_{15:0}$, $ai\text{-C}_{15:0}$ and $\text{C}_{16:1}$ may be biomarkers representative of methane assimilation. Analysis of stable carbon isotopes, microbial communities via molecular analysis, and sulfate reduction rates all suggest the SRB are not one of the primary contributors to the removal of methane in PC13 from the MITAS expedition.

Though there is not a strong tie of SRB to methanotrophy at this site, other saturated FAMES can be used as markers for origins of organic matter contributing to the sedimentary carbon based on the $\delta^{13}\text{C}$ signature (shown in Table 3.6). Short chain FAMES (SC-FAMES) are typically attributed to marine sources, while even-numbered long chain FAMES (LC-FAMES) (specifically $\text{C}_{24:0}$, $\text{C}_{26:0}$, and $\text{C}_{28:0}$) are widely considered to originate from C3 vascular plants (Yunker et al. 2005). The $\text{C}_{16:0}$ and $\text{C}_{18:0}$ biomarkers are common to many different groups including bacteria, algae and zooplankton (Volkman et al. 1998; Birgel, Stein, and Hefter 2004; Yunker et al. 2005), therefore they lack specificity of origin as a biomarker. The $\delta^{13}\text{C}$ for terrestrial carbon inputs are typically -28 to -26‰ (Goñi et al. 2005), but a typical range for marine $\delta^{13}\text{C}$ is

more difficult to pinpoint. In the Arctic, marine biomarkers have been reported to range from -27 to -16‰ (Faux, Belicka, and Harvey 2011).

The $\delta^{13}\text{C}$ signature of even-numbered LC-FAMES in PC13 ranged from -31.4 to -27.0‰ (Fig. 3.10). The value of these $\delta^{13}\text{C}$ signatures cannot be explained completely by terrestrial influences, which are reported to range from -28 to -26‰. In work done by Nauhaus and Ishiwatari (2000), a comparison of the $\delta^{13}\text{C}$ signatures for long chain alkanes and LC-FAMES (both attributed to terrestrial sources) indicated a mixed origin for the FAMES. In their study, LC-FAMES cannot be attributed solely to C3 vascular plants, as designated by the photosynthetic pathway, and may even have a marine source (Naraoka and Ishiwatari 2000). Based on an isotopic enrichment relative to the n-alkanes, a mixed origin from both marine and terrestrial sources was hypothesized (Naraoka and Ishiwatari 2000; Ratnayake, Suzuki, and Matsubara 2005). Marine sources are more ^{13}C -enriched than terrestrial sources, but methane from PC13 had $\delta^{13}\text{C}$ values ranging from -100.0‰ to -74.6‰. This ^{13}C -depleted methane may be a contributing source to the mixed origin of the even-numbered LC-FAMES, resulting in a ^{13}C -depleted signature relative to the accepted terrestrial range. This result highlights the caution with attributing these LC-FAMES to only terrestrial inputs and may suggest a role for methane in PC13.

Odd-numbered LC-FAMES are not attributed to a specific origin. The lipid biomarker studies of FAMES typically only include odd-numbered LC-FAMES in the discussion of the abundance relative to the even-number LC-FAMES, and fail to suggest an origin for these compounds. The fact that these odd-numbered LC-FAMES (as identified by the NIST05a.L database) are seemingly the most ^{13}C -depleted of all the

FAMES ($C_{21:0}$ to $C_{27:0}$), particularly $C_{21:0}$ and $C_{23:0}$, may suggest that methane metabolism was involved in their formation. Each has a seemingly uniform abundance regardless of depth in the core for both PC09 and PC13, but the sample from the depth at the SMTZ in PC13 was not analyzed, so a comparison to the depth where methanotrophy occurs cannot be made. The ^{13}C -depleted signature for $C_{21:0}$ and $C_{23:0}$ FAMES may warrant investigation for other metabolic pathways for methane in this environment.

Previous investigations from the Alaska Beaufort Shelf identified high methane concentrations in ice-trapped water of the Beaufort Sea, likely implicating direct methane contributions to the atmosphere once ice melt occurred (Kvenvolden et al. 1993). In fact, recent atmospheric investigations over the Arctic ocean found methane emissions from the surface waters (Kort et al. 2012). Core PC09 was collected at the same location noted for high methane concentrations in the earlier study (Kvenvolden et al. 1993). However, in 2009 during the MITAS cruise, the peak methane concentration in PC09 was only approximately 3.2×10^{-3} mM, four orders of magnitude smaller than the maximum concentration observed at the “active” core, PC13. Although the previous work at this site was limited to methane investigations in the water column (Kvenvolden et al. 1993), where there was an enrichment in concentration relative to sites in the Arctic in absence of ice cover, it is inferred that the only methane source was from the sediments. The stable carbon isotopic signature of the water column methane at the Beaufort site covered in sea ice was reported as -78.4‰ (Kvenvolden et al. 1993). Based on an assumption that the sedimentary methane is the source of the water column methane, it can be inferred the isotopic signature of the sedimentary methane would also be ^{13}C -depleted at the time of the previous investigation. The $\delta^{13}\text{C}$ signatures for individual compounds from the

FAMEs fraction in PC09 may be representative of a residual methane effect from this previously observed occurrence of methane (Kvenvolden et al. 1993).

The identification of the reference core as a site of methane influences decades earlier is the likely cause of the modestly depleted $\delta^{13}\text{C}$ values observed for FAMEs in PC09. The interpretation of PC13 FAMEs relative to the reference core PC09 needs to be considered with this framework. The $\delta^{13}\text{C}$ signatures for each FAME (represented in Figures 3.9 and 3.10) cannot be compared directly to PC09 to infer methane's contribution due to the potential of a residual methane influence on the $\delta^{13}\text{C}$ signature. Instead, PC13 should be compared to other work in this region as the baseline, with PC09 a representation of how lasting methane's ^{13}C -depleted signature may be, even when a site is no longer indicative of high methane concentrations.

5.4 Further Investigations

Based on the methane concentration profile versus depth in PC13 (Fig. 3.5), there is an obvious sink for methane at approximately 110 cmbsf. The process by which the biogenic methane at this site is removed from the sediments is unknown on the Alaska Beaufort Shelf. Even at sites of with strong evidence for the coupling of methane oxidation and sulfate reduction, the specific roles of the archaeal and bacterial partners and the flow of carbon and reduced species between them remains poorly understood (Holler et al. 2011). Though Boetius et al. (2000) showed that the microbial players are often clustered together, the SRB are not always present in associations with archaeal methanotrophs, further complicating understanding of the AOM process (Orphan et al. 2002).

AOM is typically studied in two unique marine environments – anoxic sediments where methane flux is controlled by molecular diffusion, and seep sites where phylogenetic studies have focused due to the large microbial population resulting from high methane concentrations near the sediment-water interface. Methane availability in anoxic sediments is one important factor influencing AOM, but is a difficult value to accurately measure because methane is lost from the sediments during the sediment collection process (Knab et al. 2008). Additionally, high methane concentrations are not necessary for sulfate dependent AOM, which has been observed at diffusive sites with considerably low methane flux resulting in low AOM rates (Parkes et al. 2007; Knab et al. 2008). Even with abundant methane availability at seep sites, evidence for a decoupling of sulfate reduction and methane oxidation based on rate measurements has been observed (Orcutt et al. 2005). It seems there is no single AOM environment that can give a consistently clear understanding of the process based on standard lines of investigation: sulfate and methane concentrations; AOM and sulfate reduction rates; stable carbon isotope signatures of biomarkers; and phylogenetic studies. Future work should target other potential pathways beyond sulfate dependent AOM based on another important factor influencing AOM, the sedimentary material (Valentine 2002).

The unexpected observation of methanotrophy occurring without an obvious sulfate reduction dependence in PC13 illustrates that the Arctic may be a unique environment for processing methane well suited for future AOM investigations. The sources of organic material differ between the Arctic and other AOM sites, and this difference could be a factor in the decoupling of sulfate reduction and methanotrophy. The Arctic region is a naturally colder climate than the more temperate regions of prior

AOM investigations, e.g., Gulf of Mexico, New Zealand, and Chile. The climate influences the sources of sedimentary material to the Arctic, particularly the ice cover for part of the year. Unlike other regions whose sedimentary material is significantly influenced by marine primary production, the main source of organic material to the Arctic shelves is terrestrial, either from river inputs and coastal erosion or current deposition of transported material. The variable sources of organic matter likely influence the electron acceptors available for use by microorganisms in the sea floor and may be the mitigating factor for the processes occurring in anoxic sediments rather than just an abundance of both sulfate and methane. Terrestrial material may contain nitrogen, manganese, and/or iron, all proposed electron acceptors coupled to methane oxidation (Dekas, Poretsky, and Orphan 2009; Beal, House, and Orphan 2009). The terrestrial influence on marine sediments in the Arctic could allow for an AOM process that occurs by a pathway other than sulfate dependent AOM.

The processes for methanotrophy occurring in Arctic marine sediment are not currently understood in the framework established by present AOM research. The Arctic presents a microbial community that may operate by an undetermined pathway for AOM. Arctic sediments warrant further investigations into methanotrophy and its implications on methane release and climate change.

Chapter 6: Conclusion

The isolated biomarkers for the sulfate reducing bacteria do not have a $\delta^{13}\text{C}$ isotopic signature consistent with the incorporation of methane derived carbon. Despite a seemingly well-defined sulfate-methane transition zone (SMTZ) in PC13, the stable carbon isotopic signature is not ^{13}C -depleted, like the biogenic methane present in this core. Stable carbon investigations suggest sulfate dependent methane oxidation is not the primary process for methanotrophy at this site. This result is consistent with measured sulfate reduction rates and phylogenetic studies of microorganisms populating PC13. Radiocarbon analysis of the bacterial biomarkers from PC13 were not utilized for the analysis of methanotrophic pathways because the biomarkers targeted were for phylotypes whose dominant function at this site is not tied to methanotrophy. In the absence of sulfate dependent anaerobic oxidation of methane (AOM), the radiocarbon age of the isolated bacterial biomarkers may be useful as a chronology tool when foraminifera are not available to infer sedimentation rates. However, significant research is required to substantiate this correlation through radiocarbon dating of foraminifera and bacterial biomarkers from the same sediment horizons.

This work presents one of the first investigations of AOM from marine sediments in the Arctic. However, sulfate dependent AOM is not the dominant process explaining the methanotrophy at the SMTZ in PC13. The pathway for methane removal at this site remains unidentified, as well as the potential microbial communities responsible for this process. Due to the terrestrial sources of sedimentary matter in the Arctic regions and the

abundance of unclassified phylotypes, specifically archaea, alternative methane oxidation pathways involving nitrogen, manganese and/or iron are candidates for investigations.

Future work in the Arctic region is essential to determine if sulfate independent methanotrophy is the dominant process for the removal of methane in marine sediments. Determining this process will continue to broaden the current understanding of AOM and the process by which the majority of sedimentary methane is removed from the global carbon cycle. In order to further understand methane cycling in Arctic sediments, more expeditions focusing on the collection of piston cores from methane hydrate sites need to take place. Target cores for compound specific carbon isotope investigations would be selected after both rate studies and phylogenetic probing have identified sediments functioning with either sulfate dependent or sulfate independent methane oxidation. A comparison analysis of a core where the methanotrophy appears similar to PC13 and another core from any region cited as AOM occurring via the well-documented ANME/SRB consortia pathway may reveal the essential parameters resulting in alternative occurrences of methanotrophy.

Advances in radiocarbon analysis technologies will need to achieve routine measurement of microgram quantities of carbon for progress to be made in understanding methane cycling in marine environments. Measurement of samples this size would allow for the analysis of individual biomarkers with higher resolution throughout the depth of a sediment core. Current work necessitated multiple biomarkers and sediment horizons to be combined in order to collect greater than 25 µg of carbon for a single radiocarbon measurement. The assessment of biomarkers as a tool for determining deposition rates in

marine sediments, radiocarbon analysis of both bacterial biomarkers and foraminifera, will be possible when the sample size requirements for radiocarbon analysis are lessened.

Appendix 1: Assessment of a New Radiocarbon Technology for Compound Specific Radiocarbon Analysis

A1.1 Introduction

The goal of this appendix is to address the contributions made to the development and assessment of the Intracavity Optogalvanic Spectroscopy (ICOGS) system at Rutgers University in Newark, NJ. The Naval Research Laboratory (NRL) is well suited to help Rutgers address issues associated with small sample radiocarbon analysis, due to their expertise in the field as an Accelerator Mass Spectrometry (AMS) facility. Additionally, the interest in compound specific radiocarbon analysis (CSRA) and its applications to microbial communities responsible for anaerobic oxidation of methane (AOM) was an exciting challenge to highlight the potential of ICGOS to the AMS community. The active contribution made to the collaboration was in providing carbon dioxide gas samples of known percent modern carbon to test the robustness and limitations of the ICGOS system. This work presented its own challenges at NRL in the preparation of such materials. This appendix is a record of the efforts made in gas sample preparation for measurement via the ICGOS system. Also included in this section are the preliminary results from comparison of ICGOS to another new radiocarbon technique, the gas ion source at Woods Hole Oceanographic Institute, as well as a commentary on the progress made and the future obstacles ICGOS needs to overcome to be a viable alternative to AMS for CSRA. This appendix is written sequentially – showing progress and barriers overcome throughout this collaboration.

A1.2 Background

For more than three decades, radiocarbon has been measured using AMS. Though the systematics and analyses vary for each accelerator used, the principles of operation are the same (please refer to the Chap. 2 of this document for general information about AMS (Donahue 1995; Gove 2000)). The measurement of all three naturally occurring isotopes of carbon is essential to radiocarbon analysis. Radiocarbon content is reported relative to the ^{12}C isotope while the ^{13}C to ^{12}C ratio is used to correct for fractionation during sample processing and measurement in the reporting of a radiocarbon value. Though this technique can be a powerful tool in determining the age of a sample, the measurement is time consuming and costly. Perhaps the greatest disadvantage to AMS is the sample size requirement. Most conventional AMS measurements require a minimum of 1 mg of carbon (mg C). Over the years, techniques in sample preparation and system hardware have been developed to push the limits of this technology and reduce the minimum sample size (Pearson et al. 2006; Santos et al. 2007). Despite the improvements in small sample radiocarbon analysis, natural samples for compound specific measurements are limited in size and often times the small sample techniques employed cannot adequately measure the radiocarbon content (Shah and Pearson 2007).

The work involved to prepare a single biomarker for radiocarbon analysis is a testament to the importance of sensitive and reliable technologies to make the measurement. Reducing the time and/or cost of making a radiocarbon measurement, even at a loss of sensitivity, would be a major advancement in the field of radiocarbon. A technique that could increase sensitivity and/or measure smaller samples would allow for

small sample radiocarbon analysis to be routine, facilitating the ^{14}C analysis of biomarkers as a tool for understanding the carbon cycle in the environment. To this end, collaborative efforts have been made to assess the emerging technology of intracavity optogalvanic spectroscopy (ICOGS) for radiocarbon measurement by a direct comparison to the industry standard AMS technique.

Intracavity optogalvanic spectroscopy is a laser based technique that employs the optogalvanic effect and combines it with intracavity absorption spectroscopy, a technique that independently cannot achieve the sensitivity required for radiocarbon measurements to compete with AMS techniques. ICOGS uses a tunable $^{14}\text{CO}_2$ laser to irradiate the sample and measures the impedance in the gas discharge with a simple electrical circuit. The impedance is proportional to the amount of absorbing species present in the sample. The lasing transition for $^{14}\text{CO}_2$ is well separated from the other isotopic forms of carbon dioxide, specifically $^{13}\text{CO}_2$ and $^{12}\text{CO}_2$ (Murnick and Okil 2005). One advantage of this technique compared to AMS is CO_2 gas is measured directly, eliminating the need for graphitization. Additionally, the technique is non-destructive, so the sample gas can be measured repeatedly to improve counting statistics and, in theory, retained for future analysis. Dr. Murnick and his group have already demonstrated the usefulness of the ICOGS system in measuring $^{13}\text{C}/^{12}\text{C}$ ratios and atmospheric monitoring of $^{14}\text{CO}_2$ (Murnick and Okil 2005), but ICOGS could make an even greater impact in CSRA. The major limitation of AMS for CSRA is sample size. At the present time, routine AMS measurements are made on samples as small as 25 $\mu\text{g C}$ at the National Oceanographic Sciences Accelerator Mass Spectrometer (NOSAMS) facility, but a sample this size is not always attainable for microbial biomarkers from sediment samples associated with

AOM. This collaboration is a way to explore the potential capabilities of ICOGS for CSRA.

An additional benefit to analyzing a sample as carbon dioxide as opposed to graphite is the possibility of interfacing other analytical instruments (e.g., gas chromatograph or high pressure liquid chromatograph) with the analysis system. This coupling could be extremely beneficial for compound specific radiocarbon measurements but has the requirement of oxidizing the carbon eluted from a complex mixture to carbon dioxide and flowing it through an interface into the analysis system rapidly before another component elutes. The ICOGS system is designed for sample introduction as CO₂ gas, already eliminating the need for graphitization, but requires the development of an interface for the laser based instrument. Alternatively, AMS is challenged with the need to develop an ion source capable of accepting samples as CO₂ gas rather than loading graphite targets. NOSAMS has made substantial progress in the development of a gas chromatograph coupled to a gas accepting ion source for AMS (Roberts et al. 2007; McIntyre, Sylva, and Roberts 2009; McIntyre et al. 2010; Roberts et al. 2011). This appendix represents the first effort to directly compare ICOGS to the gas accepting continuous flow AMS for the radiocarbon measurement and presents preliminary results.

A1.3 Preparation of Gas Mixtures – Series 1

Beyond applications for CSRA, ICOGS systems are also currently in development for use by pharmaceutical companies using ¹⁴C as a tracer. Natural samples contain orders of magnitude less ¹⁴C atoms than biomedical samples enriched in ¹⁴C. In the ICOGS system, parameters like laser power and laser modulation frequency can be modified to achieve optimal operating conditions depending on the amount of

radiocarbon present in the sample analyzed. One example for the ICOGS system shows non-linearity in signal enhancements when the samples cover a large dynamic range (i.e., less than 1 modern to 12 modern) (Ilkmen 2009). Biomedical samples enriched in radiocarbon (sample greater than 1 modern carbon) exhibit an enhancement of the optogalvanic signal at lower laser power than natural samples (sample less than 1 modern carbon) (Ilkmen 2009). Therefore, it is imperative to calibrate and optimize the ICOGS system for measuring in the 0 to 1 modern range for natural samples. To assess the linearity of the system over the range of natural samples and determine the sensitivity of the ICOGS system in comparison to AMS, a priority was placed on preparing mixtures with well known composition on the dead end of the natural radiocarbon scale.

Dr. Murnick's group expressed the need for access to materials of well known composition (percent modern carbon) to fill in the gaps left by industry standards in the 0 to 1 modern range – particularly samples close to 0 modern, the “dead” end of the natural range. The distillation/graphitization apparatus at NRL was already capable of manipulating and quantifying CO₂ gas in the preparation of materials for AMS analysis (Pohlman et al. 2000). Minor modifications (discussed later in this section) were made to the apparatus for the preparation of gas mixtures to provide the ICOGS system with small CO₂ samples ranging from radiocarbon dead to modern. This work necessitated the capability of making an accurate determination of the percent modern carbon in the gas mixtures – thereby allowing the optogalvanic signal achieved to correlate to a predicted percent modern carbon. The percent modern carbon of the prepared gas mixtures from two end members (modern and dead CO₂ gas) was determined as the ratio of the modern

CO₂ to the total CO₂ gas (modern CO₂ + dead CO₂) based on the pressure measured at an area of the distillation/graphitization apparatus with a constant volume.

Samples can be introduced for measurement into the ICOGS system in a manner comparable to graphitization systems for AMS with the carbon dioxide gas sealed in quartz (for combustion reactions) or Pyrex tubes (~8" in length and 6 mm o.d.). These tubes are then scored and placed into a break-seal, which is a component of the distillation/graphitization apparatus that can be evacuated and then used to crack the sample tube to introduce the CO₂ gas to the system. This is the accepted technique in radiocarbon work because it allows for the tubes to be baked before samples are transferred to them, removing possible contaminants and reducing the contributing blank. There are limitations to the amount of CO₂ gas that can be transferred to and sealed in a quartz or Pyrex tube. AMS sample preparation typically controls the amount of sample transferred to a combustion tube for conversion to CO₂ gas, so as not to over pressurize the sealed tube causing the tube to break and a sample to be lost.

Measuring the pressure of CO₂ in a small enough quantity to make samples of precisely determined modern carbon values at the radiocarbon dead range is difficult due to the sensitivity of the gauge used. It is essential for the pressure gauges on the distillation/graphitization apparatus to have a large dynamic range and the capability of withstanding pressures above atmosphere. Due to this requirement, none of the pressure gauges are extremely sensitive at low pressures. To accurately prepare gas mixtures close to dead, small volumes of modern gas need to be mixed with larger volumes of dead carbon dioxide, essentially diluting the amount of modern carbon present without over pressurizing the sample tube. Two different techniques utilizing the

distillation/graphitization apparatus were explored to prepare gas mixtures of well known near dead compositions – a gas expansion and a sample dilution.

The gas expansion technique utilizes a series of reservoirs on the distillation/graphitization apparatus that can be isolated with valves to allow for the expansion of the gas from the Volume Manipulator Unit (VMU) into three additional fixed volumes (described in Sec. A1.3.2, Table A1.1 and Fig. A1.5). Due to the low sensitivity of the transducer at the minimum pressure threshold, the pressure of such small amounts of gases cannot be accurately measured. To address this issue, the fixed volume reservoirs were used to expand the carbon dioxide gas. A calibration series was performed to expand the gas into each of the successive reservoirs and measure the pressure with each expansion. Based on this work, pressures of less than 100 torr modern carbon dioxide could be measured at “reservoir 1” and the pressure once the gas had been expanded to all the reservoirs could be extrapolated, resulting in a few torr of pressure.

The dilution technique requires preparing a sample with a nearly dead and accurately measured composition. This sample is then reintroduced to the distillation/graphitization apparatus through the break-seal and then used as the “modern” gas. A small aliquot of this diluted modern gas can then be measured and diluted with dead CO₂ gas to achieve a gas mixture at least two orders of magnitude more dilute than the original.

The CO₂ gas samples were prepared by transferring measured amounts of dead and modern carbon dioxide gas to quartz tubes and sealing with an acetylene torch. The end member gas bottles were attached directly to the distillation apparatus. The modern CO₂ gas bottle was incorporated into the system as a standard gas for preparing AMS

targets at NRL (Pohlman et al. 2000). The dead CO₂ gas source was from a coal gasification process purchased through MESA Gas in September 2008. The dead tank was attached to the distillation apparatus using ¼” copper tubing and a Swagelok valve near the connection point on the still. The two bottles of end member gases were at different pressures (dead at 6 psi gauge and modern at the equivalent pressure to the source bottle (Pohlman et al. 2000)), therefore the process of transferring a measured aliquot of each gas to the sample tube varied for the two end member gases. Each process is described in Sec. A1.3.1 and A1.3.2.

A1.3.1 Dead CO₂

When preparing the gas mixtures, combusted quartz tubes were attached to the graphitization units in an ultra-torr fitting with an O-ring shown in Fig. A1.1. All the sample tubes were first evacuated using the roughing pump and then with the turbo pump.

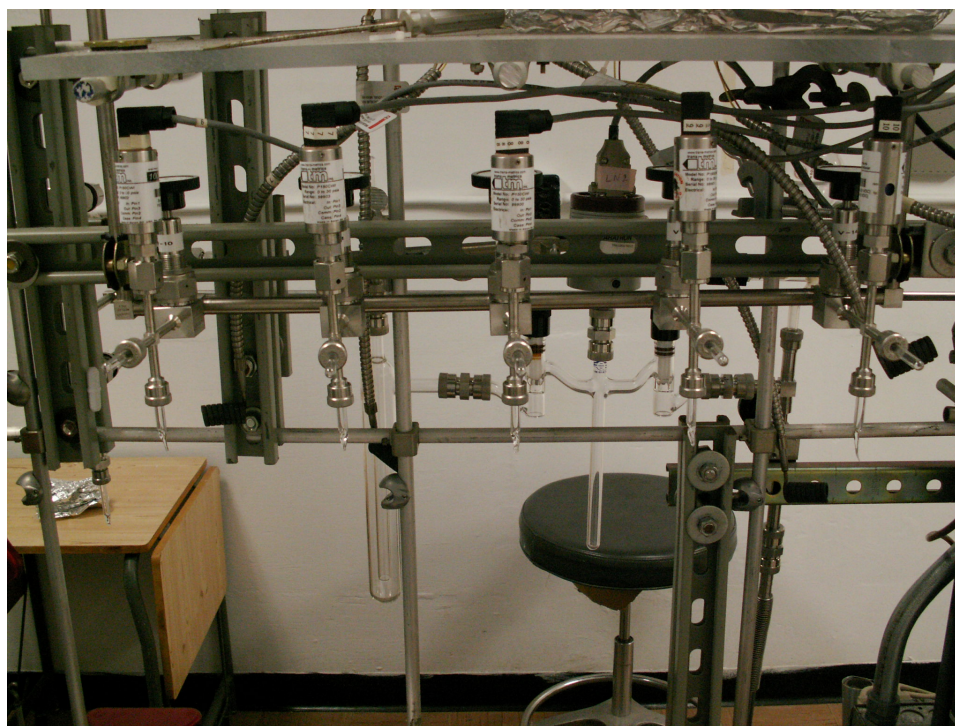


Figure A1. 1. Graphitization units on the distillation/graphitization apparatus at NRL. These stations are each equipped with a pressure transducer and modified to serve as a sealing station for gas preparation in relation to the ICOGS instrument in order to accommodate multiple sample preparations at a single time.

Prior to initiating gas transfers, each section of the still utilized in this gas preparation was evacuated for an hour prior and systematically leak-checked by isolating sections from the pump and monitoring the pressure after reopening to vacuum. When transferring the dead CO₂ for gas mixtures, the line of copper tubing connecting the tank to the still was evacuated using the roughing pump, then the turbo pump. A quick leak check was performed by closing the line to vacuum at V-26 (see Fig. A1.3) and allowed to sit for 5 minutes before opening to vacuum again and monitoring the pressure at a vacuum gauge. The transfer period of five minutes is allowed when expanding the gas into an evacuated volume to allow the gas to equilibrate and minimize fractionation. The lighter isotopes of carbon dioxide will travel faster than the heavier ¹⁴CO₂, resulting in a sample with less ¹⁴C relative to ¹²C and to a lesser extent ¹³C. Allowing time for the gas

to equilibrate when expanding the gas into a larger volume will minimize fractionation in the sample preparation. The Swagelok valve connecting the copper line directly to the still was closed and the tank valve opened to allow gas to expand and fill the volume of the copper tubing. After allowing the gas to equilibrate for approximately 5 minutes, the tank valve was closed and only aliquots of the dead CO₂ gas contained in the copper line were used to make the mixtures. The valve to the copper line was opened to allow gas to fill the section on the still referred to as the loading area between V-25 and V-26 (see Figure A1.2 and Figure A1.3) and closed again. The same region is where modern CO₂ was expanded from the bottle attached to the still by opening V-25 (discussed in A1.3.2).

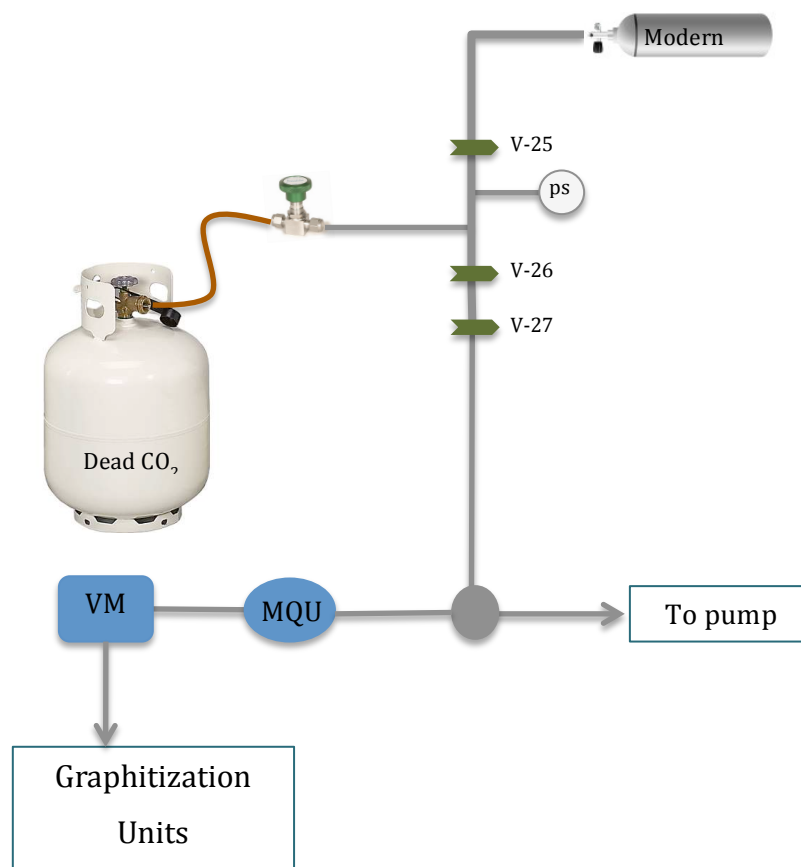


Figure A1. 2. Area of the distillation/graphitization apparatus where the two end member gases are connected. Valves connecting the gas bottles to the still can be opened to allow CO₂ gas to expand into the “loading area”. From there, the gas can be subsampled and transferred to other components of the still.

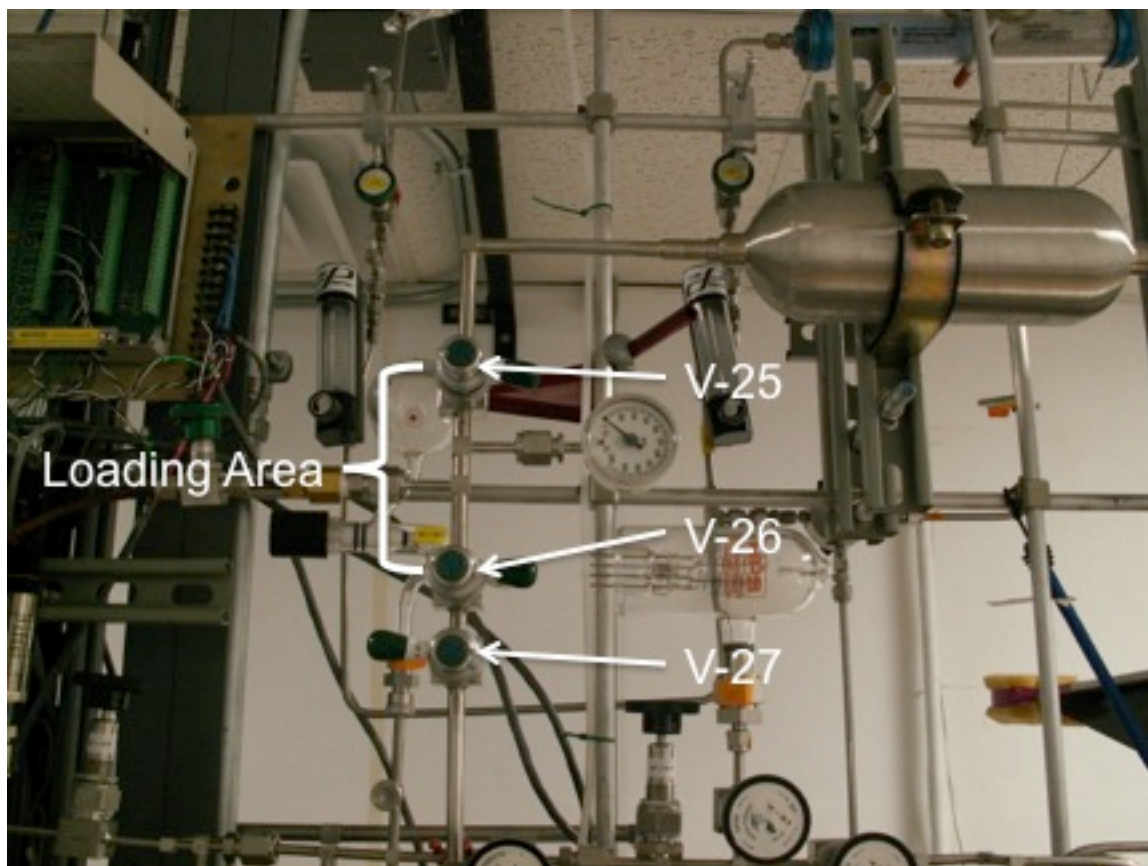


Figure A1. 3. Picture of the area on the distillation/graphitization apparatus depicted in Fig. A1.2.

The gas contained in the loading area was cryogenically transferred to the component of the distillation/graphitization apparatus known as the molar quantification unit (MQU) by placing a liquid nitrogen Dewar flask (LN_2) on bulb #1 of the MQU (Fig. A1.5) and opening V-27. After three minutes, the roughing pump was opened to pump away any impurities (e.g., H_2 gas) in the dead CO_2 . After one minute of pumping the valve to the pump and MQU was closed and the LN_2 flask was removed, allowing the gas to return to room temperature. A dry ice/ethanol slurry (temperature is approximately -78°C) was placed on the MQU and a LN_2 trap on the cold finger of the volume manipulator unit (VMU) (Figure A1.4). After two minutes the valve to the MQU was opened and the carbon dioxide was cryogenically transferred to the VMU for two minutes, leaving

behind any contaminants (i.e., water) frozen at the MQU in the dry ice/ethanol slurry. The dead CO₂ gas was allowed to come to room temperature and the pressure was measured. The VMU is equipped with an adjustable syringe that can be used to increase the volume of this area, thereby lowering the measured pressure at the transducer. This pressure correlates directly to the amount of CO₂ contained in this volume and V-16 can be closed (Fig. A1.4), isolating an aliquot of gas at a specific pressure, while the remainder of the gas is retained in the syringe. The VMU allows for replicate samples to be made from a single gas.

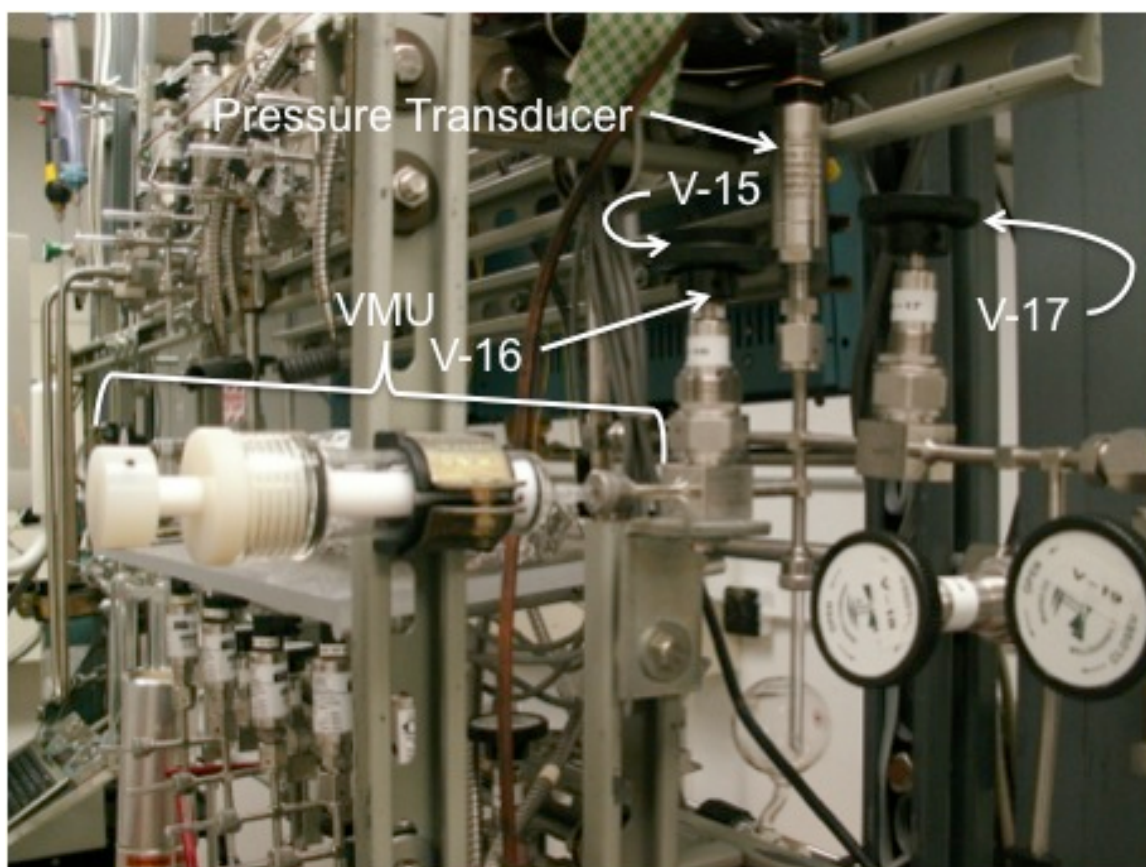


Figure A1. 4. The volume manipulator unit (VMU) on the distillation/graphitization apparatus at NRL. The VMU is designed with an adjustable syringe used to change the volume of this region. The user can control the amount of CO₂ gas by increasing or decreasing the volume, then isolating the desired quantity (by closing V-16) for transfer to the sample tubes.

To achieve the small quantity of modern CO₂ relative to dead, a pressure of approximately 100 torr was targeted for the dead carbon dioxide and transferred to the sample tubes. For more “dead” samples, 200 or 300 torr was used to make a more dilute sample once modern CO₂ was added (additional techniques to achieve small quantities of modern CO₂ are addressed in the following section A1.3.2). The VMU was used to adjust the volume to achieve the target pressure of dead CO₂, the isolation valve (V-16) was closed, and the pressure recorded. A LN₂ trap was placed on one of the quartz tubes set in a graphitization unit and the aliquot of dead CO₂ was cryogenically transferred for three minutes. Then the valve on the graphitization unit was closed, trapping the quantified gas in a sample tube. This process was repeated with the CO₂ gas remaining in the VMU or by filling the loading area with CO₂ from the copper line and repeating for the desired number of samples, up to five total samples located at the graphitization units.

A1.3.2 Modern CO₂

To prepare a small volume of modern CO₂, an aliquot of gas was transferred from the modern CO₂ bottle to the distillation apparatus by opening V-25, filling the loading area. Valve 26 was opened and allowed to sit open for two minutes, then closed. This allowed for only the volume between V-26 and V-27 to be filled with the modern CO₂, but the pressure in this region was comparable to the pressure of the source bottle and would overload the pressure transducer at the VMU. To obtain a measurable amount of modern CO₂, the VMU was isolated from the rest of the system by closing V-17 and the valve closing off the roughing pump. Valve 27 was opened allowing the gas to expand into a larger volume and equilibrate. Then V-27 was closed and the gas contained in the volume was opened to the roughing pump. By repeating this process of expansion,

isolation and pumping away gas - particularly in instances when the loading area is first filled with the modern CO₂ - the amount of CO₂ can be significantly reduced. The carbon dioxide that remains was cryogenically transferred to the VMU, isolated and the pressure at the strain gauge was recorded.

The distillation/graphitization apparatus was constructed in modules to allow for the isolation of gas through a series of valves. This design allows for various components of the still to be under vacuum while gas is being manipulated in a different section. The MQU was designed for the gas expansion into pre-determined fixed volumes as a means to quantify the amount of carbon dioxide present in a sample. This same principle was employed as a means to quantify the pressure of a very small amount of gas when the pressure could not be accurately measured at the transducer. Starting at the VMU, the gas could be expanded sequentially into three additional fixed volumes by opening a valve. The regions of the still incorporated in these volumes are described in Table A1.1 and pictures of these components are shown in Fig. A1.5.

Table A1. 1. Designated areas on the distillation/graphitization apparatus for gas expansion.

Reservoir	Area on distillation/graphitization apparatus	Designation in gas law equations
1	VMU with V-15, V-16 and V-17 closed	V_1
2	Reservoir 1 + V-17 open with MQU closed (V-29 and V-31 closed), V-27 open, V-26 closed, V-20 (to roughing pump) closed	$V_1 + V_2$
3	Reservoir 1 & 2 + V-29 (Bulb #1 and #2 on MQU) open	$V_1 + V_2 + V_3$
4	Reservoir 1, 2 & 3 + V-31 (Bulb #3 on MQU) open	$V_1 + V_2 + V_3 + V_4$

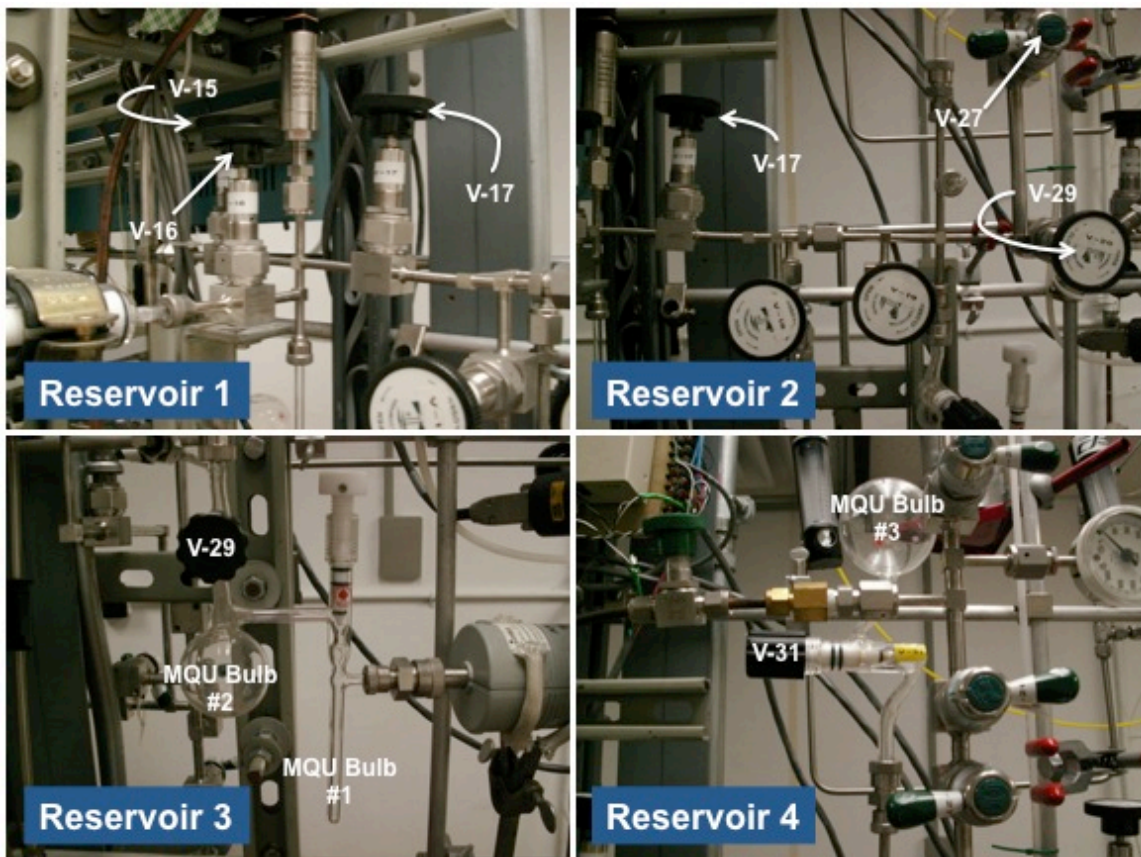


Figure A1. 5. Pictures of the designated reservoirs (Table A1.1) on the distillation/graphitization apparatus.

The volume of each of these reservoirs is unknown, but using the ideal gas law, $PV = nRT$, the ratio of one volume to another could be determined and used to solve for the pressure once the gas was expanded to fill the four designated reservoirs,

$$P_1 V_1 = P_2 (V_1 + V_2) = P_3 (V_1 + V_2 + V_3) = P_4 (V_1 + V_2 + V_3 + V_4), \quad (\text{A1.1})$$

$$\frac{V_2}{V_1} = \frac{P_1 - P_2}{P_2}, \quad (\text{A1.2})$$

$$\frac{V_3}{V_1} = \left(\frac{P_2}{P_3} \left(1 + \frac{V_2}{V_1} \right) \right) - \frac{V_2}{V_1} - 1, \quad (\text{A1.3})$$

$$\frac{V_4}{V_1} = \left(\frac{P_3}{P_4} \left(1 + \frac{V_2}{V_1} + \frac{V_3}{V_1} \right) \right) - \frac{V_2}{V_1} - \frac{V_3}{V_1} - 1. \quad (\text{A1.4})$$

Using the volume ratios determined in Eq. A1.2, A1.3 and A1.4, the pressure of the expanded gas could be extrapolated from the pressure in Reservoir 1 and the calibration series according to

$$P_4 = \frac{P_1}{1 + \frac{V_2}{V_1} + \frac{V_3}{V_1} + \frac{V_4}{V_1}}. \quad (\text{A1.5})$$

Based on the expansion calibrations of the three additional reservoirs, the pressure of the gas after expansion was extrapolated. This volume of gas was then cryogenically transferred to a selected graphitization station with dead CO₂ already in the quartz tube. The new gas mixture was frozen at the end of the quartz tube using a LN₂ trap and the tube was sealed with an acetylene torch under vacuum.

A1.3.3 Analysis of Gas Mixtures

A total of seventeen gas samples were prepared for analysis via ICOGS. Select samples were analyzed in batch mode on the ICOGS system. The initial analysis of select samples reported in Table A1.2 is presented in Figure A1.6 and is part of the dissertation work of Dr. Erhan Ilkmen (Ilkmen 2009). Initial results from the gas preparation determined a nearly linear relationship between the optogalvanic signal and the predicted modern carbon based on pressure determinations on the distillation/graphitization apparatus. The ICOGS analysis highlighted the usefulness of the gas preparation techniques at NRL and the potential for the calibration of the system using gas mixtures of well known modern ratios as determined manometrically.

Table A1. 2. Select samples from the prepared gas mixtures analyzed by the ICOGS system.

Sample #	Dead CO ₂ (torr)	Modern CO ₂ (torr)	Estimated Total P (torr)	Ratio
2	82.6	10.48	93.08	0.1126
14	175.5	1.39	176.89	0.00785
17	132	0	132.00	0

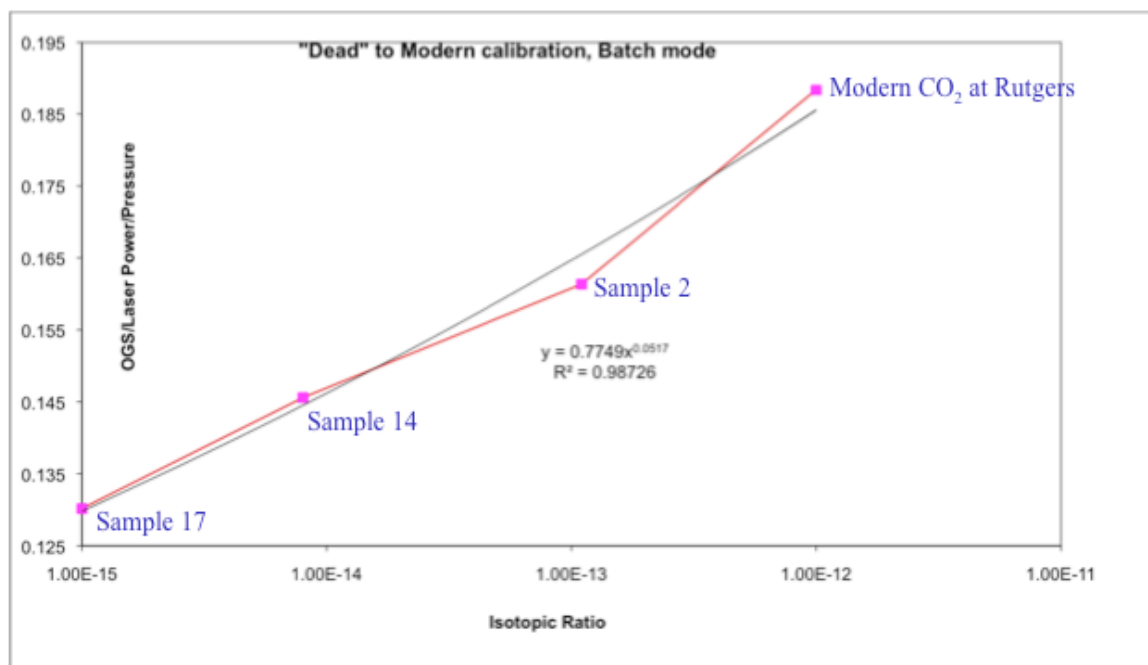


Figure A1. 6. Calibration of optogalvanic signal compared ratios calculated based on pressures determined at NRL. The modern sample is a standard modern gas used at Rutgers and measured by AMS at LLNL.

A1.4 Modifications and Additional Gas Series Preparation

A1.4.1 Modifications to the Distillation/Graphitization Apparatus

Modifications to the distillation apparatus were made after select samples from the first prepared series were measured. A new pressure transducer from Stellar Technologies was placed at the VMU with better precision over the range of 0 to 30 psi absolute (with 0.1% accuracy). A National Instruments LabVIEW program was written to record the pressure at this gauge at a designated time interval, therefore an average

could be determined over a length of time, rather than recording an instantaneous pressure. This modification allowed for an improved determination of the percent modern calculation based on this pressure measurement. Additionally, the cold finger at the VMU was replaced with a longer tube to allow for the use of a LN₂ trap without the risk of freezing the O-ring. Due to the change in volumes from the new transducer and the switching of the cold finger, the gas expansion reservoirs were recalibrated. The pressure transducer was determined to be sensitive to changes in atmospheric pressure and therefore was re-calibrated over night before use each day.

A1.4.2 Preparation of Gas Mixtures – Series 2

A second series of gas mixtures was prepared using the listed modifications made to the distillation/graphitization apparatus for analysis at Rutgers. These samples were used to optimize operating conditions on the ICOGS system for natural sample measurement in batch mode. To achieve near dead mixtures, dilutions were done by preparing three sample tubes with a small volume of modern CO₂ (ranging from 0.82 to 0.87 torr as determined by the new strain gauge and gas expansion calibration) and approximately 100 torr dead CO₂. These mixtures were then re-introduced into the distillation/graphitization apparatus through the break-seal (Pohlman et al. 2000). This starting mixture of CO₂ was frozen with LN₂ and any non-condensable gases that may have been introduced in the sealing or re-introduction process were pumped away. The gas was then frozen in a dry ice/ethanol slurry and cryogenically transferred to the MQU, then transferred to the VMU. The VMU was used to partition an aliquot of this starting gas and measure the initial pressure (target of 20 torr) before the gas was expanded to fill reservoir 4. The gas was then transferred to a sample tube at the sealing station and the

process was repeated for 2 – 3 more aliquots of the initial gas. The remaining initial gas was transferred and sealed in a Pyrex tube for analysis via ICOGS, serving as another calibration standard and a check for potential contamination or fractionation associated with the dilution process. Dead CO₂ at pressures of 100 – 300 torr was introduced into each dilution vial as described in A1.3.1.

A1.4.3 Preparation of Gas Mixtures – Series 3

A third series of mixtures was prepared for a comparison study between AMS and ICOGS. The samples in this series were made in duplicate for analysis by ICOGS and AMS, with the exception of five samples prepared in triplicate to include analysis via the gas ion source at NOSAMS. Duplicates of a single mixture were prepared by cryogenically transferring the gas, a mixture of two end members, from the sealing station to the VMU rather than directly sealing the sample tube. A portion of this prepared mixture was then allocated back to the sealing station and the Pyrex tube was sealed and the process was repeated with the remaining gas. The amount of carbon contained within the sample tube was estimated based on the pressure recorded at the VMU transducer. The sources of CO₂ gases were both dead making the prepared samples a comparison of sensitivity between the two techniques. Lawrence Livermore National Laboratory (LLNL) Center for Accelerator Mass Spectrometry measured these mixtures reported in Table A1.3. The modern ratio was calculated using the measured values of the two end member gases as measured at LLNL and the pressures of each gas measured on the distillation/graphitization apparatus at NRL.

Table A1. 3. Results from the analysis of the near dead series at LLNL.

Sample Name	$\delta^{13}\text{C}$	Fm	\pm	$\Delta^{14}\text{C}$	\pm	^{14}C age	\pm	Predicted % Modern
A	-25	0.0012	0.0003	-998.8	0.3	54010	2110	0.0011
End Member 1	-23	0.0037	0.0003	-996.3	0.3	44980	710	0.0037
C	-27	0.0027	0.0003	-997.4	0.3	47650	970	0.0023
D	-25	0.0010	0.0003	-999.0	0.3	55610	2570	0.0010
End Member 2	-16	0.0010	0.0003	-999.0	0.3	55580	2520	0.0010
E	-32	0.0019	0.0003	-998.1	0.3	50300	1350	0.0010
F	-25	0.0010	0.0003	-999.0	0.3	55190	2450	0.0011
G	-23	0.0014	0.0003	-998.7	0.3	53070	1860	0.0010
H	-21	0.0020	0.0003	-998.0	0.3	49990	1280	0.0010
I	-18	0.0010	0.0003	-999.0	0.3	55320	2450	0.0010
J	-22	0.0014	0.0003	-998.6	0.3	52840	1870	0.0010
K	-15	0.0024	0.0003	-997.6	0.3	48390	1040	0.0023
L	-12	0.0012	0.0003	-998.8	0.3	53840	2020	0.0011
M	-16	0.0028	0.0003	-997.2	0.3	47140	890	0.0023
N	-28	0.0061	0.0005	-994.0	0.5	40990	630	0.0013
O	-14	0.0018	0.0003	-998.2	0.3	50900	1410	0.0017
P	-20	0.0010	0.0003	-999.0	0.3	55280	2440	0.0010
Q	-25	0.0006	0.0003	-999.4	0.3	59130	3950	0.0011
R	-16	0.0021	0.0003	-997.9	0.3	49490	1200	0.0023

Deviations from the predicted values based on the measured pressures from the AMS measurements are indicative of the need for the ICOGS system. Because these samples were prepared as mixtures of two dead CO_2 gases and therefore there are a very small number of ^{14}C atoms present to be detected, the AMS measurement of each end member gas individually or the mixtures may not be sensitive enough to provide an accurate ^{14}C measurement. For radiocarbon, the practical limit is approximately 60,000 years, therefore anything older than this is reported as radiocarbon dead. There is a potential for the ICOGS system to have a greater precision than current AMS technology (Murnick, Dogru, and Ilkmen 2010). The mixtures of dead gases can be used to test the limitations of the technique. A number of the gas mixtures analyzed by LLNL were reported at values inconsistent with the predicted fraction modern based on the pressures measured on the distillation/graphitization apparatus at NRL, for example sample N was measured at $F_m = 0.0061$ by LLNL shown in Fig. A1.7. Another inconsistency is sample Q (Table A1.3), measured by AMS to have a $F_m = 0.0006$, more dead than both the gases mixed together to make the sample.

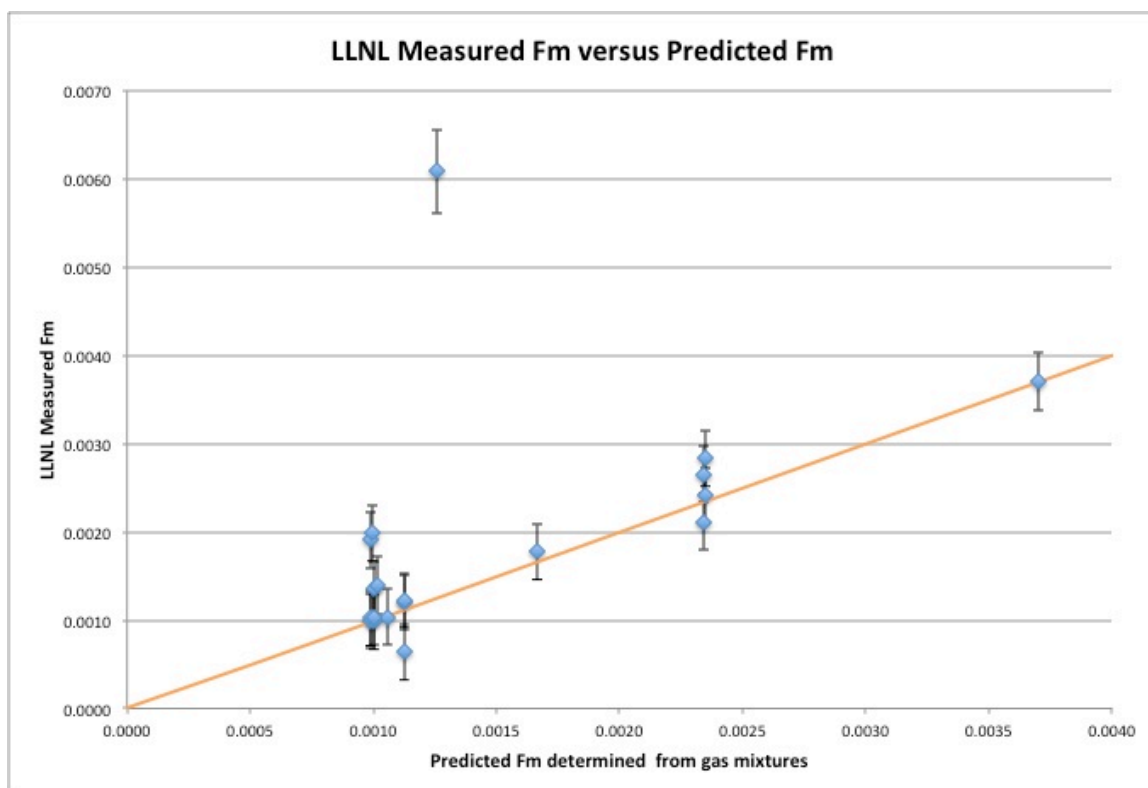


Figure A1. 7. Measured F_m at LLNL value plotted versus the predicted F_m calculated from measured pressures and AMS determined composition of end members. The error bars are the reported error on the F_m from LLNL.

Aside from highlighting the usefulness of an instrument capable of having a greater sensitivity to the few radiocarbon atoms present in “dead” samples, it is imperative to assess the gas preparation technique. The prepared duplicates of these samples are available to be analyzed by ICOGS once a dedicated system has been established for the measurement of CSRA samples.

A1.5 Large Volume Calibration Gases

The success of the first prepared gas mixtures lead to the need for larger quantities of CO_2 to be used for routine calibration of the ICOGS instrument. Gas mixtures were prepared from tanks of dead and modern CO_2 gas based on regional sources of Airgas suppliers with the dead CO_2 as a petroleum by-product from Virginia and the modern

CO₂ from an ethanol plant in Wisconsin. The gas “standards” were made by mixing dead and modern gases together to achieve compositions of roughly 0, .25, .50, .75, and 1 modern. Lecture bottles were filled completely with dead or modern CO₂ from the Airgas tanks. Each filled bottle was then split into two lecture bottles, one containing mostly liquid CO₂ and the other containing gas phase CO₂ determined by the mass of carbon dioxide in the filled bottles. The masses of dead and modern CO₂ contained in the lecture bottles were used to determine which gas bottles to mix to target the intermediate points between dead and modern.

The two bottles to be mixed were attached to the distillation/graphitization apparatus using Swagelok hoses. The hoses were evacuated by pumping with the roughing pump and then the turbo pump attached to the still. The hoses were closed to vacuum and allowed to sit for 10 minutes then opened again to the roughing pump. This served as a leak check for the hose connections to the bottles; if the pressure did not increase when the valves on the still were reopened to the roughing pump it was determined that the hoses were free of major leaks. The gases were mixed by freezing the whole quantity of gas into a single bottle at a lower height, while heating the other illustrated in Fig. A1.8, to ensure the liquid CO₂ would flow to the lower bottle. This process allowed for a temperature gradient between the two bottles to be created, condensing the gas in the cold bottle. This transfer/mixing procedure (shown pictorially in Fig. A1.8) was repeated two more times, by raising and heating the bottle with the condensed CO₂ and lowering the empty bottle to cool. Each transfer was allowed 1-2 hours to complete. After the final transfer, the bottles were allowed to equilibrate to room temperature. The bottle at the lower height was the last one frozen, allowing for a

larger volume of CO₂ to remain condensed in the bottle. After both bottles reached room temperature, both bottles were closed and weighed to determine the mass of mixed gas present in the bottles.

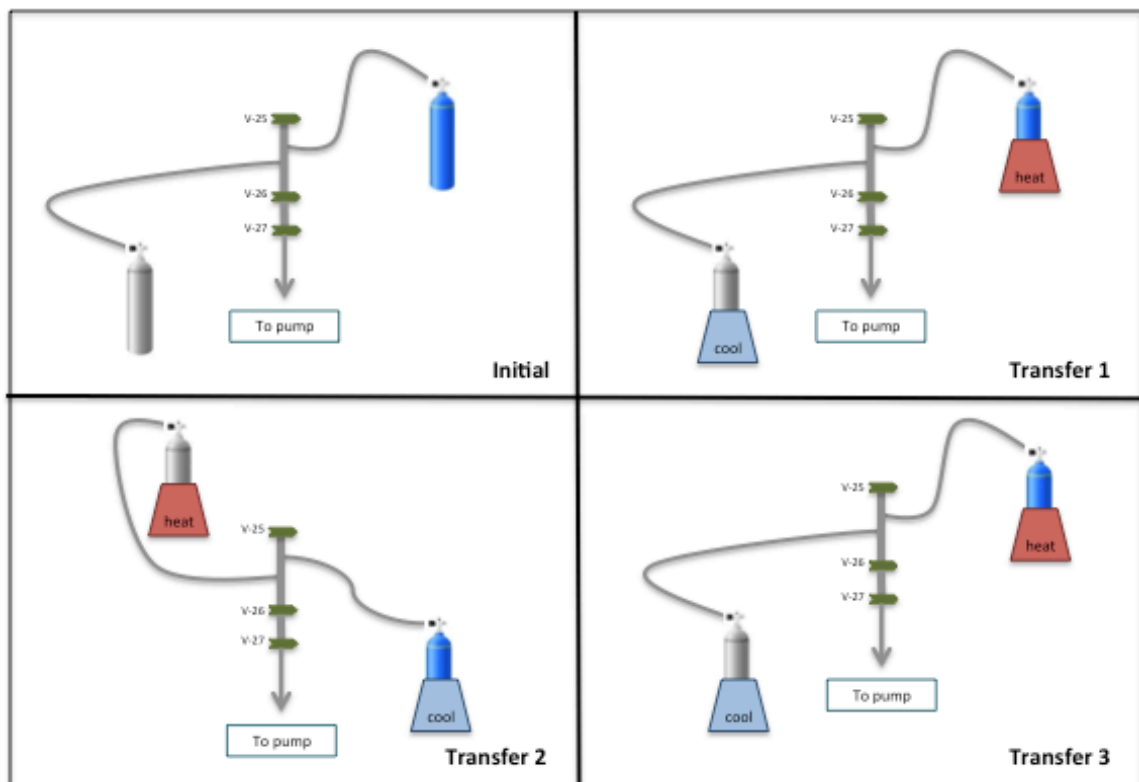


Figure A1. 8. Depiction of the mixing process for preparing gas bottles.

This mixing process was repeated for the preparation of two additional gas mixtures. Heat tape was wrapped around the Swagelok hoses to minimize CO₂ condensing in the hose volume. The composition of the bottles (Table A1.4) was estimated as a mass based mixture of the two gases present in the starting bottles, with the assumption the two gases mixed well and an identical composition was retained in both bottles. Rutgers made an initial measurement of the gases using the ¹³CO₂ laser system in June 2011, shown in Fig. A1.9, and analyzed the two end members on the ¹⁴CO₂ apparatus. This measurement indicated the nominal gas values predicted based on

mass of end member gases mixed were appropriate estimations and the process of mixing the gases in large quantities was successful.

Table A1. 4. Composition of the prepared large volume gas bottles and the facility to which they were distributed.

Bottle #	Mass CO ₂ (g)	Phase	Composition (% Modern)	Destination
1	89.4	gas	50.15%	WHOI
2	345.6	liquid	0.00%	Rutgers
3	337.2	liquid	100.00%	Rutgers
4	91.8	gas	70.80%	WHOI
5	91.2	gas	0.00%	WHOI
6	182.2	liquid	50.15%	Rutgers
7	182.4	liquid	70.80%	Rutgers
8	93.8	gas	31.80%	WHOI
9	153.6	liquid	31.80%	Rutgers
10	96.1	gas	100.00%	WHOI

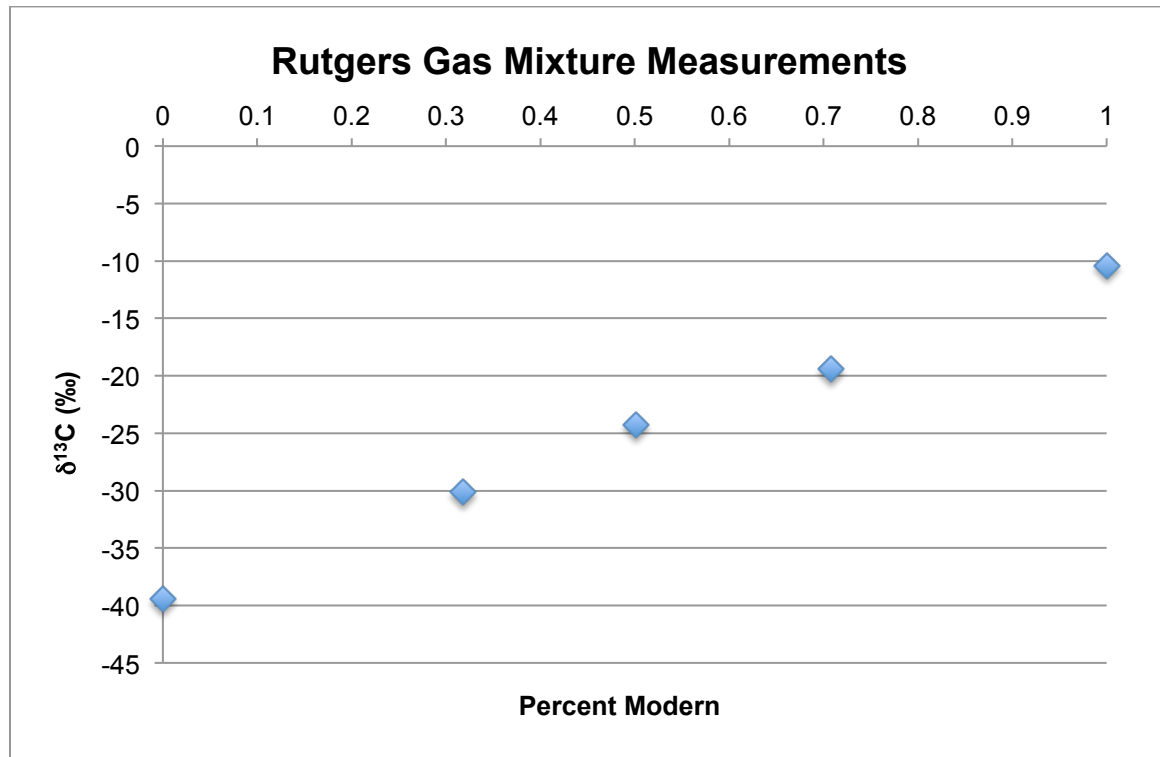


Figure A1. 9. Initial measurement of the calibration gases by ICOGS system equipped with ¹³CO₂ laser.

The calibration gases were measured at NOSAMS and Rutgers, with aliquots of the Rutgers bottles being sent to Groningen for analysis via AMS. Radiocarbon content

of samples from the gas bottles were measured at NOSAMS via AMS and a separate measurement of the ^{13}C was made at NOSAMS on another mass spectrometer used to analyze for the offline ^{13}C correction. Groningen measured the ^{14}C and ^{13}C by AMS. These four samples served as the basis to calculate a “true” value for the gas composition contained in the bottles. This average was a weighted average calculated using the errors reported by the facilities. If an error was not given (like on the ^{13}C values), it was assumed to be 1/1000. Both NOSAMS and Groningen are experienced in isotope measurement; therefore a weighted average from both laboratories should be a best representation of “true” composition. The gases were also measured by ICOGS using a $^{13}\text{CO}_2$ laser and with the new gas ion source continuous flow AMS at NOSAMS. This work is the first intercomparison of the two new technologies for radiocarbon measurement.

The reported value for the two end members from each technique was used to calculate the fraction modern (Fm) value for each gas bottle using based on the assumption the for the dead gas Fm = 0 and for the modern gas Fm = 1, and the reported value was representative of a perfect mixing of these to gases following

$$\text{Fm} = (\text{sample} - \text{dead}) / (\text{modern} - \text{dead}). \quad (\text{A1.6})$$

The residuals for each measurement were calculated following

$$\text{Residual} = \text{Reported value} - \text{“true” weighted average}. \quad (\text{A1.7})$$

The residuals are plotted versus the “true” calculated average in Fig. A1.10. The error for each residual was calculated, propagating the reported (or assumed error) through the Fm calculation (Eq. A1.6) to include error bars on residuals. In addition, Fig. A1.11 compares the reported values to that of the ^{13}C measurement at NOSAMS, not measured

via AMS. This is considered to be the best representation of the actual ratios made from the mixing of two end member gases because it is a well-established stable carbon isotope measurement technique used to correct the AMS measurements when calculating the fraction modern.

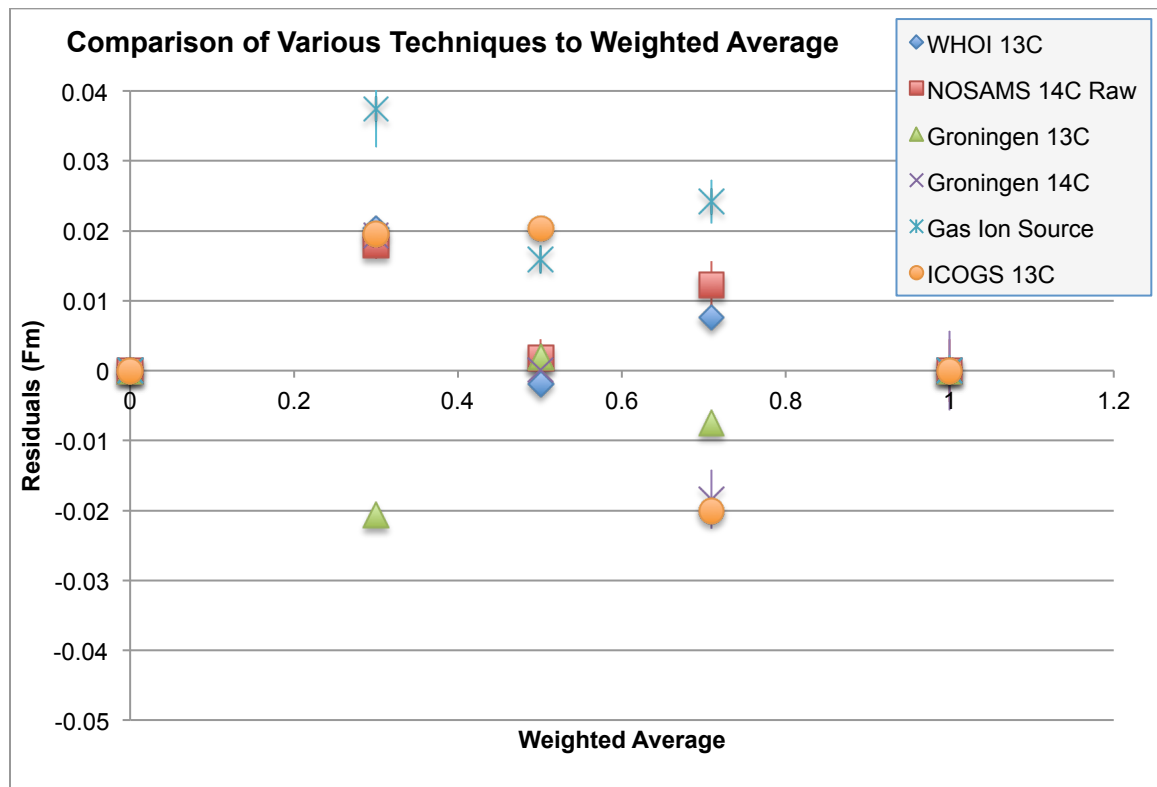


Figure A1. 10. Residuals plotted versus a weighted average.

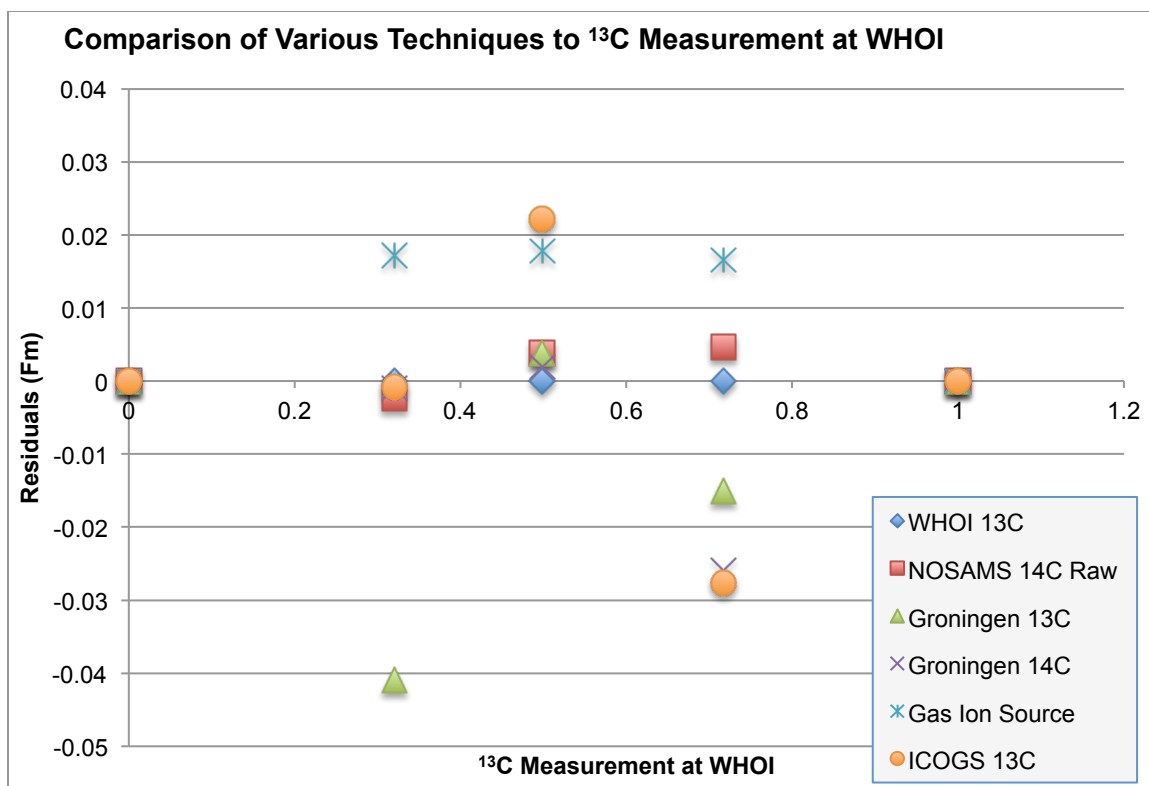


Figure A1. 11. Residuals plotted versus the ^{13}C measurement at WHOI.

From both residual analyses (Fig. A1.10 and A1.11) it seems apparent the gas ion source is measuring radiocarbon resulting in a Fm value higher for all three intermediate mixtures than the calculated average or the $\delta^{13}\text{C}$ measured on the NOSAMS mass spectrometer system. This is potentially a systematic error in the measurement. The nominal 70.8% gas was contained in bottles 4 and 7. Bottle 4 was measured at WHOI by AMS with a split taken for the independent measurement of ^{13}C and the bottle was connected directly to the gas ion source AMS system for analysis. Bottle 7 was measured by the $^{13}\text{CO}_2$ laser system at Rutgers (results shown in Fig. A1.9) and an aliquot was taken from the bottle for measurement at Groningen of both ^{13}C and ^{14}C via AMS. Groningen's $\delta^{13}\text{C}$ AMS measurement is the most variable. This may be because AMS is not the best technique for achieving high precision for stable carbon isotope measurements.

The gas contained within these two bottles may be fractionated as the systems measuring bottle 4 were all higher than the calculated average and the partner, bottle 7, was measured lower than the average. This result may be indicative of fractionation when preparing the gas bottles. Preparation of this sample composition occurred prior to the addition of heat tape wrapped around the Swagelok hoses and could be a result of incomplete mixing. Another major concern is that the bottles may fractionate as they are used and subsampled for analysis, if the gas is not allowed to equilibrate. Tests need to be conducted to determine if the calibration gases are being fractionated every time they are used on the ICOGS system. Over time, this continual fractionation would affect the contents of the bottle, but the immediate concern would be the gas used for the calibration would be isotopically depleted compared to the source gas because the lighter carbon dioxide molecules would travel out of the orifice of the gas bottle faster than the heavier isotopes. The results from this analysis are inconclusive. There are too many uncertainties associated with the measurement techniques and gas handling procedures when these gas samples were analyzed. At NOSAMS, the gas bottle was connected to a distillation/graphitization apparatus and allowed to equilibrate when an aliquot was sampled for AMS measurements and a ^{13}C split was taken, but the same may not be true for the other systems and subsamples taken from the gas bottles. Standard operating procedures in gas handling to minimize fractionation while sampling would need to be developed and followed before an intercomparison of prepared gas mixtures could validate the new technologies.

A1.6 Discussion

A1.6.1 ICOGS Requirements

An ICOGS system dedicated to small sample radiocarbon analysis is essential for progress towards a system competitive with AMS for CSRA. Currently, the Rutgers group is making improvements and modifications to a number of their systems, as well as assisting other groups in the construction of new ICOGS instruments. A dedicated system for small sample analysis of natural materials requires a number of sensitivity considerations unimportant for the biomedical system used for samples enriched in ^{14}C .

Measuring quantities less than 50 $\mu\text{g C}$ would require an analysis cell equipped with a cold trap to cryogenically transfer the entire sample to the cell for irradiation with the laser, which the current ICOGS system lacks (D. Murnick personal communication). A small sample system would also need to incorporate a $^{13}\text{CO}_2$ laser in addition to the $^{14}\text{CO}_2$ and $^{12}\text{CO}_2$ lasers. All AMS measurements for radiocarbon are reported with a correction based on the measurement of the $^{13}\text{C}/^{12}\text{C}$, therefore to be competitive with AMS, ICOGS would require simultaneous measurement of the impedance resulting from the irradiation of sample tuned for the ^{13}C isotope.

Small sample analysis will require the system to be operated in batch mode. Most biomarker samples will not have enough carbon present to allow for continuous flow analysis. Batch mode analysis has been shown to have a memory effect in the sample cell of the laser system, but the memory effect can be eliminated by baking out the cell or flowing UHP N_2 through the analysis cell (Ilkmen 2009). This is the preferred method of analysis for CSRA due to the precision gained from increased measurement times, particularly advantageous when measuring small samples. Optimization of conditions for

this analysis technique, as well as instrument calibration in batch mode, would be imperative.

A1.6.2 Preparation of Materials

The long-term goal of ICOGS is to couple the laser system to an analytical instrument, i.e., HPLC or GC, similar to the gas ion source at NOSAMS, coupled to a gas chromatograph as the preparative end of the system (Murnick, Dogru, and Ilkmen 2008). Until that time, sample preparation techniques comparable to those for radiocarbon analysis via AMS for conversion of samples to CO₂ gas, minus the graphitization step, are necessary.

The preparation in this work of CO₂ gas mixtures for the calibration of new radiocarbon measurement techniques utilized a number of different processes on the distillation/graphitization apparatus at NRL in an attempt to create samples of well known, near dead composition. Though no direct comparison of the different preparation techniques was performed, internal work done at NRL by Dr. Sunita Shah indicates distillation/graphitization apparatus itself contributes background to the samples processed through the system, particularly when a sample is introduced at the break-seal. Sample processing is a large contribution to the blank in any radiocarbon sample preparation. The amount of blank added to samples prepared from dead and modern CO₂ sources is unknown, but could be determined by incorporating a known dead CO₂ gas common in the AMS community (i.e., CO₂ produced from the combustion of coal known as a coal blank). Preparing a large quantity of gas from coal and attaching the gas in a vessel directly to the distillation/graphitization apparatus could be used in the assessment of the blank contribution from the system. The dead CO₂ would also serve as a standard

prepared with batches of samples, as is done in AMS sample preparation. The dilution method, introducing initial gas mixtures sealed in Pyrex tubes into the break-seal and mixing aliquots with dead CO₂, would likely have the highest contribution of blank due to a single sample being processed through the still once, sealed, and then re-introduced through the break-seal. The gas expansion technique with the improved sensitivity of the pressure gauge at the VMU would most likely be the more viable method moving forward, but the technique needs to be evaluated.

The gas expansion preparation technique can be assessed for its accuracy and reproducibility, particularly for near dead gas compositions. An exact target composition will be difficult to attain based on the manner in which the carbon dioxide is manipulated on the distillation/graphitization apparatus, but it is not necessary if the measured pressures can be used to accurately determine the composition of the gas. Predicting the composition based on the pressure and knowing how well the calculated value correlates with the fraction modern as determined by AMS would be beneficial in the assessment of the ICOGS system. If the gas expansion method proves viable for preparing samples, the ICOGS system could be evaluated without the additional time and cost of analyzing a duplicate of each sample via AMS. Sources of gases with intermediate compositions are difficult to find, therefore the preparation of any target composition between two end member gases (0 to 1 modern) would be invaluable in the actualization of ICOGS as a system competitive with AMS.

A series of identical CO₂ gases needs to be prepared to compare the ICOGS technique to multiple existing AMS systems. This was the goal of the preparation of the large quantities of CO₂ in the gas bottles, but fractionation may be a factor when

subsampling. Preparing individual samples of identical gas using the sealing stations on the distillation/graphitization apparatus could allow for a direct comparison of measurement systems without concerns for fractionation during sample introduction. A large volume gas mixture composed of manometrically determined amounts of dead and modern CO₂ would be prepared by methods described earlier in this appendix. Without sealing the sample tube, the known gas mixture should be allowed to expand into the entire sealing station manifold and up to five total sample tubes. After allowing the gas to equilibrate, all the sealing station valves are closed and the gas cryogenically frozen in the sample tube for sealing. The gas remaining in the manifold (less the gas isolated in each sample tube) can be transferred back to the VMU then cryogenically transferred to a sealing station to determine if any fractionation occurred in the gas expansion. Ideally, all the sample tubes should contain gas of identical composition and the measurement of each would assess the reproducibility of the ICOGS instrument for the same sample and/or a comparison to AMS carried out over a range from 0 to 1 modern CO₂.

Another essential component for the use of the ICOGS system will be in the routine preparation and measurement of standards used in AMS, coal blanks serving as a dead standard and oxalic acid II as a modern radiocarbon standard available through the National Institute of Standards and Technology. The radiocarbon age reported is corrected using the blank and modern standards according to methods described by Stuiver and Polach (1977) and would need to be adopted as part of the standard operating procedures for the ICOGS system. Additionally, there are secondary standards and materials used in the International Radiocarbon Intercomparison available (Scott, Harkness, and Cook 1998; Boaretto et al. 2002). The measurement of these

internationally accepted materials could validate the utility of ICOGS in the AMS community.

Three individual bacterial FAME biomarkers (presented in this dissertation) were combined from adjacent sediment depths to ensure enough carbon was collected for a radiocarbon measurement without suffering from the uncertainty added from the combustion step and with enough carbon for a ^{13}C split offline AMS correction. A size series calibration is essential for determining how little carbon is required for an ICOGS radiocarbon measurement. ICOGS has the potential to measure as small as 1-microgram samples of carbon as CO_2 gas non-destructively (D. Murnick, personal communication). If the ICOGS technique proves to be a viable instrument for measuring radiocarbon, the size of the instrument and cost of sample analysis will revolutionize the measurement of radiocarbon, even for samples of 1 mg C or larger. AMS may have reached its limit with current small sample AMS preparation and measurement techniques having a threshold of 20 $\mu\text{g C}$ (Shah and Pearson 2007). If ICOGS can surpass this threshold it will be the greatest advancement in radiocarbon measurement since the advent of AMS and change the landscape of CSRA.

A1.7 Conclusions

This appendix presents the work completed to date as part of a collaborative effort to assess the viability of ICOGS for CSRA. The techniques in gas sample preparation are detailed here (Sec. A1.3.1 to A1.3.2, A1.4.2 to A1.4.3), as well as preliminary results from the measurement of the prepared gases via ICOGS. The ICOGS system has shown its usefulness in measuring $^{13}\text{C}/^{12}\text{C}$ ratios and atmospheric monitoring of $^{14}\text{CO}_2$ (Murnick and Okil 2005), but has yet to be accepted as a viable analysis system by the AMS

community for radiocarbon analysis. This appendix calls for a number of analyses in order for the ICOGS instrument to be competitive with AMS for radiocarbon analysis particularly for small samples. Essential work will be a size series to determine the minimum sample threshold, a comparison to AMS systems with the measurement of the same gas by multiple analysis systems, and the measurement of standards and materials valued by the AMS community

The original goal of this collaboration was to measure the bacterial FAME biomarkers presented in this dissertation via ICOGS. Though this goal was not realized, the contributions presented in this appendix have been important in the development of an ICOGS system capable of CSRA.

Appendix 2: Total Lipid Extraction

Soxhlet Extraction Procedure Modified from *Lipid Analysis in Marine Particles and Sediment Samples: A Laboratory Handbook* (Wakeham and Pearse 2004)

Required Supplies:

- Gloves
- Combusted aluminum foil
- Spatulas
- Soxhlet extractor
- Thimble
- Condenser
- Round bottom flask
- Teflon boiling chips
- Large tweezers (to grab the thimble when removing from the set up)
- Chiller and tubing to connect condensers
- Large graduated cylinder (for volumes greater than 300 mL, use a 1-L graduated cylinder)
- 100-mL graduated cylinder
- Large beaker for waste solvents

All glassware, spatulas and foil should be pre-baked for 6 hours at 450 °C before using for the Soxhlet extraction. All solvents are GC² Honeywell Burdick & Jackson ®).

Preparation of sediment for lipid extraction

- Transport sample from -80 °C freezer to lab in cooler with dry ice.
- Lay out a piece of combusted aluminum foil.
- Turn the sample jar upside down onto piece of combusted foil.
- Allow for sample to thaw so it can be removed from jar, using a combusted spatula if necessary to scrape the sediment onto the foil.
- Rinse combusted 500-mL round bottom flask with methanol (MeOH) using Teflon squirt bottles then repeat with dichloromethane (DCM).
- Shake into flask pre-washed Teflon boiling chips.
- Rinse Soxhlet extractor with MeOH, then DCM (be sure to squirt solvents into the side arm).
- Attach the extractor to the round bottom flask and place in cork holder inside ring stand (in case the glassware tips the ring stand close to the top of the Soxhlet extractor will prevent a loss of sample or solvent throughout the preparation of the apparatus).
- Pre-weigh baked thimbles (use the foil to transfer) taking care not to touch the sides of the thimble.
- Split the sediment from a single sample between two thimbles (for the jars used on MITAS the amount of sediment fits well in two thimbles). Fill the thimbles about half way, so the sediment level remains lower than the siphon arm when transferred to the Soxhlet extractor.
- Use foil to transfer the thimble to the balance and weigh with sediment.
- Rinse already combusted, LARGE tweezers with DCM.

- Grab the thimble with the tweezers from the top and place inside the Soxhlet extractor, angling the extractor to gently place the thimble inside.
- Remove and wash tweezers.

Soxhlet Extraction

- Prepare solvents in a large graduated cylinder.
- Measure out 9:1 DCM:MeOH solvent mixture in large graduated cylinder (315 mL DCM to 35 mL MeOH).
- Gently pour the solvent into the thimble, allowing for some fluid to go directly into the flask, but not down the side arm of the extractor (also be sure to not overfill the thimble allowing for sediment to run over the sides).
- Repeat as thimble drains until the solvent mixture is all transferred to the soxhlet extractor.
- Rinse the condenser with MeOH, then repeat with DCM.
- Move apparatus to appropriate heating well, connect the condenser and fasten with clamp.
- Repeat this process for all the samples to be extracted.
- Daisy-chain the condensers to one another with the bottom as the inlet for chilled water and the top for the outlet (to connect to the next bottom condenser).
- Be sure the chiller outlet is connected to the first apparatus' bottom port and the chiller inlet is connected to the top port of the last condenser.
- Turn on the chiller and check to make sure there are no leaks.
- Turn on the heating mantle and allow solvent to reach a low boil.

- Well 1: Just past off
 - Well 2: Just below the 1
 - Well 3: Dead
 - Well 4: 1/3 of the way between 0 and 1
 - Well 5: Dead
 - Well 6: Almost at the 2
- Allow to extract for 48 hours, check on the extractions at the 24-hour mark.

Changing the solvent ratio to increase polarity

- Turn off all heating mantles.
- Once the solutions stop boiling, take Kimwipe and wrap it around the extractor/condenser connection to remove some of the condensation formed.
- Remove the condenser and allow it to hang off the rack with clamp.
- Move the extractor and round bottom to the cork holder and ring stand set up.
- Allow remaining liquid to drain from the Soxhlet extractor.
- Angle the apparatus so the liquid at the bottom of the extractor can siphon down to the round bottom flask.
- Remove the round bottom flask and pour into a combusted 1-L Wheaton bottle.
- Reattach round bottom flask to the Soxhlet extractor.
- Rinse the cap with methanol 3 times and cover 1-L Wheaton bottle and set aside.
- Use a 2:1 DCM:MeOH mixture (250 mL DCM to 125 mL MeOH for a total of 375 mL solvent).

- Pour solvent into the top of the extractor, pouring down the sides (away from the arm) and into the thimble.
- Allow the extractor to drain and repeat until all the solvent is used.
- Move apparatus back to the same mantle and reconnect the condenser.
- Repeat with the remaining Soxhlet extractors.
- Adjust heating mantle to a slightly higher heat than previous extraction.
- Allow to extract for 24 hours.

Finish Extraction

- Turn off all the heating mantles.
- Once boiling has stopped, wipe off the condensation around the Soxhlet extractor/round bottom flask connection with a Kimwipe.
- Disconnect the condenser and allow it to hang from clamp on the ring stand.
- Move the extractor and round bottom to the cork holder and ring stand set up.
- Allow the remaining solvent to drain from the thimble and angle the extractor so the remaining solution siphons into the round bottom.
- Pour the contents of the round bottom flask into the other solvent from the same sediment.
- Pull out the thimble with combusted tweezers that have been rinsed with DCM.
- Pour off the liquid remaining at the bottom of the Soxhlet extractor.
- Cap and freeze or proceed to the next series of step for “washing the TLE”.

Washing the TLE

Required Supplies:

- Separatory funnels
- Stoppers for funnels
- Teflon stopcocks
- Large 1-L bottles (amount for number of samples processing)
- Graduated cylinder
- Scoopula
- Small tweezers (to rinse the cap for sample vials)
- Turbovap flasks
- Pasteur pipettes
- Teflon pipette bulb

Separatory Funnel Steps

- Transfer all of the all the extracted contents to a large combusted separatory funnel (1 L is preferable, if not you will to separate the extract and do twice in a 500 mL separatory funnel).

Note, if you use a funnel for this step, be sure to keep the stem from touching anything.

- Rinse round bottom or flask with DCM and transfer this wash to the separatory funnel.
- Repeat with a MeOH wash.
- Add 5% NaCl solution to form two phases (aqueous and MeOH/DCM). Solution should be 1:1 MeOH/H₂O (basically total the amount of methanol used in the extractions and add this amount of NaCl solution to the flask, in this case ~160 mL).

- Cap the separatory funnel (do not touch the ground cap or the joint), invert and open stopcock to release any pressure.
- Shake approximately 30 times, relieving built up pressure periodically.
- Place back in ring stand and drain the organic phase into a labeled and combusted solvent-rinsed bottle (like the 1-L Wheaton bottles).
- Add DCM (approximately the same volume as used of NaCl solution, ~160 mL) to the separatory funnel.
- Cap the funnel and extract the aqueous phase second time (shaking 30 times), allowing the phases to separate, then draining the organic phase into the labeled bottle. Repeat for a 3rd time with DCM.
- Discard the aqueous phase (what remains in the funnel).
- Carefully transfer the organic extracts (based on the amount of solvent used we estimated about 1/3 of the volume and transferred that, repeating 3 times) into a combusted 500 mL separatory funnel.
- Add 5% NaCl solution with a volume of approximately 1/3 the volume of organic extract being washed.
- Gently shake the separatory funnel and rest in ring stand, allowing the phases to separate.
- Collect the organic phase in a baked turbovap flask.
- Place the turbovap flask(s) in the turbovap (be sure the water level is appropriate) and set (Turbovap settings: 50 °C used sensor dried with UHP N₂ to ~1 mL volume).
- Transfer the ~1 mL sample from the turbovap flask to the sample vial using a Pasteur pipette. Rinse the turbovap flask down the sides with < 1 mL DCM. Suck up the

solvent in the pipette and squirt down the side a number of times, then transfer the solvent to the sample vial. Repeat this rinsing process with DCM and then twice with MeOH.

- Add a little pre-baked Na_2SO_4 to dry any remaining water (it should look a mix of slightly clumpy and then individual grains).
- Rinse the cap using the Teflon squirt bottles with hexane, DCM (quickly because this will eat away at the glue) and MeOH.
- Cap and secure the cap with Teflon tape. Label the sample and keep in the refrigerated room until the chromatography steps.

Appendix 3: Sample Preparation at WHOI

Saponification

- Transfer to larger vial that fits into the heat block by filtering sample through a Pasteur pipette plugged with quartz wool (pre-baked and rinsed with DCM twice) to remove the Na_2SO_4 .
- Wash vial with DCM and transfer (usually until the solvent is clear ~3 times).
Note, you can use pipette bulb to gently push liquid through.
- Rinse needles for UHP N_2 with DCM.
- Start to dry sample down with UHP N_2 , raise lab jack as the liquid level lowers, temperature control at 50 °C (at approximately 4.5).
- Prepare 0.5 M KOH (MW 56.11 g/mol) solution in 4:1 MeOH:H₂O solution.
200 mL MeOH:50 mL H₂O, weighed out 6.98 g KOH.
- Do not completely dry the sample, allow some liquid to remain.
- Add KOH solution (go above the drying line for the sample).
- Place cap and raise the temperature in the heat block to 80 °C (at 7 on the dial then turn down to 6.5 once it hits 80 °C).
- Let heat for 2 hours.
- Remove from heat block and cool.

Note, you can speed this up by placing the vial in water bath to cool.

Neutral Fraction

- Add Milli-Q water in 1:1 ratio with contents of the sample vial.
- Set heat block to 50 °C.

- Add hexane (again 1:1:1 sample:H₂O:hexane) and shake vigorously (aqueous layer on bottom, organic layer on top).
- Transfer the organic layer (top) with pipette to new vial (same size labeled as sample number with N for neutral).
- Repeat this hexane extraction 2 more times (for a total of 3 extractions).
- To the neutral sample vial add Milli-Q water and shake to wash.
- Use pipette to remove the water (the bottom layer) and transfer to a waste beaker.
- Repeat this wash process a second time.
- Add Na₂SO₄ that was pre-baked to the vial to dry sample.

Note, the neutral fraction can be stored in the refrigerator at this point until archaeal biomarker work.

- Transfer to a new clean vial with pipette and use DCM for transfer. Be sure to use a pipette with quartz wool in the tip as a filter to remove the sodium sulfate.
- Dry down with UHP N₂ gas (first rinse needle with DCM) to reduce the volume and then transfer to a 4-mL vial with DCM (rinse with DCM 3 times to transfer).
- Store in the refrigerator.

Acid Fraction

- To the remaining solution from the original vial (the TLE vial that was saponified for 2 hours) add 1:1 HCl/H₂O, mix by drawing up in pipette and the squirting out again, test the pH (want it to be acidic).
- Add 4:1 hexane to DCM (need to make a large quantity ~750 mL to use for the rest of samples) and shake to mix.
- Allow layers to separate and transfer the organic layer into another vial.

- Repeat the process 2 more times (for 3 times total).
- To the acidic sample vial add Milli-Q water and shake to wash.
- Use pipette to remove the water (the bottom layer) and transfer to a waste beaker.
- Repeat this wash process a second time.
- Add Na₂SO₄ that was pre-baked to the vial to dry sample and allow sample to sit for at least 10 minutes.

Note, this can sit overnight the refrigerator and continued the next day.

- Transfer to a new clean vial with pipette and use DCM for transfer. Be sure to use a pipette with quartz wool in the tip as a filter to remove the Na₂SO₄.
- Dry down with UHP N₂ gas (first rinse needle with DCM) to reduce the volume and then transfer to a 4-mL vial with DCM (rinse vial with DCM 3 times to transfer), then dry sample again to reduce the volume.
- Add MeOH with a known isotopic composition
- Allow to react in vial in heat block for 3 to 9 hours at 50 °C.
- Add water to create 2 layers for extraction.
- Add 10% ethyl acetate (EtOAc) in hexane, shake vigorously and extract the organic layer.
- Repeat the extraction 2 more times (for 3 times total) then wash with H₂O twice.
- Dry with Na₂SO₄ and allow the sample to dry.

Preparing sample for GC-FID

- Transfer acidic, methylated sample to a new 4-mL vial using DCM to remove the Na₂SO₄ (quartz wool in a pipette rinse with DCM, transfer sample with another

pipette through the “filter” into fresh vial). Wash Na_2SO_4 with DCM to transfer the entire sample.

- Dry sample with UHP N_2 gas to reduce the volume and remove all the polar solvent and bring it up in hexane.
- Prepare a column:
 - Pack quartz wool in pipette with short tip (use long tipped pipette or luer-lock needle to push it down);
 - Add silica gel with 5% deactivated H_2O using a long pipette as a scoop and funnel;
 - Silica gel should measure 4 cm from where the pipette diameter becomes uniform and tap to settle the silica gel;
 - Bake prepared column overnight at $450\text{ }^\circ\text{C}$ for 6 hours;
 - Rinse column with pure hexane pushing hexane through with a pipette bulb to force out air pockets (should get a color change in the gel-it looks wet);
 - Dispose hexane from column rinse.
- Label 3, 4-mL vials (FAME “F1”, “F2” and “F3”)
- Rinse vial with hexane 3 times.
- Transfer sample to column and use hexane until you reach ~4 mL.
- Add 5% ethyl acetate in hexane to column and move to collect in F2 (get 4 mL).
- Then add 10% ethyl acetate in hexane (or change to 1:4 EtOAc/DCM to elute hydroxy FAME) to the column to collect F3 for safe keeping.
- Dry down each fraction vial to approximately 0.5 mL to reduce the volume.

- Transfer to 2-mL GC vial with hexane (be sure to rinse the 4 mL vial with hexane to ensure sample is transferred) bringing volume up to 1 mL.
- Analyze with GC-FID.

Preparation for PCGC

- Combine interested F2 (FAMES) fractions together based on geochemical data provided for the core:
 - Transfer sample from GC vial used to run the F2 on GC-FID with a Pasteur pipette to a combusted and rinsed with hexane 4-mL vial;
 - Wash the GC vial 3 times with hexane and transfer each wash to the 4-mL vial;
 - Repeat this procedure for all the samples being combined;
 - Dry off the solvent using UHP N₂ to reduce the sample volume;
 - Transfer with pipette to 250-μL GC vial insert;
 - The goal is to collect as much of the original sample as possible, so the vial should be washed with hexane, dried down and added to the GC insert as needed;
 - The waste vial from the GC is also rinsed with hexane and added back to the GC vial to minimize lost sample.
- Once PCGC is done running, the sample was removed from the u-shaped trap “Trap 1” into a pre-weighed, combusted and rinsed 4-mL vial by rinsing the tube with hexane using a 500-μL syringe with 200-300 μL hexane 5 times.
- “Trap 0” was washed into a second 4-mL vial using DCM (sometimes it was hexane or a combination of the two solvents).

- “Trap 1” vial was weighed again, then 50 μ L was transferred to a GC vial insert and run on the GC-FID to confirm the collection of i-C_{15:0}, ai-C_{15:0}, and C_{16:1}.
- The contents of the insert were transferred back to the sample vial and refrigerated.
- “Trap 0” was retained for analysis via GC-IRMS.

Removing column bleed

- Prepare a column:
 - Pack quartz wool in pipette with short tip (use long tipped pipette or luer-lock needle to push it down);
 - Add silica gel with 5% deactivated H₂O using a long pipette as a scoop and funnel;
 - Silica gel should measure 4 cm from where the pipette diameter becomes uniform and tap to settle the silica gel;
 - Bake prepared column overnight at 450 °C for 6 hours;
 - Rinse column with pure hexane pushing hexane through with a pipette bulb to force out air pockets (should get a color change in the gel-it looks wet);
 - Dispose hexane from column rinse.
- Prepare 3 4-mL pre combusted vials labeling with sample name and “F1” “F2” & “F3”.
- Once column is prepared, place in vial labeled “F1” and add sample to the washed column.
- Rinse the sample vial twice with hexane and add to the column.

- After the solvent level has reached the top of the silica gel, retain the contents of “F1” and add 1.5mL 1:1 DCM:pentane to the column.
- Once all has eluted, move to “F2” and add 1:1 DCM:pentane until then volume reaches 4.5 mL.
- Transfer column to the 3rd vial and add DCM to the top on the column. Allow to drain and repeat.
- Run “F1” and “F3” on GC-FID to confirm sample is not present, retain “F2” for analysis by AMS (greater than 98% recovery of sample).

Appendix 4: Matreya LLC – Bacterial acid methyl esters CP Mix

SAVE THIS DATA SHEET!

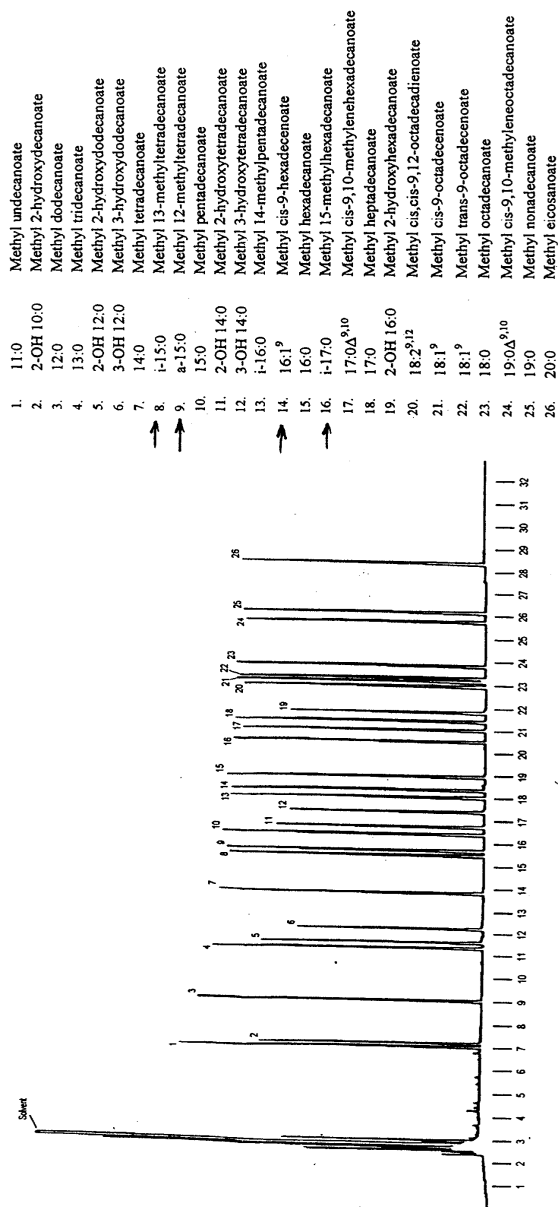
It contains important information about this product.

Bacterial acid methyl esters CP™ mix

Catalog No.: 1114

This mixture contains a total 10 mg/ml methyl esters in methyl caproate

This is a qualitative mixture composed of equal amounts of the compounds listed next to the chromatogram shown below.



SPB™-1 fused silica capillary column, 30 meter x 0.25mm I.D. x 0.20μm film thickness.

Col. Temp.: hold 4 min. at 150°C then to 250°C at 4°C/min., Inj. Temp.: 250°C, Det. Temp: 280°C

Linear Velocity: 20cm/sec, Helium, Det.: FID, Sens.: 10⁻¹¹ x 2 AFS.

Sample: 1.0μl of catalog number: 1114, Split Ratio: 100:1

Form No.: 1114DS
9/27/07



Appendix 5: Gas Chromatography Mass Spectrometry Data

This appendix presents the data from the analysis of samples from PC09 and PC13 via Gas Chromatography Mass Spectrometry data and discussed in detail in Chap. 3. Peak identifications represent the best match from the NIST05.a.L mass spectral database associated with the Agilent software.

C:\Users\Mara\Data\24FAME_OCT11\S111 F2_1.D
Wed Nov 09 14:09:41 2011

PK	RT	Area Pct	Library/ID	Ref	CAS	Qual
1	18.4411	1.594	Methyl tetradecanoate	86751	000124-10-7	95
2	20.3043	0.6696	Methyl 9-methyltetradecanoate	96259	213617-69-7	95
3	21.0301	0.5518	Pentadecanoic acid, methyl ester	96270	007132-64-1	98
4	23.0649	1.3489	9-Hexadecenoic acid, methyl ester, (Z)-	104152	001120-25-8	99
5	23.5735	8.0507	Hexadecanoic acid, methyl ester	105639	000112-39-0	98
6	25.9226	0.4556	Heptadecanoic acid, methyl ester	114854	001731-92-6	98
7	27.5401	0.3609	Hexadecanoic acid, 3,7,11,15-tetramethyl-, methyl ester	140343	001118-77-0	97
8	27.6887	0.5495	9-Octadecenoic acid, methyl ester, (E)-	122326	001937-62-8	99
9	27.8144	0.5691	8-Octadecenoic acid, methyl ester	122297	002345-29-1	99
10	28.2431	2.636	Octadecanoic acid, methyl ester	123709	000112-61-8	99
11	30.5007	0.3754	Nonadecanoic acid, methyl ester	132331	001731-94-8	98
12	33.1298	3.5736	Eicosanoic acid, methyl ester	140313	001120-28-1	98
13	35.4503	18.709	Tetracosane	146923	000646-31-1	99
14	36.2047	0.7047	Heneicosanoic acid, methyl ester	147946	006064-90-0	99
15	40.0055	7.6884	Docosanoic acid, methyl ester	154650	000929-77-1	99
16	42.8461	3.3873	Tricosanoic acid, methyl ester	160636	002433-97-8	98
17	43.4862	0.3288	Cyclononanone	18017	003350-30-9	52
18	44.3778	0.3014	Tricosane	139232	000638-67-5	97
19	45.1037	18.688	Tetracosanoic acid, methyl ester	165888	002442-49-1	99
20	46.8069	4.3033	Docosanoic acid, methyl ester	154654	000929-77-1	97
21	47.3099	0.5581	Docosanedioic acid, dimethyl ester	170755	022399-98-0	43
22	47.9786	0.328	Nonacosane	173139	000630-03-5	98
23	48.6759	14.9505	Hexacosanoic acid, methyl ester	173512	005802-82-4	95
24	50.5048	2.2026	Tetracosanoic acid, methyl ester	165888	002442-49-1	96
25	52.6881	7.1146	Octacosanoic acid, methyl ester	178460	055682-92-3	98

C:\Users\Mara\Data\24FAME_OCT11\S111 F2_2.D

Wed Nov 09 14:09:52 2011

PK	RT	Area Pct	Library/ID	Ref	CAS	Qual
1	18.4266	1.5135	Methyl tetradecanoate	86751	000124-10-7	95
2	20.2899	0.6238	Methyl 9-methyltetradecanoate	96259	213617-69-7	97
3	21.01	0.5199	Pentadecanoic acid, methyl ester	96270	007132-64-1	97
4	23.0505	1.2379	9-Hexadecenoic acid, methyl ester, (Z)-	104152	001120-25-8	99
5	23.5534	7.9638	Hexadecanoic acid, methyl ester	105639	000112-39-0	98
6	25.9139	0.4442	Heptadecanoic acid, methyl ester	114854	001731-92-6	98
7	27.68	0.5133	9-Octadecenoic acid, methyl ester, (E)-	122326	001937-62-8	99
8	27.8	0.5286	9-Octadecenoic acid, methyl ester	122299	002462-84-2	99
9	28.2287	2.6973	Octadecanoic acid, methyl ester	123709	000112-61-8	99
10	30.492	0.3569	Nonadecanoic acid, methyl ester	132330	001731-94-8	98
11	33.1154	3.5622	Eicosanoic acid, methyl ester	140313	001120-28-1	98
12	35.4359	18.527	Tetracosane	146923	000646-31-1	99
13	36.196	0.6876	Heneicosanoic acid, methyl ester	147951	006064-90-0	99
14	39.9911	7.7878	Docosanoic acid, methyl ester	154650	000929-77-1	99
15	42.8431	3.4003	Tricosanoic acid, methyl ester	160636	002433-97-8	99
16	44.3691	0.2978	Eicosane	113492	000112-95-8	98
17	45.1007	18.9555	Tetracosanoic acid, methyl ester	165890	002442-49-1	98
18	46.8039	4.2964	Docosanoic acid, methyl ester	154653	000929-77-1	98
19	47.3069	0.5919	Docosanedioic acid, dimethyl ester	170754	022399-98-0	74
20	47.9756	0.3297	Nonacosane	173139	000630-03-5	98
21	48.6786	15.1888	Hexacosanoic acid, methyl ester	173512	005802-82-4	96
22	50.5018	2.2564	Heptacosanoic acid, methyl ester	176204	055682-91-2	94
23	51.1305	0.364	Benzo[h]quinoline, 2,4-dimethyl-	62243	000605-67-4	30
24	52.6909	7.3554	Octacosanoic acid, methyl ester	178460	055682-92-3	98

C:\Users\Mara\Data\24FAME_OCT11\S111 F2_3.D

Wed Nov 09 14:10:04 2011

PK	RT	Area Pct	Library/ID	Ref	CAS	Qual
1	18.4211	1.4886	Methyl tetradecanoate	86750	000124-10-7	95
2	20.29	0.6192	Methyl 9-methyltetradecanoate	96259	213617-69-7	94
3	21.0102	0.524	Pentadecanoic acid, methyl ester	96270	007132-64-1	98
4	23.0449	1.2056	9-Hexadecenoic acid, methyl ester, (Z)-	104152	001120-25-8	99
5	23.5536	8.0494	Hexadecanoic acid, methyl ester	105639	000112-39-0	98
6	25.9083	0.4226	Heptadecanoic acid, methyl ester	114854	001731-92-6	98
7	27.6744	0.5314	9-Octadecenoic acid, methyl ester, (E)-	122326	001937-62-8	99
8	27.8001	0.5711	8-Octadecenoic acid, methyl ester	122297	002345-29-1	99
9	28.2288	2.7301	Octadecanoic acid, methyl ester	123707	000112-61-8	99
10	30.4921	0.3587	Nonadecanoic acid, methyl ester	132330	001731-94-8	99
11	33.1098	3.5856	Eicosanoic acid, methyl ester	140313	001120-28-1	98
12	35.436	18.5941	Tetracosane	146923	000646-31-1	99
13	36.1904	0.688	Heneicosanoic acid, methyl ester	147946	006064-90-0	99
14	39.9912	7.7399	Docosanoic acid, methyl ester	154650	000929-77-1	99
15	42.8375	3.4231	Tricosanoic acid, methyl ester	160636	002433-97-8	99
16	44.3693	0.2976	Heptacosane	165301	000593-49-7	98
17	45.0951	18.9572	Tetracosanoic acid, methyl ester	165890	002442-49-1	99
18	46.8041	4.3519	Docosanoic acid, methyl ester	154653	000929-77-1	97
19	47.3013	0.575	Docosanedioic acid, dimethyl ester	170754	022399-98-0	81
20	47.9757	0.3049	Eicosane	113492	000112-95-8	95
21	48.673	15.1396	Hexacosanoic acid, methyl ester	173512	005802-82-4	96
22	50.502	2.3292	Heptacosanoic acid, methyl ester	176204	055682-91-2	91
23	52.691	7.5134	Octacosanoic acid, methyl ester	178460	055682-92-3	98

C:\Users\Mara\Data\24FAME_OCT11\S112 F2_1.D
Wed Nov 09 14:10:21 2011

PK	RT	Area Pct	Library/ID	Ref	CAS	Qual
1	18.4155	1.5478	Methyl tetradecanoate	86750	000124-10-7	95
2	20.2845	0.6487	Methyl 9-methyltetradecanoate	96259	213617-69-7	93
3	21.0047	0.5193	Pentadecanoic acid, methyl ester	96270	007132-64-1	95
4	23.0451	1.5163	7-Hexadecenoic acid, methyl ester, (Z)-	104151	056875-67-3	99
5	23.5423	7.8697	Hexadecanoic acid, methyl ester	105639	000112-39-0	98
6	25.9085	0.4233	Heptadecanoic acid, methyl ester	114854	001731-92-6	98
7	27.6746	0.5853	9-Octadecenoic acid, methyl ester, (E)-	122326	001937-62-8	99
8	27.7946	0.6292	11-Octadecenoic acid, methyl ester	122316	052380-33-3	99
9	28.2233	2.8003	Octadecanoic acid, methyl ester	123709	000112-61-8	99
10	30.4923	0.3488	Nonadecanoic acid, methyl ester	132330	001731-94-8	98
11	33.1043	3.4859	Eicosanoic acid, methyl ester	140313	001120-28-1	98
12	35.419	20.1167	Tetracosane	146923	000646-31-1	99
13	36.1906	0.7075	Heneicosanoic acid, methyl ester	147951	006064-90-0	97
14	39.98	8.0226	Docosanoic acid, methyl ester	154650	000929-77-1	99
15	42.832	3.6494	Tricosanoic acid, methyl ester	160643	002433-97-8	98
16	43.4721	0.4735	6-Octadecenoic acid, methyl ester	122301	052355-31-4	47
17	45.0839	19.2585	Tetracosanoic acid, methyl ester	165888	002442-49-1	99
18	46.7928	4.2466	Docosanoic acid, methyl ester	154653	000929-77-1	98
19	47.3015	0.7235	Docosanedioic acid, dimethyl ester	170755	022399-98-0	76
20	48.6504	13.7929	Hexacosanoic acid, methyl ester	173512	005802-82-4	95
21	50.4907	1.8993	Tetracosanoic acid, methyl ester	165887	002442-49-1	94
22	51.1309	0.4898	3-(1-Methyl-piperidin-2-yl)-octahydro-quinolizine-1-carboxylic acid	111810	1000296-60-0	25
23	52.6626	6.2451	Octacosanoic acid, methyl ester	178460	055682-92-3	98

C:\Users\Mara\Data\24FAME_OCT11\S112 F2_2.D
Wed Nov 09 14:10:31 2011

PK	RT	Area Pct	Library/ID	Ref	CAS	Qual
1	18.4149	1.5873	Methyl tetradecanoate	86750	000124-10-7	95
2	20.2781	0.6682	Tetradecanoic acid, 12-methyl-, methyl ester	96284	005129-66-8	83
3	21.004	0.533	Pentadecanoic acid, methyl ester	96270	007132-64-1	98
4	23.0387	1.5817	9-Hexadecenoic acid, methyl ester, (Z)-	104152	001120-25-8	99
5	23.5416	8.1786	Hexadecanoic acid, methyl ester	105639	000112-39-0	98
6	25.9078	0.4476	Heptadecanoic acid, methyl ester	114854	001731-92-6	99
7	27.6739	0.6132	8-Octadecenoic acid, methyl ester	122297	002345-29-1	99
8	27.7939	0.651	11-Octadecenoic acid, methyl ester	122316	052380-33-3	99
9	28.2226	2.9179	Octadecanoic acid, methyl ester	123709	000112-61-8	99
10	30.4859	0.3658	Nonadecanoic acid, methyl ester	132330	001731-94-8	98
11	33.1036	3.6708	Eicosanoic acid, methyl ester	140314	001120-28-1	98
12	35.3955	17.6273	Tetracosane	146923	000646-31-1	99
13	36.1785	0.75	Heneicosanoic acid, methyl ester	147951	006064-90-0	97
14	39.9736	8.3107	Docosanoic acid, methyl ester	154650	000929-77-1	99
15	42.8313	3.8685	Tricosanoic acid, methyl ester	160636	002433-97-8	98
16	43.4772	0.4574	16-Octadecenoic acid, methyl ester	122315	056554-49-5	81
17	45.0775	20.0419	Tetracosanoic acid, methyl ester	165890	002442-49-1	98
18	46.7921	4.3609	Docosanoic acid, methyl ester	154653	000929-77-1	98
19	47.3008	0.7472	Docosanedioic acid, dimethyl ester	170755	022399-98-0	68
20	48.6497	14.0119	Hexacosanoic acid, methyl ester	173512	005802-82-4	95
21	50.4901	2.0336	Tetracosanoic acid, methyl ester	165887	002442-49-1	95
22	52.6562	6.5755	Octacosanoic acid, methyl ester	178460	055682-92-3	98

C:\Users\Mara\Data\24FAME_OCT11\S112 F2_3.D
Wed Nov 09 14:10:39 2011

PK	RT	Area Pct	Library/ID	Ref	CAS	Qual
1	18.421	1.6066	Methyl tetradecanoate	86750	000124-10-7	94
2	20.2785	0.6725	Methyl 9-methyltetradecanoate	96259	213617-69-7	92
3	21.0043	0.5466	Pentadecanoic acid, methyl ester	96270	007132-64-1	97
4	23.0448	1.6335	9-Hexadecenoic acid, methyl ester, (Z)-	104152	001120-25-8	99
5	23.542	8.3889	Hexadecanoic acid, methyl ester	105639	000112-39-0	98
6	27.6743	0.6093	9-Octadecenoic acid, methyl ester, (E)-	122326	001937-62-8	99
7	27.7943	0.6277	11-Octadecenoic acid, methyl ester	122316	052380-33-3	99
8	28.223	2.9113	Octadecanoic acid, methyl ester	123709	000112-61-8	99
9	30.4863	0.3712	Nonadecanoic acid, methyl ester	132331	001731-94-8	99
10	33.104	3.6941	Eicosanoic acid, methyl ester	140313	001120-28-1	98
11	35.3845	16.6657	Tetracosane	146923	000646-31-1	99
12	36.1789	0.7537	Heptadecanoic acid, 16-methyl-, methyl ester	123729	005129-61-3	97
13	39.974	8.4165	Docosanoic acid, methyl ester	154650	000929-77-1	99
14	42.8317	3.8455	Tricosanoic acid, methyl ester	160636	002433-97-8	99
15	43.4719	0.4848	2-Benzothiazolesulfenamide, N-cyclohexyl-	101041	000095-33-0	38
16	45.0779	20.3819	Tetracosanoic acid, methyl ester	165888	002442-49-1	98
17	46.7925	4.5166	Docosanoic acid, methyl ester	154653	000929-77-1	98
18	47.2955	0.7679	Docosanedioic acid, dimethyl ester	170755	022399-98-0	70
19	48.6501	14.4607	Hexacosanoic acid, methyl ester	173512	005802-82-4	97
20	50.4847	1.9977	Tetracosanoic acid, methyl ester	165888	002442-49-1	91
21	52.6566	6.6473	Octacosanoic acid, methyl ester	178460	055682-92-3	98

C:\Users\Mara\Data\24FAME_OCT11\S113 F2_1.D
Wed Nov 09 14:10:54 2011

PK	RT	Area Pct	Library/ID	Ref	CAS	Qual
1	18.4158	1.7668	Methyl tetradecanoate	86750	000124-10-7	95
2	20.2847	0.7236	Methyl 9-methyltetradecanoate	96259	213617-69-7	93
3	21.0049	0.6624	Pentadecanoic acid, methyl ester	96270	007132-64-1	98
4	23.0453	1.755	9-Hexadecenoic acid, methyl ester, (Z)-	104152	001120-25-8	99
5	23.554	8.538	Hexadecanoic acid, methyl ester	105639	000112-39-0	98
6	25.9087	0.5012	Heptadecanoic acid, methyl ester	114854	001731-92-6	98
7	27.5205	0.4102	Hexadecanoic acid, 3,7,11,15-tetramethyl-, methyl ester	140345	001118-77-0	94
8	27.6748	0.6779	9-Octadecenoic acid, methyl ester, (E)-	122326	001937-62-8	99
9	27.7948	0.6582	11-Octadecenoic acid, methyl ester, (Z)-	122331	001937-63-9	99
10	28.2292	2.9829	Octadecanoic acid, methyl ester	123709	000112-61-8	99
11	30.4868	0.4129	Nonadecanoic acid, methyl ester	132330	001731-94-8	98
12	33.1159	3.9632	Eicosanoic acid, methyl ester	140313	001120-28-1	98
13	35.3621	10.1731	Tetracosane	146921	000646-31-1	99
14	36.1794	0.8347	Heneicosanoic acid, methyl ester	147951	006064-90-0	99
15	40.0031	9.0708	Docosanoic acid, methyl ester	154650	000929-77-1	99
16	42.8437	4.0711	Tricosanoic acid, methyl ester	160636	002433-97-8	98
17	43.4724	0.3463	13-Octadecenoic acid, methyl ester	122313	056554-47-3	43
18	45.107	21.7432	Tetracosanoic acid, methyl ester	165888	002442-49-1	99
19	46.8045	4.7103	Docosanoic acid, methyl ester	154653	000929-77-1	97
20	47.3017	0.7086	Docosanedioic acid, dimethyl ester	170755	022399-98-0	87
21	48.6734	15.3224	Hexacosanoic acid, methyl ester	173512	005802-82-4	95
22	50.4967	2.1642	Tetracosanoic acid, methyl ester	165887	002442-49-1	95
23	51.1311	0.5649	Cyclobutanone, 2-tetradecyl-	102835	035493-47-1	25
24	52.68	7.2382	Octacosanoic acid, methyl ester	178460	055682-92-3	98

C:\Users\Mara\Data\24FAME_OCT11\S113 F2_2.D
Wed Nov 09 14:11:06 2011

PK	RT	Area Pct	Library/ID	Ref	CAS	Qual
1	18.4268	1.7825	Methyl tetradecanoate	86750	000124-10-7	95
2	20.2843	0.727	Methyl 9-methyltetradecanoate	96259	213617-69-7	95
3	21.0102	0.6734	Pentadecanoic acid, methyl ester	96270	007132-64-1	97
4	23.0506	1.7984	9-Hexadecenoic acid, methyl ester, (Z)-	104152	001120-25-8	99
5	23.5593	8.6191	Hexadecanoic acid, methyl ester	105639	000112-39-0	98
6	25.914	0.4968	Heptadecanoic acid, methyl ester	114854	001731-92-6	99
7	27.5258	0.4121	Hexadecanoic acid, 3,7,11,15-tetramethyl-, methyl ester	140342	001118-77-0	97
8	27.6744	0.6767	9-Octadecenoic acid, methyl ester, (E)-	122326	001937-62-8	99
9	27.7944	0.663	8-Octadecenoic acid, methyl ester	122297	002345-29-1	99
10	28.2288	3.0091	Octadecanoic acid, methyl ester	123709	000112-61-8	99
11	30.4921	0.4023	Nonadecanoic acid, methyl ester	132330	001731-94-8	98
12	33.1155	4.0209	Eicosanoic acid, methyl ester	140312	001120-28-1	98
13	35.3617	10.0338	Tetracosane	146923	000646-31-1	99
14	36.179	0.8384	Heneicosanoic acid, methyl ester	147946	006064-90-0	99
15	40.0027	9.0865	Docosanoic acid, methyl ester	154650	000929-77-1	99
16	42.8432	4.0434	Tricosanoic acid, methyl ester	160643	002433-97-8	99
17	43.472	0.3116	1-(3,3,3-Trifluoro-2-hydroxypropyl)piperidine	55182	1000283-75-5	38
18	45.1066	21.7189	Tetracosanoic acid, methyl ester	165890	002442-49-1	98
19	46.8041	4.6247	Docosanoic acid, methyl ester	154653	000929-77-1	97
20	47.3013	0.7081	Docosanedioic acid, dimethyl ester	170755	022399-98-0	74
21	48.673	15.4167	Hexacosanoic acid, methyl ester	173513	005802-82-4	95
22	50.4905	2.1615	Heptacosanoic acid, methyl ester	176206	055682-91-2	95
23	51.1249	0.5686	Tridecanedioic acid, dimethyl ester	106737	001472-87-3	38
24	52.6796	7.2064	Octacosanoic acid, methyl ester	178460	055682-92-3	98

C:\Users\Mara\Data\24FAME_OCT11\S113 F2_3.D

Wed Nov 09 14:11:20 2011

PK	RT	Area Pct	Library/ID	Ref	CAS	Qual
1	18.4211	1.7804	Methyl tetradecanoate	86750	000124-10-7	95
2	20.2843	0.7259	Methyl 9-methyltetradecanoate	96259	213617-69-7	94
3	21.0102	0.6892	Pentadecanoic acid, methyl ester	96270	007132-64-1	98
4	23.0506	1.7703	9-Hexadecenoic acid, methyl ester, (Z)-	104152	001120-25-8	99
5	23.5593	8.6647	Hexadecanoic acid, methyl ester	105639	000112-39-0	98
6	25.9083	0.4901	Heptadecanoic acid, methyl ester	114852	001731-92-6	98
7	27.5201	0.4051	Hexadecanoic acid, 3,7,11,15-tetramethyl-, methyl ester	140342	001118-77-0	97
8	27.6744	0.6837	9-Octadecenoic acid, methyl ester, (E)-	122326	001937-62-8	99
9	27.7945	0.6746	11-Octadecenoic acid, methyl ester	122316	052380-33-3	99
10	28.2288	2.9866	Octadecanoic acid, methyl ester	123709	000112-61-8	99
11	30.4865	0.4208	Nonadecanoic acid, methyl ester	132330	001731-94-8	98
12	33.1155	3.9509	Eicosanoic acid, methyl ester	140313	001120-28-1	98
13	35.356	10.0617	Tetracosane	146923	000646-31-1	99
14	36.179	0.7922	Heneicosanoic acid, methyl ester	147951	006064-90-0	99
15	40.0027	9.0186	Docosanoic acid, methyl ester	154650	000929-77-1	99
16	42.8433	4.0855	Tricosanoic acid, methyl ester	160636	002433-97-8	99
17	43.472	0.363	2,3-Dihydro-6-hydroxy-3-oxo-2-(piperidinomethyl)pyridazine	63472	014628-38-7	41
18	45.1066	21.8252	Tetracosanoic acid, methyl ester	165890	002442-49-1	98
19	46.7984	4.6461	Docosanoic acid, methyl ester	154647	000929-77-1	96
20	47.3013	0.6972	Docosanedioic acid, dimethyl ester	170755	022399-98-0	87
21	48.6731	15.427	Hexacosanoic acid, methyl ester	173512	005802-82-4	96
22	50.4906	2.1059	Heptacosanoic acid, methyl ester	176204	055682-91-2	94
23	51.125	0.544	Cyclopentaneundecanoic acid, methyl ester	104158	025779-85-5	38
24	52.6796	7.1914	Octacosanoic acid, methyl ester	178460	055682-92-3	98

C:\Users\Mara\Data\24FAME_OCT11\S114 F2_1.D

Wed Nov 09 14:11:33 2011

PK	RT	Area Pct	Library/ID	Ref	CAS	Qual
1	18.4151	1.2783	Methyl tetradecanoate	86750	000124-10-7	94
2	23.0389	1.2697	9-Hexadecenoic acid, methyl ester, (Z)-	104152	001120-25-8	99
3	23.519	6.6859	Pentadecanoic acid, 14-methyl-, methyl ester	105662	005129-60-2	99
4	28.2114	2.3179	Octadecanoic acid, methyl ester	123709	000112-61-8	99
5	33.081	2.8044	Eicosanoic acid, methyl ester	140313	001120-28-1	99
6	35.3957	33.022	Tetracosane	146923	000646-31-1	99
7	39.9224	6.6096	Docosanoic acid, methyl ester	154650	000929-77-1	99
8	42.803	3.3769	Tricosanoic acid, methyl ester	160636	002433-97-8	99
9	45.032	18.2641	Tetracosanoic acid, methyl ester	165890	002442-49-1	99
10	46.7695	4.0178	Docosanoic acid, methyl ester	154647	000929-77-1	98
11	48.6042	13.0905	Hexacosanoic acid, methyl ester	173512	005802-82-4	95
12	50.4674	1.8744	Heptacosanoic acid, methyl ester	176204	055682-91-2	93
13	52.6107	5.3885	Octacosanoic acid, methyl ester	178460	055682-92-3	98

C:\Users\Mara\Data\24FAME_OCT11\S114 F2_2.D

Wed Nov 09 14:11:52 2011

PK	RT	Area Pct	Library/ID	Ref	CAS	Qual
1	18.4126	1.2521	Methyl tetradecanoate	86753	000124-10-7	95
2	23.0365	1.235	9-Hexadecenoic acid, methyl ester, (Z)-	104152	001120-25-8	97
3	23.5165	6.6582	Hexadecanoic acid, methyl ester	105639	000112-39-0	98
4	28.209	2.2682	Octadecanoic acid, methyl ester	123707	000112-61-8	99
5	33.0785	2.7452	Eicosanoic acid, methyl ester	140313	001120-28-1	98
6	35.399	33.2959	Tetracosane	146923	000646-31-1	99
7	39.92	6.5642	Docosanoic acid, methyl ester	154650	000929-77-1	99
8	42.8062	3.3357	Tricosanoic acid, methyl ester	160636	002433-97-8	99
9	45.0296	18.2328	Tetracosanoic acid, methyl ester	165890	002442-49-1	99
10	46.7671	4.0711	Docosanoic acid, methyl ester	154654	000929-77-1	98
11	48.6075	13.0007	Hexacosanoic acid, methyl ester	173512	005802-82-4	95
12	50.465	1.8827	Heptacosanoic acid, methyl ester	176206	055682-91-2	91
13	52.614	5.4582	Octacosanoic acid, methyl ester	178460	055682-92-3	98

C:\Users\Mara\Data\24FAME_OCT11\S114 F2_3.D
Wed Nov 09 14:12:05 2011

PK	RT	Area Pct	Library/ID	Ref	CAS	Qual
1	18.4143	1.268	Methyl tetradecanoate	86753	000124-10-7	94
2	23.0381	1.2175	9-Hexadecenoic acid, methyl ester, (Z)-	104152	001120-25-8	99
3	23.5182	6.6891	Hexadecanoic acid, methyl ester	105639	000112-39-0	98
4	28.2049	2.2763	Octadecanoic acid, methyl ester	123709	000112-61-8	99
5	33.0802	2.7594	Eicosanoic acid, methyl ester	140313	001120-28-1	98
6	35.395	33.5566	Tetracosane	146923	000646-31-1	99
7	39.9159	6.5323	Docosanoic acid, methyl ester	154650	000929-77-1	99
8	42.8022	3.3741	Tricosanoic acid, methyl ester	160636	002433-97-8	98
9	45.0313	18.3552	Tetracosanoic acid, methyl ester	165888	002442-49-1	99
10	46.7687	4.0859	Docosanoic acid, methyl ester	154654	000929-77-1	99
11	48.6034	12.6852	Hexacosanoic acid, methyl ester	173512	005802-82-4	95
12	50.4667	1.8389	Heptacosanoic acid, methyl ester	176204	055682-91-2	90
13	52.6099	5.3616	Octacosanoic acid, methyl ester	178460	055682-92-3	98

C:\Users\Mara\Data\24FAME_OCT11\S118_5 F2_1.D
Wed Nov 09 14:12:15 2011

PK	RT	Area Pct	Library/ID	Ref	CAS	Qual
1	18.4177	1.8449	Methyl tetradecanoate	86750	000124-10-7	95
2	20.281	0.905	Methyl 9-methyltetradecanoate	96259	213617-69-7	92
3	21.0068	0.5015	Pentadecanoic acid, methyl ester	96270	007132-64-1	98
4	23.0415	1.757	9-Hexadecenoic acid, methyl ester, (Z)-	104152	001120-25-8	99
5	23.5445	9.832	Hexadecanoic acid, methyl ester	105639	000112-39-0	98
6	25.905	0.5425	Heptadecanoic acid, methyl ester	114854	001731-92-6	98
7	27.6654	0.6856	8-Octadecenoic acid, methyl ester	122297	002345-29-1	99
8	27.7911	0.7201	11-Octadecenoic acid, methyl ester, (Z)-	122331	001937-63-9	99
9	28.2198	3.3997	Octadecanoic acid, methyl ester	123709	000112-61-8	99
10	30.4831	0.4434	Nonadecanoic acid, methyl ester	132331	001731-94-8	98
11	33.1007	4.2898	Eicosanoic acid, methyl ester	140313	001120-28-1	98
12	35.3469	12.4421	Tetracosane	146923	000646-31-1	99
13	36.1643	0.8371	Heneicosanoic acid, methyl ester	147946	006064-90-0	99
14	39.965	9.1092	Docosanoic acid, methyl ester	154650	000929-77-1	99
15	42.8228	3.9913	Tricosanoic acid, methyl ester	160636	002433-97-8	99
16	45.0746	20.8259	Tetracosanoic acid, methyl ester	165888	002442-49-1	99
17	46.7836	4.5365	Docosanoic acid, methyl ester	154653	000929-77-1	98
18	47.2923	0.7293	Docosanedioic acid, dimethyl ester	170754	022399-98-0	90
19	48.6411	14.275	Hexacosanoic acid, methyl ester	173512	005802-82-4	97
20	50.4758	2.0271	Tetracosanoic acid, methyl ester	165887	002442-49-1	99
21	52.6419	6.3049	Octacosanoic acid, methyl ester	178460	055682-92-3	98

C:\Users\Mara\Data\24FAME_OCT11\S118_5 F2_2.D
Wed Nov 09 14:12:23 2011

PK	RT	Area Pct	Library/ID	Ref	CAS	Qual
1	18.4143	1.8555	Tridecanoic acid, 12-methyl-, methyl ester	86778	005129-58-8	95
2	20.2775	0.9133	Methyl 9-methyltetradecanoate	96259	213617-69-7	93
3	21.0034	0.5084	Pentadecanoic acid, methyl ester	96270	007132-64-1	98
4	23.0438	1.7581	9-Hexadecenoic acid, methyl ester, (Z)-	104152	001120-25-8	99
5	23.5468	9.8324	Hexadecanoic acid, methyl ester	105639	000112-39-0	98
6	25.9015	0.5378	Heptadecanoic acid, methyl ester	114854	001731-92-6	99
7	27.6676	0.6988	9-Octadecenoic acid, methyl ester, (E)-	122326	001937-62-8	99
8	27.7876	0.7331	11-Octadecenoic acid, methyl ester	122316	052380-33-3	99
9	28.222	3.3992	Octadecanoic acid, methyl ester	123709	000112-61-8	99
10	30.4854	0.4449	Nonadecanoic acid, methyl ester	132329	001731-94-8	95
11	33.103	4.2908	Eicosanoic acid, methyl ester	140313	001120-28-1	98
12	35.3492	12.511	Tetracosane	146923	000646-31-1	99
13	36.1665	0.8545	Heneicosanoic acid, methyl ester	147946	006064-90-0	98
14	39.9673	9.1338	Docosanoic acid, methyl ester	154650	000929-77-1	99
15	42.8193	3.9876	Tricosanoic acid, methyl ester	160636	002433-97-8	99
16	45.0712	20.7821	Tetracosanoic acid, methyl ester	165888	002442-49-1	99
17	46.7859	4.4663	Pentacosanoic acid, methyl ester	170267	055373-89-2	98
18	47.2888	0.7217	Docosanedioic acid, dimethyl ester	170755	022399-98-0	62
19	48.6377	14.2498	Hexacosanoic acid, methyl ester	173512	005802-82-4	96
20	50.4781	2.0276	Tetracosanoic acid, methyl ester	165888	002442-49-1	97
21	52.6442	6.2937	Octacosanoic acid, methyl ester	178460	055682-92-3	98

C:\Users\Mara\Data\24FAME_OCT11\S118_5 F2_3.D

Wed Nov 09 14:12:35 2011

PK	RT	Area Pct	Library/ID	Ref	CAS	Qual
1	18.4178	1.8107	Methyl tetradecanoate	86750	000124-10-7	95
2	20.281	0.9066	Methyl 9-methyltetradecanoate	96259	213617-69-7	95
3	21.0069	0.5082	Pentadecanoic acid, methyl ester	96270	007132-64-1	98
4	23.0416	1.7685	9-Hexadecenoic acid, methyl ester, (Z)-	104152	001120-25-8	99
5	23.5503	9.8807	Hexadecanoic acid, methyl ester	105639	000112-39-0	98
6	25.9051	0.5368	Heptadecanoic acid, methyl ester	114854	001731-92-6	98
7	27.6711	0.6865	9-Octadecenoic acid, methyl ester, (E)-	122326	001937-62-8	99
8	27.7911	0.7256	9-Octadecenoic acid (Z)-, methyl ester	122323	000112-62-9	99
9	28.2198	3.3848	Octadecanoic acid, methyl ester	123709	000112-61-8	99
10	30.4831	0.4435	Nonadecanoic acid, methyl ester	132330	001731-94-8	98
11	33.1008	4.3027	Eicosanoic acid, methyl ester	140313	001120-28-1	98
12	35.347	12.6434	Tetracosane	146923	000646-31-1	99
13	36.1643	0.8801	Heneicosanoic acid, methyl ester	147951	006064-90-0	99
14	39.9708	9.0396	Docosanoic acid, methyl ester	154650	000929-77-1	99
15	42.8228	3.9857	Tricosanoic acid, methyl ester	160636	002433-97-8	98
16	45.0747	20.8028	Tetracosanoic acid, methyl ester	165890	002442-49-1	98
17	46.7837	4.4621	Docosanoic acid, methyl ester	154653	000929-77-1	97
18	47.2923	0.7137	Docosanedioic acid, dimethyl ester	170754	022399-98-0	68
19	48.6412	14.3102	Hexacosanoic acid, methyl ester	173512	005802-82-4	96
20	50.4759	1.9976	Tetracosanoic acid, methyl ester	165887	002442-49-1	94
21	52.642	6.2102	Octacosanoic acid, methyl ester	178460	055682-92-3	98

C:\Users\Mara\Data\24FAME_OCT11\S119 F2_1.D

Wed Nov 09 14:12:42 2011

PK	RT	Area Pct	Library/ID	Ref	CAS	Qual
1	18.4154	1.4642	Methyl tetradecanoate	86750	000124-10-7	95
2	20.2786	0.8841	Methyl 9-methyltetradecanoate	96259	213617-69-7	94
3	23.0392	1.4126	9-Hexadecenoic acid, methyl ester, (Z)-	104152	001120-25-8	99
4	23.5364	7.7161	Hexadecanoic acid, methyl ester	105639	000112-39-0	98
5	25.9026	0.4464	Heptadecanoic acid, methyl ester	114854	001731-92-6	98
6	27.6687	0.6123	9-Octadecenoic acid, methyl ester, (E)-	122326	001937-62-8	99
7	27.7887	0.5076	8-Octadecenoic acid, methyl ester	122297	002345-29-1	99
8	28.2174	2.6822	Octadecanoic acid, methyl ester	123709	000112-61-8	99
9	30.4807	0.3907	Nonadecanoic acid, methyl ester	132330	001731-94-8	98
10	33.0927	3.1953	Eicosanoic acid, methyl ester	140313	001120-28-1	99
11	35.4303	24.6501	Tetracosane	146923	000646-31-1	99
12	36.1733	0.759	Heneicosanoic acid, methyl ester	147946	006064-90-0	99
13	39.957	7.4729	Docosanoic acid, methyl ester	154650	000929-77-1	99
14	42.8204	3.7148	Tricosanoic acid, methyl ester	160643	002433-97-8	98
15	43.4663	0.5055	13-Octadecenoic acid, methyl ester	122313	056554-47-3	35
16	45.0666	18.3694	Tetracosanoic acid, methyl ester	165888	002442-49-1	98
17	46.7812	4.1854	Docosanoic acid, methyl ester	154647	000929-77-1	97
18	47.2899	0.8954	Docosanedioic acid, dimethyl ester	170755	022399-98-0	81
19	48.633	12.6829	Hexacosanoic acid, methyl ester	173512	005802-82-4	95
20	50.4734	1.792	Tetracosanoic acid, methyl ester	165887	002442-49-1	94
21	51.1193	0.5745	9-Octadecenoic acid (Z)-, methyl ester	122321	000112-62-9	41
22	52.6281	5.0867	Octacosanoic acid, methyl ester	178460	055682-92-3	98

C:\Users\Mara\Data\24FAME_OCT11\S119 F2_2.D
Wed Nov 09 14:12:53 2011

PK	RT	Area Pct	Library/ID	Ref	CAS	Qual
1	18.4126	1.4569	Methyl tetradecanoate	86753	000124-10-7	95
2	20.2758	0.8866	Methyl 9-methyltetradecanoate	96259	213617-69-7	86
3	23.0364	1.38	9-Hexadecenoic acid, methyl ester, (Z)-	104152	001120-25-8	99
4	23.5337	7.7116	Hexadecanoic acid, methyl ester	105639	000112-39-0	98
5	25.8999	0.4591	Heptadecanoic acid, methyl ester	114854	001731-92-6	99
6	27.6659	0.6287	9-Octadecenoic acid, methyl ester, (E)-	122326	001937-62-8	99
7	27.786	0.6205	9-Octadecenoic acid, methyl ester	122299	002462-84-2	99
8	28.2146	2.6638	Octadecanoic acid, methyl ester	123709	000112-61-8	99
9	30.4837	0.3956	Nonadecanoic acid, methyl ester	132330	001731-94-8	98
10	33.0899	3.2198	Eicosanoic acid, methyl ester	140313	001120-28-1	99
11	35.4275	24.4596	Tetracosane	146923	000646-31-1	99
12	36.1763	0.7452	Heneicosanoic acid, methyl ester	147951	006064-90-0	97
13	39.9542	7.4732	Docosanoic acid, methyl ester	154650	000929-77-1	99
14	42.8177	3.6905	Tricosanoic acid, methyl ester	160643	002433-97-8	98
15	43.4635	0.4819	9-Octadecenoic acid (Z)-, methyl ester	122321	000112-62-9	46
16	45.0638	18.4324	Tetracosanoic acid, methyl ester	165888	002442-49-1	98
17	46.7785	4.1034	Docosanoic acid, methyl ester	154654	000929-77-1	98
18	47.2929	0.9209	Docosanedioic acid, dimethyl ester	170755	022399-98-0	87
19	48.6303	12.7574	Hexacosanoic acid, methyl ester	173512	005802-82-4	95
20	50.4764	1.7847	Tetracosanoic acid, methyl ester	165887	002442-49-1	95
21	51.1165	0.597	9-Octadecenoic acid (Z)-, methyl ester	122321	000112-62-9	20
22	52.6311	5.1313	Octacosanoic acid, methyl ester	178460	055682-92-3	98

C:\Users\Mara\Data\24FAME_OCT11\S119 F2_3.D
Wed Nov 09 14:13:07 2011

PK	RT	Area Pct	Library/ID	Ref	CAS	Qual
1	18.4143	1.4316	Methyl tetradecanoate	86750	000124-10-7	94
2	20.2718	0.8769	Tetradecanoic acid, 12-methyl-, methyl ester	96284	005129-66-8	86
3	23.0381	1.4	9-Hexadecenoic acid, methyl ester, (Z)-	104152	001120-25-8	99
4	23.5353	7.6973	Hexadecanoic acid, methyl ester	105639	000112-39-0	98
5	25.9072	0.4492	Heptadecanoic acid, methyl ester	114854	001731-92-6	99
6	27.6676	0.6247	8-Octadecenoic acid, methyl ester	122297	002345-29-1	99
7	27.7933	0.6123	11-Octadecenoic acid, methyl ester	122316	052380-33-3	99
8	28.2163	2.6495	Octadecanoic acid, methyl ester	123709	000112-61-8	99
9	30.4796	0.3934	Nonadecanoic acid, methyl ester	132330	001731-94-8	98
10	33.0916	3.2169	Eicosanoic acid, methyl ester	140310	001120-28-1	98
11	35.4292	24.4163	Tetracosane	146923	000646-31-1	99
12	36.1837	0.7425	Heneicosanoic acid, methyl ester	147946	006064-90-0	99
13	39.9558	7.4242	Docosanoic acid, methyl ester	154650	000929-77-1	99
14	42.8193	3.7079	Tricosanoic acid, methyl ester	160636	002433-97-8	99
15	43.4652	0.4913	16-Octadecenoic acid, methyl ester	122315	056554-49-5	60
16	45.0655	18.5173	Tetracosanoic acid, methyl ester	165890	002442-49-1	99
17	46.7801	4.1968	Docosanoic acid, methyl ester	154654	000929-77-1	98
18	47.2945	0.9103	Docosanedioic acid, dimethyl ester	170755	022399-98-0	87
19	48.6319	12.779	Hexacosanoic acid, methyl ester	173512	005802-82-4	95
20	50.4723	1.807	Heptacosanoic acid, methyl ester	176206	055682-91-2	93
21	51.1182	0.5451	2-(Heptadec-10-enyl)-N-methylimidazoline(Z)	137104	1000280-19-2	18
22	52.6328	5.1106	Octacosanoic acid, methyl ester	178460	055682-92-3	98

C:\Users\Mara\Data\24FAME_OCT11\S119_5 F2_1.D
Wed Nov 09 14:13:27 2011

PK	RT	Area Pct	Library/ID	Ref	CAS	Qual
1	18.4152	1.5754	Methyl tetradecanoate	86750	000124-10-7	95
2	20.2784	1.0512	Tridecanoic acid, 12-methyl-, methyl ester	86778	005129-58-8	83
3	23.039	1.5774	9-Hexadecenoic acid, methyl ester, (Z)-	104152	001120-25-8	99
4	23.5362	8.7009	Hexadecanoic acid, methyl ester	105639	000112-39-0	98
5	27.6685	0.7412	9-Octadecenoic acid, methyl ester, (E)-	122326	001937-62-8	99
6	27.7942	0.7282	9-Octadecenoic acid, methyl ester, (E)-	122326	001937-62-8	99
7	28.2172	2.7401	Octadecanoic acid, methyl ester	123708	000112-61-8	98
8	30.4805	0.4096	Nonadecanoic acid, methyl ester	132330	001731-94-8	98
9	33.0868	3.4083	Eicosanoic acid, methyl ester	140314	001120-28-1	98
10	35.3558	16.7497	Tetracosane	146921	000646-31-1	99
11	36.1674	0.7797	Heneicosanoic acid, methyl ester	147946	006064-90-0	99
12	39.9453	7.7681	Docosanoic acid, methyl ester	154650	000929-77-1	99
13	42.8145	3.7838	Tricosanoic acid, methyl ester	160636	002433-97-8	99
14	43.466	0.5688	2-Dodecylcyclobutanone	83998	035493-46-0	41
15	45.0607	19.939	Tetracosanoic acid, methyl ester	165888	002442-49-1	99
16	46.781	4.5105	Docosanoic acid, methyl ester	154654	000929-77-1	97
17	47.2897	1.0847	Docosanedioic acid, dimethyl ester	170755	022399-98-0	64
18	48.6328	14.8091	Hexacosanoic acid, methyl ester	173512	005802-82-4	95
19	50.4732	2.1822	Tetracosanoic acid, methyl ester	165887	002442-49-1	95
20	51.1191	0.6279	Tridecanoic acid, methyl ester	77301	001731-88-0	20
21	52.6337	6.2641	Octacosanoic acid, methyl ester	178460	055682-92-3	98

C:\Users\Mara\Data\24FAME_OCT11\S119_5 F2_2.D
Wed Nov 09 14:13:39 2011

PK	RT	Area Pct	Library/ID	Ref	CAS	Qual
1	18.4149	1.57	Methyl tetradecanoate	86750	000124-10-7	95
2	20.2839	1.0759	Tetradecanoic acid, 12-methyl-, methyl ester	96284	005129-66-8	86
3	23.0387	1.6126	7-Hexadecenoic acid, methyl ester, (Z)-	104151	056875-67-3	99
4	23.536	8.7639	Hexadecanoic acid, methyl ester	105639	000112-39-0	98
5	27.6682	0.7454	9-Octadecenoic acid, methyl ester, (E)-	122326	001937-62-8	99
6	27.7883	0.7301	9-Octadecenoic acid, methyl ester, (E)-	122326	001937-62-8	99
7	28.2112	2.7332	Octadecanoic acid, methyl ester	123709	000112-61-8	99
8	30.486	0.4183	Nonadecanoic acid, methyl ester	132330	001731-94-8	98
9	33.0865	3.4102	Eicosanoic acid, methyl ester	140313	001120-28-1	98
10	35.3556	16.8073	Tetracosane	146923	000646-31-1	99
11	36.1671	0.7845	Heneicosanoic acid, methyl ester	147946	006064-90-0	99
12	39.9451	7.7738	Docosanoic acid, methyl ester	154650	000929-77-1	99
13	42.8142	3.8341	Tricosanoic acid, methyl ester	160636	002433-97-8	98
14	43.4658	0.5605	6-Octadecenoic acid, methyl ester	122301	052355-31-4	45
15	45.0547	19.602	Tetracosanoic acid, methyl ester	165890	002442-49-1	99
16	46.775	4.5555	Docosanoic acid, methyl ester	154653	000929-77-1	98
17	47.2894	1.0642	Docosanedioic acid, dimethyl ester	170755	022399-98-0	87
18	48.6269	14.8599	Hexacosanoic acid, methyl ester	173512	005802-82-4	97
19	50.4729	2.1321	Tetracosanoic acid, methyl ester	165887	002442-49-1	95
20	51.1188	0.6254	8-Methyl-2-(2-piperidin-1-ylethylsulfanyl) quinoline-3-carbonitrile	131540	1000311-60-9	25
21	52.6277	6.3412	Octacosanoic acid, methyl ester	178460	055682-92-3	98

C:\Users\Mara\Data\24FAME_OCT11\S119_5 F2_3.D
Wed Nov 09 14:13:55 2011

PK	RT	Area Pct	Library/ID	Ref	CAS	Qual
1	18.4231	1.5629	Methyl tetradecanoate	86750	000124-10-7	95
2	20.2863	1.068	Tetradecanoic acid, 12-methyl-, methyl ester	96284	005129-66-8	86
3	23.0411	1.6304	9-Hexadecenoic acid, methyl ester, (Z)-	104152	001120-25-8	99
4	23.5384	8.8604	Hexadecanoic acid, methyl ester	105639	000112-39-0	98
5	27.6707	0.7575	9-Octadecenoic acid, methyl ester	122299	002462-84-2	99
6	27.7907	0.7472	9-Octadecenoic acid, methyl ester, (E)-	122326	001937-62-8	99
7	28.2137	2.7885	Octadecanoic acid, methyl ester	123709	000112-61-8	99
8	33.0889	3.3895	Eicosanoic acid, methyl ester	140314	001120-28-1	99
9	35.358	16.9201	Tetracosane	146923	000646-31-1	99
10	36.1639	0.7814	Heneicosanoic acid, methyl ester	147951	006064-90-0	98
11	39.9418	7.7783	Docosanoic acid, methyl ester	154652	000929-77-1	99
12	42.8109	3.8444	Tricosanoic acid, methyl ester	160636	002433-97-8	99
13	43.4625	0.5762	2-Dodecylcyclohexanone	102826	015674-95-0	64
14	45.0571	19.8084	Tetracosanoic acid, methyl ester	165888	002442-49-1	99
15	46.7775	4.519	Docosanoic acid, methyl ester	154653	000929-77-1	98
16	47.2919	1.0277	Docosanedioic acid, dimethyl ester	170755	022399-98-0	87
17	48.6293	14.9282	Hexacosanoic acid, methyl ester	173512	005802-82-4	97
18	50.4697	2.1118	Tetracosanoic acid, methyl ester	165887	002442-49-1	95
19	51.1155	0.6554	Nonanoic acid, 9-oxo-, methyl ester	47033	001931-63-1	47
20	52.6301	6.2447	Octacosanoic acid, methyl ester	178460	055682-92-3	98

C:\Users\Mara\Data\24FAME_OCT11\S122 F2_1.D
Wed Nov 09 14:14:04 2011

PK	RT	Area Pct	Library/ID	Ref	CAS	Qual
1	18.4202	1.6441	Methyl tetradecanoate	86750	000124-10-7	94
2	20.2834	1.2823	Methyl 9-methyltetradecanoate	96259	213617-69-7	93
3	23.044	1.7953	7-Hexadecenoic acid, methyl ester, (Z)-	104151	056875-67-3	99
4	23.5355	8.7953	Hexadecanoic acid, methyl ester	105639	000112-39-0	98
5	27.6678	0.9072	9-Octadecenoic acid, methyl ester, (E)-	122326	001937-62-8	99
6	27.7878	0.9098	9-Octadecenoic acid, methyl ester	122299	002462-84-2	99
7	28.2165	3.0365	Octadecanoic acid, methyl ester	123709	000112-61-8	99
8	33.0861	3.5775	Eicosanoic acid, methyl ester	140312	001120-28-1	98
9	35.3665	18.5996	Tetracosane	146921	000646-31-1	99
10	36.161	0.7445	Heneicosanoic acid, methyl ester	147951	006064-90-0	98
11	39.9389	7.7679	Docosanoic acid, methyl ester	154650	000929-77-1	99
12	42.8081	3.7425	Tricosanoic acid, methyl ester	160636	002433-97-8	99
13	45.0543	19.5729	Tetracosanoic acid, methyl ester	165890	002442-49-1	99
14	46.7746	4.3434	Pentacosanoic acid, methyl ester	170267	055373-89-2	99
15	47.2833	0.5414	Docosanedioic acid, dimethyl ester	170754	022399-98-0	47
16	48.6264	14.331	Hexacosanoic acid, methyl ester	173512	005802-82-4	95
17	50.4725	2.0865	Heptacosanoic acid, methyl ester	176204	055682-91-2	94
18	52.6273	6.3221	Octacosanoic acid, methyl ester	178460	055682-92-3	98

C:\Users\Mara\Data\24FAME_OCT11\S122 F2_2.D
Wed Nov 09 14:14:13 2011

PK	RT	Area Pct	Library/ID	Ref	CAS	Qual
1	18.4176	1.6432	Methyl tetradecanoate	86751	000124-10-7	93
2	20.2809	1.2613	Methyl 9-methyltetradecanoate	96259	213617-69-7	95
3	23.0414	1.8228	9-Hexadecenoic acid, methyl ester, (Z)-	104152	001120-25-8	99
4	23.533	8.7681	Hexadecanoic acid, methyl ester	105639	000112-39-0	98
5	27.6652	0.9023	7-Octadecenoic acid, methyl ester	122298	057396-98-2	99
6	27.791	0.9029	9-Octadecenoic acid, methyl ester	122299	002462-84-2	99
7	28.2139	2.9807	Octadecanoic acid, methyl ester	123709	000112-61-8	99
8	33.0835	3.585	Eicosanoic acid, methyl ester	140314	001120-28-1	99
9	35.364	18.5123	Tetracosane	146923	000646-31-1	99
10	36.1641	0.7562	Heneicosanoic acid, methyl ester	147946	006064-90-0	98
11	39.9421	7.7703	Docosanoic acid, methyl ester	154652	000929-77-1	99
12	42.8112	3.6452	Tricosanoic acid, methyl ester	160636	002433-97-8	99
13	45.0517	19.6521	Tetracosanoic acid, methyl ester	165890	002442-49-1	99
14	46.7778	4.35	Docosanoic acid, methyl ester	154647	000929-77-1	98
15	47.2864	0.5423	Docosanedioic acid, dimethyl ester	170755	022399-98-0	81
16	48.6238	14.5156	Hexacosanoic acid, methyl ester	173512	005802-82-4	97
17	50.4699	2.1766	Tetracosanoic acid, methyl ester	165887	002442-49-1	94
18	52.6304	6.213	Octacosanoic acid, methyl ester	178460	055682-92-3	98

C:\Users\Mara\Data\24FAME_OCT11\S122 F2_3.D
Wed Nov 09 14:14:24 2011

PK	RT	Area Pct	Library/ID	Ref	CAS	Qual
1	18.4208	1.6584	Methyl tetradecanoate	86752	000124-10-7	96
2	20.2783	1.2754	Methyl 9-methyltetradecanoate	96259	213617-69-7	97
3	23.0389	1.8281	9-Hexadecenoic acid, methyl ester, (Z)-	104152	001120-25-8	99
4	23.5361	8.8201	Pentadecanoic acid, 14-methyl-, methyl ester	105662	005129-60-2	98
5	27.6684	0.9086	8-Octadecenoic acid, methyl ester	122297	002345-29-1	99
6	27.7884	0.9149	11-Octadecenoic acid, methyl ester, (Z)-	122331	001937-63-9	99
7	28.2113	3.0163	Octadecanoic acid, methyl ester	123709	000112-61-8	98
8	33.0866	3.5298	Eicosanoic acid, methyl ester	140314	001120-28-1	98
9	35.3614	18.5808	Tetracosane	146923	000646-31-1	99
10	36.1616	0.7154	Heptadecanoic acid, 16-methyl-, methyl ester	123729	005129-61-3	97
11	39.9395	7.7831	Docosanoic acid, methyl ester	154650	000929-77-1	99
12	42.8087	3.6781	Tricosanoic acid, methyl ester	160636	002433-97-8	99
13	45.0548	19.6411	Tetracosanoic acid, methyl ester	165890	002442-49-1	98
14	46.7752	4.4061	Docosanoic acid, methyl ester	154647	000929-77-1	97
15	47.2839	0.5439	Docosanedioic acid, dimethyl ester	170755	022399-98-0	70
16	48.6213	14.4717	Hexacosanoic acid, methyl ester	173512	005802-82-4	97
17	50.4674	2.0828	Tetracosanoic acid, methyl ester	165887	002442-49-1	95
18	52.6278	6.1453	Octacosanoic acid, methyl ester	178460	055682-92-3	96

C:\Users\Mara\Data\24FAME_OCT11\S123 F2_1.D

Wed Nov 09 14:14:32 2011

PK	RT	Area Pct	Library/ID	Ref	CAS	Qual
1	23.0303	2.3435	9-Hexadecenoic acid, methyl ester, (Z)-	104152	001120-25-8	99
2	23.4989	3.6924	Hexadecanoic acid, methyl ester	105639	000112-39-0	98
3	28.2028	1.1237	Octadecanoic acid, methyl ester	123709	000112-61-8	99
4	35.4385	74.9101	Tetracosane	146921	000646-31-1	99
5	39.868	2.072	Docosanoic acid, methyl ester	154650	000929-77-1	99
6	43.4573	1.2079	9-Octadecenoic acid (Z)-, methyl ester	122321	000112-62-9	64
7	44.9719	5.4768	Tetracosanoic acid, methyl ester	165890	002442-49-1	98
8	46.7495	1.0496	Pentacosanoic acid, methyl ester	170267	055373-89-2	96
9	47.2867	3.1982	Docosanedioic acid, dimethyl ester	170755	022399-98-0	90
10	48.5498	3.0916	Hexacosanoic acid, methyl ester	173512	005802-82-4	95
11	51.1103	1.8343	Tridecanoic acid, methyl ester	77299	001731-88-0	38

C:\Users\Mara\Data\24FAME_OCT11\S123 F2_2.D

Wed Nov 09 14:14:39 2011

PK	RT	Area Pct	Library/ID	Ref	CAS	Qual
1	23.0327	2.3212	9-Hexadecenoic acid, methyl ester, (Z)-	104152	001120-25-8	99
2	23.5013	3.6888	Hexadecanoic acid, methyl ester	105639	000112-39-0	98
3	28.1995	1.077	Heptadecanoic acid, 16-methyl-, methyl ester	123732	005129-61-3	95
4	35.4353	75.126	Tetracosane	146923	000646-31-1	98
5	39.8704	2.1278	Docosanoic acid, methyl ester	154650	000929-77-1	99
6	43.4541	1.193	2-Dodecylcyclohexanone	102826	015674-95-0	49
7	44.9686	5.3963	Tetracosanoic acid, methyl ester	165890	002442-49-1	99
8	46.7462	1.0502	Pentacosanoic acid, methyl ester	170267	055373-89-2	99
9	47.2834	3.2073	Docosanedioic acid, dimethyl ester	170755	022399-98-0	90
10	48.5465	3.0384	Hexacosanoic acid, methyl ester	173512	005802-82-4	95
11	51.1071	1.7739	2-(Heptadec-8-enyl)-N-methylimidazoline(Z)	137102	1000280-19-3	38

C:\Users\Mara\Data\24FAME_OCT11\S123 F2_3.D

Wed Nov 09 14:14:47 2011

PK	RT	Area Pct	Library/ID	Ref	CAS	Qual
1	23.0281	2.2696	7-Hexadecenoic acid, methyl ester, (Z)-	104151	056875-67-3	96
2	23.4967	3.6705	Pentadecanoic acid, 14-methyl-, methyl ester	105662	005129-60-2	98
3	28.1948	1.1018	Octadecanoic acid, methyl ester	123709	000112-61-8	99
4	35.4306	75.3334	Tetracosane	146921	000646-31-1	99
5	39.8601	2.0743	Docosanoic acid, methyl ester	154650	000929-77-1	99
6	43.4551	1.2513	2,3-Dihydro-6-hydroxy-3-oxo-2-(piperidinomethyl)pyridazine	63472	014628-38-7	45
7	44.964	5.3562	Tetracosanoic acid, methyl ester	165890	002442-49-1	99
8	46.7415	1.0267	Pentacosanoic acid, methyl ester	170267	055373-89-2	99
9	47.2845	3.1176	Docosanedioic acid, dimethyl ester	170755	022399-98-0	90
10	48.5476	3.0422	Hexacosanoic acid, methyl ester	173512	005802-82-4	95
11	51.1024	1.7564	Cyclobutanone, 2-tetradecyl-	102835	035493-47-1	30

C:\Users\Mara\Data\21FAME_OCT11\1C1 T0_1.D
 Mon Nov 07 14:25:03 2011

PK	RT	Area Pct	Library/ID	Ref	CAS	Qual
1	18.4328	1.2058	Methyl tetradecanoate	86750	000124-10-7	95
2	21.0105	0.5712	Pentadecanoic acid, methyl ester	96270	007132-64-1	98
3	22.5937	0.1254	Hexadecanoic acid, methyl ester	105639	000112-39-0	98
4	23.6168	8.1404	Hexadecanoic acid, methyl ester	105639	000112-39-0	98
5	25.0285	0.1665	Hexadecanoic acid, 14-methyl-, methyl ester	114864	002490-49-5	98
6	25.2457	0.1135	Hexadecanoic acid, 14-methyl-, methyl ester	114866	002490-49-5	98
7	25.9029	0.5376	Heptadecanoic acid, methyl ester	114854	001731-92-6	99
8	26.1601	0.0674	5-(1-Iodo-1-methyl-ethyl)-3,3-dimethyl-dihydro-furan-2-one	113599	1000190-61-9	12
9	27.5147	0.3466	Hexadecanoic acid, 3,7,11,15-tetramethyl-, methyl ester	140343	001118-77-0	98
10	27.669	0.547	9-Octadecenoic acid, methyl ester, (E)-	122326	001937-62-8	99
11	27.7948	0.6981	8-Octadecenoic acid, methyl ester	122297	002345-29-1	99
12	28.2577	3.3845	Octadecanoic acid, methyl ester	123709	000112-61-8	99
13	30.481	0.4219	Nonadecanoic acid, methyl ester	132330	001731-94-8	98
14	31.104	0.1649	Tridecanedioic acid, dimethyl ester	106736	001472-87-3	53
15	33.1616	4.3939	Eicosanoic acid, methyl ester	140313	001120-28-1	99
16	35.4935	10.9644	Tetracosane	146923	000646-31-1	99
17	36.2079	0.9839	Heneicosanoic acid, methyl ester	147946	006064-90-0	99
18	37.111	0.2687	Octadecanedioic acid, dimethyl ester	148829	001472-93-1	72
19	40.1001	9.3367	Docosanoic acid, methyl ester	154650	000929-77-1	99
20	42.8779	4.0195	Tricosanoic acid, methyl ester	160636	002433-97-8	98
21	43.4666	0.471	Eicosanedioic acid, dimethyl ester	161411	042235-38-1	90
22	44.5639	0.3441	15-Tetracosenoic acid, methyl ester	165278	056554-33-7	93
23	44.6782	0.2731	2-Pentadecanone, 6,10,14-trimethyl-	104263	000502-69-2	86
24	45.2041	18.6618	Tetracosanoic acid, methyl ester	165888	002442-49-1	98
25	45.5356	0.5345	Tetracosanoic acid, methyl ester	165890	002442-49-1	95
26	46.8387	4.803	Docosanoic acid, methyl ester	154653	000929-77-1	97
27	47.3016	0.7025	Docosanedioic acid, dimethyl ester	170755	022399-98-0	91
28	47.8732	0.1985	Hexacosanoic acid, methyl ester	173513	005802-82-4	95
29	48.1761	0.1613	Silicic acid, diethyl bis(trimethylsilyl) ester	121708	003555-45-1	38
30	48.3419	0.4148	2-Heptacosanone	169707	007796-19-2	68
31	48.7648	14.4433	Hexacosanoic acid, methyl ester	173512	005802-82-4	96
32	49.1534	0.1999	Eicosanedioic acid, dimethyl ester	161412	042235-38-1	45
33	49.9536	0.5895	Octadecanoic acid, 11-methyl-, methyl ester	132359	074484-77-8	78
34	50.5194	2.2948	Tetracosanoic acid, methyl ester	165887	002442-49-1	95
35	51.1082	0.2953	d-Gulopyranoside, 2,3:4,6-di-O-(ethylboranediyl)-1-O-methyl-	104987	1000149-94-5	45
36	52.3427	0.3521	2-Nonacosanone	175866	017600-99-6	35
37	52.7656	8.594	Octacosanoic acid, methyl ester	178460	055682-92-3	98
38	53.3486	0.2087	Methanamine, N-(diphenylethenylidene)-	62245	013911-54-1	41

C:\Users\Mara\Data\21FAME_OCT11\1C1 T0_2.D
 Mon Nov 07 14:25:19 2011

PK	RT	Area Pct	Library/ID	Ref	CAS	Qual
1	18.4287	1.2192	Tridecanoic acid, 12-methyl-, methyl ester	86778	005129-58-8	95
2	21.0063	0.5827	Pentadecanoic acid, methyl ester	96270	007132-64-1	97
3	22.5952	0.1311	Pentadecanoic acid, 14-methyl-, methyl ester	105662	005129-60-2	97
4	23.6126	8.1761	Hexadecanoic acid, methyl ester	105639	000112-39-0	98
5	25.03	0.1824	Hexadecanoic acid, 14-methyl-, methyl ester	114864	002490-49-5	98
6	25.2415	0.1148	Hexadecanoic acid, 14-methyl-, methyl ester	114866	002490-49-5	96
7	25.8988	0.5339	Heptadecanoic acid, methyl ester	114854	001731-92-6	99
8	26.156	0.0701	5-(1-Iodo-1-methyl-ethyl)-3,3-dimethyl-dihydro-furan-2-one	113599	1000190-61-9	43
9	27.5105	0.3189	Hexadecanoic acid, 3,7,11,15-tetramethyl-, methyl ester	140343	001118-77-0	98
10	27.6706	0.5046	9-Octadecenoic acid, methyl ester, (E)-	122326	001937-62-8	99
11	27.7906	0.5714	9-Octadecenoic acid, methyl ester, (E)-	122326	001937-62-8	99
12	28.2593	3.3822	Octadecanoic acid, methyl ester	123709	000112-61-8	99
13	30.4769	0.4014	Nonadecanoic acid, methyl ester	132331	001731-94-8	99
14	31.1056	0.1626	Hexadecanedioic acid, dimethyl ester	133343	019102-90-0	62
15	33.1574	4.4408	Eicosanoic acid, methyl ester	140313	001120-28-1	99
16	35.4893	11.1078	Tetracosane	146923	000646-31-1	99
17	36.2038	1.0373	Heneicosanoic acid, methyl ester	147951	006064-90-0	99
18	37.1068	0.2586	Octadecanedioic acid, dimethyl ester	148829	001472-93-1	86
19	40.0903	9.4149	Docosanoic acid, methyl ester	154650	000929-77-1	99
20	42.8737	4.0099	Tricosanoic acid, methyl ester	160636	002433-97-8	99
21	43.4624	0.4787	Eicosanedioic acid	148821	002424-92-2	46
22	44.5655	0.0848	15-Tetracosenoic acid, methyl ester	165278	056554-33-7	89
23	44.5884	0.0305	15-Tetracosenoic acid, methyl ester, (Z)-	165279	002733-88-2	99
24	45.2056	18.731	Tetracosanoic acid, methyl ester	165888	002442-49-1	98
25	45.5314	0.3027	Tetracosanoic acid, methyl ester	165890	002442-49-1	95
26	46.8345	4.7689	Docosanoic acid, methyl ester	154647	000929-77-1	98
27	47.2975	0.7145	Docosanedioic acid, dimethyl ester	170755	022399-98-0	91
28	47.869	0.2176	Hexacosanoic acid, methyl ester	173512	005802-82-4	66
29	48.1662	0.1996	Silicic acid, diethyl bis(trimethylsilyl) ester	121708	003555-45-1	43
30	48.3377	0.4471	2-Heptacosanone	169707	007796-19-2	93
31	48.7606	14.6873	Hexacosanoic acid, methyl ester	173512	005802-82-4	96
32	49.1493	0.2727	Eicosanedioic acid, dimethyl ester	161411	042235-38-1	64
33	49.9438	0.5261	Hexacosanoic acid, methyl ester	173513	005802-82-4	78
34	50.5096	2.323	Tetracosanoic acid, methyl ester	165887	002442-49-1	99
35	51.104	0.285	Triacantanedioic acid, dimethyl ester	185167	024397-43-1	43
36	52.3443	0.3725	2-Ethylacridine	62222	055751-83-2	30
37	52.7557	8.7292	Octacosanoic acid, methyl ester	178460	055682-92-3	99
38	53.3559	0.2081	Vitamin E	177300	010191-41-0	46

C:\Users\Mara\Data\21FAME_OCT11\IC1 T0_3.D
Mon Nov 07 14:25:35 2011

PK	RT	Area Pct	Library/ID	Ref	CAS	Qual
1	18.4258	1.187	Methyl tetradecanoate	86750	000124-10-7	94
2	21.0035	0.556	Pentadecanoic acid, methyl ester	96270	007132-64-1	98
3	22.5924	0.1204	Pentadecanoic acid, 14-methyl-, methyl ester	105662	005129-60-2	97
4	23.6097	8.0006	Pentadecanoic acid, 14-methyl-, methyl ester	105662	005129-60-2	98
5	25.0214	0.1769	Hexadecanoic acid, 14-methyl-, methyl ester	114864	002490-49-5	98
6	25.2386	0.1091	Hexadecanoic acid, 14-methyl-, methyl ester	114866	002490-49-5	98
7	25.9016	0.5298	Heptadecanoic acid, methyl ester	114854	001731-92-6	99
8	26.1588	0.0697	Cyclohexanol, 1-methyl-4-(1-methylethyl)-, cis-	27165	003901-95-9	11
9	27.5134	0.3123	Hexadecanoic acid, 3,7,11,15-tetramethyl-, methyl ester	140342	001118-77-0	96
10	27.662	0.4902	9-Octadecenoic acid, methyl ester, (E)-	122326	001937-62-8	99
11	27.7877	0.5669	9-Octadecenoic acid, methyl ester, (E)-	122326	001937-62-8	99
12	28.2564	3.3341	Octadecanoic acid, methyl ester	123709	000112-61-8	99
13	30.474	0.4186	Nonadecanoic acid, methyl ester	132330	001731-94-8	98
14	31.097	0.1577	16-Nitrobicyclo[10.4.0]hexadecan-1-ol-13-one	122752	079880-69-6	38
15	33.1546	4.366	Eicosanoic acid, methyl ester	140313	001120-28-1	99
16	35.4808	10.9154	Tetracosane	146923	000646-31-1	99
17	36.1952	1.0058	Octadecanoic acid, methyl ester	123709	000112-61-8	98
18	37.1039	0.2605	Octadecanedioic acid, dimethyl ester	148831	001472-93-1	80
19	40.0931	9.3295	Docosanoic acid, methyl ester	154650	000929-77-1	99
20	42.8708	4.0074	Tricosanoic acid, methyl ester	160636	002433-97-8	99
21	43.4595	0.4795	Eicosanebioic acid, dimethyl ester	161411	042235-38-1	87
22	44.5626	0.2495	15-Tetracosenoic acid, methyl ester	165278	056554-33-7	96
23	44.6141	0.0779	15-Tetracosenoic acid, methyl ester	165278	056554-33-7	89
24	44.6712	0.2765	2-Pentadecanone, 6,10,14-trimethyl-	104263	000502-69-2	74
25	45.2028	18.658	Tetracosanoic acid, methyl ester	165888	002442-49-1	99
26	45.5285	0.3053	Octadecanoic acid, 11-methyl-, methyl ester	132359	074484-77-8	89
27	46.8317	4.7336	Docosanoic acid, methyl ester	154647	000929-77-1	98
28	47.2946	0.719	Docosanedioic acid, dimethyl ester	170755	022399-98-0	91
29	48.3348	0.3186	2-Heptacosanone	169707	007796-19-2	49
30	48.7578	14.2399	Hexacosanoic acid, methyl ester	173512	005802-82-4	96
31	49.1464	0.1958	Eicosanebioic acid, dimethyl ester	161411	042235-38-1	66
32	49.9409	0.4532	Hexacosanoic acid, methyl ester	173513	005802-82-4	78
33	50.5124	2.3058	Tetracosanoic acid, methyl ester	165887	002442-49-1	95
34	51.1068	0.2922	Imidazo[4,5-d]imidazole-2,5-dione, perhydro-1,6-dimethyl-3,4-bis(1-piperidyl)methyl-	158773	300389-09-7	25
35	52.3414	0.7077	2-Nonacosanone	175866	017600-99-6	58
36	52.7586	9.2903	Octacosanoic acid, methyl ester	178460	055682-92-3	96
37	53.3473	0.783	Vitamin E	177303	000059-02-9	42

C:\Users\Mara\Data\21FAME_OCT11\IC2 T0_1.D
Wed Nov 09 13:54:22 2011

PK	RT	Area Pct	Library/ID	Ref	CAS	Qual
1	18.5063	1.6926	Tridecanoic acid, 12-methyl-, methyl ester	86778	005129-58-8	95
2	18.7007	0.192	Tridecanoic acid, 12-methyl-, methyl ester	86778	005129-58-8	96
3	19.7752	0.2051	Tridecanoic acid, 4,8,12-trimethyl-, methyl ester	105664	010339-74-9	49
4	21.0611	0.7067	Pentadecanoic acid, methyl ester	96270	007132-64-1	98
5	22.6386	0.1977	Hexadecanoic acid, methyl ester	105639	000112-39-0	96
6	23.6845	9.483	Hexadecanoic acid, methyl ester	105639	000112-39-0	98
7	25.0562	0.227	Hexadecanoic acid, 14-methyl-, methyl ester	114864	002490-49-5	98
8	25.2677	0.1736	Hexadecanoic acid, 14-methyl-, methyl ester	114864	002490-49-5	97
9	25.9307	0.6465	Heptadecanoic acid, methyl ester	114854	001731-92-6	99
10	26.1879	0.2483	5-(1-Iodo-1-methyl-ethyl)-3,3-dimethyl-dihydro-furan-2-one	113599	1000190-61-9	14
11	26.2451	0.1568	2,6-Piperazinedione, 4,4'-(1-methyl-1,2-ethanediyl)bis-, (S)-	103570	024584-09-6	35
12	27.3824	0.1479	Heptadecanoic acid, 16-methyl-, methyl ester	123732	005129-61-3	91
13	27.5482	0.4971	Hexadecanoic acid, 3,7,11,15-tetramethyl-, methyl ester	140343	001118-77-0	98
14	27.7025	0.9268	9-Octadecenoic acid, methyl ester, (E)-	122326	001937-62-8	99
15	27.8168	0.7407	9-Octadecenoic acid, methyl ester	122299	002462-84-2	99
16	28.3141	4.7022	Octadecanoic acid, methyl ester	123709	000112-61-8	99
17	30.4974	0.5924	Nonadecanoic acid, methyl ester	132330	001731-94-8	98
18	31.1261	0.15	Tridecanedioic acid, dimethyl ester	106736	001472-87-3	64
19	31.6176	0.2984	Ethyl 5,8,11,14,17-icosapentaenoate	142611	084494-70-2	94
20	32.5892	0.1827	11-Eicosenoic acid, methyl ester	139171	003946-08-5	97
21	33.2008	4.5944	Eicosanoic acid, methyl ester	140313	001120-28-1	99
22	35.4698	7.1052	Tetracosane	146923	000646-31-1	99
23	36.2243	1.0343	Heneicosanoic acid, methyl ester	147951	006064-90-0	99
24	37.1273	0.1383	Octadecanedioic acid, dimethyl ester	148831	001472-93-1	91
25	39.2478	0.2297	13-Docosenoic acid, methyl ester, (Z)-	153714	001120-34-9	92
26	40.1565	9.1062	Docosanoic acid, methyl ester	154650	000929-77-1	99
27	40.8023	0.1253	Nonadecanedioic acid, dimethyl ester	155389	023130-41-8	38
28	42.9057	3.9246	Tricosanoic acid, methyl ester	160636	002433-97-8	98
29	43.4829	0.4894	Eicosanebioic acid, dimethyl ester	161411	042235-38-1	90
30	44.5803	0.6165	15-Tetracosenoic acid, methyl ester	165278	056554-33-7	99
31	44.6775	0.3179	15-Tetracosenoic acid, methyl ester	165278	056554-33-7	97
32	45.2433	17.4237	Tetracosanoic acid, methyl ester	165887	002442-49-1	99
33	45.5519	0.6074	Tetracosanoic acid, methyl ester	165890	002442-49-1	86
34	46.1178	0.0857	Pentacosanoic acid, methyl ester	170268	055373-89-2	94
35	46.8608	4.3104	Docosanoic acid, methyl ester	154653	000929-77-1	97
36	47.0322	0.6081	Pentacosanoic acid, methyl ester	170267	055373-89-2	47
37	47.318	0.8179	Docosanedioic acid, dimethyl ester	170755	022399-98-0	91
38	47.8781	0.2993	Hexacosanoic acid, methyl ester	173513	005802-82-4	95
39	48.181	0.2444	22-Tricosenoic acid	153711	065119-95-1	42
40	48.3525	0.4848	2-Heptacosanone	169707	007796-19-2	86
41	48.7983	13.0819	Hexacosanoic acid, methyl ester	173512	005802-82-4	96
42	49.1698	0.214	Eicosanebioic acid, dimethyl ester	161411	042235-38-1	53
43	50.0271	0.7073	Hexacosanoic acid, methyl ester	173513	005802-82-4	60
44	50.5415	2.1411	Heptacosanoic acid, methyl ester	176204	055682-91-2	94
45	51.1245	0.3815	Octadecanedioic acid	133331	000871-70-5	35
46	52.3705	0.5332	2-Nonacosanone	175866	017600-99-6	49
47	52.7991	8.0149	Octacosanoic acid, methyl ester	178460	055682-92-3	96
48	53.3707	0.1952	Antra-9,10-quinone, 1-(3-hydroxy-3-phenyl-1-triazenyl)-	149262	098496-82-3	90

C:\Users\Mara\Data\21FAME_OCT11\IC2 T0_2.D
Wed Nov 09 13:54:52 2011

PK	RT	Area Pct	Library/ID	Ref	CAS	Qual
1	18.5063	1.7092	Methyl tetradecanoate	86750	000124-10-7	94
2	18.6949	0.1914	Tridecanoic acid, 12-methyl-, methyl ester	86778	005129-58-8	97
3	19.7751	0.1649	Tridecanoic acid, 4,8,12-trimethyl-, methyl ester	105664	010339-74-9	95
4	21.0554	0.7178	Pentadecanoic acid, methyl ester	96270	007132-64-1	98
5	22.6385	0.2043	Pentadecanoic acid, 14-methyl-, methyl ester	105659	005129-60-2	97
6	23.6845	9.5781	Pentadecanoic acid, 14-methyl-, methyl ester	105662	005129-60-2	99
7	25.0505	0.2162	Hexadecanoic acid, 14-methyl-, methyl ester	114864	002490-49-5	98
8	25.2677	0.1373	Hexadecanoic acid, 14-methyl-, methyl ester	114864	002490-49-5	96
9	25.9307	0.6489	Heptadecanoic acid, methyl ester	114854	001731-92-6	99
10	26.1879	0.2588	Phthalic acid, ethyl furfuryl ester	110513	1000314-91-3	22
11	26.245	0.149	2,6-Piperazinedione, 4,4'-(1-methyl-1,2-ethanediyl)bis-, (S)-	103570	024584-09-6	35
12	27.3824	0.1388	Heptadecanoic acid, 15-methyl-, methyl ester	123730	054833-55-5	90
13	27.5424	0.4938	Hexadecanoic acid, 3,7,11,15-tetramethyl-, methyl ester	140345	001118-77-0	93
14	27.7024	0.9269	9-Octadecenoic acid, methyl ester, (E)-	122326	001937-62-8	99
15	27.8168	0.7354	9-Octadecenoic acid, methyl ester	122299	002462-84-2	99
16	28.3083	4.6649	Octadecanoic acid, methyl ester	123709	000112-61-8	99
17	30.4973	0.5993	Nonadecanoic acid, methyl ester	132330	001731-94-8	98
18	31.1203	0.1584	Hexadecanedioic acid, dimethyl ester	133343	019102-90-0	68
19	31.6176	0.326	5,8,11,14,17-Eicosapentaenoic acid, methyl ester, (all-Z)-	134757	002734-47-6	93
20	32.5892	0.1856	11-Eicosenoic acid, methyl ester	139171	003946-08-5	97
21	33.2007	4.6586	Eicosanoic acid, methyl ester	140313	001120-28-1	99
22	35.4641	7.2428	Tetracosane	146923	000646-31-1	99
23	36.2185	1.0488	Heneicosanoic acid, methyl ester	147951	006064-90-0	99
24	37.1215	0.292	Octadecanedioic acid, dimethyl ester	148831	001472-93-1	90
25	39.2534	0.2444	13-Docosenoic acid, methyl ester, (Z)-	153714	001120-34-9	95
26	40.1508	9.1407	Docosanoic acid, methyl ester	154650	000929-77-1	99
27	42.9056	3.9424	Tricosanoic acid, methyl ester	160636	002433-97-8	98
28	43.4772	0.4885	Eicosanebioic acid, dimethyl ester	161411	042235-38-1	83
29	44.5859	0.9345	15-Tetracosenoic acid, methyl ester	165278	056554-33-7	97
30	45.2432	17.5577	Tetracosanoic acid, methyl ester	165888	002442-49-1	99
31	45.4776	0.1563	Tetracosanoic acid, methyl ester	165890	002442-49-1	98
32	45.5519	0.3265	Tetracosanoic acid, methyl ester	165890	002442-49-1	89
33	46.1177	0.0975	Pentacosanoic acid, methyl ester	170268	055373-89-2	94
34	46.5235	0.1433	1-Hexacosene	159039	018835-33-1	58
35	46.865	4.6026	Docosanoic acid, methyl ester	154647	000929-77-1	98
36	47.3179	0.8025	Docosanedioic acid, dimethyl ester	170754	022399-98-0	91
37	47.8723	0.2962	Hexacosanoic acid, methyl ester	173512	005802-82-4	83
38	48.181	0.2688	1,22-Docosanediol	148950	022513-81-1	20
39	48.3524	0.4829	2-Heptacosanone	169707	007796-19-2	76
40	48.7982	13.4234	Hexacosanoic acid, methyl ester	173512	005802-82-4	96
41	49.1698	0.2718	Eicosanebioic acid, dimethyl ester	161411	042235-38-1	52
42	49.9756	0.4563	Hexacosanoic acid, methyl ester	173513	005802-82-4	78
43	50.5358	2.1637	Tetracosanoic acid, methyl ester	165887	002442-49-1	95
44	51.1244	0.3508	2-(Heptadec-10-enyl)-N-methylimidazoline(Z)	137104	1000280-19-2	25
45	52.239	0.1587	1H-Indole-2-carboxylic acid, 6-(4-ethoxyphenyl)-3-methyl-4-oxo-4,5,6,7-tetrahydro-, isopropyl ester	154967	1000316-17-5	38
46	52.3704	0.2887	3-Heptadecanol	96328	084534-30-5	35
47	52.7933	7.5512	Octacosanoic acid, methyl ester	178460	055682-92-3	99
48	53.3649	0.4032	Antra-9,10-quinone, 1-(3-hydroxy-3-phenyl-1-triazenyl)-	149262	098496-82-3	90

C:\Users\Mara\Data\21FAME_OCT11\C2 T0_3.D
Wed Nov 09 13:55:12 2011

PK	RT	Area Pct	Library/ID	Ref	CAS	Qual
1	18.5057	1.6518	Methyl tetradecanoate	86750	000124-10-7	94
2	18.6944	0.1868	Tridecanoic acid, 12-methyl-, methyl ester	86778	005129-58-8	96
3	19.7803	0.1619	Tridecanoic acid, 4,8,12-trimethyl-, methyl ester	105664	010339-74-9	90
4	21.0548	0.8662	Pentadecanoic acid, methyl ester	96270	007132-64-1	98
5	22.638	0.1982	Pentadecanoic acid, 14-methyl-, methyl ester	105659	005129-60-2	97
6	23.684	9.364	Pentadecanoic acid, 14-methyl-, methyl ester	105662	005129-60-2	98
7	25.05	0.2171	Hexadecanoic acid, 14-methyl-, methyl ester	114864	002490-49-5	98
8	25.2671	0.1282	Hexadecanoic acid, 14-methyl-, methyl ester	114864	002490-49-5	96
9	25.9301	0.634	Heptadecanoic acid, methyl ester	114854	001731-92-6	99
10	26.1816	0.4009	5-(1-Iodo-1-methyl-ethyl)-3,3-dimethyl-dihydro-furan-2-one	113599	1000190-61-9	38
11	27.3819	0.1237	Heptadecanoic acid, 16-methyl-, methyl ester	123732	005129-61-3	95
12	27.5419	0.4791	Hexadecanoic acid, 3,7,11,15-tetramethyl-, methyl ester	140343	001118-77-0	97
13	27.7019	0.8964	9-Octadecenoic acid, methyl ester, (E)-	122326	001937-62-8	99
14	27.8105	0.7113	9-Octadecenoic acid, methyl ester	122299	002462-84-2	99
15	28.3078	4.5566	Octadecanoic acid, methyl ester	123709	000112-61-8	99
16	30.4968	0.4781	Nonadecanoic acid, methyl ester	132330	001731-94-8	98
17	31.1198	0.1425	Tridecanedioic acid, dimethyl ester	106736	001472-87-3	58
18	31.617	0.3106	5,8,11,14,17-Eicosapentaenoic acid, methyl ester, (all-Z)-	134757	002734-47-6	94
19	32.5887	0.1753	11-Eicosenoic acid, methyl ester	139171	003946-08-5	97
20	33.1945	4.5062	Eicosanoic acid, methyl ester	140313	001120-28-1	99
21	35.4635	7.1103	Tetracosane	146923	000646-31-1	99
22	36.218	1.0276	Heneicosanoic acid, methyl ester	147946	006064-90-0	99
23	37.121	0.2936	Octadecanedioic acid, dimethyl ester	148831	001472-93-1	91
24	39.2415	0.2438	13-Docosenoic acid, methyl ester, (Z)-	153714	001120-34-9	97
25	40.1502	9.1233	Docosanoic acid, methyl ester	154650	000929-77-1	99
26	40.8018	0.161	Cyclododecanamine, N-cyclohexylidene-	100713	079014-38-3	45
27	42.9051	3.8347	Tricosanoic acid, methyl ester	160636	002433-97-8	98
28	43.4766	0.4867	Eicosanebioic acid, dimethyl ester	161411	042235-38-1	91
29	44.5797	0.8137	15-Tetracosenoic acid, methyl ester	165278	056554-33-7	99
30	45.2427	17.0547	Tetracosanoic acid, methyl ester	165888	002442-49-1	99
31	45.5513	0.4723	Tetracosanoic acid, methyl ester	165890	002442-49-1	95
32	46.1114	0.0912	Pentacosanoic acid, methyl ester	170268	055373-89-2	94
33	46.523	0.1369	2-Nonadecanone	113459	000629-66-3	41
34	46.8545	4.4991	Docosanoic acid, methyl ester	154647	000929-77-1	98
35	47.3174	0.7859	Docosanedioic acid, dimethyl ester	170755	022399-98-0	91
36	47.8661	0.2324	Hexacosanoic acid, methyl ester	173513	005802-82-4	86
37	48.1805	0.2347	22-Tricosenoic acid	153711	065119-95-1	38
38	48.3519	0.4084	2-Heptacosanone	169707	007796-19-2	94
39	48.7977	12.9813	Hexacosanoic acid, methyl ester	173512	005802-82-4	96
40	49.1692	0.2134	5-(1-Methyl-2-piperidyl)-2,3'-bipyridine	94069	1000224-90-0	46
41	49.9751	0.5417	Octadecanoic acid, 11-methyl-, methyl ester	132359	074484-77-8	78
42	50.5352	2.1311	Tetracosanoic acid, methyl ester	165887	002442-49-1	95
43	51.1239	0.32	2-(Heptadec-10-enyl)-N-methylimidazoline(Z)	137104	1000280-19-2	25
44	52.2499	0.4572	5-Methyl-2-trimethylsilyloxy-acetophenone	72509	097389-69-0	25
45	52.3585	0.562	2-Nonacosanone	175866	017600-99-6	53
46	52.7928	8.7818	Octacosanoic acid, methyl ester	178460	055682-92-3	96
47	53.3644	0.812	Vitamin E	177299	000059-02-9	38

C:\Users\Mara\Data\21FAME_OCT11\IC3 TO_1.D
Wed Nov 09 13:55:36 2011

PK	RT	Area Pct	Library/ID	Ref	CAS	Qual
1	16.8319	0.1157	Benzoic acid, 2,5-bis(trimethylsiloxy)-, trimethylsilyl ester	161131	003618-20-0	38
2	18.5351	1.3492	Methyl tetradecanoate	86750	000124-10-7	94
3	18.7294	0.1385	Tridecanoic acid, 12-methyl-, methyl ester	86778	005129-58-8	98
4	19.8096	0.1659	Tridecanoic acid, 4,8,12-trimethyl-, methyl ester	105664	010339-74-9	91
5	20.9527	0.0534	Cyclononasiloxane, octadecamethyl-	189575	000556-71-8	91
6	21.0899	0.5903	Pentadecanoic acid, methyl ester	96270	007132-64-1	98
7	22.6673	0.3018	Pentadecanoic acid, 14-methyl-, methyl ester	105659	005129-60-2	97
8	23.3303	0.1092	9-Hexadecenoic acid, methyl ester, (Z)-	104152	001120-25-8	99
9	23.7361	8.2273	Hexadecanoic acid, methyl ester	105639	000112-39-0	98
10	24.5535	0.0736	Pentadecanoic acid, 14-methyl-, methyl ester	105659	005129-60-2	93
11	24.6163	0.1054	Heptadecanoic acid, methyl ester	114852	001731-92-6	53
12	24.7078	0.1807	Cyclononasiloxane, octadecamethyl-	189575	000556-71-8	49
13	25.0793	0.2403	Hexadecanoic acid, 14-methyl-, methyl ester	114864	002490-49-5	98
14	25.2965	0.177	Hexadecanoic acid, 14-methyl-, methyl ester	114864	002490-49-5	98
15	25.4451	0.0601	9-Hexadecenoic acid, methyl ester, (Z)-	104156	001120-25-8	94
16	25.9595	0.6664	Heptadecanoic acid, methyl ester	114854	001731-92-6	99
17	26.2167	0.2323	Cyclohexanol, 1-methyl-4-(1-methylethyl)-, cis-	27165	003901-95-9	11
18	26.2795	0.1688	Methyl (11R,12R,13S)-(Z)-12,13-epoxy-11-methoxy-9-octadecenoate	147798	088335-39-1	38
19	27.4055	0.1676	Heptadecanoic acid, 16-methyl-, methyl ester	123732	005129-61-3	90
20	27.577	0.5053	Hexadecanoic acid, 3,7,11,15-tetramethyl-, methyl ester	140343	001118-77-0	98
21	27.737	0.9437	9-Octadecenoic acid, methyl ester, (E)-	122326	001937-62-8	99
22	27.8513	0.7685	9-Octadecenoic acid, methyl ester, (E)-	122326	001937-62-8	99
23	28.3428	3.6631	Octadecanoic acid, methyl ester	123709	000112-61-8	99
24	29.4173	0.0494	Cyclopentadecanone, 2-hydroxy-	85349	004727-18-8	83
25	29.5488	0.0798	Hexadecanoic acid, butyl ester	132322	000111-06-8	94
26	30.5318	0.6236	Nonadecanoic acid, methyl ester	132330	001731-94-8	98
27	30.6576	0.1139	3-Cyano-5,5-dimethoxycarbonyl-N-methylisoxazolidine	77633	071167-53-8	15
28	31.1548	0.1947	Hexadecanedioic acid, dimethyl ester	133343	019102-90-0	52
29	31.5378	0.1012	Cyclononasiloxane, octadecamethyl-	189576	000556-71-8	59
30	31.6521	0.3598	5,8,11,14,17-Eicosapentaenoic acid, methyl ester, (all-Z)-	134757	002734-47-6	94
31	32.4408	0.2286	11-Eicosenoic acid, methyl ester	139171	003946-08-5	99
32	32.6237	0.1828	11-Eicosenoic acid, methyl ester	139171	003946-08-5	97
33	33.2467	4.2856	Eicosanoic acid, methyl ester	140313	001120-28-1	99
34	35.6586	10.6076	Tetracosane	146923	000646-31-1	99
35	36.3216	1.1754	Octadecanoic acid, methyl ester	123709	000112-61-8	98
36	37.1961	0.2633	Octadecanedioic acid, dimethyl ester	148831	001472-93-1	90
37	39.2822	0.2501	13-Docosenoic acid, methyl ester, (Z)-	153714	001120-34-9	97
38	40.2081	6.1181	Docosanoic acid, methyl ester	154650	000929-77-1	99
39	40.2482	2.8573	Docosanoic acid, methyl ester	154650	000929-77-1	99
40	40.7968	0.217	Benzoic acid, 2,4-bis(trimethylsilyloxy)-, trimethylsilyl ester	161138	010586-16-0	25
41	42.9687	4.2883	Tricosanoic acid, methyl ester	160636	002433-97-8	98
42	43.5288	0.7565	Eicosanebioic acid, dimethyl ester	161411	042235-38-1	87
43	44.3061	0.1726	Hexasiloxane, tetradecamethyl-	180792	000107-52-8	50
44	44.6091	0.3514	15-Tetracosenoic acid, methyl ester, (Z)-	165279	002733-88-2	99
45	44.6491	0.3882	15-Tetracosenoic acid, methyl ester, (Z)-	165279	002733-88-2	99
46	45.3178	15.8013	Tetracosanoic acid, methyl ester	165888	002442-49-1	99
47	45.5978	0.2298	Hencosanedioic acid, dimethyl ester	166463	042235-57-4	86
48	46.0208	0.0558	Oxiraneundecanoic acid, 3-pentyl-, methyl ester, trans-	132223	038520-31-9	87
49	46.1408	0.0771	Pentacosanoic acid, methyl ester	170268	055373-89-2	94
50	46.398	0.0886	1,3-Dioxolane, 4-ethyl-5-octyl-2,2-bis(trifluoromethyl)-, trans-	152414	038274-73-6	27
51	46.5466	0.1148	3-Tetradecanol	67325	001653-32-3	22
52	46.9066	4.5383	Docosanoic acid, methyl ester	154653	000929-77-1	97
53	47.3867	1.5488	Docosanedioic acid, dimethyl ester	170755	022399-98-0	91
54	47.9012	0.1665	Hexacosanoic acid, methyl ester	173512	005802-82-4	86
55	48.1069	0.0715	Antra-9,10-quinone, 1-(3-hydroxy-3-phenyl-1-triazenyl)-	149262	098496-82-3	64
56	48.2098	0.2205	Androstan(B)-3-formoxy-11-ol-17-one	144804	004589-70-2	90
57	48.2898	0.0221	22-Tricosenoic acid	153711	065119-95-1	42
58	48.3584	0.3074	2-Heptacosanone	169707	007796-19-2	89
59	48.8671	12.1267	Hexacosanoic acid, methyl ester	173512	005802-82-4	95
60	49.2157	0.4468	Triacontanedioic acid, dimethyl ester	185167	024397-43-1	43
61	49.993	0.0779	Tetracosanoic acid, methyl ester	165887	002442-49-1	74
62	50.5874	2.1815	Tetracosanoic acid, methyl ester	165887	002442-49-1	95
63	51.199	1.1545	Cyclobutanone, 2-tetradecyl-	102835	035493-47-1	43
64	51.8105	0.1773	2,4,6-(1H,3H,5H)-Pyrimidinetrione, 5-ethyl-5-(3-methylbutyl)-1,3-bis(trimethylsilyl)-	161170	052937-67-4	44
65	52.2735	0.1981	2,4,6-Cycloheptatrien-1-one, 3,5-bis(trimethylsilyl)-	91822	1000161-21-8	25
66	52.3764	0.2751	Anthracene, 9-ethyl-9,10-dihydro-9,10-dimethyl-	82678	054947-86-3	22
67	52.8565	6.9902	Octacosanoic acid, methyl ester	178460	055682-92-3	96
68	53.4109	0.3413	Docosanedioic acid, dimethyl ester	170755	022399-98-0	43
69	55.0683	0.1185	Hexacosanoic acid, methyl ester	173513	005802-82-4	92

C:\Users\Mara\Data\21FAME_OCT11\IC3 T0_2.D
Wed Nov 09 13:56:04 2011

PK	RT	Area Pct	Library/ID	Ref	CAS	Qual
1	16.789	0.1121	1,3,5,7-Tetraethyl-1-ethylbutoxysiloxycyclotetrasiloxane	178859	073420-30-1	43
2	18.5094	1.3187	Tridecanoic acid, 12-methyl-, methyl ester	86778	005129-58-8	95
3	18.7094	0.1425	Tridecanoic acid, 12-methyl-, methyl ester	86778	005129-58-8	97
4	19.7725	0.1633	Tridecanoic acid, 4,8,12-trimethyl-, methyl ester	105664	010339-74-9	95
5	20.9327	0.0527	Cyclononasiloxane, octadecamethyl-	189575	000556-71-8	87
6	21.0642	0.5745	Pentadecanoic acid, methyl ester	96270	007132-64-1	99
7	22.6417	0.211	Pentadecanoic acid, 14-methyl-, methyl ester	105659	005129-60-2	97
8	23.3104	0.1103	9-Hexadecenoic acid, methyl ester, (Z)-	104152	001120-25-8	99
9	23.7105	7.9944	Hexadecanoic acid, methyl ester	105639	000112-39-0	98
10	24.5278	0.0756	Cyclopropaneoctanoic acid, 2-hexyl-, methyl ester	113414	010152-61-1	91
11	24.5906	0.0964	Hexadecanoic acid, methyl ester	105645	000112-39-0	64
12	24.6878	0.1777	Cyclodecasiloxane, eicosamethyl-	190220	018772-36-6	55
13	25.0593	0.2387	Hexadecanoic acid, 14-methyl-, methyl ester	114864	002490-49-5	98
14	25.2822	0.1719	Hexadecanoic acid, 14-methyl-, methyl ester	114866	002490-49-5	97
15	25.4251	0.0546	Cyclopropaneoctanoic acid, 2-hexyl-, methyl ester	113414	010152-61-1	93
16	25.9452	0.6558	Heptadecanoic acid, methyl ester	114854	001731-92-6	99
17	26.1967	0.2297	Phthalic acid, furfuryl hexyl ester	144738	1000314-92-4	22
18	26.2538	0.0365	Sulfurous acid, decyl 2-pentyl ester	119568	1000309-15-9	43
19	26.271	0.1266	3-Methyl-thiophene-2-carboxamide	18249	076655-99-7	27
20	27.3855	0.1439	Heptadecanoic acid, 15-methyl-, methyl ester	123730	054833-55-5	95
21	27.557	0.4925	Hexadecanoic acid, 3,7,11,15-tetramethyl-, methyl ester	140345	001118-77-0	93
22	27.7227	0.9211	9-Octadecenoic acid, methyl ester, (E)-	122326	001937-62-8	99
23	27.8313	0.7544	9-Octadecenoic acid, methyl ester, (E)-	122326	001937-62-8	99
24	28.3228	3.5821	Octadecanoic acid, methyl ester	123709	000112-61-8	99
25	29.4088	0.0444	Octadec-9-enoic acid	113356	1000190-13-7	93
26	29.5288	0.0791	Hexadecanoic acid, butyl ester	132322	000111-06-8	95
27	30.5176	0.6084	Nonadecanoic acid, methyl ester	132330	001731-94-8	98
28	30.6433	0.1129	Coumarin-3-carboxylic acid, 8-allyl-, cyclohexyl ester	132156	325472-94-4	15
29	31.1406	0.1995	Tridecanedioic acid, dimethyl ester	106736	001472-87-3	53
30	31.5235	0.1039	2H-1,4-Benzodiazepin-2-one, 7-chloro-1,3-dihydro-5-phenyl-1-(trimethylsilyl)-3-[(trimethylsilyl)oxy]-	177154	055319-93-2	59
31	31.6435	0.3615	5,8,11,14,17-Eicosapentaenoic acid, methyl ester, (all-Z)-	134757	002734-47-6	94
32	32.3465	0.1446	11-Eicosenoic acid, methyl ester	139171	003946-08-5	76
33	32.4208	0.1056	11-Eicosenoic acid, methyl ester	139171	003946-08-5	99
34	32.598	0.1823	11-Eicosenoic acid, methyl ester	139171	003946-08-5	96
35	33.2324	4.116	Eicosanoic acid, methyl ester	140313	001120-28-1	99
36	35.6444	10.226	Tetracosane	146923	000646-31-1	99
37	36.3074	1.1379	Heneicosanoic acid, methyl ester	147951	006064-90-0	99
38	37.1818	0.49	Octadecanedioic acid, dimethyl ester	148831	001472-93-1	91
39	39.2622	0.2504	13-Docosenoic acid, methyl ester, (Z)-	153714	001120-34-9	98
40	40.2339	8.6908	Docosanoic acid, methyl ester	154650	000929-77-1	99
41	40.7826	0.1969	Pentasiloxane, dodecamethyl-	166196	000141-63-9	30
42	42.9601	4.0592	Tricosanoic acid, methyl ester	160636	002433-97-8	98
43	43.5203	0.7449	Eicosanebioic acid, dimethyl ester	161411	042235-38-1	83
44	44.2976	0.1472	Trisiloxane, 1,1,1,5,5,5-hexamethyl-3,3-bis[(trimethylsilyl)oxy]-	166198	003555-47-3	30
45	44.5891	0.2679	15-Tetracosenoic acid, methyl ester	165278	056554-33-7	99
46	44.6405	0.342	15-Tetracosenoic acid, methyl ester	165278	056554-33-7	99
47	45.3149	15.3798	Tetracosanoic acid, methyl ester	165888	002442-49-1	99
48	45.5092	0.1245	Heptacosanoic acid, 25-methyl-, methyl ester	178463	1000112-14-5	96
49	45.5893	0.3509	Tetracosanoic acid, methyl ester	165890	002442-49-1	86
50	46.0179	0.0526	Spiro[6-bromo-2,3-dihydroindol-3,5'-2'-oxazoline], 2'-methylthio-2-oxo	131678	1000311-76-1	53
51	46.1265	0.0757	Pentacosanoic acid, methyl ester	170267	055373-89-2	95
52	46.2122	0.0586	Octadecane, 1,1'-[(1-methyl-1,2-ethanediy)bis(oxy)]bis-	187968	035545-51-8	45
53	46.3951	0.0885	Silicic acid, diethyl bis(trimethylsilyl) ester	121708	003555-45-1	27
54	46.5438	0.0997	2-Octadecyl-propane-1,3-diol	141492	005337-61-1	51
55	46.9038	4.4399	Docosanoic acid, methyl ester	154652	000929-77-1	98
56	47.0353	0.2579	Pentacosanoic acid, methyl ester	170267	055373-89-2	86
57	47.3782	1.5416	Docosanedioic acid, dimethyl ester	170755	022399-98-0	91
58	47.8926	0.1534	Hexacosanoic acid, methyl ester	173512	005802-82-4	78
59	48.2012	0.2119	9-Octadecenoic acid (Z)-, methyl ester	122321	000112-62-9	60
60	48.3613	0.3324	2-Heptacosanone	169707	007796-19-2	60
61	48.8585	11.7419	Hexacosanoic acid, methyl ester	173512	005802-82-4	96
62	49.2129	0.4289	Eicosanebioic acid, dimethyl ester	161411	042235-38-1	51
63	50.0016	0.1528	Octadecanoic acid, 11-methyl-, methyl ester	132359	074484-77-8	78
64	50.0187	0.2976	Hexacosanoic acid, methyl ester	173513	005802-82-4	78
65	50.5846	2.1163	Tetracosanoic acid, methyl ester	165887	002442-49-1	99
66	51.1961	1.1863	Cyclobutanone, 2-tetradecyl-	102835	035493-47-1	45
67	51.7963	0.3352	3,3,7,11-Tetramethyltricyclo[5.4.0.0(4,11)]undecan-1-ol	72963	117591-80-7	25
68	52.2707	0.4445	Cyclotrisiloxane, hexamethyl-	73122	000541-05-9	27
69	52.3678	0.4493	2-Nonacosanone	175866	017600-99-6	35
70	52.8536	7.7376	Octacosanoic acid, methyl ester	178460	055682-92-3	97
71	53.408	0.7862	Docosanedioic acid, dimethyl ester	170755	022399-98-0	46
72	55.0655	0.108	Hexacosanoic acid, methyl ester	173513	005802-82-4	93

C:\Users\Mara\Data\21FAME_OCT11\IC3 T0_3.D
Wed Nov 09 13:56:32 2011

PK	RT	Area Pct	Library/ID	Ref	CAS	Qual
1	16.7921	0.12	Benzeneacetic acid, alpha,3,4-tris[(trimethylsilyl)oxy]-, methyl ester	174160	055268-65-0	46
2	18.5125	1.3262	Methyl tetradecanoate	86750	000124-10-7	94
3	18.7068	0.146	Tridecanoic acid, 12-methyl-, methyl ester	86778	005129-58-8	96
4	19.787	0.1662	Tridecanoic acid, 4,8,12-trimethyl-, methyl ester	105664	010339-74-9	91
5	20.9358	0.0498	Cyclononasiloxane, octadecamethyl-	189575	000556-71-8	91
6	21.0673	0.5746	Pentadecanoic acid, methyl ester	96270	007132-64-1	98
7	22.6447	0.2208	Pentadecanoic acid, 14-methyl-, methyl ester	105659	005129-60-2	95
8	23.3192	0.1092	9-Hexadecenoic acid, methyl ester, (Z)-	104152	001120-25-8	99
9	23.7193	8.0246	Hexadecanoic acid, methyl ester	105639	000112-39-0	98
10	24.5309	0.0795	Pentadecanoic acid, 14-methyl-, methyl ester	105659	005129-60-2	91
11	24.5995	0.1031	Hexadecanoic acid, 14-methyl-, methyl ester	114866	002490-49-5	83
12	24.6909	0.191	Cycloheptasiloxane, tetradecamethyl-	185541	000107-50-6	47
13	25.0681	0.3033	Hexadecanoic acid, 14-methyl-, methyl ester	114864	002490-49-5	98
14	25.2796	0.2232	Hexadecanoic acid, 14-methyl-, methyl ester	114864	002490-49-5	96
15	25.4282	0.1124	Cyclopropaneoctanoic acid, 2-hexyl-, methyl ester	113414	010152-61-1	89
16	25.9483	0.6666	Heptadecanoic acid, methyl ester	114854	001731-92-6	99
17	26.1998	0.2223	Phthalic acid, ethyl furfuryl ester	110513	1000314-91-3	22
18	26.2626	0.1723	3-Methyl-thiophene-2-carboxamide	18249	076655-99-7	43
19	27.3886	0.1649	Heptadecanoic acid, 15-methyl-, methyl ester	123730	054833-55-5	64
20	27.5658	0.5053	Hexadecanoic acid, 3,7,11,15-tetramethyl-, methyl ester	140343	001118-77-0	98
21	27.7258	0.9338	9-Octadecenoic acid, methyl ester, (E)-	122326	001937-62-8	99
22	27.8344	0.7656	9-Octadecenoic acid, methyl ester, (E)-	122326	001937-62-8	99
23	28.3316	3.6144	Octadecanoic acid, methyl ester	123709	000112-61-8	99
24	29.4062	0.0444	Octadecane, 1-(ethenyl)-	122415	000930-02-9	56
25	29.5319	0.0778	Hexadecanoic acid, 1,1-dimethylethyl ester	132348	031158-91-5	97
26	30.2463	0.0733	Cyclopropaneoctanoic acid, 2-octyl-, methyl ester	131111	010152-62-2	96
27	30.5207	0.6138	Nonadecanoic acid, methyl ester	132330	001731-94-8	98
28	30.6407	0.1136	Tetrahydrofuran-2-carboxylic acid, dibenzofuran-3-ylamide	112592	1000316-12-2	20
29	31.1437	0.1972	d-Gulopyranoside, 2,3,4,6-di-O-(ethylboranediyl)-1-O-methyl-	104987	1000149-94-5	44
30	31.5266	0.1171	Cyclononasiloxane, octadecamethyl-	189576	000556-71-8	81
31	31.6409	0.4303	5,8,11,14,17-Eicosapentaenoic acid, methyl ester, (all-Z)-	134757	002734-47-6	94
32	32.3553	0.1545	Z-7-Tetradecenoic acid	75854	1000130-98-4	55
33	32.4296	0.132	11-Eicosenoic acid, methyl ester	139171	003946-08-5	99
34	32.6011	0.1988	11-Eicosenoic acid, methyl ester	139171	003946-08-5	91
35	33.2412	4.0964	Eicosanoic acid, methyl ester	140313	001120-28-1	99
36	35.6531	10.3086	Tetracosane	146923	000646-31-1	99
37	36.3162	1.1447	Heneicosanoic acid, methyl ester	147951	006064-90-0	99
38	37.1906	0.49	Octadecanedioic acid, dimethyl ester	148831	001472-93-1	86
39	39.2825	0.2455	13-Docosenoic acid, methyl ester, (Z)-	153716	001120-34-9	96
40	40.2427	8.7342	Docosanoic acid, methyl ester	154650	000929-77-1	99
41	40.7914	0.1959	Pentasiloxane, dodecamethyl-	166195	000141-63-9	30
42	42.9632	4.1877	Tricosanoic acid, methyl ester	160636	002433-97-8	98
43	43.5234	0.7586	Eicosanebioic acid, dimethyl ester	161412	042235-38-1	90
44	44.3006	0.2464	Heptasiloxane, hexadecamethyl-	186165	000541-01-5	18
45	44.5921	0.37	15-Tetracosenoic acid, methyl ester	165278	056554-33-7	97
46	44.6436	0.4823	15-Tetracosenoic acid, methyl ester	165278	056554-33-7	99
47	45.318	15.6231	Tetracosanoic acid, methyl ester	165888	002442-49-1	99
48	45.5066	0.163	Tetracosanoic acid, methyl ester	165890	002442-49-1	99
49	45.5924	0.3914	Hencosanedioic acid, dimethyl ester	166463	042235-57-4	90
50	46.021	0.0789	9-Octadecenoic acid (Z)-, methyl ester	122321	000112-62-9	40
51	46.1353	0.0969	Pentacosanoic acid, methyl ester	170268	055373-89-2	94
52	46.2153	0.1197	(+/-)-cis-3,4-Dimethyl-2-phenyltetrahydro-1,4-thiazine	62165	092772-63-9	12
53	46.3182	0.0722	Pentacosanoic acid, methyl ester	170268	055373-89-2	95
54	46.3925	0.1077	2-(Acetoxymethyl)-3-(methoxycarbonyl)biphenylene	113217	093103-70-9	25
55	46.5411	0.1052	Stearic acid hydrazide	123617	004130-54-5	78
56	46.9069	4.6877	Docosanoic acid, methyl ester	154647	000929-77-1	96
57	47.3813	1.5607	Docosanedioic acid, dimethyl ester	170755	022399-98-0	91
58	47.89	0.2197	Hexacosanoic acid, methyl ester	173512	005802-82-4	70
59	48.0957	0.0804	Antra-9,10-quinone, 1-(3-hydroxy-3-phenyl-1-triazenyl)-	149262	098496-82-3	56
60	48.2043	0.2347	22-Tricosenoic acid	153711	065119-95-1	35
61	48.3586	0.3498	2-Heptacosanone	169707	007796-19-2	86
62	48.8673	11.7345	Hexacosanoic acid, methyl ester	173512	005802-82-4	96
63	49.2102	0.431	Eicosanebioic acid, dimethyl ester	161411	042235-38-1	80
64	50.0047	0.3699	Hexacosanoic acid, methyl ester	173513	005802-82-4	83
65	50.582	2.1077	Tetracosanoic acid, methyl ester	165887	002442-49-1	95
66	51.1992	1.1601	8-Methyl-2-(2-piperidin-1-ylethylsulfanyl) quinoline-3-carbonitrile	131540	1000311-60-9	51
67	51.6736	0.0858	2-Ethylacridine	62222	056751-83-2	42
68	51.7993	0.1996	Silane, trimethyl[5-methyl-2-(1-methylethyl)phenoxy]-	72681	055012-80-1	25
69	52.2737	0.1775	Benzol[h]quinoline, 2,4-dimethyl-	62243	000605-67-4	35
70	52.2909	0.0218	Cyclohexane, 1,1'-(2-propyl-1,3-propanediyl)bis-	92245	055030-21-2	35
71	52.3766	0.2655	2-Nonacosanone	175866	017600-99-6	42
72	52.8567	6.9129	Octacosanoic acid, methyl ester	178460	055682-92-3	96
73	53.4111	0.3252	Docosanedioic acid, dimethyl ester	170755	022399-98-0	38
74	55.0572	0.1092	Hexacosanoic acid, methyl ester	173513	005802-82-4	90

C:\Users\Mara\Data\19FAME_OCT11\S208 T0_1.D
Wed Nov 09 14:08:11 2011

PK	RT	Area Pct	Library/ID	Ref	CAS	Qual
1	26.1714	0.6315	4-Amino-furazan-3-carboxylic acid (2-O-tolyloxy-ethyl)-amide	99649	1000275-82-3	38
2	26.4972	0.6641	Hexadecanoic acid, 2-hydroxy-, methyl ester	116045	016742-51-1	72
3	27.1773	0.3741	Hexadecanoic acid, 3-hydroxy-, methyl ester	116046	051883-36-4	80
4	27.4459	0.558	Cyclohexadecane	74524	000295-65-8	97
5	27.7831	0.4147	2-Tetradecanone	65975	002345-27-9	56
6	28.2232	1.13	Nonanoic acid, 9-oxo-, methyl ester	47033	001931-63-1	27
7	28.8519	0.6664	Octadecanoic acid, 3-hydroxy-, methyl ester	133429	002420-36-2	72
8	30.3037	2.7428	Tridecanoic acid, 12-methyl-, methyl ester	86778	005129-58-8	50
9	31.1552	1.1298	Cyclononanone	18017	003350-30-9	49
10	31.9554	0.3243	Octadecanoic acid, 3-hydroxy-, methyl ester	133429	002420-36-2	87
11	32.2126	3.1806	1-Octadecene	93544	000112-88-9	95
12	33.1957	0.7086	11-Dodecenoic acid, 2,4,6-trimethyl-, methyl ester, (R,R,R)-(-)-	94829	030459-92-8	46
13	34.1159	0.6744	4,8,12,16-Tetramethylheptadecan-4-olide	139173	096168-15-9	97
14	35.539	21.7295	Tetracosane	146921	000646-31-1	99
15	36.082	1.0382	6-Octadecenoic acid, methyl ester, (Z)-	122324	002777-58-4	90
16	36.2706	0.4825	9-Octadecenal, (Z)-	102821	002423-10-1	91
17	37.1851	0.7235	Octadecanedioic acid, dimethyl ester	148831	001472-93-1	53
18	37.3222	0.5914	1-Heptadecene	84041	006765-39-5	70
19	38.9054	8.8219	1-Nonadecene	102860	018435-45-5	98
20	39.9342	0.4067	Docosanoic acid, methyl ester	154650	000929-77-1	97
21	40.14	0.4421	Acetamide, N-[(3.beta.,5.alpha.)-androstan-3-yl]-N-ethyl-	150347	055320-49-5	50
22	40.9744	0.3075	1-Heptadecene	84041	006765-39-5	83
23	42.0889	0.7622	9-Tricosene, (Z)-	138120	027519-02-4	97
24	42.8491	3.5463	Octadecanoic acid, 10-methyl-, methyl ester	132363	002490-19-9	66
25	42.9806	0.406	Oxirane, hexadecyl-	104256	007390-81-0	95
26	43.5292	0.5966	Eicosanebioic acid, dimethyl ester	161412	042235-38-1	74
27	43.6836	2.8117	Z-5-Nonadecene	102861	1000131-11-8	78
28	44.4952	3.909	1-Docosene	129888	001599-67-3	99
29	45.0038	0.6872	Tetracosanoic acid, methyl ester	165890	002442-49-1	99
30	45.1353	0.6041	1-Hexacosene	159039	018835-33-1	92
31	45.2896	0.3616	1-Hexacosene	159039	018835-33-1	89
32	45.4211	0.2613	Methyl 7,9-tridecadienyl ether	64387	1000131-00-0	64
33	45.6954	2.0818	Cyclohexane, 1-(1,5-dimethylhexyl)-4-(4-methylpentyl)-	112117	056009-20-2	62
34	46.2098	0.3412	Octacosane	169719	000630-02-4	94
35	46.3584	0.1794	1-Hexacosene	159039	018835-33-1	97
36	46.4327	1.1792	Cyclotetracosane	145923	000297-03-0	59
37	46.9699	8.0964	Heneicosanoic acid, methyl ester	147946	006064-90-0	78
38	47.1471	1.8918	1,3-Dioxolane, 4-ethyl-5-octyl-2,2-bis(trifluoromethyl)-, cis-	152413	038274-72-5	38
39	47.3929	0.7137	Docosanedioic acid	161406	000505-56-6	50
40	47.5815	6.8644	1-Triacontanol	178480	000593-50-0	53
41	47.9987	0.677	Tricosane	139233	000638-67-5	93
42	48.1931	1.9673	9-Tricosene, (Z)-	138120	027519-02-4	98
43	48.6103	0.3603	Hexacosanoic acid, methyl ester	173512	005802-82-4	96
44	48.7932	0.4662	1-Nonadecene	102860	018435-45-5	70
45	48.9704	0.6618	9-Octadecenoic acid (Z)-, methyl ester	122321	000112-62-9	90
46	49.0961	0.7158	Cyclopentadecanone, 2-hydroxy-	85349	004727-18-8	59
47	49.3704	1.5495	1-Nonadecene	102860	018435-45-5	64
48	49.862	0.2274	1,3-Dioxolane, 4-ethyl-5-octyl-2,2-bis(trifluoromethyl)-, trans-	152414	038274-73-6	35
49	50.805	4.2155	Tricosanoic acid, methyl ester	160636	002433-97-8	80
50	51.0051	1.1323	Antra-9,10-quinone, 1-(3-hydroxy-3-phenyl-1-triazenyl)-	149262	098496-82-3	53
51	51.2223	0.5377	9-Octadecenoic acid (Z)-, methyl ester	122321	000112-62-9	68
52	51.4109	1.184	Antra-9,10-quinone, 1-(3-hydroxy-3-phenyl-1-triazenyl)-	149262	098496-82-3	53
53	51.9481	0.0344	9H-Fluorene, 9-[(t-butylamino)dimethylsilyl]-	121622	154283-79-1	25
54	52.2396	1.1395	1-Hexacosene	159039	018835-33-1	97
55	53.2341	1.0635	Hexacosanoic acid, 25-oxo, methyl ester	176178	1000111-39-4	25
56	53.3541	1.031	Hexacosanoic acid, methyl ester	173513	005802-82-4	56

C:\Users\Mara\Data\19FAME_OCT11\S208 T0_2.D
Wed Nov 09 14:08:32 2011

PK	RT	Area Pct	Library/ID	Ref	CAS	Qual
1	26.1716	0.6045	5-(1-Iodo-1-methyl-ethyl)-3,3-dimethyl-dihydro-furan-2-one	113599	1000190-61-9	40
2	26.5031	0.6412	Hexadecane-1,2-diol	97546	006920-24-7	64
3	27.1889	0.3366	Octadecanoic acid, 3-hydroxy-, methyl ester	133429	002420-36-2	83
4	27.4576	0.5081	Z-8-Hexadecene	74523	1000130-87-5	95
5	27.7891	0.3818	2-Nonadecanone	113459	000629-66-3	93
6	28.2292	1.0679	[1,1'-Biphenyl]-4-amine	35743	000092-67-1	25
7	28.8578	0.6327	Octadecanoic acid, 3-hydroxy-, methyl ester	133429	002420-36-2	80
8	30.3096	2.5039	9-Hexadecenoic acid, methyl ester, (Z)-	104156	001120-25-8	53
9	31.1612	1.1043	Tridecanedioic acid, dimethyl ester	106736	001472-87-3	68
10	31.9613	0.2883	Octadecanoic acid, 3-hydroxy-, methyl ester	133429	002420-36-2	87
11	32.2186	3.0335	1-Octadecene	93544	000112-88-9	97
12	34.1161	0.6304	4,8,12,16-Tetramethylheptadecan-4-olide	139173	096168-15-9	97
13	35.545	21.0578	Tetracosane	146921	000646-31-1	99
14	36.0879	0.9955	9-Octadecenoic acid (Z)-, methyl ester	122321	000112-62-9	78
15	36.2822	0.5145	13-Octadecenal, (Z)-	102822	058594-45-9	81
16	37.1967	0.6695	10-Undecenyl chloride	58206	038460-95-6	38
17	37.3339	0.5766	13-Tetradecen-1-ol acetate	94752	056221-91-1	55
18	38.9171	8.4892	1-Nonadecene	102860	018435-45-5	97
19	39.9516	0.3347	Octadecanoic acid, 11-methyl-, methyl ester	132359	074484-77-8	95
20	40.163	0.4209	Dodecanedioic acid, 2,2,11,11-tetramethyl-	115946	022092-64-4	43
21	40.9918	0.2936	Cyclooctacosane	169156	000297-24-5	70
22	42.1006	0.7369	1-Docosanol, acetate	160634	000822-26-4	94
23	42.855	3.4659	Octadecanoic acid, 10-methyl-, methyl ester	132363	002490-19-9	64
24	42.9808	0.4412	9-Octadecenoic acid (Z)-, methyl ester	122321	000112-62-9	90
25	43.5352	0.5763	Eicosanebioic acid, dimethyl ester	161411	042235-38-1	80
26	43.6895	2.7026	1-Nonadecene	102860	018435-45-5	70
27	44.2668	0.2065	Cyclopropaneundecanal, 2-nonyl-	145910	056196-17-9	94
28	44.3753	0.1477	Octacosane	169719	000630-02-4	95
29	44.5011	4.0435	1-Docosene	129888	001599-67-3	98
30	45.0097	0.688	Tetracosanoic acid, methyl ester	165890	002442-49-1	99
31	45.1412	0.6698	1-Hexacosene	159039	018835-33-1	95
32	45.2955	0.3663	1-Docosene	129888	001599-67-3	90
33	45.427	0.2414	Erucic acid	146863	000112-86-7	60
34	45.5642	0.1751	1-Hexacosene	159039	018835-33-1	91
35	45.7013	1.9217	1-Docosene	129889	001599-67-3	64
36	46.2157	0.3628	Eicosane	113492	000112-95-8	94
37	46.4386	1.3117	Pentadec-7-ene, 7-bromomethyl-	125926	1000259-58-5	80
38	46.5358	0.4866	Cyclopentadecanone, 2-hydroxy-	85349	004727-18-8	55
39	46.9759	8.3988	Heneicosanoic acid, methyl ester	147946	006064-90-0	70
40	47.1531	2.3607	9-Octadecenoic acid (Z)-, 9-hexadecenyl ester, (Z)-	184836	022393-99-3	52
41	47.3988	0.9525	Docosanedioic acid, dimethyl ester	170754	022399-98-0	72
42	47.5874	7.1759	1-Docosene	129889	001599-67-3	70
43	48.0047	1.0696	Nonacosane	173139	000630-03-5	90
44	48.2047	2.3548	1-Docosene	129888	001599-67-3	99
45	48.6105	0.49	Hexacosanoic acid, methyl ester	173512	005802-82-4	95
46	48.7934	0.6551	1-Nonadecene	102860	018435-45-5	70
47	48.982	0.7676	9-Octadecenoic acid (Z)-, methyl ester	122321	000112-62-9	90
48	49.1135	1.0681	Antra-9,10-quinone, 1-(3-hydroxy-3-phenyl-1-triazenyl)-	149262	098496-82-3	53
49	49.3821	1.6528	1-Docosene	129889	001599-67-3	87
50	49.8565	0.259	Antra-9,10-quinone, 1-(3-hydroxy-3-phenyl-1-triazenyl)-	149262	098496-82-3	53
51	50.811	3.8264	Tricosanoic acid, methyl ester	160636	002433-97-8	80
52	51.011	0.8938	1-Octadecene	93544	000112-88-9	70
53	51.2282	0.4143	cis-Inositol tri-methylboronate	93668	1000064-40-1	59
54	51.4225	0.9833	Cyclohexane, 1,1'-(2-ethyl-1,3-propanediyl)bis-	82661	054833-34-0	38
55	51.9483	0.2966	Antra-9,10-quinone, 1-(3-hydroxy-3-phenyl-1-triazenyl)-	149262	098496-82-3	53
56	52.257	0.805	1-Hexacosene	159039	018835-33-1	95
57	53.24	1.1188	Antra-9,10-quinone, 1-(3-hydroxy-3-phenyl-1-triazenyl)-	149262	098496-82-3	56
58	53.3658	0.8273	Tetracosanoic acid, methyl ester	165890	002442-49-1	62

C:\Users\Mara\Data\19FAME_OCT11\S208 T0_3.D
Wed Nov 09 14:09:02 2011

PK	RT	Area Pct	Library/ID	Ref	CAS	Qual
1	26.1762	0.579	Cyclopentene-3-carboxylic acid, 1-(trimethylsilyloxy-, methyl ester	66811	1000151-78-8	38
2	26.5077	0.5955	Hexadecanoic acid, 2-hydroxy-, methyl ester	116045	016742-51-1	74
3	27.1936	0.2996	Hexadecanoic acid, 3-hydroxy-, methyl ester	116046	051883-36-4	86
4	27.4736	0.3405	Z-8-Hexadecene	74523	1000130-87-5	95
5	28.2395	0.9016	Decanoic acid, methyl ester	47245	000110-42-9	38
6	28.8682	0.5817	Octadecanoic acid, 3-hydroxy-, methyl ester	133429	002420-36-2	74
7	30.3199	2.3879	Pentadecanoic acid, methyl ester	96271	007132-64-1	46
8	31.1658	0.9884	d-Gulopyranoside, 2,3:4,6-di-O-(ethylboranediyl)-1-O-methyl-	104987	1000149-94-5	44
9	31.966	0.3028	Octadecanoic acid, 3-hydroxy-, methyl ester	133429	002420-36-2	87
10	32.2289	2.8657	1-Octadecene	93544	000112-88-9	95
11	33.2291	0.6455	Undecanoic acid, 2,4,6-trimethyl-, methyl ester	86784	055955-76-5	38
12	34.1264	0.6098	4,8,12,16-Tetramethylheptadecan-4-olide	139173	096168-15-9	98
13	35.561	19.6292	Tetracosane	146921	000646-31-1	99
14	36.1097	0.8882	9-Octadecenoic acid, methyl ester, (E)-	122326	001937-62-8	84
15	36.2869	0.3242	13-Octadecenal, (Z)-	102822	058594-45-9	81
16	36.344	0.1434	E-10-Octadecen-1-ol acetate	131079	002195-92-8	83
17	37.2128	0.6484	Octadecanedioic acid, dimethyl ester	148829	001472-93-1	53
18	37.3442	0.5343	1-Nonadecene	102860	018435-45-5	87
19	38.9331	8.153	3-Eicosene, (E)-	112107	074685-33-9	97
20	39.9505	0.3214	Docosanoic acid, methyl ester	154650	000929-77-1	96
21	40.1734	0.3902	11-Dodecenoic acid, 2,4,6-trimethyl-, methyl ester, (2S,4R,6R)-(+)-	94831	030459-93-9	43
22	41.0021	0.428	1-Nonadecene	102860	018435-45-5	83
23	42.1224	0.6882	9-Tricosene, (Z)-	138120	027519-02-4	99
24	42.8654	3.1161	Octadecanoic acid, 10-methyl-, methyl ester	132363	002490-19-9	64
25	42.9911	0.3485	Oxirane, hexadecyl-	104256	007390-81-0	91
26	43.5455	0.5681	9-Octadecenoic acid (Z)-, methyl ester	122321	000112-62-9	70
27	43.6941	2.5549	1-Nonadecene	102860	018435-45-5	55
28	44.38	0.1471	Tetrapentacontane, 1,54-dibromo-	190704	1000156-09-4	93
29	44.5114	3.9907	Cyclotetrasiloxane	145923	000297-03-0	97
30	45.0144	0.8432	Tetracosanoic acid, methyl ester	165890	002442-49-1	99
31	45.1459	0.9165	1-Hexacosene	159039	018835-33-1	76
32	45.3002	0.541	1-Hexacosene	159039	018835-33-1	91
33	45.4374	0.5026	Erucic acid	146863	000112-86-7	70
34	45.5688	0.3936	9-Tricosene, (Z)-	138120	027519-02-4	83
35	45.706	2.4422	1-Docosene	129889	001599-67-3	83
36	46.2204	0.7478	Eicosane	113492	000112-95-8	89
37	46.449	1.7684	22-Tricosenoic acid	153711	065119-95-1	84
38	46.5519	0.7084	Pentadec-7-ene, 7-bromomethyl-	125926	1000259-58-5	56
39	46.9862	8.6791	Heneicosanoic acid, methyl ester	147946	006064-90-0	70
40	47.1577	2.5552	Cyclopentane, 1,1'-[3-(2-cyclopentylethyl)-1,5-pentanediy]bis-	127513	055255-85-1	50
41	47.4092	1.084	Docosanedioic acid, dimethyl ester	170754	022399-98-0	46
42	47.5921	7.1574	Cyclooctacosane	169156	000297-24-5	78
43	48.015	1.1953	Tetracosane	146920	000646-31-1	93
44	48.2151	2.5689	9-Tricosene, (Z)-	138120	027519-02-4	99
45	48.6152	0.644	Hexacosanoic acid, methyl ester	173512	005802-82-4	95
46	48.8038	0.7591	22-Tricosenoic acid	153711	065119-95-1	49
47	48.9866	0.837	9-Octadecenoic acid (Z)-, methyl ester	122321	000112-62-9	90
48	49.1238	1.0744	1-Nonadecene	102860	018435-45-5	47
49	49.3867	1.6882	2-Octadecyl-propane-1,3-diol	141492	005337-61-1	60
50	49.8611	0.3188	Antra-9,10-quinone, 1-(3-hydroxy-3-phenyl-1-triazenyl)-	149262	098496-82-3	53
51	50.8213	3.663	9-Hexadecenoic acid, methyl ester, (Z)-	104156	001120-25-8	64
52	51.0213	0.9461	9-Octadecenoic acid (Z)-, methyl ester	122321	000112-62-9	70
53	51.2271	0.4423	2-Oxabicyclo[4.4.0]dec-9-en-8-one, 1,3,7,7-tetramethyl-, (-)-(1R,3S,6R)-	62880	122723-58-4	42
54	51.4329	0.9104	Antra-9,10-quinone, 1-(3-hydroxy-3-phenyl-1-triazenyl)-	149262	098496-82-3	53
55	52.2616	0.7906	1-Docosene	129889	001599-67-3	95
56	53.2561	1.1018	22-Tricosenoic acid	153711	065119-95-1	60
57	53.3819	0.7494	Tetracosanoic acid, methyl ester	165889	002442-49-1	47

Appendix 6: Isotope Ratio Mass Spectrometry Data

This appendix presents the data from the analysis of samples from PC09 and PC13 via Isotope Ratio Mass Spectrometry and discussed in detail in Chap. 3. The reported measurements in this appendix are voltages (mV) and $^{13}\text{C}/^{12}\text{C}$ ratio (‰). Each sample was analyzed in triplicate. Samples with voltage readings less than 250 mV and greater than 10,000 mV were eliminated from the data set. A standard, tetracosane, was added to each sample (analyzed on October 19, 2011 and later) prior to analysis. Each run was later corrected for the internal standard of known $\delta^{13}\text{C}$ composition ($\delta^{13}\text{C} = -31.548\text{‰}$), to account for chromatographic effects on isotope ratio and that average of the three corrected values was reported as the $\delta^{13}\text{C}$ signature.

δ ¹³ C - October 12, 2011		CO ₂ Standard												
	Retention Time (min)	48.1	75.2	129.4	868	1020.9	1119.4	1174.5	1251.9	1327.9	1343.3	1358.2	1394.3	1423.1
	Sample ID													
	'STD_3'	-40.845	-41.1	-41.064	-27.521	-28.785	0	-25.882	-24.017	-32.885	0	0	0	-25.36
	'STD_2'	-41.304	-41.1	-41.188	-28.475	-28.919	0	-26.112	-24.095	-33.02	0	0	0	-25.883
	'STD_1'	-41.188	-41.1	-41.288	-27.854	-29.47	0	-26.515	-24.175	-33.262	0	0	0	-26.789
	'S208_3'	-41.146	-41.1	-41.048	0	0	0	-24.52	0	-24.277	0	0	0	0
	'S208_2'	-41.34	-41.1	-41.084	0	0	0	-26.702	0	-25.672	0	0	0	0
	'S208_1'	-41.159	-41.1	-41.116	0	0	0	-26.012	0	-24.593	0	0	0	0
	'C1_3'	-41.027	-41.1	-41.107	0	0	0	-25.524	-20.339	-24.013	0	0	0	-27.087
	'C1_2'	-40.756	-41.1	-41.12	0	0	0	-26.315	-23.73	-24.917	0	0	0	-28.957
	'C1_1'	-41.23	-41.1	-40.773	0	0	0	-25.643	-24.822	-24.208	-28.997	0	0	-26.689
	'C2_3'	-41.205	-41.1	-40.801	-26.724	-23.811	-27.238	-24.826	-24.516	-23.113	-28.099	-23.674	-24.258	-28.626
	'C2_2'	-41.423	-41.1	-41.312	-25.801	-24.258	-26.743	-25.054	-24.701	-23.842	-29.475	-22.714	-27.768	-27.389
Voltages - October 12, 2011		CO ₂ Standard												
	Retention Time (min)	48.1	75.2	129.4	868	1020.9	1119.4	1174.5	1251.9	1327.9	1343.3	1358.2	1394.3	1423.1
	Sample ID													
	'STD_3'	1838	1814	1823	68	97	0	130	208	163	0	0	0	144
	'STD_2'	1843	1832	1848	71	99	0	132	210	168	0	0	0	142
	'STD_1'	1840	1833	1834	71	100	0	136	211	172	0	0	0	131
	'S208_3'	1858	1846	1840	0	0	0	233	0	197	0	0	0	0
	'S208_2'	1829	1833	1847	0	0	0	230	0	199	0	0	0	0
	'S208_1'	1820	1821	1834	0	0	0	230	0	199	0	0	0	0
	'C1_3'	1836	1849	1840	0	0	0	719	65	410	0	0	0	78
	'C1_2'	1832	1853	1827	0	0	0	708	63	402	0	0	0	78
	'C1_1'	1832	1848	1846	0	0	0	710	66	400	82	0	0	78
	'C2_3'	1840	1839	1842	71	82	80	1547	156	920	159	90	55	159
	'C2_2'	1839	1847	1835	68	80	76	1528	151	883	154	88	53	148

$\delta^{13}\text{C}$ - October 12, 2011	Retention Time (min)	1481.7	1541.1	1567.6	1580.2	1589.5	1619.4	1637.8	1677.5	1725.8	1760.3	1877	1891.9	1929.7
	Sample ID													
	'STD_3'	-29.562	0	-24.04	0	-29.261	-30.238	0	0	-30.054	-24.083	-29.385	-29.944	0
	'STD_2'	-29.57	0	-23.908	0	-28.936	-30.187	0	0	-30.255	-25.005	-29.363	-28.756	0
	'STD_1'	-30.632	0	-23.921	0	-29.759	-30.679	0	0	-30.504	-24.439	-30.844	-29.266	0
	'S208_3'	-26.106	0	0	0	0	-27.547	0	0	-25.637	-29.066	0	-30.44	0
	'S208_2'	-26.919	0	0	0	0	-29.181	0	0	-27.121	-29.808	0	-31.266	0
	'S208_1'	-26.517	0	0	0	0	-28.045	0	0	-24.925	-28.926	0	-28.054	0
	'C1_3'	-25.412	0	-25.239	-28.606	0	-28.034	-23.528	0	-28.362	-30.158	0	-29.659	-44.321
	'C1_2'	-26.376	0	-27.322	-30.584	0	-29.421	-27.214	0	-29.881	-31.158	0	-31.363	-39.831
	'C1_1'	-25.388	0	-25.177	-27.769	0	-28.356	-25.442	0	-28.255	-30.026	0	-24.884	-37.33
	'C2_3'	-24.988	-30.183	-28.042	-30.369	-32.838	-30.194	-28.863	0	-25.335	-28.098	-28.544	-27.46	-33.058
	'C2_2'	-25.962	-30.923	-27.898	-30.44	-31.667	-29.617	-26.466	-27.426	-25.358	-28.415	-33.842	-34.15	-29.748
	'C2_1'	-25.285	-26.442	-22.764	-28.483	0	-28.062	-19.193	0	-26.039	-28.998	0	-29.647	-33.805
	'C3_3'	-25.745	0	-23.835	-29.175	0	-28.21	-20.326	0	-25.946	-29.209	0	-28.668	-39.247
	'C3_2'	-25.433	0	-23	-28.638	0	-27.598	-13.362	0	-25.635	-28.394	0	-29.502	0
	'C3_1'	-26.76	0	0	-38.803	0	-34.859	0	0	-33.926	-29.505	0	-29.448	0
Voltages - October 12, 2011	Retention Time (min)	1481.7	1541.1	1567.6	1580.2	1589.5	1619.4	1637.8	1677.5	1725.8	1760.3	1877	1891.9	1929.7
	Sample ID													
	'STD_3'	209	0	202	0	200	225	0	0	229	247	206	207	0
	'STD_2'	211	0	207	0	200	227	0	0	220	245	211	219	0
	'STD_1'	213	0	219	0	213	236	0	0	220	257	230	239	0
	'S208_3'	2438	0	0	0	0	130	0	0	233	931	0	131	0
	'S208_2'	2398	0	0	0	0	129	0	0	235	940	0	131	0
	'S208_1'	2458	0	0	0	0	131	0	0	233	939	0	147	0
	'C1_3'	5473	0	85	78	0	328	79	0	311	2273	0	304	52
	'C1_2'	5474	0	86	81	0	325	79	0	311	2274	0	305	51
	'C1_1'	5416	0	86	81	0	328	78	0	317	2320	0	357	52
	'C2_3'	9663	163	225	213	97	637	258	0	948	4930	113	689	75
	'C2_2'	9628	168	232	216	100	631	278	63	959	4899	58	610	78
	'C2_1'	9371	81	147	137	0	600	274	0	949	4758	0	561	75
	'C3_3'	4022	0	61	67	0	231	65	0	380	1749	0	265	51
	'C3_2'	3991	0	59	66	0	224	51	0	339	1743	0	258	0
	'C3_1'	4261	0	0	172	0	351	0	0	399	1816	0	256	0

$\delta^{13}\text{C}$ - October 12, 2011	Retention Time (min)	1961.1	2015.5	2048.3	2224.9	2281.1	2404.2	2456.2	2504.1	2631.1	2669.9	2740.3	2771.9	2848.5
	Sample ID													
	'STD_3'	0	0	-26.758	0	0	0	0	0	0	0	0	0	0
	'STD_2'	0	0	-26.709	0	0	0	0	0	0	0	0	0	0
	'STD_1'	0	0	-26.511	0	0	-29.304	0	0	0	0	0	0	0
	'S208_3'	0	0	-30.08	-32.135	0	0	-32.363	0	-32.583	-32.962	-23.587	-34.332	0
	'S208_2'	0	0	-30.922	-31.794	0	0	-32.949	0	-33.597	-32.252	-24.953	-35.748	0
	'S208_1'	0	0	-29.527	-34.612	0	0	-31.778	0	-32.152	-25.226	0	-31.358	0
	'C1_3'	0	0	-31.422	-30.951	-30.603	0	-31.467	-29.645	-32.066	-34.379	0	-30.09	0
	'C1_2'	0	0	-32.591	-37.485	-32.937	0	-32.394	0	-34.17	-32.605	0	-33.725	0
	'C1_1'	0	0	-31.232	-35.76	-30.062	0	-30.983	0	-32.103	-31.996	0	-29.285	0
	'C2_3'	-23.905	-25.334	-30.993	-38.132	-32.524	-21.144	-32.483	-32.908	-33.229	-30.181	-24.895	-84.273	0
	'C2_2'	-24.732	-25.51	-31.078	-37.143	-32.462	-21.635	-32.113	-32.25	-32.795	-31.783	-26.386	-85.08	-34.394
	'C2_1'	0	-26.164	-30.822	-37.055	-30.486	-20.543	-31.564	-33.828	-32.604	-30.794	-26.787	-35.266	0
	'C3_3'	0	0	-30.652	-37.354	-31.587	0	-31.354	0	-32.363	-30.873	0	-35.697	0
	'C3_2'	0	0	-30.846	-35.634	-30.319	0	-30.884	0	-31.803	-31.816	-26.156	-31.587	0
	'C3_1'	0	-32.302	-30.135	-35.715	-31.196	0	-30.603	0	-31.867	-31.03	-26.959	-32.412	0
Voltages - October 12, 2011	Retention Time (min)	1961.1	2015.5	2048.3	2224.9	2281.1	2404.2	2456.2	2504.1	2631.1	2669.9	2740.3	2771.9	2848.5
	Sample ID													
	'STD_3'	0	0	154	0	0	0	0	0	0	0	0	0	0
	'STD_2'	0	0	164	0	0	0	0	0	0	0	0	0	0
	'STD_1'	0	0	193	0	0	234	0	0	0	0	0	0	0
	'S208_3'	0	0	944	157	0	0	1299	0	659	60	64	96	0
	'S208_2'	0	0	923	158	0	0	1322	0	672	63	69	90	0
	'S208_1'	0	0	940	167	0	0	1357	0	680	64	0	4147	0
	'C1_3'	0	0	2299	379	67	0	3360	77	2034	178	0	370	0
	'C1_2'	0	0	2309	378	65	0	3336	0	2046	236	0	351	0
	'C1_1'	0	0	2363	394	68	0	3425	0	2098	244	0	347	0
	'C2_3'	62	98	3835	697	116	66	5066	122	3241	400	404	12645	0
	'C2_2'	67	107	3827	714	124	69	5075	120	3219	403	394	12649	77
	'C2_1'	0	101	3722	703	120	66	5008	112	3215	397	374	528	0
	'C3_3'	0	0	1637	332	84	0	2512	0	1682	240	0	432	0
	'C3_2'	0	0	1617	329	78	0	2533	0	1637	233	137	208	0
	'C3_1'	0	105	1674	352	91	0	2545	0	1672	277	150	1952	0

$\delta^{13}\text{C}$ - October 12, 2011				CO ₂ Standard			
	Retention Time (min)	2874.7	2904	2933.9	3258.8	3277.6	3300.4
	Sample ID						
	'STD_3'	0	0	0	-40.466	-40.554	-40.698
	'STD_2'	0	0	-36.239	-40.782	-40.879	-41.106
	'STD_1'	0	0	-35.5	-40.386	-40.253	-40.373
	'S208_3'	-34.358	-35.12	-22.578	-41.308	-41.032	-41.18
	'S208_2'	-36.247	-34.799	69.392	-41.543	-41.709	-41.81
	'S208_1'	-30.867	-29.866	0	-40.471	-40.348	-40.218
	'C1_3'	-30.69	-30.61	-27.594	-40.615	-40.511	-40.44
	'C1_2'	-33.744	-33.064	-45.384	-41.473	-41.493	-41.295
	'C1_1'	-30.81	-30.724	-26.98	-40.253	-40.095	-40.319
	'C2_3'	-31.954	-31.603	-28.295	-41.008	-41.098	-40.952
	'C2_2'	-33.368	-32.788	-12.647	-41.547	-41.22	-41.418
	'C2_1'	-31.548	-31.855	-30.534	-41.494	-41.181	-41.295
	'C3_3'	-31.699	-31.927	-28.562	-41.187	-41.106	-41.018
'C3_2'	-30.963	-32.177	-34.067	-41.256	-41.099	-40.868	
'C3_1'	-31.457	-32.446	-52.338	-40.837	-40.951	-40.754	
Voltages - October 12, 2011				CO ₂ Standard			
	Retention Time (min)	2874.7	2904	2933.9	3258.8	3277.6	3300.4
	Sample ID						
	'STD_3'	0	0	0	1823	1824	1836
	'STD_2'	0	0	62	1857	1840	1845
	'STD_1'	0	0	70	1841	1810	1835
	'S208_3'	742	211	142	1849	1840	1843
	'S208_2'	762	212	150	1825	1850	1824
	'S208_1'	889	333	0	1845	1816	1815
	'C1_3'	2794	665	493	1830	1821	1838
	'C1_2'	2600	524	321	1830	1829	1837
	'C1_1'	2830	700	519	1833	1824	1834
	'C2_3'	4199	1167	719	1829	1830	1847
	'C2_2'	3956	1005	510	1822	1822	1831
	'C2_1'	4099	1138	615	1849	1821	1826
	'C3_3'	2161	1048	415	1850	1834	1848
	'C3_2'	2050	1056	75	1838	1826	1834
	'C3_1'	1967	829	224	1834	1845	1847

$\delta^{13}\text{C}$ - October 13, 2011		CO ₂ Standard												
	Retention Time (min)	47.3	75.4	129.4	1359.3	1401.9	1415.6	1472.8	1511.3	1600.7	1616.6	1636.8	1654.4	1706.6
	Sample ID													
	'S203_F3_3'	-41.287	-41.1	-41.163	0	0	0	0	0	0	0	0	-29.314	-31.22
	'S203_F3_2'	-41.421	-41.1	-41.214	0	0	0	0	0	0	0	0	-30.002	-29.882
	'S203_F3_1'	-40.973	-41.1	-40.928	0	0	0	0	0	0	0	0	-29.197	-29.059
	'S203_F1_3'	-41.277	-41.1	-41.153	0	0	0	0	0	0	0	0	0	-30.244
	'S203_F1_2'	-41.211	-41.1	-41.064	0	0	0	0	0	0	0	0	0	-31.045
	'S203_F1_1'	-41.326	-41.1	-41.019	0	0	0	0	0	0	0	0	0	-30.973
	'S204_F3_3'	-41.187	-41.1	-41.11	-24.861	-25.732	-28.682	-23.384	-27.701	-30.11	-27.286	-22.994	-28.461	-30.753
	'S204_F3_2'	-41.124	-41.1	-40.878	-26.925	-27.446	-31.637	-24.828	-27.095	-29.893	-28.275	-22.715	-28.399	-28.256
	'S204_F3_1'	-41.099	-41.1	-40.873	-29.566	0	0	-23.114	-25.062	0	-27.726	-22.281	-28.279	-28.972
	'S204_F1_3'	-41.417	-41.1	-41.057	-28.411	0	-29.67	0	0	-29.438	0	0	0	-30.042
	'S204_F1_2'	-41.146	-41.1	-40.954	-23.762	0	-31.734	0	0	-27.991	0	0	0	-29.74
	'S204_F1_1'	-41.164	-41.1	-40.943	0	0	0	0	0	0	0	0	0	0
	'S208_F3_3'	-41.566	-41.1	-41.014	0	0	0	0	0	0	0	0	0	0
	'S208_F3_2'	-40.905	-41.1	-41.049	0	0	0	0	0	0	0	0	0	0
	'S208_F3_1'	-41.314	-41.1	-41.197	0	0	0	0	0	0	0	0	0	0
	'S208_F1_3'	-41.098	-41.1	-41.04	0	0	0	0	0	0	0	0	0	-29.168
	'S208_F1_2'	-41.151	-41.1	-40.95	0	0	0	0	0	0	0	0	0	-28.662
	'S208_F1_1'	-41.269	-41.1	-41.039	0	0	0	0	0	0	0	0	0	-28.745
	'Zero CO2'	-41.166	-41.1	-41.128	0	0	0	0	0	0	0	0	0	0
	'Zero CO2'	-41.056	-41.1	-40.839	0	0	0	0	0	0	0	0	0	0

Voltages - October 13, 2011		CO ₂ Standard												
	Retention Time (min)	47.3	75.4	129.4	1359.3	1401.9	1415.6	1472.8	1511.3	1600.7	1616.6	1636.8	1654.4	1706.6
	Sample ID													
	'S203_F3_3'	1785	1774	1795	0	0	0	0	0	0	0	0	231	91
	'S203_F3_2'	1795	1792	1801	0	0	0	0	0	0	0	0	216	83
	'S203_F3_1'	1793	1783	1807	0	0	0	0	0	0	0	0	158	71
	'S203_F1_3'	1804	1808	1771	0	0	0	0	0	0	0	0	0	81
	'S203_F1_2'	1784	1768	1797	0	0	0	0	0	0	0	0	0	101
	'S203_F1_1'	1781	1783	1778	0	0	0	0	0	0	0	0	0	114
	'S204_F3_3'	1783	1772	1771	80	66	63	65	89	101	145	350	454	184
	'S204_F3_2'	1787	1773	1764	75	55	55	57	82	93	128	344	430	205
	'S204_F3_1'	1773	1781	1774	79	0	0	57	70	0	96	292	352	129
	'S204_F1_3'	1781	1788	1793	54	0	111	0	0	139	0	0	0	359
	'S204_F1_2'	1777	1777	1796	191	0	135	0	0	171	0	0	0	446
	'S204_F1_1'	1792	1777	1791	0	0	0	0	0	0	0	0	0	0
	'S208_F3_3'	1787	1784	1762	0	0	0	0	0	0	0	0	0	0
	'S208_F3_2'	1770	1788	1770	0	0	0	0	0	0	0	0	0	0
	'S208_F3_1'	1786	1769	1781	0	0	0	0	0	0	0	0	0	0
	'S208_F1_3'	1791	1800	1785	0	0	0	0	0	0	0	0	0	83
	'S208_F1_2'	1796	1770	1798	0	0	0	0	0	0	0	0	0	60
'S208_F1_1'	1822	1801	1801	0	0	0	0	0	0	0	0	0	68	
'Zero CO2'	1803	1789	1800	0	0	0	0	0	0	0	0	0	0	
'Zero CO2'	1800	1818	1796	0	0	0	0	0	0	0	0	0	0	

$\delta^{13}\text{C}$ - October 13, 2011	Retention Time (min)	1756.5	1794.5	1830.8	1880.2	1933.5	1990.2	2017.6	2049.8	2106	2147.3	2165.5	2215.3	2288.8
	Sample ID													
	'S203_F3_3'	-25.41	-29.969	0	-33.027	-30.513	-33.464	-32.311	-28.552	-28.983	0	-31.074	-29.576	-33.016
	'S203_F3_2'	-25.632	-30.247	0	-32.52	-29.885	-32.057	0	-30.128	-29.507	0	-30.379	-29.686	-32.63
	'S203_F3_1'	-26.463	-31.373	0	-34.489	-31.6	-32.115	-31.663	-29.493	-48.776	0	-30.989	-31.59	-29.858
	'S203_F1_3'	0	0	0	-30.514	0	-30.682	0	0	0	0	-30.501	0	0
	'S203_F1_2'	0	0	-30.834	0	0	-30.827	0	0	0	0	-30.208	0	0
	'S203_F1_1'	0	0	-30.093	0	0	-30.851	0	0	0	0	-30.407	0	0
	'S204_F3_3'	-27.774	-30.922	-33.255	-33.336	-30.712	-33.408	-30.329	-29.74	-29.794	-33.672	-32.743	-32.004	-32.084
	'S204_F3_2'	-27.026	-29.323	-31.754	-33.172	-31.496	-32.752	-31.223	-30.011	-28.573	-27.643	-32.3	-31.477	-32.074
	'S204_F3_1'	-26.303	-28.915	0	-32.159	-30.988	-31.14	-30.512	-26.647	-27.818	0	-29.492	-29.287	-31.182
	'S204_F1_3'	0	0	-30.852	-30.852	0	-30.552	0	0	0	0	-31.389	0	0
	'S204_F1_2'	0	0	-29.574	0	0	-30.901	0	0	0	0	-30.399	0	0
	'S204_F1_1'	0	0	0	0	0	0	0	0	0	0	0	0	0
	'S208_F3_3'	0	0	0	0	0	0	0	0	0	0	0	0	0
	'S208_F3_2'	0	0	0	0	0	0	0	0	0	0	0	0	0
	'S208_F3_1'	-26.755	0	0	-31.327	-34.321	-30.687	0	0	-22.565	0	-30.854	-24.224	0
	'S208_F1_3'	0	0	0	-29.25	0	-30.467	0	0	0	0	-28.75	0	0
	'S208_F1_2'	0	0	0	-28.817	0	-29.853	0	0	0	0	-29.193	0	0
	'S208_F1_1'	0	0	0	-27.454	0	-30.152	0	0	0	0	-29.913	0	0
	'Zero CO2'	0	0	0	0	0	0	0	0	0	0	0	0	0
	'Zero CO2'	0	0	0	0	0	0	0	0	0	0	0	0	0

Voltages - October 13, 2011	Retention Time (min)	1756.5	1794.5	1830.8	1880.2	1933.5	1990.2	2017.6	2049.8	2106	2147.3	2165.5	2215.3	2288.8
	Sample ID													
	'S203_F3_3'	266	286	0	725	294	297	70	97	236	0	292	214	172
	'S203_F3_2'	253	272	0	704	289	288	0	132	235	0	281	209	167
	'S203_F3_1'	178	215	0	532	242	240	61	84	176	0	234	193	134
	'S203_F1_3'	0	0	0	111	0	322	0	0	0	0	130	0	0
	'S203_F1_2'	0	0	126	0	0	341	0	0	0	0	138	0	0
	'S203_F1_1'	0	0	127	0	0	336	0	0	0	0	149	0	0
	'S204_F3_3'	531	534	55	1279	664	872	147	220	306	57	511	359	441
	'S204_F3_2'	537	542	51	1239	643	827	127	199	272	56	459	314	383
	'S204_F3_1'	449	418	0	1052	537	756	149	127	250	0	435	348	341
	'S204_F1_3'	0	0	353	353	0	914	0	0	0	0	313	0	0
	'S204_F1_2'	0	0	428	0	0	1060	0	0	0	0	408	0	0
	'S204_F1_1'	0	0	0	0	0	0	0	0	0	0	0	0	0
	'S208_F3_3'	0	0	0	0	0	0	0	0	0	0	0	0	0
	'S208_F3_2'	0	0	0	0	0	0	0	0	0	0	0	0	0
	'S208_F3_1'	935	0	0	221	139	109	0	0	94	0	96	92	0
	'S208_F1_3'	0	0	0	90	0	267	0	0	0	0	76	0	0
	'S208_F1_2'	0	0	0	75	0	252	0	0	0	0	73	0	0
	'S208_F1_1'	0	0	0	62	0	277	0	0	0	0	77	0	0
	'Zero CO2'	0	0	0	0	0	0	0	0	0	0	0	0	0
	'Zero CO2'	0	0	0	0	0	0	0	0	0	0	0	0	0

$\delta^{13}\text{C}$ - October 13, 2011	Retention Time (min)	2378.5	2449.5	2473.6	2513.7	2580.2	2628.7	2681.2	2732.2	2806.4	2882.7	2918.8	2957.2	3005.1
	Sample ID													
	'S203_F3_3'	-33.536	-25.792	0	-29.584	-31.582	-33.151	-30.16	-31.263	-29.463	-31.389	-31.023	-32.272	0
	'S203_F3_2'	-32.651	-25.103	-29.957	-30.896	-32.727	-32.949	-29.936	-29.01	-32.557	-33.743	-32.357	-34.048	0
	'S203_F3_1'	-33.329	-26.759	0	-31.129	-34.687	-35.028	-32.666	-36.541	-34.776	-34.376	-33.727	-35.668	0
	'S203_F1_3'	-30.805	0	0	0	-31.9	0	0	-32.632	-32.343	0	0	-31.693	0
	'S203_F1_2'	-31.025	0	0	0	-32.726	0	0	-32.59	-32.773	0	0	-33.166	0
	'S203_F1_1'	-31.524	0	0	0	-30.839	0	0	-31.5	-28.95	-29.159	0	-33.22	0
	'S204_F3_3'	-32.04	-27.861	0	-30.73	0	-31.875	-31.39	-32.804	-29.918	-32.065	-31.538	-32.859	0
	'S204_F3_2'	-31.893	-25.167	-28.72	-30.14	-40.689	-34.869	-32.334	-32.9	-31.807	-32.854	-32.794	-37.093	-27.225
	'S204_F3_1'	-30.975	-28.187	0	-28.049	-31.472	-32.23	-30.906	-31.232	-29.713	-30.331	-34.708	-56.739	-30.023
	'S204_F1_3'	-30.645	0	0	0	-31.367	0	0	-31.539	-31.712	0	0	-33.01	0
	'S204_F1_2'	-30.554	0	0	0	-30.245	0	0	-30.281	-31.192	-27.508	0	-31.099	0
	'S204_F1_1'	0	0	0	0	0	0	0	-107.727	-29.376	0	0	-30.874	0
	'S208_F3_3'	0	0	0	0	0	0	0	0	0	0	0	0	0
	'S208_F3_2'	0	0	0	0	0	0	0	0	0	0	0	0	0
	'S208_F3_1'	0	0	0	0	0	0	0	0	0	0	0	0	0
	'S208_F1_3'	-30.364	0	0	0	-29.883	0	0	-28.977	-30.633	0	0	-31.313	0
	'S208_F1_2'	-30.062	0	0	0	-30.174	0	0	-31.902	-30.094	0	0	-31.686	0
	'S208_F1_1'	-29.968	0	0	0	-29.794	0	0	-31.422	-30.919	0	-28.594	-31.88	0
	'Zero CO2'	0	0	0	0	0	0	0	0	0	0	0	0	0
	'Zero CO2'	0	0	0	0	0	0	0	0	0	0	0	0	0

Voltages - October 13, 2011	Retention Time (min)	2378.5	2449.5	2473.6	2513.7	2580.2	2628.7	2681.2	2732.2	2806.4	2882.7	2918.8	2957.2	3005.1
	Sample ID													
	'S203_F3_3'	842	140	0	144	110	851	908	1394	883	2374	2103	1408	0
	'S203_F3_2'	827	134	58	103	107	782	841	105	570	694	1826	1094	0
	'S203_F3_1'	744	110	0	90	103	751	780	1208	653	822	1981	1326	0
	'S203_F1_3'	277	0	0	0	115	0	0	645	143	0	0	609	0
	'S203_F1_2'	289	0	0	0	133	0	0	767	185	0	0	693	0
	'S203_F1_1'	348	0	0	0	169	0	0	868	232	53	0	669	0
	'S204_F3_3'	2130	205	0	226	0	1121	973	1459	746	1950	1961	897	0
	'S204_F3_2'	2204	146	65	159	170	907	1020	1921	831	2111	2252	657	143
	'S204_F3_1'	2588	251	0	137	140	1252	1480	2853	1224	3350	2867	1092	161
	'S204_F1_3'	765	0	0	0	324	0	0	1662	284	0	0	1374	0
	'S204_F1_2'	903	0	0	0	389	0	0	1778	333	218	0	1463	0
	'S204_F1_1'	0	0	0	0	0	0	0	12797	4914	0	0	1875	0
	'S208_F3_3'	0	0	0	0	0	0	0	0	0	0	0	0	0
	'S208_F3_2'	0	0	0	0	0	0	0	0	0	0	0	0	0
	'S208_F3_1'	0	0	0	0	0	0	0	0	0	0	0	0	0
	'S208_F1_3'	193	0	0	0	64	0	0	73	63	0	0	285	0
	'S208_F1_2'	191	0	0	0	65	0	0	65	68	0	0	292	0
	'S208_F1_1'	216	0	0	0	75	0	0	139	80	0	1205	61	0
	'Zero CO2'	0	0	0	0	0	0	0	0	0	0	0	0	0
	'Zero CO2'	0	0	0	0	0	0	0	0	0	0	0	0	0

$\delta^{13}\text{C}$ - October 13, 2011								CO ₂ Standard		
	Retention Time (min)	3026.1	3109.4	3121.9	3145	3193.9	3234.8	3252.6	3278.4	3300.4
	Sample ID									
	'S203_F3_3'	0	-31.486	0	0	-32.554	-32.397	-46.278	-45.131	-41.98
	'S203_F3_2'	-38.122	-36.185	-35.02	-37.669	-33.473	-35.287	-60.776	-51.324	-40.812
	'S203_F3_1'	-35.901	-37.373	0	-37.881	-34.621	-33.754	-53.74	-42.853	-42.651
	'S203_F1_3'	-31.977	0	0	0	-32.642	-35.94	-42.545	-41.008	-41.752
	'S203_F1_2'	-35.143	0	0	0	-32.058	-31.526	-44.242	-40.834	-40.97
	'S203_F1_1'	-28.086	-27.141	0	0	-32.548	-32.826	-49.426	-40.688	-40.659
	'S204_F3_3'	-31.774	-32.451	0	0	0	-32.575	-59.315	-52.14	-41.775
	'S204_F3_2'	-32.099	-33.892	-33.32	-34.9	-35.074	-31.088	-95.92	-60.192	-42.757
	'S204_F3_1'	-40.336	-32.02	-32.311	-31.588	-34.036	-31.451	-57.359	-49.271	-40.403
	'S204_F1_3'	-31.718	0	0	0	-32.598	-30.1	-42.29	-41.283	-41.131
	'S204_F1_2'	-29.88	0	0	0	-32.719	-29.309	-41.452	-39.998	-39.925
	'S204_F1_1'	-37.437	0	0	0	-35.433	-31.343	-45.767	-41.578	-41.7
	'S208_F3_3'	0	0	0	0	0	0	-40.708	-40.707	-40.551
	'S208_F3_2'	0	0	0	0	0	0	-41.551	-41.41	-41.548
	'S208_F3_1'	0	0	0	0	0	0	-41.497	-41.478	-41.619
	'S208_F1_3'	0	0	0	0	-31.334	-29.182	-41.233	-41.202	-40.87
	'S208_F1_2'	0	0	0	0	-31.448	-36.854	-41.179	-40.633	-40.78
	'S208_F1_1'	0	0	0	-31.334	0	-35.658	-41.369	-40.62	-40.593
	'Zero CO2'	0	0	0	0	0	0	0	0	0
	'Zero CO2'	0	0	0	0	0	0	0	0	0

Voltages - October 13, 2011								CO ₂ Standard		
	Retention Time (min)	3026.1	3109.4	3121.9	3145	3193.9	3234.8	3252.6	3278.4	3300.4
	Sample ID									
	'S203_F3_3'	0	1171	0	0	1012	1167	1598	1545	1800
	'S203_F3_2'	154	841	413	313	612	734	1219	1212	1798
	'S203_F3_1'	536	961	0	439	692	716	1330	1787	1778
	'S203_F1_3'	67	0	0	0	434	120	1574	1790	1773
	'S203_F1_2'	79	0	0	0	524	162	1515	1806	1793
	'S203_F1_1'	137	123	0	0	558	258	1322	1793	1783
	'S204_F3_3'	686	945	0	0	0	1176	1297	1225	1792
	'S204_F3_2'	379	682	344	268	342	827	1073	1002	1783
	'S204_F3_1'	52	858	385	285	459	733	1249	1229	1795
	'S204_F1_3'	140	0	0	0	149	129	1609	1771	1782
	'S204_F1_2'	164	0	0	0	151	180	1597	1771	1776
	'S204_F1_1'	190	0	0	0	149	216	1461	1786	1785
	'S208_F3_3'	0	0	0	0	0	0	1757	1780	1784
	'S208_F3_2'	0	0	0	0	0	0	1764	1798	1782
	'S208_F3_1'	0	0	0	0	0	0	1770	1785	1768
	'S208_F1_3'	0	0	0	0	136	71	1701	1785	1779
	'S208_F1_2'	0	0	0	0	159	76	1670	1788	1811
	'S208_F1_1'	0	0	0	212	0	90	1669	1794	1813
	'Zero CO2'	0	0	0	0	0	0	0	0	0
	'Zero CO2'	0	0	0	0	0	0	0	0	0

	Retention Time (min)	CO ₂ Standard			1362	1404.5	1418.7	1512.5	1602.8	1618.9	1638.1	1656.5	1709.2	1759.1
		49.2	89.8	115.4										
$\delta^{13}\text{C}$ - October 14, 2011	Sample ID													
	'S196_F3_1'	-41.375	-41.1	-40.983	0	0	0	0	0	0	0	0	0	0
	'S196_F1_3'	-41.363	-41.1	-40.976	-31.601	0	-34.86	0	-30.624	0	0	0	-34.037	0
	'S196_F1_2'	-41.195	-41.1	-40.75	-29.091	0	-34.133	0	-30.886	0	0	0	-32.701	0
	'S196_F1_1'	-41.662	-41.1	-41.104	-33.458	0	-35.37	0	-33.169	0	0	0	-33.868	0
	'S197_F3_3'	-41.389	-41.1	-41.017	-30.395	-26.784	-32.476	-32.649	-31.361	-30.75	-25.416	-29.698	-30.654	-27.141
	'S197_F3_2'	-41.387	-41.1	-41.048	-29.289	-27.991	-32.9	-30.267	-33.588	-30.978	-26.256	-30.239	-31.755	-28.403
	'S197_F3_1'	-41.352	-41.1	-41.047	-28.707	0	0	-27.775	0	-30.948	-26.187	-29.956	-29.988	-27.824
	'S197_F1_3'	-41.44	-41.1	-41.067	-33.099	0	-35.547	0	-32.12	0	0	0	-33.675	0
	'S197_F1_2'	-41.411	-41.1	-41.081	-32.42	0	-35.091	0	-31.696	0	0	0	-31.526	0
	'S197_F1_1'	-41.341	-41.1	-40.911	-32.41	0	-33.901	0	-32.1	0	0	0	-32.948	0
	'S202_F3_3'	-41.314	-41.1	-40.975	0	0	0	0	0	0	0	-31.474	0	-28.668
	'S202_F3_2'	-41.273	-41.1	-40.92	0	0	0	0	0	0	0	-30.478	0	-27.765
	'S202_F3_1'	-41.183	-41.1	-40.946	0	0	0	0	0	0	0	-27.911	-27.284	-26.677
	'S202_F1_3'	-41.486	-41.1	-41.455	0	0	-30.756	0	-31.145	0	0	0	-30.887	0
	'S202_F1_2'	-41.372	-41.1	-41.075	0	0	-30.699	0	-31.811	0	0	0	-32.966	0
	'S202_F1_1'	-41.21	-41.1	-40.918	0	0	-31.993	0	-30.272	0	0	0	-32.338	0
	'S210_F3_3'	-41.396	-41.1	-41.258	0	0	0	0	0	0	0	-31.29	0	-26.89
	'S210_F3_2'	-40.995	-41.1	-40.849	0	0	0	0	0	0	0	-30.407	0	-24.817
	'S210_F3_1'	-41.073	-41.1	-40.959	0	0	0	0	0	0	0	-29.21	0	-24.49
	'S210_F1_3'	-41.055	-41.1	-41.03	0	0	0	0	0	0	0	0	-30.438	0
	'S210_F1_2'	-41.362	-41.1	-41.089	0	0	0	0	0	0	0	0	-30.902	0
	'S210_F1_1'	-41.322	-41.1	-40.989	0	0	0	0	0	0	0	0	-31.786	0
	'S211_F3_3'	-41.417	-41.1	-40.832	-25.198	-28.825	0	-22.343	-32.131	-28.826	-23.221	-28.635	-26.851	-25.334
	'S211_F3_2'	-41.136	-41.1	-40.906	-19.947	0	0	-24.549	-32.13	-29.562	-23.185	-28.904	-28.905	-26.673
	'S211_F3_1'	-41.215	-41.1	-40.953	-27.314	0	0	-25.796	0	0	-26.805	-29.264	-28.115	-26.383
	'S211_F1_3'	-41.108	-41.1	-40.816	0	0	0	0	-30.438	0	0	0	-31.187	0
	'S211_F1_2'	-41.283	-41.1	-40.847	0	0	0	0	-30.458	0	0	0	-30.784	0
	'S211_F1_1'	-41.277	-41.1	-41.117	0	0	-30.811	0	-29.43	0	0	0	-30.661	0

	Retention Time (min)	CO ₂ Standard			1362	1404.5	1418.7	1512.5	1602.8	1618.9	1638.1	1656.5	1709.2	1759.1
		49.2	89.8	115.4										
Voltages - October 14, 2011	Sample ID													
	'S196_F3_1'	1859	1871	1863	0	0	0	0	0	0	0	0	0	0
	'S196_F1_3'	1834	1807	1811	57	0	86	0	126	0	0	0	307	0
	'S196_F1_2'	1859	1858	1839	60	0	94	0	139	0	0	0	323	0
	'S196_F1_1'	1826	1829	1818	60	0	94	0	142	0	0	0	346	0
	'S197_F3_3'	1807	1815	1824	74	60	76	68	92	102	73	361	204	338
	'S197_F3_2'	1813	1813	1816	74	58	74	67	92	100	77	358	192	420
	'S197_F3_1'	1820	1808	1825	73	0	0	58	0	87	71	322	165	376
	'S197_F1_3'	1798	1810	1821	64	0	218	0	315	0	0	0	822	0
	'S197_F1_2'	1808	1798	1807	64	0	224	0	339	0	0	0	857	0
	'S197_F1_1'	1804	1808	1805	63	0	245	0	359	0	0	0	883	0
	'S202_F3_3'	1811	1804	1805	0	0	0	0	0	0	0	165	0	290
	'S202_F3_2'	1862	1844	1830	0	0	0	0	0	0	0	170	0	285
	'S202_F3_1'	1844	1837	1845	0	0	0	0	0	0	0	157	75	262
	'S202_F1_3'	1804	1815	1821	0	0	52	0	85	0	0	0	209	0
	'S202_F1_2'	1804	1795	1806	0	0	54	0	79	0	0	0	209	0
	'S202_F1_1'	1786	1807	1793	0	0	55	0	86	0	0	0	214	0
	'S210_F3_3'	1834	1831	1830	0	0	0	0	0	0	0	121	0	85
	'S210_F3_2'	1838	1830	1816	0	0	0	0	0	0	0	117	0	83
	'S210_F3_1'	1826	1817	1778	0	0	0	0	0	0	0	107	0	79
	'S210_F1_3'	1792	1824	1806	0	0	0	0	0	0	0	0	70	0
	'S210_F1_2'	1801	1823	1821	0	0	0	0	0	0	0	0	68	0
	'S210_F1_1'	1815	1796	1797	0	0	0	0	0	0	0	0	68	0
	'S211_F3_3'	1783	1798	1793	64	54	0	72	73	105	207	423	171	356
	'S211_F3_2'	1787	1802	1806	55	0	0	66	61	90	197	390	178	422
	'S211_F3_1'	1798	1804	1767	53	0	0	61	0	0	189	366	145	362
	'S211_F1_3'	1804	1768	1792	0	0	0	0	68	0	0	0	192	0
	'S211_F1_2'	1791	1781	1804	0	0	0	0	75	0	0	0	210	0
	'S211_F1_1'	1789	1775	1792	0	0	57	0	87	0	0	0	228	0

$\delta^{13}\text{C}$ - October 14, 2011	Retention Time (min)	1796.5	1882.7	1936	1993.8	2021.2	2052.4	2109.3	2150.9	2180.5	2219.2	2235.8	2294.4	2384
	Sample ID													
	'S196_F3_1'	0	0	0	0	0	0	0	0	0	0	0	0	0
	'S196_F1_3'	0	-32.973	0	-34.143	0	0	0	0	-34.221	0	0	0	-35.096
	'S196_F1_2'	0	-31.509	0	-32.259	0	0	0	0	-32.709	0	0	0	-33.524
	'S196_F1_1'	0	-32.832	0	-32.926	0	0	0	0	-34.063	0	0	0	-34.258
	'S197_F3_3'	-29.504	-33.17	-30.196	-33.483	-29.221	-29.161	-28.885	-32.135	-32.741	-32.706	-31.53	-29.218	-32.253
	'S197_F3_2'	-29.982	-33.095	-29.168	-33.287	-28.586	-27.644	-28.649	-28.259	-32.38	-33.278	-32.677	-28.809	-32.951
	'S197_F3_1'	-30.064	-32.274	-29.361	-33.101	-31.579	-30.779	-30.56	0	-30.651	-30.517	0	-32.753	-29.385
	'S197_F1_3'	0	-33.02	0	-34.353	0	0	0	0	-34.989	0	0	0	-34.064
	'S197_F1_2'	0	-33.269	0	-33.816	0	0	0	0	-34.979	0	0	0	-33.875
	'S197_F1_1'	0	-33.042	0	-33.175	0	0	0	0	-33.652	0	0	0	-33.153
	'S202_F3_3'	-30.688	-32.268	-30.556	-33.603	-31.103	-30.826	-52.825	0	-31.279	-31.11	0	-33.821	-26.663
	'S202_F3_2'	-29.909	-33.27	-30.447	-32.719	-29.959	-29.146	-53.49	0	-31.414	0	-31.743	-33.25	-25.291
	'S202_F3_1'	-29.028	-32.144	-29.308	-32.265	0	-24.964	-29.214	0	-30.465	0	-31.358	-32.992	-26.117
	'S202_F1_3'	0	-32.195	0	-33.128	0	0	0	0	-33.648	0	0	0	-35.325
	'S202_F1_2'	0	-32.199	0	-34.068	0	0	0	0	-34.635	0	0	0	-35.76
	'S202_F1_1'	0	-31.41	0	-33.862	0	0	0	0	-33.909	0	0	0	-34.755
	'S210_F3_3'	-38.843	-33.173	-32.198	-32.852	0	0	-64.267	0	-30.42	0	-30.41	-33.084	-28.875
	'S210_F3_2'	-29.226	-31.604	-27.513	-31.493	0	0	-28.496	0	-29.666	0	-30.072	-32.752	-26.619
	'S210_F3_1'	-31.454	-32.793	-30.975	-31.133	0	0	-54.746	0	-29.455	0	-29.243	-31.077	-28.225
	'S210_F1_3'	0	-30.243	0	-32.535	0	0	0	0	-30.883	0	0	0	-33.083
	'S210_F1_2'	0	-31.012	0	-32.233	0	0	0	0	-33.205	0	0	0	-33.083
	'S210_F1_1'	0	-31.486	0	-33.82	0	0	0	0	-36.103	0	0	0	-31.918
	'S211_F3_3'	-28.469	-32.417	-30.133	-31.611	-30.102	-28.828	-28.005	-29.558	-31.813	-31.329	0	-30.574	-26.542
	'S211_F3_2'	-28.304	-31.982	-29.83	-31.933	-30.523	-28.918	-29.067	-31.663	-31.387	-31.067	0	-31.595	-26.113
	'S211_F3_1'	-28.355	-32.428	-31.435	-31.673	-32.208	-30.102	-29.265	0	-30.041	0	-30.777	-30.545	-28.752
	'S211_F1_3'	0	-31.682	0	-31.864	0	0	0	0	-31.499	0	0	0	-34.046
	'S211_F1_2'	0	-30.876	0	-31.705	0	0	0	0	-31.413	0	0	0	-32.191
	'S211_F1_1'	0	-30.387	0	-31.835	0	0	0	0	-32.287	0	0	0	-31.719

Voltages - October 14, 2011	Retention Time (min)	1796.5	1882.7	1936	1993.8	2021.2	2052.4	2109.3	2150.9	2180.5	2219.2	2235.8	2294.4	2384
	Sample ID													
	'S196_F3_1'	0	0	0	0	0	0	0	0	0	0	0	0	0
	'S196_F1_3'	0	330	0	878	0	0	0	0	360	0	0	0	813
	'S196_F1_2'	0	351	0	947	0	0	0	0	377	0	0	0	851
	'S196_F1_1'	0	382	0	1011	0	0	0	0	425	0	0	0	975
	'S197_F3_3'	53	1354	396	979	173	215	299	61	625	490	308	290	2829
	'S197_F3_2'	409	1373	386	995	174	210	312	56	621	496	314	288	2875
	'S197_F3_1'	92	1252	286	893	170	119	273	0	537	398	0	215	239
	'S197_F1_3'	0	780	0	1898	0	0	0	0	711	0	0	0	1635
	'S197_F1_2'	0	789	0	1891	0	0	0	0	720	0	0	0	1675
	'S197_F1_1'	0	851	0	2046	0	0	0	0	803	0	0	0	1812
	'S202_F3_3'	245	747	283	390	72	90	130	0	337	229	0	172	146
	'S202_F3_2'	237	676	233	382	74	122	138	0	334	0	235	163	58
	'S202_F3_1'	216	601	183	353	0	86	165	0	310	0	241	134	105
	'S202_F1_3'	0	195	0	433	0	0	0	0	148	0	0	0	309
	'S202_F1_2'	0	197	0	420	0	0	0	0	144	0	0	0	302
	'S202_F1_1'	0	198	0	440	0	0	0	0	152	0	0	0	345
	'S210_F3_3'	107	397	195	87	0	0	84	0	173	0	176	137	78
	'S210_F3_2'	104	378	170	86	0	0	110	0	165	0	167	132	74
	'S210_F3_1'	99	362	162	84	0	0	89	0	154	0	140	120	66
	'S210_F1_3'	0	74	0	165	0	0	0	0	66	0	0	0	117
	'S210_F1_2'	0	73	0	161	0	0	0	0	68	0	0	0	122
	'S210_F1_1'	0	77	0	187	0	0	0	0	77	0	0	0	172
	'S211_F3_3'	54	1290	620	709	128	201	277	58	586	422	0	482	263
	'S211_F3_2'	434	1223	599	694	125	194	279	57	576	400	0	437	243
	'S211_F3_1'	73	1073	507	602	111	174	241	0	487	0	326	346	193
	'S211_F1_3'	0	193	0	430	0	0	0	0	131	0	0	0	226
	'S211_F1_2'	0	213	0	474	0	0	0	0	150	0	0	0	272
	'S211_F1_1'	0	225	0	526	0	0	0	0	183	0	0	0	344

$\delta^{13}\text{C}$ - October 14, 2011	Retention Time (min)	2584.5	2632.4	2684.3	2735.7	2768.6	2809.2	2853.8	2885.4	2921.2	2960.3	3008.1	3028.7	3041.7
	Sample ID													
	'S196_F3_1'	0	0	0	0	0	0	0	0	0	0	0	0	0
	'S196_F1_3'	-35.376	0	0	-34.565	0	0	-30.641	0	0	-34.355	-27.307	0	-34.376
	'S196_F1_2'	-33.405	0	0	-31.909	0	0	-32.153	0	0	-32.027	0	0	-49.439
	'S196_F1_1'	-31.059	0	0	-30.585	0	0	-31.51	-29.194	-32.975	-27.377	0	0	-54.531
	'S197_F3_3'	-29.926	-34.542	-29.997	-31.263	0	-29.01	0	-30.637	-29.972	-31.259	0	-29.863	0
	'S197_F3_2'	-30.359	-34.593	-31.288	-32.733	-29.407	-32.178	-33.82	-32.923	-32.698	-37.924	-31.929	-32.249	-36.221
	'S197_F3_1'	-35.237	-33.024	-31.054	-32.195	0	-30.13	0	-31.678	-31.423	-32.277	0	-30.857	0
	'S197_F1_3'	-34.961	0	0	-33.297	0	0	-31.259	0	0	-33.044	0	0	-32.491
	'S197_F1_2'	-34.404	0	0	-32.535	0	0	-31.287	0	0	-33.428	-26.792	-29.879	-22.833
	'S197_F1_1'	-32.264	0	0	-31.416	0	0	-32.074	0	0	-32.965	-30.308	0	-33.507
	'S202_F3_3'	-31.861	-32.929	-31.121	-36.136	-33.952	-34.396	0	-34.148	-32.66	-34.706	0	-34.093	0
	'S202_F3_2'	-33.409	-32.89	-31.43	-35.771	-33.193	-33.972	0	-30.493	-33.222	-34.186	0	-33.759	0
	'S202_F3_1'	-34.646	-32.826	-30.819	-32.185	0	-29.543	0	-31.639	-31.409	-31.677	0	-31.033	0
	'S202_F1_3'	-35.175	0	0	-34.469	0	0	-34.855	0	0	-33.187	0	0	-34.78
	'S202_F1_2'	-35.43	0	0	-35.119	0	0	-29.32	0	0	-34.888	0	0	-34.501
	'S202_F1_1'	-33.738	0	0	-33.674	0	0	-32.066	0	0	-34.873	0	-30.828	-33.774
	'S210_F3_3'	-33.837	-32.87	-31.631	-30.52	0	-30.259	0	-31.92	-31.44	0	0	-30.768	0
	'S210_F3_2'	-30.36	-32.885	-30.879	-29.871	-30.678	-32.355	0	-33.472	-32.404	-32.586	0	-33.994	0
	'S210_F3_1'	-31.702	-34.088	-32.884	-33.329	-28.846	-32.962	0	-33.61	-32.796	0	0	-32.506	0
	'S210_F1_3'	-34.193	0	0	-33.041	0	0	-34.174	0	0	-33.076	0	0	0
	'S210_F1_2'	-33.622	0	0	-33.357	0	0	-37.869	0	0	-36.139	0	0	0
	'S210_F1_1'	-29.242	0	0	-31.408	0	0	-30.714	0	0	-40.294	0	0	-59.337
	'S211_F3_3'	-29.154	-30.988	-29.702	-30.658	0	-29.491	0	-29.769	-32.776	-46.14	-30.339	-31.21	0
	'S211_F3_2'	-34	-31.88	-30.38	-32.053	0	-29.684	0	-31.001	-30.789	-31.483	0	-30.628	0
	'S211_F3_1'	-32.81	-32.776	-31.473	-31.792	0	-30.061	0	-31.318	-31.141	-32.08	0	-31.186	0
	'S211_F1_3'	-34.05	0	0	-34.103	0	0	-33.651	0	0	-32.545	0	0	0
	'S211_F1_2'	-33.384	0	0	-32.889	0	0	-34.327	0	0	-36.396	0	0	0
	'S211_F1_1'	-31.101	0	0	-31.106	0	0	-30.602	0	0	-32.527	0	0	-31.209

Voltages - October 14, 2011	Retention Time (min)	2584.5	2632.4	2684.3	2735.7	2768.6	2809.2	2853.8	2885.4	2921.2	2960.3	3008.1	3028.7	3041.7
	Sample ID													
	'S196_F3_1'	0	0	0	0	0	0	0	0	0	0	0	0	0
	'S196_F1_3'	361	0	0	1922	0	0	562	0	0	2015	76	0	54
	'S196_F1_2'	382	0	0	2189	0	0	461	0	0	2105	0	0	60
	'S196_F1_1'	580	0	0	2596	0	0	485	113	69	52	0	0	59
	'S197_F3_3'	556	1508	1419	3279	0	1441	0	4176	3835	2740	0	1332	0
	'S197_F3_2'	533	1531	1374	3055	443	963	596	3658	2874	1831	332	535	89
	'S197_F3_1'	321	1597	1303	3372	0	1306	0	4041	3513	2755	0	1179	0
	'S197_F1_3'	721	0	0	3741	0	0	872	0	0	3815	0	0	304
	'S197_F1_2'	730	0	0	3882	0	0	1014	0	0	3760	110	78	114
	'S197_F1_1'	849	0	0	4147	0	0	860	0	0	3905	157	0	216
	'S202_F3_3'	157	892	1072	1469	218	798	0	919	2778	1164	0	766	0
	'S202_F3_2'	158	820	998	1486	209	780	0	887	2761	1143	0	756	0
	'S202_F3_1'	150	769	886	1581	0	828	0	2412	2738	1230	0	779	0
	'S202_F1_3'	117	0	0	674	0	0	122	0	0	522	0	0	58
	'S202_F1_2'	115	0	0	675	0	0	129	0	0	543	0	0	61
	'S202_F1_1'	139	0	0	759	0	0	262	0	0	608	0	66	78
	'S210_F3_3'	80	496	812	355	0	710	0	1741	2022	0	0	643	0
	'S210_F3_2'	78	487	780	339	82	537	0	531	1780	214	0	414	0
	'S210_F3_1'	70	470	662	227	76	507	0	565	1720	0	0	424	0
	'S210_F1_3'	53	0	0	260	0	0	73	0	0	186	0	0	0
	'S210_F1_2'	62	0	0	310	0	0	91	0	0	217	0	0	0
	'S210_F1_1'	175	0	0	430	0	0	363	0	0	205	0	0	57
	'S211_F3_3'	316	1644	2031	2249	0	1851	0	3813	3728	677	252	829	0
	'S211_F3_2'	193	1420	1760	1929	0	1534	0	3402	4166	1364	0	1379	0
	'S211_F3_1'	187	1347	1590	1923	0	1372	0	3170	3787	1197	0	1144	0
	'S211_F1_3'	81	0	0	507	0	0	108	0	0	442	0	0	0
	'S211_F1_2'	97	0	0	554	0	0	120	0	0	446	0	0	0
	'S211_F1_1'	141	0	0	617	0	0	157	0	0	446	0	0	98

$\delta^{13}\text{C}$ - October 14, 2011								CO ₂ Standard		
	Retention Time (min)	3112.1	3125.4	3149	3199.1	3237.2	3245.2	3252.5	3277.2	3299
	Sample ID									
	'S196_F3_1'	0	0	0	0	0	0	0	0	0
	'S196_F1_3'	0	0	0	-33.335	-29.605	0	-44.674	-40.944	-40.685
	'S196_F1_2'	0	0	0	-32.199	-31.594	0	-47.336	-40.584	-40.568
	'S196_F1_1'	0	-23.349	0	-47.015	-31.529	0	-62.741	-40.987	-41.138
	'S197_F3_3'	-31.127	0	0	-31.415	-29.998	0	-63.875	-54.001	-40.659
	'S197_F3_2'	-33.061	-30.45	-32.116	-35.936	-32.258	-1.534	15.697	-171.559	-41.333
	'S197_F3_1'	-32.2	0	0	-32.217	-30.568	0	-45.953	-44.736	-41.263
	'S197_F1_3'	0	0	0	-26.9	-32.034	0	-46.505	-41.349	-41.419
	'S197_F1_2'	0	0	0	-30.772	-31.575	0	-48.097	-41.231	-41.148
	'S197_F1_1'	-32.951	0	0	-47.088	-26.892	0	-50.777	-40.984	-41.085
	'S202_F3_3'	-35.62	0	-35.559	-37.054	-33.275	0	-54.086	-48.921	-41.035
	'S202_F3_2'	-34.975	0	-26.025	-34.662	-32.908	0	-61.508	-41.727	-41.707
	'S202_F3_1'	-32.016	0	-32.656	-33.734	-33.507	0	-44.563	-43.76	-41.499
	'S202_F1_3'	0	0	-35.497	-30.594	-31.534	0	-41.545	-40.223	-40.068
	'S202_F1_2'	0	0	-35.273	0	-38.888	0	-43.042	-40.839	-40.77
	'S202_F1_1'	0	0	-35.201	-34.878	-32.459	0	-43.574	-41.311	-41.257
	'S210_F3_3'	-32.15	0	-31.641	0	-32.171	0	-43.486	-41.264	-41.262
	'S210_F3_2'	-33.518	0	-32.731	0	-33.574	0	-46.313	-41.014	-41
	'S210_F3_1'	-34.637	0	-34.184	0	-33.745	0	-46.697	-41.526	-41.507
	'S210_F1_3'	0	0	-32.464	0	0	-36.57	-43.071	-40.865	-40.776
	'S210_F1_2'	0	0	-34.622	0	0	-35.98	-43.696	-40.592	-40.915
	'S210_F1_1'	-26.492	0	-33.239	0	-36.198	0	-50.684	-42.398	-42.282
	'S211_F3_3'	-27.394	-33.15	-33.127	-33.9	-31.854	-4.378	425.582	-86.546	-40.974
	'S211_F3_2'	-31.148	0	-31.13	0	-31.697	0	-47.782	-45.631	-41.464
	'S211_F3_1'	-31.871	0	-31.766	0	-31.273	0	-44.027	-43.36	-41.131
	'S211_F1_3'	0	0	-34.045	0	-33.346	0	-42.776	-41.115	-41.403
	'S211_F1_2'	0	0	-33.585	0	-32.932	0	-43.236	-41.107	-41.066
	'S211_F1_1'	-22.729	0	-35.847	0	-32.865	0	-44.777	-40.635	-40.652

Voltages - October 14, 2011								CO ₂ Standard		
	Retention Time (min)	3112.1	3125.4	3149	3199.1	3237.2	3245.2	3252.5	3277.2	3299
	Sample ID									
	'S196_F3_1'	0	0	0	0	0	0	0	0	0
	'S196_F1_3'	0	0	0	1715	289	0	1481	1824	1798
	'S196_F1_2'	0	0	0	1819	327	0	1454	1862	1875
	'S196_F1_1'	0	101	0	270	425	0	1204	1798	1795
	'S197_F3_3'	1916	0	0	1883	2783	0	1276	1172	1822
	'S197_F3_2'	1311	621	532	1269	2080	1072	771	660	1801
	'S197_F3_1'	1876	0	0	1882	2363	0	1605	1526	1800
	'S197_F1_3'	0	0	0	455	404	0	1472	1796	1835
	'S197_F1_2'	0	0	0	448	418	0	1435	1766	1824
	'S197_F1_1'	146	0	0	460	445	0	1322	1788	1794
	'S202_F3_3'	1164	0	632	648	1075	0	1395	1335	1817
	'S202_F3_2'	1163	0	280	443	802	0	1253	1865	1858
	'S202_F3_1'	1181	0	659	753	1011	0	1671	1648	1853
	'S202_F1_3'	0	0	395	55	119	0	1585	1812	1792
	'S202_F1_2'	0	0	412	0	102	0	1541	1798	1815
	'S202_F1_1'	0	0	439	51	168	0	1533	1791	1779
	'S210_F3_3'	816	0	492	0	765	0	1690	1838	1835
	'S210_F3_2'	550	0	222	0	515	0	1447	1816	1830
	'S210_F3_1'	619	0	318	0	494	0	1483	1796	1806
	'S210_F1_3'	0	0	99	0	0	137	1589	1844	1825
	'S210_F1_2'	0	0	104	0	0	168	1533	1827	1829
	'S210_F1_1'	112	0	150	0	241	0	1360	1800	1810
	'S211_F3_3'	1184	590	726	440	1409	859	900	852	1801
	'S211_F3_2'	1603	0	1136	0	1763	0	1535	1459	1817
	'S211_F3_1'	1417	0	996	0	1520	0	1634	1585	1789
	'S211_F1_3'	0	0	320	0	120	0	1602	1810	1775
	'S211_F1_2'	0	0	305	0	139	0	1536	1767	1780
	'S211_F1_1'	59	0	327	0	190	0	1479	1788	1801

Voltages - October 19, 2011

	CO ₂ Standard												
Retention Time (min)	49	74.6	129	928	1371.2	1416.5	1437.2	1487.5	1524.3	1629.9	1649	1668.4	1710
Sample ID													
'C3 T0_1'	1814	1801	1812	0	371	0	108	2947	55	243	128	0	0
'S208 T0_3'	1859	1856	1859	87	148	96	0	195	177	166	312	446	213
'S208 T0_2'	1830	1843	1850	86	146	95	92	140	114	158	310	443	212
'S208 T0_1'	1789	1788	1778	83	135	88	87	131	108	152	297	419	204
'S188_F3_3'	1799	1791	1789	0	98	86	0	125	105	149	290	408	193
'S188_F3_2'	1805	1783	1778	0	92	86	0	121	103	143	283	407	191
'S188_F3_1'	1787	1807	1780	0	93	84	87	118	101	145	284	409	185
'S188.5_F3_3'	1786	1790	1776	56	150	123	423	169	205	334	0	607	0
'S188.5_F3_2'	1781	1782	1774	54	145	123	415	170	203	330	0	600	0
'S188.5_F3_1'	1783	1803	1773	51	141	118	394	165	198	308	0	561	0
'S189_F3_3'	1775	1787	1781	0	85	86	68	76	92	133	87	460	198
'S189_F3_2'	1801	1781	1769	0	81	86	105	76	95	131	85	457	195
'S189_F3_1'	1779	1799	1794	0	81	86	107	71	92	128	86	469	200
'S191_F3_3'	1808	1800	1811	0	118	104	68	59	92	152	301	411	220
'S191_F3_2'	1802	1806	1774	99	111	100	66	57	94	148	297	406	215
'S191_F3_1'	1769	1786	1787	96	112	95	64	53	85	143	285	388	215
'S194_F3_3'	1780	1786	1789	0	56	72	57	59	85	115	175	442	204
'S194_F3_2'	1791	1799	1769	0	53	69	55	56	82	106	160	406	192
'S194_F3_1'	1785	1779	1787	0	55	56	0	57	82	106	155	396	189
'S196_F3_3'	1764	1772	1764	86	79	81	0	65	97	120	0	487	229
'S196_F3_2'	1785	1763	1780	90	77	80	0	66	93	114	0	466	215
'S196_F3_1'	1760	1752	1757	86	81	78	0	65	93	116	0	465	208
'S197_F3_3'	1756	1765	1744	127	167	183	0	192	249	0	0	924	0
'S197_F3_2'	1759	1767	1776	140	289	191	0	189	250	0	0	931	414
'S197_F3_1'	1740	1768	1759	149	294	271	0	0	335	0	0	1007	0
'S202_F3_3'	1761	1743	1735	0	84	80	0	73	98	102	51	402	182
'S202_F3_2'	1740	1766	1754	0	78	74	0	67	90	94	89	400	160
'S202_F3_1'	1770	1738	1763	0	76	66	0	0	139	0	0	452	170
'S210_F3_3'	1775	1747	1742	0	55	0	0	0	61	0	0	320	109
'S210_F3_2'	1755	1758	1732	0	61	0	0	0	62	0	0	316	107
'S210_F3_1'	1771	1776	1754	0	53	0	0	0	0	66	0	232	69
'S211_F3_3'	1747	1775	1762	0	0	0	0	0	0	0	0	0	0
'S211_F3_2'	1764	1760	1769	0	0	0	0	0	0	0	0	0	0
'S211_F3_1'	1797	1787	1787	0	0	0	0	0	0	0	0	0	0
'Tetracosane_3'	1783	1788	1767	0	0	0	0	0	0	0	0	0	0
'Tetracosane_2'	1781	1796	1778	0	0	0	0	0	0	0	0	0	0
'Tetracosane_1'	1796	1821	1804	0	0	0	0	0	0	0	0	0	0

$\delta^{13}\text{C}$ - October 19, 2011	Retention Time (min)	1727.1	1773.4	1809.8	1867	1898.7	1949.9	1997	2013.3	2071.6	2126.4	2171.7	2210.6	2244.7
	Sample ID													
	'C3 T0_1'	-28.746	-30.947	0	0	-30.926	-33.634	-26.954	-28.709	-32.861	0	0	-32.105	-27.333
	'S208 T0_3'	-31.193	-28.175	-29.63	-36.125	-32.665	-30.615	-29.684	-32.919	-32.938	-29.168	-31.611	-32.033	-30.782
	'S208 T0_2'	-30.939	-27.955	-29.651	-33.632	-33.103	-31.034	-30.259	-33.971	-32.203	-31.278	-28.07	-32.343	-30.951
	'S208 T0_1'	-30.857	-27.943	-29.162	-32.548	-32.566	-30.155	-29.421	-33.051	-33.638	-28.571	-30.986	-31.403	-29.595
	'S188 F3_3'	-31.701	-28.724	-29.643	0	-32.576	-30.867	-28.568	-33.459	-29.634	-29.147	-29.957	-32.052	-30.357
	'S188 F3_2'	-32.016	-28.837	-40.749	-34.213	-33.383	-30.629	-30.082	-33.678	-30.749	-31.268	-31.496	-31.627	-29
	'S188 F3_1'	-31.35	-28.534	-29.145	0	-31.804	-30.463	0	-32.294	-29.419	-29.369	-34.542	-31.885	-29.32
	'S188.5 F3_3'	-30.351	-28.134	-28.646	0	-30.985	-29.256	0	-29.018	0	-29.2	0	-31.106	-29.673
	'S188.5 F3_2'	-31.744	-28.561	-29.612	-30.844	-32.74	-31.066	-28.697	-29.399	-34.134	-30.155	-33.619	-31.59	-31.117
	'S188.5 F3_1'	-32.05	-28.404	-29.558	-38.797	-33.394	-30.229	-29.472	-24.94	-32.513	-31.242	-31.9	-32.205	-29.499
	'S189 F3_3'	-32.339	-30.008	-30.876	0	-33.925	-30.182	-30.616	-27.811	-23.36	-31.711	0	-32.713	-29.098
	'S189 F3_2'	-31.906	-29.287	-30.499	0	-32.495	-30.287	-28.865	-28.706	-32.374	-29.016	0	-32.009	-28.072
	'S189 F3_1'	-32.19	-29.669	-30.399	0	-32.805	-30.499	0	-33.05	-30.167	-30.78	0	-32.107	-30.213
	'S191 F3_3'	-31.337	-29.473	-31.05	0	-33.214	-32.016	0	-32.273	-31.419	-31.687	0	-31.54	-31.288
	'S191 F3_2'	-30.157	-28.779	-30.545	-35.398	-32.77	-30.953	-29.175	-30.079	-30.74	-30.123	-33.941	-31.433	-30.73
	'S191 F3_1'	0	-29.951	-30.382	-31.788	-33.369	-31.392	-30.204	-32.406	-31.07	-30.422	-37.498	-31.682	-31.676
	'S194 F3_3'	0	-29.596	-31.596	0	-33.073	-31.196	-32.971	-27.849	-27.588	-28.983	-35.34	-31.924	-32.254
	'S194 F3_2'	0	-27.911	-31.671	0	-33	-30.726	-34.147	-31.088	-27.627	-30.946	-31.629	-32.185	-31.77
	'S194 F3_1'	0	-30.259	-31.342	0	-33.215	-31.425	-34.317	0	-33.95	-30.371	0	-32.379	-31.393
	'S196 F3_3'	0	-29.468	-30.523	0	-32.59	-30.273	-32.341	0	-29.924	-31.647	0	-32.457	-30.042
	'S196 F3_2'	0	-30.004	-30.934	0	-32.686	-30.501	-34.763	-30.739	-29.991	-30.943	-28.825	-33.593	-30.692
	'S196 F3_1'	0	-27.689	-34.519	0	-33.618	-30.237	-35.468	0	-23.902	-28.406	-34.313	-32.915	-31.801
	'S197 F3_3'	0	-28.636	-29.25	0	-31.011	-29.542	-31.588	0	0	-29.507	0	-31.516	-31.618
	'S197 F3_2'	0	-27.771	-29.496	0	-31.526	-29.815	-33.079	-30.921	-28.833	-28.951	0	-31.42	-32.744
	'S197 F3_1'	0	-29.049	-29.977	0	-31.371	-30.238	-32.045	0	0	-30.116	0	-31.718	-32.464
	'S202 F3_3'	0	-28.247	-30.801	0	-32.733	-31.086	-32.71	0	-30.758	-30.053	-32.857	0	-33.799
	'S202 F3_2'	0	-30.609	-38.446	0	-33.342	-30.822	-33.548	-33.555	-30.35	-29.665	-31.541	0	-32.673
	'S202 F3_1'	0	-30.222	-40.418	0	-33.68	-30.293	-33.973	-26.529	-29.135	-30.881	-32.205	0	-32.034
	'S210 F3_3'	0	-28.601	-35.101	0	-33.52	-32.41	-30.42	-33.863	-30.432	-29.358	-32.414	0	-32.369
	'S210 F3_2'	0	-28.025	-33.14	0	-33.01	-29.274	-26.856	-32.356	-29.664	-29.738	-32.225	0	-32.245
	'S210 F3_1'	0	-29.096	-31.43	0	-33.579	-31.993	-28.496	-34.332	-32.892	-31.101	-33.083	0	-32.612
	'S211 F3_3'	0	0	0	0	0	0	0	0	0	0	0	0	0
	'S211 F3_2'	0	0	0	0	0	0	0	0	0	0	0	0	0
	'S211 F3_1'	0	0	0	0	0	0	0	0	0	0	0	0	0
	'Tetracosane_3'	0	0	0	0	0	0	0	0	0	0	-33.149	0	0
	'Tetracosane_2'	0	0	0	0	0	0	0	0	0	0	-32.208	0	0
	'Tetracosane_1'	0	0	0	0	0	0	0	0	0	0	-31.489	0	0

Voltages - October 19, 2011	Retention Time (min)	1727.1	1773.4	1809.8	1867	1898.7	1949.9	1997	2013.3	2071.6	2126.4	2171.7	2210.6	2244.7
	Sample ID													
	'C3 T0_1'	523	1356	0	0	352	73	206	63	1437	0	0	6968	599
	'S208 T0_3'	312	564	437	89	1406	565	191	1617	168	384	72	7976	832
	'S208 T0_2'	305	547	438	72	1398	540	184	1615	172	371	75	7845	823
	'S208 T0_1'	293	523	417	66	1337	541	175	1548	51	359	69	7822	825
	'S188_F3_3'	285	516	418	0	1373	608	173	1512	229	351	72	7560	871
	'S188_F3_2'	281	514	262	58	1307	534	171	1507	227	346	68	7597	848
	'S188_F3_1'	279	512	426	0	1385	622	0	1573	331	451	69	7324	867
	'S188.5_F3_3'	841	774	653	0	2176	732	0	574	0	703	0	8157	1348
	'S188.5_F3_2'	701	642	524	232	2030	439	229	330	73	453	78	7834	1112
	'S188.5_F3_1'	671	610	501	111	1868	466	230	350	71	443	72	7717	1123
	'S189_F3_3'	268	523	453	0	1494	408	184	191	60	344	0	7458	1050
	'S189_F3_2'	265	535	454	0	1648	498	187	182	63	332	0	7435	1052
	'S189_F3_1'	266	537	479	0	1698	530	0	1396	343	452	0	7537	1033
	'S191_F3_3'	318	378	410	0	2555	907	0	356	332	502	0	8617	1370
	'S191_F3_2'	312	369	405	61	2391	804	200	238	217	388	66	8404	1168
	'S191_F3_1'	0	359	384	60	2295	759	196	242	214	373	58	8409	1172
	'S194_F3_3'	0	508	540	0	1635	734	889	135	64	369	53	6868	856
	'S194_F3_2'	0	390	434	0	1485	638	871	135	59	355	53	6802	854
	'S194_F3_1'	0	456	509	0	1509	716	828	0	64	355	0	6606	502
	'S196_F3_3'	0	521	578	0	1708	710	1082	0	398	385	0	6509	1007
	'S196_F3_2'	0	503	569	0	1608	697	888	167	263	388	56	6163	1035
	'S196_F3_1'	0	99	379	0	1414	569	801	0	179	342	57	5775	842
	'S197_F3_3'	0	1011	1035	0	2876	1063	2189	0	0	916	0	6625	1453
	'S197_F3_2'	0	834	857	0	2762	887	1978	293	371	572	0	7538	582
	'S197_F3_1'	0	1046	1032	0	2976	1022	2369	0	0	933	0	7890	1438
	'S202_F3_3'	0	563	499	0	1505	535	860	0	299	345	3738	0	521
	'S202_F3_2'	0	83	313	0	1286	425	677	105	198	300	3313	0	422
	'S202_F3_1'	0	77	290	0	1209	360	618	97	173	309	3296	0	424
	'S210_F3_3'	0	247	231	0	650	320	105	201	83	222	4237	0	328
	'S210_F3_2'	0	240	229	0	613	279	101	204	86	232	4291	0	343
	'S210_F3_1'	0	185	222	0	457	220	56	131	68	169	4114	0	316
	'S211_F3_3'	0	0	0	0	0	0	0	0	0	0	0	0	0
	'S211_F3_2'	0	0	0	0	0	0	0	0	0	0	0	0	0
	'S211_F3_1'	0	0	0	0	0	0	0	0	0	0	0	0	0
	'Tetracosane_3'	0	0	0	0	0	0	0	0	0	0	4115	0	0
	'Tetracosane_2'	0	0	0	0	0	0	0	0	0	0	4042	0	0
	'Tetracosane_1'	0	0	0	0	0	0	0	0	0	0	3664	0	0

$\delta^{13}\text{C}$ - October 19, 2011	Retention Time (min)	2318.6	2385.5	2414.1	2607.7	2652.6	2702.7	2752.6	2783	2807	2824.6	2870.4	2901.7	2937.8
	Sample ID													
	'C3 T0_1'	-25.573	0	-31.377	0	-31.84	0	0	-30.805	0	0	0	-31.326	0
	'S208 T0_3'	-31.161	-31.741	-29.362	0	-32.086	-31.451	-31.476	0	0	-30.747	0	-31.69	-31.872
	'S208 T0_2'	-30.413	-33.174	-32.944	-31.409	-34.695	-32.566	-33.828	-33.628	-28.692	-34.673	-35.066	-33.559	-33.225
	'S208 T0_1'	-30.052	-32.764	-30.142	0	-31.855	-31.319	-31.532	0	0	-30.622	0	-31.326	-31.159
	'S188 F3_3'	-29.619	-27.98	-29.584	-31.699	-32.625	-31.773	-31.692	-33.725	-34.117	-34.012	-35.19	-32.741	-32.108
	'S188 F3_2'	-28.264	-29.194	-29.051	0	-31.757	-30.892	-31.058	0	0	-30.723	-35.616	-32.555	-32.22
	'S188 F3_1'	-29.76	-34.202	-33.092	-31.425	-34.056	-31.557	-31.797	0	0	-30.693	0	-31.633	-31.147
	'S188.5 F3_3'	-34.258	0	-29.646	0	-32.589	-31.256	-31.494	0	0	0	0	-31.042	-31.065
	'S188.5 F3_2'	-33.409	0	-29.022	0	-32.125	-31.206	-31.396	0	0	0	0	-31.116	-31.086
	'S188.5 F3_1'	-37.174	0	-30.759	0	-32.764	-31.689	-31.859	0	0	0	0	-31.612	-31.634
	'S189 F3_3'	-38.093	0	-30.974	0	-33.252	-32.475	-32.729	0	0	-31.621	0	-32.282	-31.968
	'S189 F3_2'	-28.934	0	-30.435	0	-32.441	-31.693	-32.02	0	0	-30.9	0	-31.68	-31.439
	'S189 F3_1'	-31.216	0	-66.221	-36.903	-33.885	-31.621	-32.204	0	0	-30.527	0	-31.49	-31.126
	'S191 F3_3'	-32.124	0	-32.921	-31.843	-33.94	-32.019	-32.449	0	0	-31.274	0	-31.974	-32.226
	'S191 F3_2'	-32.388	0	-30.259	-31.883	-33.647	-31.618	-32.991	0	0	-31.949	0	-32.245	-31.975
	'S191 F3_1'	-33.11	0	-30.83	-33.482	-33.812	-32.183	-33.112	0	0	-31.919	-32.035	-32.622	-32.116
	'S194 F3_3'	-32.679	0	-30.375	0	-31.908	-31.049	-31.961	0	0	-30.703	0	-31.351	-31.094
	'S194 F3_2'	-32.574	0	-30.916	0	-32.677	-31.678	-32.042	0	0	-30.898	0	-31.496	-31.691
	'S194 F3_1'	-34.102	0	-30.476	0	-32.25	-31.295	-31.986	-38.184	-41.209	-42.73	-35.632	-32.168	-31.523
	'S196 F3_3'	-29.679	0	-30.67	-31.759	-33.01	-31.245	-31.671	-41.949	-74.794	-36.724	-35.094	-32.663	-32.627
	'S196 F3_2'	-31.252	0	-31.919	0	-33.429	-32.192	-33.096	0	0	0	0	-31.947	-32.14
	'S196 F3_1'	-32.843	-33.992	-30.081	0	-32.395	-33.191	-33.512	0	0	-31.226	-34.57	-31.33	-32.171
	'S197 F3_3'	-30.519	0	-31.854	-30.872	-35.935	-32.569	-33.129	0	0	-31.67	0	-32.367	-33.409
	'S197 F3_2'	-33.813	0	-30.853	0	-31.653	-30.844	-31.696	0	0	-30.7	0	-31.007	-31.316
	'S197 F3_1'	-31.159	0	-31.97	-31.455	-35.153	-32.536	-32.788	0	0	-32.15	0	-33.115	-32.9
	'S202 F3_3'	-33.454	-34.249	-34.652	0	-34.378	-32.83	-33.336	0	-32.474	0	0	-33.172	-33.206
	'S202 F3_2'	-30.151	-33.189	-34.168	0	-33.667	-32.156	-32.879	0	-31.73	0	0	-34.782	-32.411
	'S202 F3_1'	-32.073	-33.161	-27.972	-33.543	-34.002	-32.386	-32.687	0	-31.777	0	0	-32.485	-32.144
	'S210 F3_3'	-31.335	-34.484	-29.229	-33.559	-36.129	-33.265	-33.536	0	-32.878	0	-34.799	-32.86	-35.889
	'S210 F3_2'	-32.665	-31.543	-30.076	-41.85	-34.22	-33.146	-32.592	-31.856	-34.323	0	-35.764	-33.193	-33.236
	'S210 F3_1'	-32.334	-31.695	0	-41.04	-33.755	-33.506	-32.752	0	-32.922	0	-35.689	-32.908	-32.974
	'S211 F3_3'	0	0	0	0	0	0	0	0	0	0	0	0	0
	'S211 F3_2'	0	0	0	0	0	0	0	0	0	0	0	0	0
	'S211 F3_1'	0	0	0	0	0	0	0	0	0	0	0	0	-37.262
	'Tetracosane_3'	0	0	0	0	0	0	0	0	0	0	0	0	0
	'Tetracosane_2'	0	0	0	0	0	0	0	0	0	0	0	0	0
	'Tetracosane_1'	0	0	0	0	0	0	0	0	0	0	0	-31.513	0

Voltages - October 19, 2011	Retention Time (min)	2318.6	2385.5	2414.1	2607.7	2652.6	2702.7	2752.6	2783	2807	2824.6	2870.4	2901.7	2937.8
	Sample ID													
	'C3 T0_1'	130	0	2319	0	1480	0	0	6018	0	0	0	1949	0
	'S208 T0_3'	481	111	406	0	2150	2252	2922	0	0	2278	0	5027	5309
	'S208 T0_2'	477	109	3258	772	1716	1840	2301	272	119	1326	714	4035	4349
	'S208 T0_1'	464	100	386	0	2058	2168	2906	0	0	2217	0	4943	5204
	'S188_F3_3'	487	98	386	771	2020	2208	2942	266	115	1326	700	4093	4240
	'S188_F3_2'	66	97	385	0	1999	2181	2877	0	0	2280	630	3984	4262
	'S188_F3_1'	464	89	2985	791	1557	1742	2377	0	0	1901	0	4397	4880
	'S188.5_F3_3'	407	0	463	0	2384	2212	4658	0	0	0	0	5054	4240
	'S188.5_F3_2'	404	0	464	0	2330	2149	4624	0	0	0	0	5054	4192
	'S188.5_F3_1'	381	0	436	0	2241	2063	4562	0	0	0	0	5015	4039
	'S189_F3_3'	359	0	397	0	2136	2357	3478	0	0	2443	0	5212	6291
	'S189_F3_2'	442	0	396	0	2192	2385	3514	0	0	2476	0	5291	6373
	'S189_F3_1'	452	0	103	567	1671	1910	2940	0	0	2028	0	4731	5814
	'S191_F3_3'	715	0	3278	1181	2302	2240	4375	0	0	2279	0	6481	6759
	'S191_F3_2'	584	0	515	1037	2240	2216	4057	0	0	1945	0	6169	6338
	'S191_F3_1'	586	0	451	735	2452	2416	3953	0	0	1877	581	5567	5838
	'S194_F3_3'	491	0	383	0	2190	2253	3411	0	0	2298	0	5415	5555
	'S194_F3_2'	480	0	380	0	2083	2245	3260	0	0	2266	0	5228	5487
	'S194_F3_1'	427	0	387	0	2018	2180	3181	155	144	54	621	3765	4126
	'S196_F3_3'	468	0	400	552	1890	2186	3367	143	120	1203	619	3747	4600
	'S196_F3_2'	482	0	397	0	2025	2345	3476	0	0	0	0	4900	5696
	'S196_F3_1'	380	1937	419	0	1874	1537	2459	0	0	1765	500	1567	4062
	'S197_F3_3'	930	0	3751	1291	1946	2015	3714	0	0	2228	0	4974	3697
	'S197_F3_2'	506	0	574	0	2907	2938	5516	0	0	3080	0	6279	6643
	'S197_F3_1'	861	0	4678	1145	2470	2307	4860	0	0	2225	0	5374	5221
	'S202_F3_3'	343	2430	264	0	1831	2084	3143	0	1947	0	0	4159	4873
	'S202_F3_2'	269	1985	205	0	1505	1318	2063	0	1165	0	0	1122	3148
	'S202_F3_1'	269	2161	148	220	1364	1422	2290	0	1191	0	0	2755	2828
	'S210_F3_3'	221	310	84	124	842	1259	509	0	1061	0	149	2311	204
	'S210_F3_2'	234	285	82	62	806	1227	481	134	888	0	154	2441	2544
	'S210_F3_1'	173	245	0	62	693	1064	433	0	931	0	134	2288	2495
	'S211_F3_3'	0	0	0	0	0	0	0	0	0	0	0	0	0
	'S211_F3_2'	0	0	0	0	0	0	0	0	0	0	0	0	0
	'S211_F3_1'	0	0	0	0	0	0	0	0	0	0	0	0	75
	'Tetracosane_3'	0	0	0	0	0	0	0	0	0	0	0	0	0
	'Tetracosane_2'	0	0	0	0	0	0	0	0	0	0	0	0	0
	'Tetracosane_1'	0	0	0	0	0	0	0	0	0	0	0	150	0

	Retention Time (min)	CO ₂ Standard													
		2976.4	3022.2	3046	3075.1	3132.2	3143	3168.5	3181.3	3202.1	3216.9	3245.7	3252.5	3278.2	3295.3
δ ¹³ C - October 19, 2011	Sample ID														
	'C3 T0_1'	0	-31.277	0	0	-32.142	0	0	0	0	-32.177	-29.469	-42.552	-42.376	-40.7
	'S208 T0_3'	-31.656	0	0	0	-31.701	0	0	0	0	0	-30.958	-44.601	-44.495	-41.091
	'S208 T0_2'	-35.691	-36.305	-37.256	-44.166	-36.696	-37.436	-37.36	-40.896	-51.714	-34.459	-29.387	9.528	-1088.95	-42.033
	'S208 T0_1'	-31.541	0	0	0	-31.72	0	0	0	0	0	-30.679	-44.189	-43.801	-40.37
	'S188_F3_3'	-35.288	-35.619	-35.868	-41.417	-32.517	-33.969	-33.645	0	-38.513	-31.547	-25.005	-2.784	89.178	-40.791
	'S188_F3_2'	-35.54	-36.132	-36.256	-54.397	-33.428	-34.515	-31.9	0	-34.291	-32.223	-22.968	-8.266	247.633	-40.833
	'S188_F3_1'	-32.076	0	-32.217	0	-32.576	-38.328	-34.797	0	0	-30.353	-23.18	-13.641	37.648	-40.881
	'S188.5_F3_3'	-31.804	0	0	0	-31.803	0	0	0	0	-30.015	-24.063	-18.929	-8.802	-40.831
	'S188.5_F3_2'	-31.73	0	0	0	-31.657	0	0	0	0	-30.507	-24.17	-18.396	3.55	-40.934
	'S188.5_F3_1'	-32.09	0	0	0	-31.954	0	0	0	0	-30.467	-25.753	-16.736	0.749	-41.132
	'S189_F3_3'	-32.753	0	-32.095	-44.437	-35.708	-33.587	-35.334	0	0	-32.684	-27.291	-14.997	4.99	-41.291
	'S189_F3_2'	-32.086	0	-31.613	0	-32.127	0	0	0	0	-31.079	0	-43.515	-44.041	-40.731
	'S189_F3_1'	-32.147	0	-31.494	0	-31.928	0	-31.666	0	0	-31.988	-27.721	-13.515	22.944	-40.634
	'S191_F3_3'	-32.706	0	-32.702	-32.998	-35.794	-34.487	-34.927	0	0	-30.719	-22.435	-22.63	-17.072	-41.591
	'S191_F3_2'	-32.963	0	-32.954	0	-33.633	0	-33.077	0	0	-32.392	-26.981	33.571	-3850.01	-40.918
	'S191_F3_1'	-33.332	-33.268	-33.105	-34.786	-34.853	-31.817	-35.573	0	0	-32.326	-25.156	-13.682	2.458	-40.859
	'S194_F3_3'	-31.799	0	0	0	-31.368	0	0	0	0	0	-30.984	-43.981	-43.765	-40.47
	'S194_F3_2'	-36.813	-30.739	-35.63	-24.612	-44.261	0	-4.507	0	0	-31.374	-26.002	-12.06	4.51	-41.002
	'S194_F3_1'	-33.315	-29.104	-32.771	-31.306	-25.638	0	-31.554	0	0	-30.628	-24.575	-29.111	-2.123	-40.212
	'S196_F3_3'	-36.034	0	-36.574	-39.901	-37.228	0	-38.596	0	0	-35.198	6.991	-45.411	0	-41.253
	'S196_F3_2'	-32.741	0	0	0	-32.267	0	0	0	0	-31.909	-25.597	-17.829	-11.698	-41.83
	'S196_F3_1'	-34.341	0	-33.636	-32.759	-33.4	0	-33.495	0	0	0	-28.064	-20.662	-36.317	-40.79
	'S197_F3_3'	-40.007	-30.354	-34.977	-37.337	-35.407	-27.969	-32.443	0	0	-31.255	-26.387	-52.272	0	-41.48
	'S197_F3_2'	-31.978	-28.275	-33.802	-38.523	-36.208	-30.55	-35.842	0	0	-30.507	-24.75	-50.711	0	-41.163
	'S197_F3_1'	-34.077	0	-33.406	0	-33.542	-32.48	-33.751	0	0	-32.49	-26.098	-21.951	-42.285	-42.399
	'S202_F3_3'	-33.844	0	-33.132	0	-33.237	0	30.429	0	-36.094	0	-25.625	-11.235	204.719	-41.879
	'S202_F3_2'	-34.112	-30	-33.551	-27.909	-24.545	0	-31.88	0	-33.691	0	-28.486	-356.536	-67.5	-40.923
	'S202_F3_1'	-33.711	-32.906	-32.906	0	-33.445	-34.385	0	0	0	0	-32.198	-45.24	-44.618	-41.421
	'S210_F3_3'	0	-34.617	-34.303	-37.269	-35.108	-38.195	0	-41.597	0	0	-30.967	-49.39	-40.844	-40.804
	'S210_F3_2'	-35.365	-34.639	-34.646	0	-35.255	-38.198	0	-41.165	0	0	-30.479	-49.736	-41.475	-41.427
	'S210_F3_1'	-34.329	-34.336	0	0	-33.966	-35.853	0	-32.209	0	0	-29.892	-47.351	-44.591	-41.339
	'S211_F3_3'	0	0	0	0	0	0	0	0	0	0	-34.273	-41.72	-41.087	-41.095
	'S211_F3_2'	0	0	0	0	0	0	0	0	0	0	-33.547	-41.902	-41.172	-41.078
	'S211_F3_1'	0	0	0	0	0	0	0	0	0	0	-32.55	-41.614	-40.634	-40.662
	'Tetracosane_3'	0	0	0	0	0	0	0	0	0	0	-36.81	-42.374	-41.211	-41.006
	'Tetracosane_2'	0	0	0	0	0	0	0	0	0	0	-31.337	-42.168	-40.564	-40.298
	'Tetracosane_1'	0	0	0	-25.261	0	0	0	0	0	-26.637	0	-44.478	-40.442	-40.464

													CO ₂ Standard		
	Retention Time (min)	2976.4	3022.2	3046	3075.1	3132.2	3143	3168.5	3181.3	3202.1	3216.9	3245.7	3252.5	3278.2	3295.3
Voltages - October 19, 2011	Sample ID														
	'C3 T0_1'	0	4308	0	0	1141	0	0	0	0	3790	926	1677	1612	1813
	'S208 T0_3'	2177	0	0	0	2817	0	0	0	0	0	2755	1686	1533	1863
	'S208 T0_2'	1236	561	1058	211	1865	782	744	127	168	1537	1834	736	596	1857
	'S208 T0_1'	2132	0	0	0	2766	0	0	0	0	0	2756	1618	1490	1803
	'S188_F3_3'	1220	537	1008	213	1840	734	724	0	136	1511	1823	694	540	1808
	'S188_F3_2'	1139	493	941	131	1792	727	722	0	134	1506	1885	643	487	1786
	'S188_F3_1'	1747	0	1566	0	2358	66	391	0	0	1461	1899	555	380	1810
	'S188.5_F3_3'	4738	0	0	0	2511	0	0	0	0	4213	2117	370	180	1805
	'S188.5_F3_2'	4785	0	0	0	2558	0	0	0	0	4309	2201	399	201	1778
	'S188.5_F3_1'	4792	0	0	0	2528	0	0	0	0	4406	2230	496	293	1794
	'S189_F3_3'	3068	0	2332	133	1850	653	863	0	0	2216	1854	554	367	1783
	'S189_F3_2'	3112	0	2382	0	3023	0	0	0	0	3364	0	1658	1503	1788
	'S189_F3_1'	2642	0	1923	0	2600	0	1802	0	0	2332	2087	556	387	1787
	'S191_F3_3'	4326	0	2402	240	2490	1006	1384	0	0	4391	2831	352	115	1778
	'S191_F3_2'	3984	0	2006	0	2994	0	1911	0	0	4691	3316	875	677	1794
	'S191_F3_1'	3547	838	1580	440	2528	1110	1347	0	0	4091	2793	485	270	1817
	'S194_F3_3'	3177	0	0	0	3077	0	0	0	0	0	3221	1629	1505	1786
	'S194_F3_2'	1611	281	741	204	55	0	388	0	0	1780	2152	565	409	1782
	'S194_F3_1'	1723	414	885	226	626	0	735	0	0	1562	2123	198	207	1761
	'S196_F3_3'	2284	0	1099	380	1669	0	915	0	0	2235	1659	1571	0	1796
	'S196_F3_2'	3491	0	0	0	2835	0	0	0	0	2078	2631	288	72	1768
	'S196_F3_1'	1851	0	1049	396	681	0	956	0	0	0	2716	108	1750	1754
	'S197_F3_3'	1720	518	867	248	1405	729	877	0	0	3302	3937	1494	0	1746
	'S197_F3_2'	4400	583	919	55	1566	729	947	0	0	3374	3985	1512	0	1775
	'S197_F3_1'	3393	0	1907	0	1614	858	800	0	0	2870	3595	240	1752	1758
	'S202_F3_3'	2267	0	1755	0	2221	0	475	0	573	0	1388	611	513	1753
	'S202_F3_2'	1298	181	585	129	517	0	542	0	518	0	1187	941	867	1748
	'S202_F3_1'	1214	910	910	0	1323	798	0	0	0	0	1302	1496	1439	1773
	'S210_F3_3'	0	494	191	121	792	330	0	106	0	0	683	1305	1753	1748
	'S210_F3_2'	238	544	198	0	872	364	0	113	0	0	693	1359	1728	1751
	'S210_F3_1'	261	572	0	0	843	341	0	93	0	0	675	1433	1394	1764
	'S211_F3_3'	0	0	0	0	0	0	0	0	0	0	92	1616	1766	1767
'S211_F3_2'	0	0	0	0	0	0	0	0	0	0	99	1607	1745	1755	
'S211_F3_1'	0	0	0	0	0	0	0	0	0	0	107	1616	1782	1761	
'Tetracosane_3'	0	0	0	0	0	0	0	0	0	0	117	1595	1781	1775	
'Tetracosane_2'	0	0	0	0	0	0	0	0	0	0	141	1575	1803	1798	
'Tetracosane_1'	0	0	0	59	0	0	0	0	0	193	0	1422	1778	1769	

Voltages - October 19, 2011

	CO ₂ Standard													
	Retention Time (min)	49	81.7	129.6	877	1031.6	1129.8	1187.6	1264.3	1318.7	1341.4	1370.9	1406.1	1437
δ ¹³ C - October 21, 2011	Sample ID													
	'Tetracosane_3'	-41.636	-41.1	-41.021	0	0	0	0	0	0	0	0	0	0
	'Tetracosane_2'	-41.57	-41.1	-41.021	0	0	0	0	0	0	0	0	0	0
	'Tetracosane_1'	-41.492	-41.1	-40.924	0	0	0	0	0	0	0	0	0	0
	'S118.5_F3_3'	-41.596	-41.1	-41.139	0	0	0	0	0	0	0	-29.138	0	-26.823
	'S118.5_F3_2'	-41.508	-41.1	-41.006	0	0	0	0	0	0	0	-29.97	0	-26.114
	'S118.5_F3_1'	-41.538	-41.1	-40.901	0	0	0	0	0	0	0	-31.249	0	-27.605
	'S119_F3_3'	-41.494	-41.1	-40.751	0	0	0	0	0	0	0	-31.321	0	-27.139
	'S119_F3_2'	-41.511	-41.1	-40.825	0	0	0	0	0	0	0	-32.936	0	-27.647
	'S119_F3_1'	-41.574	-41.1	-41.07	0	0	0	0	0	0	0	-32.645	0	-27.895
	'S119.5_F3_3'	-41.489	-41.1	-41.007	0	0	0	0	0	0	0	-30.79	0	-27.507
	'S119.5_F3_2'	-41.583	-41.1	-40.777	0	0	0	0	0	0	0	-31.008	0	-27.033
	'S119.5_F3_1'	-41.798	-41.1	-40.959	0	0	0	0	0	0	0	-31.51	0	-26.453
	'S122_F3_3'	-41.748	-41.1	-41.002	0	0	0	0	0	0	0	-25.684	0	-26.741
	'S122_F3_2'	-41.509	-41.1	-41.003	0	0	0	0	0	0	0	-26.795	0	-25.917
	'S122_F3_1'	-41.535	-41.1	-41.002	0	0	0	0	0	0	0	-27.686	0	-25.68
	'S123_F3_3'	-41.405	-41.1	-40.834	0	0	0	0	0	0	0	-29.051	0	-28.482
	'S123_F3_2'	-41.51	-41.1	-40.943	0	0	0	0	0	0	0	-27.749	0	-26.909
	'S123_F3_1'	-41.56	-41.1	-40.973	0	0	0	0	0	0	0	-28.605	0	-27.212
	'S193_F3_3'	-41.472	-41.1	-40.759	0	0	0	0	0	0	0	-45.058	0	-33.838
	'S193_F3_2'	-41.697	-41.1	-40.934	0	0	0	0	0	0	0	-42.682	0	-31.458
	'S193_F3_1'	-41.681	-41.1	-41.055	0	0	0	0	0	0	0	-42.638	0	-34.771
	'S203_T0_3'	-41.73	-41.1	-40.989	-29.798	0	0	0	0	0	0	-27.182	-29.761	0
	'S203_T0_2'	-41.614	-41.1	-41.034	-30.558	0	0	0	0	0	0	-26.358	-29.381	0
	'S203_T0_1'	-41.594	-41.1	-40.931	-29.046	0	0	0	0	0	0	-30.846	-27.31	0
	'S204_T0_3'	-41.775	-41.1	-40.872	-29.468	0	-27.797	0	0	0	-27.216	-27.556	-27.499	0
	'S204_T0_2'	-41.42	-41.1	-41.088	-29.451	0	-29.173	0	0	0	-27.734	-26.283	-26.618	0
	'S204_T0_1'	-41.51	-41.1	-40.921	-28.612	0	-27.203	-32.916	0	0	-27.561	-27.357	0	-27.464
	'S208_T0_3'	-41.395	-41.1	-40.916	0	0	0	0	0	0	0	-28.941	0	-28.641
	'S208_T0_2'	-41.716	-41.1	-41.02	0	0	0	0	0	0	0	-30.64	0	-29.127
	'S208_T0_1'	-41.533	-41.1	-40.919	0	0	0	0	0	0	0	-30.016	0	-27.015
	'C1_T0_3'	-40.776	-41.1	-41.049	-30.687	-27.777	-31.744	-27.674	-28.385	0	-27.693	-25.922	0	-30.747
	'C1_T0_2'	-41.54	-41.1	-41.15	-30.797	-29.497	-34.645	-28.544	-27.526	0	-27.334	-24.872	0	-30.18
	'C1_T0_1'	-41.568	-41.1	-41.061	-30.431	-29.651	-32.93	-27.963	-32.613	0	-27.422	-24.501	0	-30.66
	'C2_T0_3'	-41.625	-41.1	-41.011	-29.45	-27.295	-31.118	-27.606	-35.062	-33.009	-27.498	-21.708	-31.445	-31.306
	'C2_T0_2'	-41.664	-41.1	-41.064	-29.08	-27.154	-30.738	-27.605	-31.121	-33.718	-27.025	-17.578	-32.381	-30.618
	'C2_T0_1'	-41.537	-41.1	-41.025	-29.261	-26.359	-34.181	-27.837	-34.155	-33.888	-27.167	-21.409	-30.943	-30.447
	'C3_T0_3'	-41.619	-41.1	-41.069	-29.01	-27.277	-33.435	-27.658	-34.623	0	-28.631	-24.211	-30.292	-30.076
	'C3_T0_2'	-41.698	-41.1	-41.044	-28.73	-28.617	-33.344	-28.488	-33.365	-36.508	-28.678	-23.452	-28.601	-29.294
	'C3_T0_1'	-41.44	-41.1	-41.333	-29.917	-28.43	-33.485	-28.123	-21.038	-38.795	-28.835	-20.573	-29.523	-29.925

Voltages - October 21, 2011

	CO ₂ Standard													
Retention Time (min)	49	81.7	129.6	877	1031.6	1129.8	1187.6	1264.3	1318.7	1341.4	1370.9	1406.1	1437	
Sample ID														
'Tetracosane_3'	1880	1877	1874	0	0	0	0	0	0	0	0	0	0	0
'Tetracosane_2'	1882	1866	1884	0	0	0	0	0	0	0	0	0	0	0
'Tetracosane_1'	1904	1911	1878	0	0	0	0	0	0	0	0	0	0	0
'S118.5_F3_3'	1885	1882	1879	0	0	0	0	0	0	0	79	0	86	
'S118.5_F3_2'	1881	1885	1885	0	0	0	0	0	0	0	80	0	85	
'S118.5_F3_1'	1879	1889	1867	0	0	0	0	0	0	0	78	0	85	
'S119_F3_3'	1888	1885	1878	0	0	0	0	0	0	0	76	0	72	
'S119_F3_2'	1880	1899	1871	0	0	0	0	0	0	0	76	0	74	
'S119_F3_1'	1885	1885	1877	0	0	0	0	0	0	0	78	0	73	
'S119.5_F3_3'	1899	1899	1870	0	0	0	0	0	0	0	89	0	83	
'S119.5_F3_2'	1897	1870	1895	0	0	0	0	0	0	0	89	0	82	
'S119.5_F3_1'	1907	1896	1895	0	0	0	0	0	0	0	94	0	82	
'S122_F3_3'	1912	1902	1895	0	0	0	0	0	0	0	104	0	86	
'S122_F3_2'	1901	1910	1905	0	0	0	0	0	0	0	105	0	87	
'S122_F3_1'	1907	1914	1899	0	0	0	0	0	0	0	101	0	85	
'S123_F3_3'	1891	1886	1889	0	0	0	0	0	0	0	84	0	65	
'S123_F3_2'	1914	1896	1898	0	0	0	0	0	0	0	87	0	68	
'S123_F3_1'	1909	1904	1890	0	0	0	0	0	0	0	92	0	70	
'S193_F3_3'	1887	1883	1882	0	0	0	0	0	0	0	75	0	62	
'S193_F3_2'	1880	1909	1865	0	0	0	0	0	0	0	72	0	81	
'S193_F3_1'	1889	1896	1871	0	0	0	0	0	0	0	72	0	60	
'S203_T0_3'	1888	1876	1890	104	0	0	0	0	0	0	114	98	0	
'S203_T0_2'	1903	1907	1909	105	0	0	0	0	0	0	120	106	0	
'S203_T0_1'	1893	1908	1917	105	0	0	0	0	0	0	127	111	0	
'S204_T0_3'	1842	1846	1838	140	0	74	0	0	0	53	215	155	0	
'S204_T0_2'	1889	1892	1878	141	0	69	0	0	0	60	229	169	0	
'S204_T0_1'	1914	1881	1895	138	0	70	67	0	0	59	200	0	129	
'S208_T0_3'	1914	1905	1887	0	0	0	0	0	0	0	94	0	72	
'S208_T0_2'	1885	1872	1880	0	0	0	0	0	0	0	77	0	66	
'S208_T0_1'	1892	1893	1876	0	0	0	0	0	0	0	73	0	63	
'C1_T0_3'	1874	1871	1870	54	57	71	833	107	0	502	87	0	139	
'C1_T0_2'	1881	1895	1874	54	58	72	835	109	0	511	87	0	145	
'C1_T0_1'	1874	1893	1877	53	57	73	846	109	0	518	85	0	144	
'C2_T0_3'	1874	1879	1880	93	111	137	1209	164	55	799	165	74	249	
'C2_T0_2'	1898	1892	1868	98	117	142	1312	169	57	811	136	78	264	
'C2_T0_1'	1893	1881	1876	97	118	125	1350	173	57	872	162	79	271	
'C3_T0_3'	1879	1862	1858	59	98	165	1629	239	0	1113	176	139	451	
'C3_T0_2'	1853	1855	1885	58	94	157	1601	232	82	1062	168	146	447	
'C3_T0_1'	1875	1865	1858	56	89	148	1595	254	77	1043	175	140	428	

δ ¹³ C - October 21, 2011	Retention Time (min)	1497.5	1581.8	1634.3	1650.9	1741.2	1776.6	1822.8	1909.6	1946.6	1977.2	2022	2035.1	2070.1
	Sample ID													
	'Tetracosane_3'	0	0	0	0	0	0	0	0	0	0	0	0	0
	'Tetracosane_2'	0	0	0	0	0	0	-33.323	0	0	0	0	0	0
	'Tetracosane_1'	0	0	0	0	0	0	0	0	0	0	0	0	0
	'S118.5_F3_3'	-28.278	0	0	-28.379	-29.374	-27.723	-30.285	-32.751	-30.485	0	-30.254	-32.366	-31.277
	'S118.5_F3_2'	-30.582	0	0	-30.964	-34.547	-27.729	-31.02	-33.026	-29.843	0	-31.219	-32.514	-31.966
	'S118.5_F3_1'	-29.502	0	0	-28.418	-30.015	-28.14	-30.782	-32.816	-31.109	0	0	-32.208	-27.933
	'S119_F3_3'	-28.257	0	0	-29.302	-29.264	-27.404	-30.519	-31.667	-30.338	0	-30.571	-32.164	-34.991
	'S119_F3_2'	-28.012	0	0	-30.815	-28.955	-27.457	-30.778	-31.685	-29.841	0	-28.163	-31.6	-28.876
	'S119_F3_1'	-30.255	0	0	-32.37	-29.169	-27.525	-30.727	-32.653	-30.326	0	-30.357	-31.775	-22.191
	'S119.5_F3_3'	-26.962	0	0	-33.613	-29.554	-28.099	-30.725	-32.221	-30.791	0	-28.631	-31.177	-29.558
	'S119.5_F3_2'	-24.115	0	0	-30.335	-29.229	-27.25	-30.047	-31.296	-29.778	0	-28.787	-31.463	-29.338
	'S119.5_F3_1'	-26.274	0	0	-30.162	-27.907	-26.918	-29.568	-31.072	-29.373	0	-28.675	-32.137	-26.763
	'S122_F3_3'	-26.764	0	0	-29.11	-29.291	-27.597	-29.476	-31.721	-30.463	0	-29.373	-31.955	-30.707
	'S122_F3_2'	-27.639	0	0	-29.065	-33.984	-26.904	-29.509	-32.045	-29.223	0	-30.286	-32.452	-25.523
	'S122_F3_1'	-28.397	0	0	-29.553	-28.753	-27.473	-29.271	-31.808	-30.79	0	-28.348	-31.961	-28.595
	'S123_F3_3'	-26.11	0	0	-30.512	-32.236	-27.269	-28.999	-33.089	-32.318	0	-32.685	-30.976	-30.576
	'S123_F3_2'	-29.36	0	0	-30.027	-30.201	-27.356	-28.658	-33.141	-31.663	0	-26.193	-36.13	-30.205
	'S123_F3_1'	-26.662	0	-28.906	-29.404	-30.457	-26.393	-27.832	-32.3	-31.32	0	-29.657	-32.32	-29.567
	'S193_F3_3'	-33.082	0	-29.191	-33.203	-30.224	-28.657	-30.285	-32.522	-31.044	0	-32.824	0	-30.107
	'S193_F3_2'	-29.22	0	-29.319	-34.068	-29.601	-28.247	-29.574	-31.657	-30.004	0	-31.632	0	-29.248
	'S193_F3_1'	-33.041	0	-28.259	-32.879	-31.861	-29.285	-30.78	-33.865	-31.366	0	-33.527	0	-30.992
	'S203_T0_3'	-55.198	0	-28.709	-29.497	-28.639	-28.52	-29.008	-31.648	-28.605	0	-30.303	0	-29.274
	'S203_T0_2'	-33.629	0	-29.937	-29.131	-29.364	-28.59	-29.43	-32.041	-29.098	0	-35.085	0	-33.928
	'S203_T0_1'	-28.631	0	-29.655	-29.837	-29.826	-28.886	-28.88	-31.775	-29.141	0	-30.413	0	-29.452
	'S204_T0_3'	-27.694	0	0	-27.776	0	-28.637	0	-30.88	-28.929	0	-30.573	0	0
	'S204_T0_2'	-27.831	0	0	-27.35	-32.237	-30.009	-29.53	-33.257	-30.401	0	-32.214	0	-30.317
	'S204_T0_1'	-28.245	0	0	-27.754	0	-29.304	0	-31.293	-28.639	0	-31.276	0	0
	'S208_T0_3'	0	0	0	-30.08	-30.48	-28.401	-30.792	-32.651	-31.328	0	0	-31.158	-29.933
	'S208_T0_2'	-28.992	0	0	-30.972	-33.399	-28.3	-32.295	-33.577	-31.457	0	-30.308	-32.921	-30.589
	'S208_T0_1'	-26.854	0	0	-29.994	-28.98	0	-29.716	-33.916	-31.494	0	-30.152	-29.981	0
	'C1_T0_3'	-29.51	-27.145	-25.526	-20.218	-29.402	-32.661	0	-32.419	-38.009	0	0	-26.467	-32.419
	'C1_T0_2'	-29.683	-27.849	-22.956	-20.609	-29.354	-33.139	0	-33.083	-40.239	0	0	-27.639	-33.375
	'C1_T0_1'	-29.897	-28.711	-25.731	-15.773	-26.591	-31.042	-22.308	-28.482	-28.851	0	0	-28.021	-33.353
	'C2_T0_3'	-29.324	0	-26.393	0	-24.685	-30.664	-25.006	-26.888	-26.626	-26.066	0	-28.04	-32.783
	'C2_T0_2'	-29.193	-27.373	-26.252	-21.988	-25.457	-30.883	-24.722	-26.751	-27.009	-26.492	-33.649	-25.748	-33.662
	'C2_T0_1'	-29.321	-27.828	-26.717	-23.284	-25.202	-31.28	-25.537	-26.82	-25.584	-25.613	0	-27.459	-33.063
	'C3_T0_3'	-29.377	-27.516	-27.649	-23.592	-27.132	-30.453	-24.929	-28.266	-28.304	-26.911	-28.005	0	-32.289
	'C3_T0_2'	-29.514	-27.21	-28.078	-23.733	-27.365	-30.555	-24.689	-28.765	-28.268	-26.874	-28.131	0	-32.87
	'C3_T0_1'	-29.302	-27.732	-28.615	-24.449	-27.711	-30.867	-25.756	-29.445	-27.892	-26.619	-27.054	0	-33.13

Voltages - October 21, 2011	Retention Time (min)	1497.5	1581.8	1634.3	1650.9	1741.2	1776.6	1822.8	1909.6	1946.6	1977.2	2022	2035.1	2070.1
	Sample ID													
	'Tetracosane_3'	0	0	0	0	0	0	0	0	0	0	0	0	0
	'Tetracosane_2'	0	0	0	0	0	0	96	0	0	0	0	0	0
	'Tetracosane_1'	0	0	0	0	0	0	0	0	0	0	0	0	0
	'S118.5_F3_3'	77	0	0	324	193	263	302	467	412	0	134	291	117
	'S118.5_F3_2'	75	0	0	327	170	248	275	436	374	0	132	301	122
	'S118.5_F3_1'	74	0	0	327	220	293	320	494	430	0	0	358	66
	'S119_F3_3'	71	0	0	256	174	248	314	473	290	0	115	246	61
	'S119_F3_2'	75	0	0	254	179	253	320	479	290	0	121	250	64
	'S119_F3_1'	75	0	0	258	183	257	326	429	232	0	120	258	66
	'S119.5_F3_3'	92	0	0	321	195	286	361	559	344	0	141	237	123
	'S119.5_F3_2'	92	0	0	340	191	281	354	557	336	0	143	234	85
	'S119.5_F3_1'	93	0	0	345	194	282	353	572	340	0	148	246	90
	'S122_F3_3'	95	0	0	370	198	294	350	506	441	0	145	259	124
	'S122_F3_2'	92	0	0	362	158	252	308	437	372	0	142	256	81
	'S122_F3_1'	92	0	0	360	196	287	336	486	433	0	143	255	126
	'S123_F3_3'	53	0	0	317	131	250	191	334	183	0	81	181	83
	'S123_F3_2'	57	0	0	324	162	295	227	347	183	0	108	188	96
	'S123_F3_1'	63	0	76	337	124	277	208	371	197	0	95	207	94
	'S193_F3_3'	60	0	114	258	208	296	278	667	317	0	443	0	162
	'S193_F3_2'	118	0	113	255	199	280	270	641	306	0	488	0	229
	'S193_F3_1'	60	0	113	248	157	243	235	564	243	0	426	0	156
	'S203_T0_3'	95	0	137	468	228	499	506	810	488	0	458	0	339
	'S203_T0_2'	108	0	140	478	234	516	519	823	487	0	350	0	212
	'S203_T0_1'	212	0	141	527	221	511	519	860	491	0	475	0	322
	'S204_T0_3'	275	0	0	734	0	823	0	1356	963	0	1041	0	0
	'S204_T0_2'	288	0	0	745	265	639	624	1108	771	0	829	0	433
	'S204_T0_1'	227	0	0	621	0	687	0	1051	832	0	839	0	0
	'S208_T0_3'	0	0	0	338	243	283	302	485	311	0	0	337	196
	'S208_T0_2'	63	0	0	266	194	224	247	387	237	0	112	277	120
	'S208_T0_1'	53	0	0	341	142	0	306	426	312	0	103	266	0
	'C1_T0_3'	2904	408	497	350	515	1456	0	379	104	0	0	124	1654
	'C1_T0_2'	2967	453	559	156	535	1506	0	394	107	0	0	127	1691
	'C1_T0_1'	3013	405	513	109	584	1577	161	438	158	0	0	127	1781
	'C2_T0_3'	4635	0	852	0	1026	2626	432	702	251	421	0	284	2314
	'C2_T0_2'	4914	630	878	630	1087	2808	415	735	247	435	101	141	2335
	'C2_T0_1'	4907	634	908	653	1145	2759	395	779	281	449	0	305	2530
	'C3_T0_3'	7136	897	1264	829	1620	3770	548	1154	447	739	462	0	3618
	'C3_T0_2'	6866	880	1190	811	1554	3725	533	1119	444	726	448	0	3492
	'C3_T0_1'	7785	748	1175	784	1629	4381	511	1091	425	685	426	0	3855

δ ¹³ C - October 21, 2011	Retention Time (min)	2108.5	2158.8	2206.9	2252.5	2307	2418.6	2435	2487.6	2528.5	2654.5	2690.1	2795.2	2894.9
	Sample ID													
	'Tetracosane_3'	0	0	0	0	0	0	0	0	0	0	0	0	0
	'Tetracosane_2'	0	-33.617	-33.293	0	0	0	0	0	-33.335	0	-33.401	-33.549	
	'Tetracosane_1'	0	0	-34.435	-27.746	0	0	0	0	-32.304	0	0	-38.202	
	'S118.5_F3_3'	-31.094	0	-33.557	-32.349	-26.9	-31.076	0	0	-33.594	-32.162	-31.348	0	
	'S118.5_F3_2'	-30.895	0	-33.55	-33.166	-27.64	-32.191	0	-30.304	-33.218	-34.069	-32.143	-31.478	0
	'S118.5_F3_1'	-31.321	0	-34.347	-35.38	-28.079	-32.647	0	-31.225	-33.664	0	-33.462	-32.952	-33.592
	'S119_F3_3'	-29.179	0	-33.215	-31.739	-26.238	-32.944	0	-33.284	-28.21	-35.801	-32.76	-31.839	-32.307
	'S119_F3_2'	-27.58	0	-33.38	-30.94	-26.934	-30.435	0	0	-35.251	-31.996	-30.979	-33.233	
	'S119_F3_1'	-30.36	0	-33.158	-31.097	-27.685	-31.249	0	0	-31.421	-31.075	-30.896	-32.005	
	'S119.5_F3_3'	-25.534	0	-33.198	-31.733	-29.07	-31.616	0	-30.336	-36.548	-34.318	-32.458	-31.893	-33.559
	'S119.5_F3_2'	-28.054	0	-32.606	-40.92	-26.339	-31.372	0	-28.525	-31.097	0	-31.333	-30.77	0
	'S119.5_F3_1'	-30.368	0	-33.212	-33.519	-28.656	-31.062	0	-29.562	-31.599	-32.541	-31.827	-32.375	-32.18
	'S122_F3_3'	-30.756	0	-32.804	-30.05	-29.628	-30.987	0	-28.349	-30.277	0	-31.542	-30.954	0
	'S122_F3_2'	-31.343	0	-33.022	-31.553	-28.915	-31.622	0	-28.09	-33.515	-33.395	-31.86	-31.001	0
	'S122_F3_1'	-30.258	0	-33.125	-32.459	-30.078	-31.982	0	-27.886	-33.543	-32.806	-31.978	-31.344	0
	'S123_F3_3'	-29.894	0	-33.252	-30.624	-28.203	-33.603	0	-35.811	-45.256	-33.855	-31.776	-31.834	0
	'S123_F3_2'	-30.507	0	-33.404	-32.976	25.543	-31.587	0	-29.811	-25.796	-32.337	-31.614	-31.034	0
	'S123_F3_1'	-30.327	0	-32.738	-31.487	-27.845	-32.574	0	0	0	-32.561	-33.964	-32.671	-32.996
	'S193_F3_3'	-29.064	0	-33.49	-30.858	-33.226	-32.673	0	0	0	-34.106	-32.17	-31.421	-31.908
	'S193_F3_2'	-29.449	0	-32.842	-29.314	-30.823	-32.889	0	0	0	-33.903	-35.941	-32.396	-32.609
	'S193_F3_1'	-34.686	0	-33.835	-31.208	-31.599	-33.177	0	0	0	-35.08	-33.418	-31.19	-32.675
	'S203_T0_3'	-29.168	0	-33.011	-30.32	-28.151	-31.616	0	-37.927	-33.44	-35.545	-33.179	-30.94	-32.054
	'S203_T0_2'	-32.179	-39.116	-34.49	-29.069	-30.07	-33.777	0	0	0	-36.172	-32.772	-31.172	-32.584
	'S203_T0_1'	-27.659	0	-32.243	-26.908	-28.674	-32.172	0	0	0	-34.381	-31.714	-30.367	-31.884
	'S204_T0_3'	-28.827	0	-31.603	-29.302	-30.284	-31.268	0	0	0	-39.398	-35.765	-31.428	-34.064
	'S204_T0_2'	-30.605	0	-33.247	-28.632	-32.315	-32.414	0	0	0	-44.095	-76.529	-32.802	-33.273
	'S204_T0_1'	-28.837	-35.224	-34.689	-30.356	-32.689	-31.83	0	0	0	-32.59	-49.163	-33.119	-33.986
	'S208_T0_3'	-29.628	0	-34.336	-32.5	-25.672	-31.632	0	-32.023	0	-34.013	-31.559	-32.471	-33.846
	'S208_T0_2'	-31.039	0	-34.973	0	-31.946	-31.678	0	-34.535	0	-35.022	-36.872	-32.813	-36.233
	'S208_T0_1'	-46.702	0	-33.93	-30.94	-25.142	-31.641	0	-35.167	-30.839	-34.806	-31.528	-30.688	0
	'C1_T0_3'	-32.822	0	-33.392	-33.565	-22.88	0	-27.003	-33.088	-32.321	-34.854	-27.839	-31.874	-29.391
	'C1_T0_2'	-33.319	0	-34.293	-34.587	-22.95	0	-30.223	-34.409	-35.203	-35.766	-30.232	-32.668	-30.898
	'C1_T0_1'	-32.315	-52.091	-34.142	-33.88	-18.407	0	-31.512	-34.599	-31.465	-35.3	-30.402	-32.967	-30.625
	'C2_T0_3'	-30.834	0	-34.332	-32.752	-26.189	0	-31.366	-33.917	-33.209	-34.352	-29.576	-48.321	-31.073
	'C2_T0_2'	-30.227	-57.558	-34.455	-32.182	-3.192	-41.051	-33.663	-33.664	-31.846	-35.531	-28.677	-59.91	-30.604
	'C2_T0_1'	-28.674	0	-34.807	-33.235	-25.089	0	-27.129	-33.976	-31.674	-33.548	-29.093	-64.728	-30.505
	'C3_T0_3'	-29.388	0	-33.722	-31.545	-28.205	-39.747	-45.189	-33.18	-31.892	-34.961	-32.71	-97.18	-32.595
	'C3_T0_2'	-28.645	0	-33.933	-31.993	-26.569	0	-24.78	-33.177	0	-35.225	-30.698	-96.649	-31.268
	'C3_T0_1'	-30.306	-28.212	-34.466	-34.515	-31.33	0	-26.209	-34.015	-37.181	-36.099	-33.695	-96.468	-32.448

Voltages - October 21, 2011	Retention Time (min)	2108.5	2158.8	2206.9	2252.5	2307	2418.6	2435	2487.6	2528.5	2654.5	2690.1	2795.2	2894.9
	Sample ID													
	'Tetracosane_3'	0	0	0	0	0	0	0	0	0	0	0	0	0
	'Tetracosane_2'	0	78	221	0	0	0	0	0	0	83	0	71	68
	'Tetracosane_1'	0	0	2851	381	0	0	0	0	0	159	0	0	62
	'S118.5_F3_3'	251	0	3245	631	512	671	0	0	0	410	1099	1193	0
	'S118.5_F3_2'	254	0	3365	641	524	623	0	223	229	492	1163	1266	0
	'S118.5_F3_1'	202	0	3380	630	496	632	0	214	223	0	1309	1013	1302
	'S119_F3_3'	193	0	3992	740	414	452	0	155	104	485	991	863	1116
	'S119_F3_2'	196	0	4057	731	390	551	0	0	0	391	898	1010	952
	'S119_F3_1'	202	0	4112	725	385	562	0	0	0	398	898	1029	968
	'S119.5_F3_3'	222	0	3669	657	363	461	0	125	141	605	1224	1330	1285
	'S119.5_F3_2'	225	0	3638	71	107	467	0	211	234	0	1340	1435	0
	'S119.5_F3_1'	225	0	3720	670	358	477	0	217	232	730	1334	1055	1563
	'S122_F3_3'	270	0	4026	649	516	551	0	221	254	0	1391	1488	0
	'S122_F3_2'	256	0	3889	643	527	556	0	123	153	564	1269	1363	0
	'S122_F3_1'	263	0	3886	634	531	530	0	97	126	456	1162	1260	0
	'S123_F3_3'	265	0	3387	511	322	309	0	147	94	381	840	908	0
	'S123_F3_2'	271	0	3469	521	135	333	0	70	95	390	837	930	0
	'S123_F3_1'	280	0	3506	524	274	360	0	0	0	347	691	621	769
	'S193_F3_3'	200	0	2484	528	253	1410	0	0	0	714	945	1092	2747
	'S193_F3_2'	295	0	2426	613	339	1365	0	0	0	681	771	950	2559
	'S193_F3_1'	188	0	2280	559	272	1338	0	0	0	641	895	1093	2164
	'S203_T0_3'	477	0	3900	994	568	1093	0	146	137	1015	1307	1531	3153
	'S203_T0_2'	335	68	3911	889	398	1000	0	0	0	827	1143	1377	2937
	'S203_T0_1'	481	0	4364	983	472	1082	0	0	0	830	1122	1371	2851
	'S204_T0_3'	699	0	2292	1043	813	3083	0	0	0	1174	1770	1686	3964
	'S204_T0_2'	530	0	2078	893	644	2902	0	0	0	1142	54	1637	4184
	'S204_T0_1'	616	79	1716	791	463	2591	0	0	0	1656	85	1578	4275
	'S208_T0_3'	288	0	3497	723	377	732	0	212	0	758	521	680	1642
	'S208_T0_2'	228	0	3272	0	68	654	0	186	0	687	491	662	1372
	'S208_T0_1'	269	0	2905	671	84	548	0	131	92	468	690	788	0
	'C1_T0_3'	352	0	3543	1050	408	0	82	2552	471	1652	456	8984	2571
	'C1_T0_2'	358	0	3743	1097	415	0	88	2643	474	1787	543	9602	2768
	'C1_T0_1'	355	104	3763	1067	396	0	86	2637	472	1793	552	9393	2729
	'C2_T0_3'	536	0	3450	1248	496	0	142	3467	601	2241	744	12344	3531
	'C2_T0_2'	373	83	3483	1179	323	53	169	3587	600	2236	632	12537	3443
	'C2_T0_1'	485	0	3589	1340	487	0	262	3528	592	2424	793	12508	3725
	'C3_T0_3'	580	0	8706	2275	998	60	196	5931	743	3753	1329	12470	5783
	'C3_T0_2'	585	0	8208	2233	1004	0	399	5774	0	3774	1303	12489	5778
	'C3_T0_1'	396	116	7358	1942	804	0	315	5526	573	3833	1258	12406	5833

$\delta^{13}\text{C}$ - October 21, 2011	Retention Time (min)	2922.5	2956.6	3010.3	3082.2	3096.5	3115.6	3151	3191.2	3232.4	CO ₂ Standard		
											3252.7	3278.9	3299.2
	Sample ID												
	'Tetracosane_3'	0	0	0	0	0	0	0	0	0	-42.944	-41.432	-41.085
	'Tetracosane_2'	0	0	0	0	0	0	0	0	0	-43.982	-41.324	-41.399
	'Tetracosane_1'	0	0	0	0	0	-27.829	-21.972	0	-29.923	-45.647	-40.984	-40.925
	'S118.5_F3_3'	0	-32.042	0	-31.789	0	0	0	-31.836	0	-50.059	-46.919	-40.977
	'S118.5_F3_2'	0	-31.752	0	-31.554	0	0	0	-31.73	0	-47.68	-40.88	-40.863
	'S118.5_F3_1'	0	-32.471	0	-32.881	0	0	-36.532	-29.646	0	-83.895	-58.105	-41.486
	'S119_F3_3'	0	-32.101	0	-32.302	0	0	0	-32.967	0	-53.264	-49.063	-41.03
	'S119_F3_2'	0	-31.171	-34.998	-32.378	0	0	-31.016	-31.359	0	-65.566	-52.369	-40.893
	'S119_F3_1'	0	-32.951	-33.822	-43.862	-36.579	0	-28.231	-34.058	0	-67.841	-53.091	-40.949
	'S119.5_F3_3'	0	-32.074	-33.417	-37.014	0	0	-31.522	-32.146	0	-88.288	-56.944	-41.275
	'S119.5_F3_2'	0	-31.217	0	-31.18	0	0	-30.484	-32.864	0	-86.189	-56.25	-40.505
	'S119.5_F3_1'	0	-32.084	0	-32.252	0	0	-32.032	-29.093	0	-81.636	-57.245	-40.933
	'S122_F3_3'	0	-31.324	0	-31.15	0	0	0	-31.471	0	-43.483	-40.671	-40.571
	'S122_F3_2'	0	-31.394	0	-31.44	0	0	0	-31.842	0	-45.95	-44.509	-40.9
	'S122_F3_1'	0	-31.906	0	-31.508	0	0	0	-31.992	0	-46.968	-45.483	-40.864
	'S123_F3_3'	-31.797	0	0	-32.14	0	0	-32.431	0	0	-54.963	-41.039	-40.871
	'S123_F3_2'	-31.551	0	0	-32.431	0	0	-32.933	0	0	-45.319	-44.108	-41.077
	'S123_F3_1'	-31.564	-31.482	-26.15	-31.676	0	0	-30.577	0	0	-67.177	-52.425	-40.22
	'S193_F3_3'	-32.114	-32.075	0	-31.95	0	0	-32.181	0	0	-53.313	-50.285	-41.603
	'S193_F3_2'	-32.168	-32.727	0	-32.635	0	0	-33.837	-33.837	0	-66.686	-54.045	-40.814
	'S193_F3_1'	-32.256	-34.059	-31.948	-31.274	-56.9	0	-35.228	0	-30.639	47.16	-93.519	-41.066
	'S203_T0_3'	0	-31.608	0	0	0	0	-31.421	0	-32.168	4.597	78.048	-40.865
	'S203_T0_2'	-32.153	-32.041	0	-31.807	0	0	-32.524	0	-30.635	-59.805	-52.384	-41.591
	'S203_T0_1'	-31.13	-31.221	0	-31.112	0	0	-31.57	0	-30.676	-72.058	-57.265	-40.051
	'S204_T0_3'	0	-30.944	-32.704	-33.307	0	0	-34.648	-33.387	-32.456	-3.269	42.578	-40.706
	'S204_T0_2'	0	-33.348	0	-33.917	0	0	-35.039	-33.664	-30.477	-18.415	-2.086	-40.858
	'S204_T0_1'	0	-31.902	-33.301	-34.493	0	0	-35.128	-35.047	-33.977	76.865	-300.364	-41.208
	'S208_T0_3'	-32.306	-32.825	0	-33.249	0	0	-33.639	0	-35.859	-59.009	-51.176	-41.517
	'S208_T0_2'	-32.83	-33.067	0	-37.392	0	0	-35.805	0	-31.077	-68.561	-53.176	-41.272
	'S208_T0_1'	-32.366	0	-30.779	-31.346	0	0	-31.431	0	0	-45.475	-43.9	-40.621
	'C1_T0_3'	-26.586	0	-30.514	-30.721	0	-31.609	-31.61	0	-30.712	-43.187	-42.621	-40.068
	'C1_T0_2'	-30.013	0	-31.681	-31.006	0	-31.974	-34.282	0	-31.22	-42.152	-42.032	-40.222
	'C1_T0_1'	-29.771	0	-31.814	-32.98	0	-32.583	-33.526	-27.431	-31.87	-47.767	-45.43	-41.168
	'C2_T0_3'	-30.829	0	-31.074	-32.47	0	-32.97	-34.177	0	-31.999	-43.15	-43.202	-41.066
	'C2_T0_2'	-30.122	-32.381	-30.902	-37.99	-121.057	-34.798	-25.627	-30.479	-31.498	-46.961	-45.147	-41.029
	'C2_T0_1'	-28.719	0	-33.167	-33.734	0	-33.132	-35.105	0	-31.872	-45.701	-45.192	-41.128
	'C3_T0_3'	-31.878	0	-26.937	-33.321	0	-33.104	-34.522	0	-47.489	-47.399	-46.788	-41.445
	'C3_T0_2'	-32.311	0	-30.923	-33.527	0	-33.607	-34.85	0	-48.16	-46.477	-45.669	-41.681
	'C3_T0_1'	-32.028	0	-31.604	-33.591	0	-33.991	-36.469	0	-51.237	-50.306	-47.177	-41.307

Retention Time (min)	CO ₂ Standard											
	2922.5	2956.6	3010.3	3082.2	3096.5	3115.6	3151	3191.2	3232.4	3252.7	3278.9	3299.2
Sample ID												
'Tetracosane_3'	0	0	0	0	0	0	0	0	0	1679	1896	1889
'Tetracosane_2'	0	0	0	0	0	0	0	0	0	1650	1895	1898
'Tetracosane_1'	0	0	0	0	0	56	85	0	242	1546	1885	1879
'S118.5_F3_3'	0	3461	0	1187	0	0	0	922	0	1493	1414	1888
'S118.5_F3_2'	0	3533	0	1257	0	0	0	992	0	1575	1882	1889
'S118.5_F3_1'	0	3290	0	1001	0	0	426	560	0	1145	1068	1890
'S119_F3_3'	0	2683	0	848	0	0	0	637	0	1408	1341	1895
'S119_F3_2'	0	324	128	512	0	0	355	460	0	1240	1168	1879
'S119_F3_1'	0	333	240	58	62	0	210	465	0	1199	1124	1893
'S119.5_F3_3'	0	386	353	81	0	0	484	573	0	1149	1077	1896
'S119.5_F3_2'	0	3661	0	1401	0	0	502	586	0	1145	1077	1906
'S119.5_F3_1'	0	3390	0	1029	0	0	503	595	0	1187	1088	1907
'S122_F3_3'	0	3956	0	1480	0	0	0	1283	0	1732	1911	1910
'S122_F3_2'	0	3867	0	1382	0	0	0	1150	0	1627	1575	1893
'S122_F3_1'	0	3736	0	1231	0	0	0	1002	0	1556	1493	1912
'S123_F3_3'	2420	0	0	863	0	0	705	0	0	1333	1899	1886
'S123_F3_2'	2412	0	0	874	0	0	715	0	0	1661	1585	1924
'S123_F3_1'	2056	260	127	424	0	0	394	0	0	1223	1160	1878
'S193_F3_3'	2768	1425	0	1073	0	0	1138	0	0	1428	1320	1907
'S193_F3_2'	2547	1275	0	923	0	0	748	748	0	1283	1203	1916
'S193_F3_1'	2205	614	155	50	62	0	352	0	1081	919	777	1888
'S203_T0_3'	0	2289	0	0	0	0	1660	0	1812	759	616	1912
'S203_T0_2'	3528	2120	0	1359	0	0	1494	0	2382	1349	1248	1889
'S203_T0_1'	3585	2051	0	1346	0	0	1456	0	2350	1296	1135	1888
'S204_T0_3'	0	5549	2640	1622	0	0	1693	1300	2667	588	461	1842
'S204_T0_2'	0	2711	0	1674	0	0	1843	1340	2484	353	187	1920
'S204_T0_1'	0	5421	2862	1650	0	0	1995	1254	2930	938	760	1891
'S208_T0_3'	2329	1057	0	786	0	0	720	0	1172	1340	1270	1914
'S208_T0_2'	2018	803	0	90	0	0	404	0	915	1213	1150	1904
'S208_T0_1'	2196	0	997	618	0	0	815	0	0	1578	1546	1905
'C1_T0_3'	943	0	7587	627	0	1701	431	0	6398	1675	1597	1870
'C1_T0_2'	1066	0	8183	745	0	1862	566	0	6734	1803	1739	1889
'C1_T0_1'	914	0	7996	673	0	1779	430	58	6645	1548	1499	1882
'C2_T0_3'	1388	0	10229	871	0	2266	727	0	8355	1805	1736	1890
'C2_T0_2'	1259	172	10236	415	52	1904	304	63	8375	1531	1457	1888
'C2_T0_1'	1260	0	11127	813	0	2335	590	0	8968	1639	1578	1872
'C3_T0_3'	2837	0	1937	939	0	3391	1985	0	12093	1656	1537	1911
'C3_T0_2'	2842	0	1781	964	0	3503	1985	0	12152	1639	1556	1876
'C3_T0_1'	2806	0	1650	447	0	3391	1900	0	12129	1568	1482	1872

Voltages - October 21, 2011

Voltages - October 24, 2011		CO ₂ Standard												
	Retention Time (min)	48.8	89.9	121.3	1184.4	1296.2	1340.2	1462.3	1491.4	1555.7	1594.8	1634.9	1653.2	1693.2
	Sample ID													
	'Tetracosane_3'	1799	1772	1776	0	0	0	0	0	0	0	0	0	0
	'Tetracosane_2'	1791	1804	1818	0	0	0	0	0	0	0	0	0	0
	'Tetracosane_1'	1784	1775	1775	0	0	0	0	0	0	0	0	0	0
	'S123_F2_3'	1790	1789	1785	55	0	0	134	201	0	0	0	0	0
	'S123_F2_2'	1802	1785	1786	54	0	0	134	201	0	0	0	0	0
	'S123_F2_1'	1788	1786	1783	56	0	0	137	206	0	0	0	0	0
	'S122_F2_3'	1798	1795	1788	181	166	66	199	737	0	0	0	0	0
	'S122_F2_2'	1793	1783	1784	184	168	66	200	727	0	0	0	0	0
	'S122_F2_1'	1802	1792	1778	187	171	67	205	744	0	0	51	0	0
	'S119.5_F2_3'	1786	1798	1784	180	148	62	189	741	0	0	50	0	0
	'S119.5_F2_2'	1777	1774	1769	180	147	72	191	726	0	0	52	0	0
	'S119.5_F2_1'	1820	1828	1816	187	151	75	197	771	0	0	51	0	0
	'S119_F2_3'	1833	1811	1828	207	153	74	205	797	96	0	58	0	0
	'S119_F2_2'	1819	1799	1812	208	153	74	200	797	0	0	60	0	0
	'S119_F2_1'	1828	1834	1816	210	156	75	205	811	102	0	62	0	0
	'S118.5_F2_3'	1828	1833	1825	252	163	84	268	985	0	0	146	0	0
	'S118.5_F2_2'	1832	1823	1833	255	159	89	268	1006	0	0	69	0	0
	'S118.5_F2_1'	1846	1829	1846	249	160	84	276	1011	0	0	70	0	0
	'S114_F2_3'	1829	1834	1824	116	0	0	123	478	0	0	0	0	0
	'S114_F2_2'	1829	1815	1826	118	0	0	126	486	0	0	0	0	0
	'S114_F2_1'	1836	1835	1801	126	51	0	131	511	0	0	0	0	0
	'S113_F2_3'	1831	1808	1816	330	166	142	357	1172	0	0	83	0	0
	'S113_F2_2'	1843	1821	1822	325	170	145	359	1189	0	0	84	0	0
	'S113_F2_1'	1823	1813	1824	320	168	144	359	1189	0	0	82	0	0
	'S112_F2_3'	1812	1841	1818	232	125	98	237	874	0	0	74	59	52
	'S112_F2_2'	1810	1834	1821	232	127	100	236	886	0	0	74	60	53
	'S112_F2_1'	1823	1813	1814	236	130	101	240	915	109	59	78	65	54
	'S111_F2_3'	1809	1835	1830	261	143	115	231	1068	0	0	78	0	0
'S111_F2_2'	1839	1813	1818	241	130	105	214	1023	0	0	71	0	0	
'S111_F2_1'	1881	1853	1878	246	127	104	193	1014	110	0	61	0	0	

$\delta^{13}\text{C}$ - October 24, 2011	Retention Time (min)	1747.5	1774.1	1910.6	2067	2204.5	2252	2308.5	2399.7	2479.1	2652.4	2691	2764.7	2787.9
	Sample ID													
	'Tetracosane_3'	0	0	0	0	-33.602	0	0	0	0	0	0	0	0
	'Tetracosane_2'	0	0	0	0	-34.335	-37.854	0	0	0	0	0	0	0
	'Tetracosane_1'	0	0	0	0	-34.509	0	0	0	0	0	0	0	0
	'S123_F2_3'	-32.877	-33.299	0	-34.851	-34.109	0	0	0	-30.957	-34.229	-39.071	0	-34.707
	'S123_F2_2'	-33.814	-33.29	0	-34.452	-34.029	0	0	0	-30.39	-33.08	-39.023	0	-31.092
	'S123_F2_1'	-31.061	-31.001	0	-32.828	-33.635	-39.367	0	0	-30.549	-34.857	-39	0	-35.787
	'S122_F2_3'	-32.921	-33.221	-33.839	-33.973	-34.54	-39.975	0	0	-36.51	-36.826	0	-27.742	-34.377
	'S122_F2_2'	-34.136	-34.125	-35.047	-34.749	-34.906	-40.967	0	0	-36.826	-37.186	0	-29.078	-34.566
	'S122_F2_1'	-33.692	-33.649	-33.914	-34.031	-34.671	-41.641	-37.077	0	-38.076	-37.801	-31.288	-35.584	-35.509
	'S119.5_F2_3'	-34.828	-33.954	-34.779	-34.818	-34.442	-40.597	0	0	-37.872	-36.147	-30.767	0	-33.012
	'S119.5_F2_2'	-33.892	-33.212	-32.534	-34.956	-35.227	-40.873	0	0	-38.121	-36.919	-31.436	-32.577	-34.63
	'S119.5_F2_1'	-33.429	-32.516	-32.859	-32.763	-34.691	-40.025	0	0	-37.353	-36.909	-31.2	-28.206	-33.679
	'S119_F2_3'	-35.295	-34.386	-34.921	-34.12	-34.917	-42.117	0	0	-35.087	-39.466	-43.845	-35.983	-35.087
	'S119_F2_2'	-35.501	-34.438	-34.903	-35.233	-35.361	-42.564	0	0	-35.413	-41.053	-44.929	-35.082	-35.599
	'S119_F2_1'	-33.547	-33.259	-33.551	-34.501	-34.793	-41.216	0	0	-33.812	-39.558	-38.562	-34.446	-34.987
	'S118.5_F2_3'	-35.496	-35.425	-34.242	-33.614	-35.083	-38.522	0	0	-36.243	-36.44	-28.725	-29.006	-33.713
	'S118.5_F2_2'	-34.683	-34.43	-34.181	-33.495	-35.133	-39.385	0	0	-35.492	-36.785	0	-33.003	-34.187
	'S118.5_F2_1'	-33.728	-34.03	-33.833	-33.866	-34.829	-46.365	0	0	-35.93	-36.372	-25.939	-28.187	-33.893
	'S114_F2_3'	0	-34.885	0	-33.635	-34.861	0	0	0	-36.997	-34.944	0	0	-35.387
	'S114_F2_2'	0	-34.966	0	-34.167	-34.507	-39.329	-28.819	0	-37.686	-35.29	0	0	-30.586
	'S114_F2_1'	0	-34.12	0	-32.123	-34.085	-38.445	0	0	-35.764	-35.217	0	0	-33.709
	'S113_F2_3'	-33.72	-33.686	-32.63	-33.924	-35.034	-36.601	0	0	-35.046	-36.027	-27.846	-29.407	-32.556
	'S113_F2_2'	-33.611	-33.542	-33.556	-34.563	-34.639	-63.812	0	0	-34.793	-36.58	-30.551	-30.165	-33.516
	'S113_F2_1'	-33.828	-33.663	-33.867	-33.376	-35.296	-37.321	0	0	-35.091	-36.769	-27.874	-31.361	-32.837
	'S112_F2_3'	-32.147	-32.156	-34.784	-33.526	-34.983	-38.765	0	0	-34.178	-36.434	-30.904	-30.318	-33.844
	'S112_F2_2'	-31.755	-31.882	-34.05	-33.62	-34.351	-38.243	0	0	-33.842	-35.355	-65.188	-29.439	-33.704
	'S112_F2_1'	-32.453	-32.447	-34.662	-33.628	-34.327	-39.732	-28.371	-20.583	-36.068	-36.776	-52.05	-36.482	-33.681
	'S111_F2_3'	-33.209	-32.773	-35.202	-33.514	-33.787	-38.274	0	0	-35.592	-35.488	0	0	-33.377
	'S111_F2_2'	-36.029	-35.682	-35.266	-34.731	-34.096	-38.193	0	0	-35.19	-37.157	0	0	-33.93
	'S111_F2_1'	-33.699	-33.28	-33.918	-34.188	-33.56	-37.983	0	0	-33.856	-35.696	-33.975	0	-33.409

Voltages - October 24, 2011	Retention Time (min)	1747.5	1774.1	1910.6	2067	2204.5	2252	2308.5	2399.7	2479.1	2652.4	2691	2764.7	2787.9
	Sample ID													
	'Tetracosane_3'	0	0	0	0	1982	0	0	0	0	0	0	0	0
	'Tetracosane_2'	0	0	0	0	1968	210	0	0	0	0	0	0	0
	'Tetracosane_1'	0	0	0	0	1975	0	0	0	0	0	0	0	0
	'S123_F2_3'	67	79	0	72	1790	0	0	0	95	60	74	0	304
	'S123_F2_2'	67	80	0	72	1799	0	0	0	93	57	73	0	56
	'S123_F2_1'	76	88	0	74	1787	264	0	0	90	59	74	0	297
	'S122_F2_3'	160	344	68	356	1145	220	0	0	543	386	0	58	1629
	'S122_F2_2'	161	343	69	351	1156	217	0	0	545	378	0	60	1628
	'S122_F2_1'	163	344	71	356	1138	221	104	0	550	386	52	61	1624
	'S119.5_F2_3'	140	325	71	344	1092	214	0	0	549	391	111	0	1665
	'S119.5_F2_2'	142	328	71	345	1106	220	0	0	550	402	112	61	1671
	'S119.5_F2_1'	149	334	75	356	1132	231	0	0	574	416	113	64	1742
	'S119_F2_3'	149	381	83	402	1606	317	0	0	696	454	93	57	1915
	'S119_F2_2'	148	379	83	396	1609	319	0	0	695	441	97	61	1881
	'S119_F2_1'	156	379	84	402	1605	335	0	0	710	452	100	65	1891
	'S118.5_F2_3'	163	439	92	489	1006	249	0	0	752	488	99	76	2022
	'S118.5_F2_2'	167	451	92	507	1054	253	0	0	799	503	0	75	2081
	'S118.5_F2_1'	171	452	92	516	1077	75	0	0	811	521	98	76	2152
	'S114_F2_3'	0	210	0	242	1437	0	0	0	410	306	0	0	1248
	'S114_F2_2'	0	210	0	245	1462	271	126	0	417	311	0	0	112
	'S114_F2_1'	0	220	0	254	1425	258	0	0	438	315	0	0	211
	'S113_F2_3'	204	521	63	618	1158	294	0	0	1016	672	129	104	2869
	'S113_F2_2'	205	542	61	618	1178	113	0	0	1043	676	127	104	2835
	'S113_F2_1'	205	529	67	615	1193	297	0	0	1036	671	127	106	2944
	'S112_F2_3'	163	436	82	469	1365	292	0	0	785	514	108	87	2172
	'S112_F2_2'	163	424	84	471	1433	296	0	0	802	515	58	87	2177
	'S112_F2_1'	166	435	83	487	1625	320	174	58	796	522	59	86	2219
	'S111_F2_3'	161	476	99	566	1774	342	0	0	905	578	0	0	2660
	'S111_F2_2'	138	432	89	521	1798	326	0	0	869	539	0	0	2568
	'S111_F2_1'	125	403	73	465	1760	289	0	0	768	481	87	0	2642

$\delta^{13}\text{C}$ - October 24, 2011	Retention Time (min)	2892	2922.4	3003	3030.1	3084.8	3114	3152	3229.4	3243.5	CO ₂ Standard		
											3257.6	3277.4	3300.2
	Sample ID												
	'Tetracosane_3'	0	0	0	0	0	0	0	0	0	-41.585	-40.94	-40.67
	'Tetracosane_2'	0	0	0	0	0	0	0	0	-30.939	-41.552	-41.042	-40.871
	'Tetracosane_1'	0	0	0	0	0	0	0	0	0	-41.827	-41.254	-41.132
	'S123_F2_3'	-33.42	-34.781	-33.295	0	0	0	-36.382	-32.36	-24.945	-41.903	-41.311	-41.074
	'S123_F2_2'	-34.4	-34.628	-35.428	0	0	0	-35.808	-32.87	-25.038	-41.85	-41.132	-40.855
	'S123_F2_1'	-34.187	-34.855	-34.07	0	0	0	-37.099	-33.372	-30.149	-42.296	-41.525	-41.384
	'S122_F2_3'	-34.194	0	-32.079	0	0	-36.509	0	-33.814	-33.038	-42.231	-41.23	-41.113
	'S122_F2_2'	-35.186	-26.773	-34.811	0	0	-37.283	-72.523	-33.647	-35.029	-42.634	-41.605	-41.662
	'S122_F2_1'	-36.708	179.483	-35.31	0	0	-38.78	0	-34.633	-39.36	-42.924	-41.895	-41.868
	'S119.5_F2_3'	-35.383	-18	-34.266	-51.32	0	-36.766	-43.178	-33.656	-33.889	-42.248	-41.251	-40.981
	'S119.5_F2_2'	-36.109	-32.953	-35.022	-52.85	0	-36.255	-44.403	-34.124	0	-42.456	-41.812	-41.847
	'S119.5_F2_1'	-36.023	-32.954	-34.566	-51.799	0	-36.302	-76.232	-35.005	-36.645	-43.591	-42.476	-42.589
	'S119_F2_3'	-38.823	-35.888	-34.753	-39.013	0	-36.271	-37.402	-36.053	-46.216	-44.915	-43.346	-43.214
	'S119_F2_2'	-39.023	-36.046	-35.054	-38.188	0	-36.573	-43.856	-36.012	-43.759	-46.275	-44.556	-44.461
	'S119_F2_1'	-36.748	-32.623	-33.243	-35.727	0	-34.859	-50.384	-34.887	-53.656	-43.39	-42.422	-42.326
	'S118.5_F2_3'	-35.033	8.254	-34.814	-65.439	-47.851	-42.33	-947.181	-32.925	-37.691	-42.125	-41.003	-41.014
	'S118.5_F2_2'	-37.265	-32.872	-34.111	-52.188	0	-35.7	0	-31.933	0	-42.011	-40.865	-40.792
	'S118.5_F2_1'	-35.24	-31.421	-33.924	-51.589	0	-35.874	-25.838	-32.416	0	-42.472	-40.892	-40.779
	'S114_F2_3'	-37.947	0	-33.795	0	0	-34.448	0	-33.59	-33.118	-42.169	-41.257	-41.153
	'S114_F2_2'	-35.078	-34.094	-33.449	0	0	-35.964	0	-33.902	-28.557	-42.169	-41.231	-41.158
	'S114_F2_1'	-33.364	-32.937	-33.428	0	-37.815	-37.994	0	-32.899	-82.369	-42.405	-41.281	-41.279
	'S113_F2_3'	-35.117	-31.331	-33.437	-52.847	-39.763	-35.645	-47.037	-31.91	0	-42.516	-40.53	-40.461
	'S113_F2_2'	-36.2	-32.466	-34.249	-50.76	-58.216	-43.826	-53.618	-33.11	-41.736	-43.796	-41.359	-41.338
	'S113_F2_1'	-35.191	-32.008	-32.925	0	0	-34.485	-47.782	-30.894	0	-42.987	-40.629	-40.673
	'S112_F2_3'	-33.691	-15.666	-33.592	-46.792	0	-35.799	-61.555	-32.935	-34.159	-42.617	-41.063	-40.921
	'S112_F2_2'	-33.162	-30.24	-32.309	-33.749	0	-32.825	-58.265	-32.35	-34.276	-42.428	-40.765	-40.735
	'S112_F2_1'	-36.815	-75.8	-34.142	-33.955	-70.392	-44.588	-49.224	-32.234	-34.308	-43.045	-41.393	-41.5
	'S111_F2_3'	-34.225	-33.962	-33.739	-47.412	-47.764	-33.961	-29.947	-32.861	0	-41.762	-41.279	-41.209
	'S111_F2_2'	-34.69	-30.881	-33.122	-46.556	0	-33.698	-24.611	-32.729	0	-41.903	-41.285	-41.319
	'S111_F2_1'	-34.904	-26.667	-32.164	-52.474	0	-31.94	-17.488	-32.371	-39.535	-48.44	-41.432	-41.533

Retention Time (min)	CO ₂ Standard											
	2892	2922.4	3003	3030.1	3084.8	3114	3152	3229.4	3243.5	3257.6	3277.4	3300.2
Sample ID												
'Tetracosane_3'	0	0	0	0	0	0	0	0	0	1771	1784	1787
'Tetracosane_2'	0	0	0	0	0	0	0	0	57	1708	1795	1803
'Tetracosane_1'	0	0	0	0	0	0	0	0	0	1760	1784	1801
'S123_F2_3'	73	209	194	0	0	0	116	171	78	1704	1804	1774
'S123_F2_2'	71	203	195	0	0	0	115	177	79	1692	1800	1791
'S123_F2_1'	73	206	197	0	0	0	119	182	78	1692	1786	1781
'S122_F2_3'	607	0	1449	0	0	258	0	1169	159	1682	1788	1790
'S122_F2_2'	468	62	1354	0	0	263	51	1168	162	1692	1794	1820
'S122_F2_1'	472	63	1376	0	0	269	0	1215	164	1678	1797	1792
'S119.5_F2_3'	645	124	1400	101	0	276	74	1232	164	1695	1786	1800
'S119.5_F2_2'	639	287	1430	103	0	278	75	1253	0	1753	1817	1786
'S119.5_F2_1'	672	290	1478	100	0	290	78	1313	173	1718	1825	1851
'S119_F2_3'	712	293	1625	221	0	394	166	1304	138	1687	1842	1823
'S119_F2_2'	706	301	1668	227	0	393	91	1314	164	1689	1836	1839
'S119_F2_1'	729	306	1645	237	0	397	91	1318	137	1695	1843	1816
'S118.5_F2_3'	555	111	1622	51	60	301	57	1516	195	1704	1828	1838
'S118.5_F2_2'	741	255	1659	125	0	331	0	1561	0	1717	1843	1850
'S118.5_F2_1'	789	295	1705	126	0	349	63	1580	0	1705	1835	1835
'S114_F2_3'	394	0	1098	0	0	207	0	949	114	1711	1840	1858
'S114_F2_2'	455	101	1096	0	0	207	0	965	118	1709	1823	1819
'S114_F2_1'	461	105	1101	0	88	195	0	981	120	1701	1836	1817
'S113_F2_3'	1066	390	2322	157	74	431	119	2155	0	1644	1810	1832
'S113_F2_2'	1077	388	2396	160	89	442	116	2196	245	1634	1830	1830
'S113_F2_1'	1109	390	2412	0	0	483	120	2268	0	1618	1816	1809
'S112_F2_3'	832	102	1843	125	0	365	77	1726	198	1645	1809	1829
'S112_F2_2'	836	298	2001	273	0	491	78	1748	203	1624	1827	1820
'S112_F2_1'	653	111	1895	121	56	324	77	1791	210	1620	1812	1817
'S111_F2_3'	805	125	2483	161	54	499	72	2411	0	1727	1802	1815
'S111_F2_2'	805	90	2532	135	0	497	68	2373	0	1737	1833	1832
'S111_F2_1'	956	96	2514	91	0	453	59	2343	257	1548	1844	1877

Voltages - October 24, 2011

$\delta^{13}\text{C}$ - October 26, 2011		CO ₂ Standard												
	Retention Time (min)	49.8	88.7	126.6	1375.2	1425.4	1471.3	1531	1650.3	1673.5	1718.7	1747.7	1784.5	1818.2
	Sample ID													
	'Tetracosane_3'	-41.669	-41.1	-41.014	0	0	0	0	0	0	0	0	0	0
	'Tetracosane_2'	-41.65	-41.1	-40.902	0	0	0	0	0	0	0	0	0	0
	'Tetracosane_1'	-41.757	-41.1	-40.983	0	0	0	0	0	0	0	0	0	0
	'S121_F3_3'	-41.697	-41.1	-40.972	0	0	0	0	-28.679	-30.656	-30.264	0	-27.568	-32.202
	'S121_F3_2'	-41.715	-41.1	-41.034	0	0	0	0	-29.634	-31.727	-30.15	0	-29.167	-34.323
	'S121_F3_1'	-41.716	-41.1	-41.371	0	0	0	0	-29.658	-30.977	-30.6	0	-28.37	-30.503
	'S114_F3_3'	-41.747	-41.1	-40.926	0	0	0	0	-28.339	-31.32	-32.034	-29.874	-31.166	-36.083
	'S114_F3_2'	-41.624	-41.1	-40.886	-26.217	0	0	0	-26.551	-30.081	-31.31	-29.961	-31.057	-36.784
	'S114_F3_1'	-41.748	-41.1	-41.024	-28.57	0	0	-28.742	-30.02	-31.87	-29.307	-28.326	-28.455	-32.07
	'S113_F3_3'	-41.706	-41.1	-41.431	-27.611	-29.454	0	-29.698	-28.839	-37.693	-30.938	-31.207	-28.736	-31.661
	'S113_F3_2'	-41.821	-41.1	-41.116	-30.004	-29.002	-31.499	-28.499	-27.594	-38.11	-30.295	-31.919	-27.581	-31.558
	'S113_F3_1'	-41.834	-41.1	-41.033	-33.958	-29.394	-32.582	-30.884	-29.2	-32.394	-32.461	-31.861	-29.326	-32.024
	'S112_F3_3'	-41.54	-41.1	-40.879	0	0	0	0	-30.249	-36.01	-31.644	-31.213	-28.691	-36.458
	'S112_F3_2'	-41.746	-41.1	-41.229	-30.12	0	0	0	-27.407	-29.798	-32.983	-30.044	-28.615	-35.276
'S112_F3_1'	-41.811	-41.1	-41.095	-29.535	0	0	0	-27.953	-29.539	-31.063	-30.234	-28.256	-33.248	
'S111_F3_3'	-41.614	-41.1	-40.928	-31.786	-28.396	0	0	-27.755	-31.085	-33.75	-30.374	-27.489	-34.967	
'S111_F3_2'	-41.87	-41.1	-41.08	-31.734	0	0	0	-26.136	-31.691	-32.474	-25.955	0	-30.685	
'S111_F3_1'	-41.413	-41.1	-41.013	0	0	0	0	-26.831	-33.618	0	-29.727	0	-32.031	
Voltages - October 26, 2011		CO ₂ Standard												
	Retention Time (min)	49.8	88.7	126.6	1375.2	1425.4	1471.3	1531	1650.3	1673.5	1718.7	1747.7	1784.5	1818.2
	Sample ID													
	'Tetracosane_3'	1690	1705	1686	0	0	0	0	0	0	0	0	0	0
	'Tetracosane_2'	1710	1719	1697	0	0	0	0	0	0	0	0	0	0
	'Tetracosane_1'	1706	1714	1696	0	0	0	0	0	0	0	0	0	0
	'S121_F3_3'	1709	1705	1729	0	0	0	0	64	163	74	0	73	111
	'S121_F3_2'	1712	1706	1720	0	0	0	0	66	169	76	0	75	113
	'S121_F3_1'	1730	1715	1717	0	0	0	0	65	168	76	0	141	178
	'S114_F3_3'	1720	1733	1720	0	0	0	0	99	173	71	77	84	129
	'S114_F3_2'	1718	1716	1714	55	0	0	0	92	175	74	89	94	136
	'S114_F3_1'	1723	1729	1719	59	0	0	51	104	208	81	68	140	187
	'S113_F3_3'	1721	1728	1734	100	69	0	123	237	219	135	269	286	329
	'S113_F3_2'	1719	1707	1724	94	68	66	69	233	203	124	217	231	271
	'S113_F3_1'	1732	1700	1715	71	64	69	61	201	223	112	225	237	286
	'S112_F3_3'	1722	1725	1718	0	0	0	0	80	128	80	110	92	105
	'S112_F3_2'	1721	1722	1730	53	0	0	0	77	140	78	103	88	103
	'S112_F3_1'	1744	1728	1721	85	0	0	0	74	135	77	98	88	104
	'S111_F3_3'	1728	1753	1735	53	54	0	0	156	191	85	99	119	148
	'S111_F3_2'	1742	1732	1731	81	0	0	0	128	178	67	59	0	137
	'S111_F3_1'	1762	1745	1748	0	0	0	0	76	93	0	100	0	150

$\delta^{13}\text{C}$ - October 26, 2011	Retention Time (min)	1894.1	1913.7	1950.2	2006.9	2031	2085.4	2128.2	2209.5	2267.7	2311.9	2399	2420.6	2630.8
	Sample ID													
	'Tetracosane_3'	0	0	0	0	0	0	0	-34.003	0	-36.423	0	0	0
	'Tetracosane_2'	0	0	0	0	0	0	0	-33.806	-37.728	0	0	-31.665	0
	'Tetracosane_1'	0	0	0	0	0	0	0	-33.682	0	0	0	0	0
	'S121_F3_3'	0	-36.822	-36.365	-30.765	-31.369	0	-25.614	-32.992	-36.512	0	0	-27.463	-31.534
	'S121_F3_2'	0	-34.108	-31.722	-33.183	-37.797	0	-31.009	-33.492	-35.841	0	0	-30.23	0
	'S121_F3_1'	0	-34.848	-32.326	-30.981	-35.038	0	-29.012	-33.978	-36.229	0	0	-29.204	0
	'S114_F3_3'	0	-31.974	-31.191	-30.697	-31.887	0	-26.42	-33.364	-34.569	0	0	-35.789	-38.574
	'S114_F3_2'	0	-31.785	-30.64	-27.983	-32.72	0	-27.37	-33.413	-34.009	0	0	-29.871	0
	'S114_F3_1'	0	-32.448	-30.157	-29.97	-33.025	0	-29.32	-33.726	-33.798	-28.479	0	-32.158	-30.952
	'S113_F3_3'	0	-32.903	-32.254	-29.531	-33.721	-30.824	-31.578	-34.165	-33.79	-34.063	-32.628	-32.992	-32.657
	'S113_F3_2'	-36.937	-33.434	-33.17	-28.592	-33.055	-31.487	-30.125	-33.69	-33.456	-34.145	-36.699	-31.978	-31.759
	'S113_F3_1'	0	-32.853	-33.003	0	-33.143	0	-32.262	-33.602	-41.524	2.136	0	-32.003	-32.364
	'S112_F3_3'	0	-35.159	-30.336	-30.917	-33.921	-30.864	-27.345	-33.964	-35.79	0	0	-31.341	-32.917
	'S112_F3_2'	0	-35.057	-32.569	-30.242	-33.446	-31.173	-30.983	-34.664	-34.942	0	0	-30.917	-31.586
	'S112_F3_1'	0	-34.166	-29.334	-29.132	-32.34	0	-33.017	-33.865	-36.686	0	0	-31.921	-32.79
	'S111_F3_3'	-33.637	-33.695	-35.106	-30.162	-32.63	0	-24.868	-33.639	-39.021	-37.842	0	-33.339	-33.839
	'S111_F3_2'	0	0	-34.102	-28.496	-31.551	0	-29.434	-33.851	-39.583	-39.253	0	-30.844	-32.914
	'S111_F3_1'	0	0	-32.676	0	-22.12	-26.436	-29.535	-31.518	-36.225	109.692	0	-28.201	-31.749
Voltages - October 26, 2011	Retention Time (min)	1894.1	1913.7	1950.2	2006.9	2031	2085.4	2128.2	2209.5	2267.7	2311.9	2399	2420.6	2630.8
	Sample ID													
	'Tetracosane_3'	0	0	0	0	0	0	0	3775	0	273	0	0	0
	'Tetracosane_2'	0	0	0	0	0	0	0	3706	315	0	0	157	0
	'Tetracosane_1'	0	0	0	0	0	0	0	3878	0	0	0	0	0
	'S121_F3_3'	0	210	149	58	105	0	116	2602	335	0	0	64	81
	'S121_F3_2'	0	218	153	61	91	0	122	2577	337	0	0	151	0
	'S121_F3_1'	0	221	150	60	94	0	124	2602	339	0	0	98	0
	'S114_F3_3'	0	234	179	62	131	0	164	2259	290	0	0	98	96
	'S114_F3_2'	0	244	175	65	143	0	170	2309	293	0	0	341	0
	'S114_F3_1'	0	257	171	71	150	0	176	2496	303	212	0	339	234
	'S113_F3_3'	0	530	436	126	395	134	232	3114	440	343	79	900	290
	'S113_F3_2'	60	435	367	119	367	123	227	3026	440	351	78	853	274
	'S113_F3_1'	0	439	406	0	398	0	282	2788	52	117	0	746	230
	'S112_F3_3'	0	254	135	71	267	76	128	2438	335	0	0	413	167
	'S112_F3_2'	0	245	131	71	254	70	124	2313	332	0	0	463	243
	'S112_F3_1'	0	229	125	69	199	0	118	2130	307	0	0	351	191
	'S111_F3_3'	54	270	256	84	199	0	153	1497	260	232	0	573	274
	'S111_F3_2'	0	0	254	72	143	0	143	1445	254	224	0	400	211
	'S111_F3_1'	0	0	255	0	53	96	152	1419	257	56	0	234	127

$\delta^{13}\text{C}$ - October 26, 2011										CO ₂ Standard		
	Retention Time (min)	2665.2	2707.6	2829.7	2942.3	3051.8	3146.1	3174.1	3246.9	3252.6	3278.1	3300.4
	Sample ID											
	'Tetracosane_3'	0	0	0	0	0	0	0	-32.167	-42.653	-41.341	-41.097
	'Tetracosane_2'	0	0	0	0	0	0	0	-32.061	-42.938	-41.167	-41.287
	'Tetracosane_1'	0	0	0	0	0	0	0	-29.823	-43.19	-40.917	-40.868
	'S121_F3_3'	0	-32.671	-32.016	-32	-31.583	0	-32.461	-27.858	-53.554	-47.438	-40.445
	'S121_F3_2'	0	-32.857	-33.15	-32.268	-32.224	0	-31.497	-27.579	-57.867	-47.177	-40.03
	'S121_F3_1'	0	-32.947	-32.369	-32.377	-31.995	0	-32.298	-30.603	-43.825	-41.201	-41.18
	'S114_F3_3'	0	-32.23	-31.615	-32.716	-37.254	0	-30.074	-28.007	-54.357	-40.874	-40.829
	'S114_F3_2'	0	-32.637	-31.263	-31.344	-30.935	0	0	-30.214	-43.057	-42.528	-40.121
	'S114_F3_1'	-32.753	-35.561	-32.646	-31.934	-32.084	-31.146	-28.965	-27.787	-64.271	-51.601	-40.854
	'S113_F3_3'	-34.217	-34.851	-32.9	-32.312	-32.009	0	-31.958	-29.527	-68.847	-57.18	-41.544
	'S113_F3_2'	-32.396	-31.665	-30.702	-31.015	-30.773	-33.834	-33.754	-27.101	121.83	-104.165	-41.298
	'S113_F3_1'	-32.7	-33.07	-31.905	-32.018	-32.304	-33.258	-33.514	-28.957	-1667.04	-79.418	-40.656
	'S112_F3_3'	-34.405	-33.446	-32.796	-31.924	-31.998	0	-31.87	-28.554	-63.454	-40.976	-41.058
	'S112_F3_2'	-32.96	-33.215	-31.521	-35.532	-35.429	0	-32.513	-27.302	-64.63	-53.093	-40.988
Voltages - October 26, 2011										CO ₂ Standard		
	Retention Time (min)	2665.2	2707.6	2829.7	2942.3	3051.8	3146.1	3174.1	3246.9	3252.6	3278.1	3300.4
	Sample ID											
	'Tetracosane_3'	0	0	0	0	0	0	0	105	1541	1696	1709
	'Tetracosane_2'	0	0	0	0	0	0	0	121	1508	1719	1710
	'Tetracosane_1'	0	0	0	0	0	0	0	159	1477	1711	1714
	'S121_F3_3'	0	606	662	1962	727	0	333	555	1224	1178	1709
	'S121_F3_2'	0	614	525	1794	302	0	334	559	1244	1183	1707
	'S121_F3_1'	0	621	694	1951	733	0	634	864	1537	1721	1714
	'S114_F3_3'	0	540	617	1277	68	0	214	567	1229	1709	1719
	'S114_F3_2'	0	539	640	1566	612	0	0	878	1521	1466	1723
	'S114_F3_1'	198	311	495	1315	313	168	231	610	1130	1063	1715
	'S113_F3_3'	419	469	1052	3419	1014	0	765	1255	1148	1013	1724
	'S113_F3_2'	399	1105	1192	3543	1176	428	468	940	866	730	1718
	'S113_F3_1'	363	1047	1138	391	148	406	424	920	904	792	1705
	'S112_F3_3'	209	515	484	1547	503	0	369	661	1146	1724	1722

Works Cited

- Alperin, M. J., and T. M. Hoehler. 2009. "Anaerobic Methane Oxidation by Archaea/sulfate-reducing Bacteria Aggregates: 1. Thermodynamic and Physical Constraints." *American Journal of Science* 309 (10) (December 1): 869–957. doi:10.2475/10.2009.01.
- . 2010. "The Ongoing Mystery of Sea-Floor Methane." *Science* 329 (5989) (July 16): 288–289. doi:10.1126/science.1189966.
- Alperin, M. J., and W. S. Reeburgh. 1985. "Inhibition Experiments on Anaerobic Methane Oxidation." *Applied and Environmental Microbiology* 50 (4) (October 1): 940–945.
- Alperin, M. J., W. S. Reeburgh, and M. J. Whiticar. 1988. "Carbon and hydrogen isotope fractionation resulting from anaerobic methane oxidation." *Global Biogeochemical Cycles* 2 (3): 279–288. doi:10.1029/GB002i003p00279.
- Aquilina, A., N. J. Knab, K. Knittel, G. Kaur, A. Geissler, S. P. Kelly, H. Fossing, et al. 2010. "Biomarker Indicators for Anaerobic Oxidizers of Methane in Brackish-marine Sediments with Diffusive Methane Fluxes." *Organic Geochemistry* 41 (4) (April): 414–426. doi:10.1016/j.orggeochem.2009.09.009.
- Archer, D. 2007. *Methane Hydrate Stability and Anthropogenic Climate Change*. <http://www.biogeosciences-discuss.net/4/993/2007/bgd-4-993-2007.pdf>, <http://www.doaj.org/doaj?func=openurl&genre=article&issn=18106277&date=2007&volume=4&issue=2&spage=993>.
- Barnes, R. O., and E. D. Goldberg. 1976. "Methane Production and Consumption in Anoxic Marine Sediments." *Geology* 4 (5) (May 1): 297–300. doi:10.1130/0091-7613(1976)4<297:MPACIA>2.0.CO;2.
- Beal, E. J., C. H. House, and V. J. Orphan. 2009. "Manganese- and Iron-Dependent Marine Methane Oxidation." *Science* 325 (5937) (July 10): 184–187. doi:10.1126/science.1169984.
- Belicka, L. L., and H. R. Harvey. 2009. "The Sequestration of Terrestrial Organic Carbon in Arctic Ocean Sediments: A Comparison of Methods and Implications for Regional Carbon Budgets." *Geochimica Et Cosmochimica Acta* 73 (20) (October 15): 6231–6248. doi:10.1016/j.gca.2009.07.020.
- Birgel, D., R. Stein, and J. Hefter. 2004. "Aliphatic Lipids in Recent Sediments of the Fram Strait/Yermak Plateau (Arctic Ocean): Composition, Sources and Transport Processes." *Marine Chemistry* 88 (3–4) (September): 127–160. doi:10.1016/j.marchem.2004.03.006.
- Blumenberg, M., R. Barnes, K. Nauhaus, T. Pape, and W. Michaelis. 2005. "In Vitro Study of Lipid Biosynthesis in an Anaerobically Methane-Oxidizing Microbial Mat." *Applied and Environmental Microbiology* 71 (8) (August 1): 4345–4351. doi:10.1128/AEM.71.8.4345-4351.2005.
- Blumenberg, M., R. Seifert, J. Reitner, T. Pape, and W. Michaelis. 2004. "Membrane Lipid Patterns Typify Distinct Anaerobic Methanotrophic Consortia." *Proceedings of the National Academy of Sciences of the United States of America* 101 (30) (July 27): 11111–11116. doi:10.1073/pnas.0401188101.

- Boaretto, E., C. Bryant, I. Carmi, G. Cook, S. Gulliksen, D. Harkness, J. Heinemeier, et al. 2002. "Summary Findings of the Fourth International Radiocarbon Intercomparison (FIRI)(1998–2001)." *Journal of Quaternary Science* 17 (7) (October 1): 633–637. doi:10.1002/jqs.702.
- Boetius, A., and K. Knittel. 2010. "Handbook of Hydrocarbon and Lipid Microbiology." In , 2193–2202. Springer Berlin Heidelberg. <http://www.springerlink.com/content/r7v48u417001j70u/abstract/>.
- Boetius, A., K. Ravensschlag, C. J. Schubert, D. Rickert, F. Widdel, A. Gieseke, R. Amann, B. B. Jørgensen, U. Witte, and O. Pfannkuche. 2000. "A Marine Microbial Consortium Apparently Mediating Anaerobic Oxidation of Methane." *Nature* 407 (6804) (October 5): 623–626. doi:10.1038/35036572.
- Bohrmann, G., and M. E. Torres. 2006. "Gas Hydrates in Marine Sediments." In *Marine Geochemistry*, ed. H. D. Schulz and M. Zabel, 481–512. Berlin/Heidelberg: Springer-Verlag. <http://www.springerlink.com/content/n633523381844333/>.
- Boyd, T. J., C. L. Osburn, K. J. Johnson, K. B. Birgl, and R. B. Coffin. 2006. "Compound-Specific Isotope Analysis Coupled with Multivariate Statistics to Source-Apportion Hydrocarbon Mixtures." *Environ. Sci. Technol.* 40 (6): 1916–1924. doi:10.1021/es050975p.
- Buffett, B., and D. Archer. 2004. "Global Inventory of Methane Clathrate: Sensitivity to Changes in the Deep Ocean." *Earth and Planetary Science Letters* 227 (3–4) (November): 185–199. doi:10.1016/j.epsl.2004.09.005.
- Coachman, L. K., K. Aagaard, and R. B. Tripp. 1975. *Bering Strait: The Regional Physical Oceanography*. University of Washington Press.
- Coffin, R. B., L. J. Hamdan, R. Plummer, J. Smith, J. Gardner, R. Hagen, and W. Wood. 2008. "Analysis of Methane and Sulfate Flux in Methane-charged Sediments from the Mississippi Canyon, Gulf of Mexico." *Marine and Petroleum Geology* 25 (9) (November): 977–987. doi:10.1016/j.marpetgeo.2008.01.014.
- Coffin, R. B., L. J. Hamdan, J. P. Smith, R. Plummer, L. Millholland, R. Larson, and W. Wood. 2011. *Beaufort Sea Methane Hydrate Exploration: Energy and Climate Change*. NAVAL RESEARCH LAB WASHINGTON DC, NAVAL RESEARCH LAB WASHINGTON DC. <http://www.dtic.mil/docs/citations/ADA550138>.
- Darby, D. A., J. F. Bischof, and G. A. Jones. 1997. "Radiocarbon Chronology of Depositional Regimes in the Western Arctic Ocean." *Deep Sea Research Part II: Topical Studies in Oceanography* 44 (8): 1745–1757. doi:10.1016/S0967-0645(97)00039-8.
- Darby, D. A., M. Jakobsson, and L. Polyak. 2005. "Icebreaker Expedition Collects Key Arctic Seafloor and Ice Data." *EOS Transactions* 86: 549–552. doi:DOI: 10.1029/2005EO520001.
- Darby, D. A., J. Ortiz, L. Polyak, S. Lund, M. Jakobsson, and R. A. Woodgate. 2009. "The Role of Currents and Sea Ice in Both Slowly Deposited Central Arctic and Rapidly Deposited Chukchi–Alaskan Margin Sediments." *Global and Planetary Change* 68 (1–2) (July): 58–72. doi:10.1016/j.gloplacha.2009.02.007.

- Darby, D. A., L. Polyak, and H. A. Bauch. 2006. "Past Glacial and Interglacial Conditions in the Arctic Ocean and Marginal Seas – a Review." *Progress In Oceanography* 71 (2–4) (October): 129–144. doi:10.1016/j.pocean.2006.09.009.
- Dekas, A. E., R. S. Poretsky, and V. J. Orphan. 2009. "Deep-Sea Archaea Fix and Share Nitrogen in Methane-Consuming Microbial Consortia." *Science* 326 (5951) (October 16): 422–426. doi:10.1126/science.1178223.
- DeLong, E. F. 2000. "Microbiology: Resolving a Methane Mystery." *Nature* 407 (6804) (October 5): 577–579. doi:10.1038/35036677.
- Devol, A. H., and S. I. Ahmed. 1981. "Are High Rates of Sulphate Reduction Associated with Anaerobic Oxidation of Methane?" *Nature* 291 (5814) (June 4): 407–408. doi:10.1038/291407a0.
- Dickens, G. R. 2003. "Rethinking the Global Carbon Cycle with a Large, Dynamic and Microbially Mediated Gas Hydrate Capacitor." *Earth and Planetary Science Letters* 213 (3–4) (August 25): 169–183. doi:10.1016/S0012-821X(03)00325-X.
- Dickens, G. R., M. Koelling, D. C. Smith, and L. Schnieders. 2007. "Rhizon Sampling of Pore Waters on Scientific Drilling Expeditions: An Example from the IODP Expedition 302, Arctic Coring Expedition (ACEX)." *Scientific Drilling* 4 (4, March 2007): 1–4. doi:10.2204/iodp.sd.4.08.2007.
- Donahue, D. J. 1995. "Radiocarbon Analysis by Accelerator Mass Spectrometry." *International Journal of Mass Spectrometry and Ion Processes* 143 (0) (May 25): 235–245. doi:10.1016/0168-1176(94)04132-Q.
- Drenzek, N. J., D. B. Montluçon, M. B. Yunker, R. W. Macdonald, and T. I. Eglinton. 2007. "Constraints on the Origin of Sedimentary Organic Carbon in the Beaufort Sea from Coupled Molecular ^{13}C and ^{14}C Measurements." *Marine Chemistry* 103 (1–2) (January 8): 146–162. doi:10.1016/j.marchem.2006.06.017.
- Eglinton, T. I., L. I. Aluwihare, J. E. Bauer, E. R. M. Druffel, and A. P. McNichol. 1996. "Gas Chromatographic Isolation of Individual Compounds from Complex Matrices for Radiocarbon Dating." *Anal. Chem.* 68 (5): 904–912. doi:10.1021/ac9508513.
- Eglinton, T. I., B. C. Benitez-Nelson, A. Pearson, A. P. McNichol, J. E. Bauer, and E. R. M. Druffel. 1997. "Variability in Radiocarbon Ages of Individual Organic Compounds from Marine Sediments." *Science* 277 (5327) (August 8): 796–799. doi:10.1126/science.277.5327.796.
- Elvert, M., A. Boetius, K. Knittel, and B. B. Jørgensen. 2003. "Characterization of Specific Membrane Fatty Acids as Chemotaxonomic Markers for Sulfate-Reducing Bacteria Involved in Anaerobic Oxidation of Methane." *Geomicrobiology Journal* 20 (4): 403–419. doi:10.1080/01490450303894.
- Elvert, M., E. Suess, J. Greinert, and M. J. Whiticar. 2000. "Archaea Mediating Anaerobic Methane Oxidation in Deep-sea Sediments at Cold Seeps of the Eastern Aleutian Subduction Zone." *Organic Geochemistry* 31 (11) (November): 1175–1187. doi:10.1016/S0146-6380(00)00111-X.
- Elvert, M., E. Suess, and M. J. Whiticar. 1999. "Anaerobic Methane Oxidation Associated with Marine Gas Hydrates: Superlight C-isotopes from Saturated

- and Unsaturated C20 and C25 Irregular Isoprenoids.” *Naturwissenschaften* 86 (6) (June 1): 295–300. doi:10.1007/s001140050619.
- Faux, J. F., L. L. Belicka, and H. R. Harvey. 2011. “Organic Sources and Carbon Sequestration in Holocene Shelf Sediments from the Western Arctic Ocean.” *Continental Shelf Research* 31 (11): 1169–1179. doi:10.1016/j.csr.2011.04.001.
- Gagnon, A. R., A. P. McNichol, J. C. Donoghue, D. R. Stuart, and K. von Reden. 2000. “The NOSAMS Sample Preparation Laboratory in the Next Millenium: Progress After the WOCE Program.” *Nuclear Instruments and Methods in Physics Research Section B: Beam Interactions with Materials and Atoms* 172 (1–4) (October): 409–415. doi:10.1016/S0168-583X(00)00201-9.
- Goñi, M. A., M. B. Yunker, R. W. Macdonald, and T. I. Eglinton. 2005. “The Supply and Preservation of Ancient and Modern Components of Organic Carbon in the Canadian Beaufort Shelf of the Arctic Ocean.” *Marine Chemistry* 93 (1) (January 1): 53–73. doi:10.1016/j.marchem.2004.08.001.
- Gove, H. E. 2000. “Some Comments On Accelerator Mass Spectrometry.” *Radiocarbon* 42 (1): 127–136. doi:10.2458/rc.v42i1.3858.
- Hamdan, L. J., P. M. Gillevet, J. W. Pohlman, M. Sikaroodi, J. Greinert, and R. B. Coffin. 2011. “Diversity and Biogeochemical Structuring of Bacterial Communities Across the Porangahau Ridge Accretionary Prism, New Zealand.” *FEMS Microbiology Ecology* 77 (3): 518–532. doi:10.1111/j.1574-6941.2011.01133.x.
- Hamdan, L. J., P. M. Gillevet, M. Sikaroodi, J. W. Pohlman, R. E. Plummer, and R. B. Coffin. 2008. “Geomicrobial Characterization of Gas Hydrate-bearing Sediments Along the mid-Chilean Margin.” *FEMS Microbiology Ecology* 65 (1): 15–30. doi:10.1111/j.1574-6941.2008.00507.x.
- Hayes, J.M., K. H. Freeman, B. N. Popp, and C. H. Hoham. 1990. “Compound-specific Isotopic Analyses: A Novel Tool for Reconstruction of Ancient Biogeochemical Processes.” *Organic Geochemistry* 16 (4–6): 1115–1128. doi:10.1016/0146-6380(90)90147-R.
- Hill, P. R., S. M. Blasco, J. R. Harper, and D. B. Fissel. 1991. “Sedimentation on the Canadian Beaufort Shelf.” *Continental Shelf Research* 11 (8–10) (August): 821–842. doi:10.1016/0278-4343(91)90081-G.
- Hinrichs, K. U., and A. Boetius. 2002. “The Anaerobic Oxidation of Methane : New Insights in Microbial Ecology and Biogeochemistry.” *Ocean Margin Systems*: 457–477.
- Hinrichs, K. U., J. M. Hayes, S. P. Sylva, P. G. Brewer, and E. F. DeLong. 1999. “Methane-consuming Archaeobacteria in Marine Sediments.” *Nature* 398 (6730) (April 29): 802–805. doi:10.1038/19751.
- Hinrichs, K. U., R. E. Summons, V. J. Orphan, S. P. Sylva, and J. M. Hayes. 2000. “Molecular and Isotopic Analysis of Anaerobic Methane-oxidizing Communities in Marine Sediments.” *Organic Geochemistry* 31 (12) (December): 1685–1701. doi:10.1016/S0146-6380(00)00106-6.
- Hoehler, T. M., M. J. Alperin, D. B. Albert, and C. S. Martens. 1994. “Field and Laboratory Studies of Methane Oxidation in an Anoxic Marine Sediment: Evidence for a Methanogen-Sulfate Reducer Consortium.” *Global*

- Biogeochemical Cycles* 8 (4) (December): PP. 451–463.
doi:199410.1029/94GB01800.
- . 1998. “Thermodynamic Control on Hydrogen Concentrations in Anoxic Sediments.” *Geochimica Et Cosmochimica Acta* 62 (10) (May): 1745–1756.
doi:10.1016/S0016-7037(98)00106-9.
- Holler, T., F. Widdel, K. Knittel, R. Amann, M. Y. Kellermann, K. U. Hinrichs, A. Teske, A. Boetius, and G. Wegener. 2011. “Thermophilic Anaerobic Oxidation of Methane by Marine Microbial Consortia.” *The ISME Journal* 5 (12) (June 23): 1946–1956. doi:10.1038/ismej.2011.77.
- Ilkmen, E. 2009. “Intracavity Optogalvanic Spectroscopy for Radiocarbon Analysis with Attomole Sensitivity”. Newark, New Jersey: Rutgers-Newark: The State University of New Jersey.
- Ingalls, A. E., and A. Pearson. 2005. “Ten Years of Compound-Specific Radiocarbon Analysis.” *Oceanography* 18 (3) (September 1): 18–31.
doi:10.5670/oceanog.2005.22.
- Ingalls, A. E., S. R. Shah, R. L. Hansman, L. I. Aluwihare, G. M. Santos, E. R. M. Druffel, and A. Pearson. 2006. “Quantifying Archaeal Community Autotrophy in the Mesopelagic Ocean Using Natural Radiocarbon” 103 (17) (April 25): 6442–6447. doi:10.1073/pnas.0510157103.
- Iversen, N., and B. B. Jørgensen. 1985. “Anaerobic Methane Oxidation Rates at the Sulfate-Methane Transition in Marine Sediments from Kattegat and Skagerrak (Denmark).” *Limnology and Oceanography* 30 (5): 944–955.
- Jardine, C. N. 2004. *Methane UK*. Environmental Change Institute, University of Oxford.
- Jørgensen, B., and S. Kasten. 2006. “Sulfur Cycling and Methane Oxidation.” In *Marine Geochemistry*, ed. H. D. Schulz and M. Zabel, 271–309. Springer Berlin Heidelberg.
<http://www.springerlink.com/content/1232764347x551k5/abstract/>.
- Judd, A. G., M. Hovland, L. I. Dimitrov, S. García Gil, and V. Jukes. 2002. “The Geological Methane Budget at Continental Margins and Its Influence on Climate Change.” *Geofluids* 2 (2) (May 1): 109–126. doi:10.1046/j.1468-8123.2002.00027.x.
- Kaneda, T. 1991. “Iso- and Anteiso-fatty Acids in Bacteria: Biosynthesis, Function, and Taxonomic Significance.” *Microbiological Reviews* 55 (2) (June 1): 288 – 302.
- Kennett, J. P. 2003. *Methane Hydrates in Quaternary Climate Change: The Clathrate Gun Hypothesis*. American Geophysical Union.
- Knab, N. J., B. A. Cragg, C. Borowski, R. J. Parkes, R. Pancost, and B. B. Jørgensen. 2008. “Anaerobic Oxidation of Methane (AOM) in Marine Sediments from the Skagerrak (Denmark): I. Geochemical and Microbiological Analyses.” *Geochimica Et Cosmochimica Acta* 72 (12) (June 15): 2868–2879.
doi:10.1016/j.gca.2008.03.016.
- Knittel, K., and A. Boetius. 2009. “Anaerobic Oxidation of Methane: Progress with an Unknown Process.” *Annual Review of Microbiology* 63 (1): 311–334.
doi:10.1146/annurev.micro.61.080706.093130.

- . 2010. “Anaerobic Methane Oxidizers.” In *Handbook of Hydrocarbon and Lipid Microbiology*, ed. K. N. Timmis, 2023–2032. Springer Berlin Heidelberg.
<http://www.springerlink.com/content/jh195617x48v3733/abstract/>.
- Knittel, K., A. Boetius, A. Lemke, H. Eilers, K. Lochte, O. Pfannkuche, P. Linke, and R. Amann. 2003. “Activity, Distribution, and Diversity of Sulfate Reducers and Other Bacteria in Sediments Above Gas Hydrate (Cascadia Margin, Oregon).” *Geomicrobiology Journal* 20 (4): 269–294.
doi:10.1080/01490450303896.
- Kort, E. A., S. C. Wofsy, B. C. Daube, M. Diao, J. W. Elkins, R. S. Gao, E. J. Hintsa, et al. 2012. “Atmospheric Observations of Arctic Ocean Methane Emissions up to 82° North.” *Nature Geoscience* 5 (5): 318–321. doi:10.1038/ngeo1452.
- Kvenvolden, K. A. 1988. “Methane Hydrate — A Major Reservoir of Carbon in the Shallow Geosphere?” *Chemical Geology* 71 (1-3) (December): 41–51.
doi:10.1016/0009-2541(88)90104-0.
- . 1998. “A Primer on the Geological Occurrence of Gas Hydrate.” *Geological Society, London, Special Publications* 137 (1) (January 1): 9–30.
doi:10.1144/GSL.SP.1998.137.01.02.
- Kvenvolden, K. A., M. D. Lilley, T. D. Lorenson, P. W. Barnes, and E. McLaughlin. 1993. “The Beaufort Sea Continental Shelf as a Seasonal Source of Atmospheric Methane.” *Geophysical Research Letters* 20 (22): PP. 2459–2462. doi:199310.1029/93GL02727.
- Liu, K. S. 1994. “Preparation of Fatty Acid Methyl Esters for Gas-chromatographic Analysis of Lipids in Biological Materials.” *Journal of the American Oil Chemists’ Society* 71 (11): 1179–1187. doi:10.1007/BF02540534.
- Londry, K. L., K. G. Dawson, H. D. Grover, R. E. Summons, and A. S. Bradley. 2008. “Stable Carbon Isotope Fractionation Between Substrates and Products of *Methanosarcina barkeri*.” *Organic Geochemistry* 39 (5) (May): 608–621.
doi:10.1016/j.orggeochem.2008.03.002.
- Londry, K. L., L. L. Jahnke, and D. J. Des Marais. 2004. “Stable Carbon Isotope Ratios of Lipid Biomarkers of Sulfate-Reducing Bacteria.” *Applied and Environmental Microbiology* 70 (2) (February 1): 745–751.
doi:10.1128/AEM.70.2.745-751.2004.
- Lösekan, T., K. Knittel, T. Nadalig, B. Fuchs, H. Niemann, A. Boetius, and R. Amann. 2007. “Diversity and Abundance of Aerobic and Anaerobic Methane Oxidizers at the Haakon Mosby Mud Volcano, Barents Sea.” *Applied and Environmental Microbiology* 73 (10) (May 15): 3348–3362.
doi:10.1128/AEM.00016-07.
- MacDonald, G. J. 1990. “Role of Methane Clathrates in Past and Future Climates.” *Climatic Change* 16 (3) (June): 247–281. doi:10.1007/BF00144504.
- Macdonald, R. W., S. M. Barrett, R. E. Cranston, H. E. Welch, M. B. Yunker, and C. Gobeil. 1998. “A Sediment and Organic Carbon Budget for the Canadian Beaufort Shelf.” *Marine Geology* 144 (4) (January): 255–273.
doi:10.1016/S0025-3227(97)00106-0.

- Martens, C. S., and R. A. Berner. 1974. "Methane Production in the Interstitial Waters of Sulfate-Depleted Marine Sediments." *Science* 185 (4157) (September 27): 1167–1169. doi:10.1126/science.185.4157.1167.
- McIntyre, C. P., E. Galutschek, M. L. Roberts, K. F. von Reden, A. P. McNichol, and W. J. Jenkins. 2010. "A Continuous-Flow Gas Chromatography 14C Accelerator Mass Spectrometry System." *Radiocarbon* 52 (2) (January 8): 295–300. doi:10.2458/rc.v52i2.3665.
- McIntyre, C. P., S. P. Sylva, and M. L. Roberts. 2009. "Gas Chromatograph-Combustion System for 14C-Accelerator Mass Spectrometry." *Analytical Chemistry* 81 (15): 6422–6428. doi:10.1021/ac900958m.
- Michaelis, W., R. Seifert, K. Nauhaus, T. Treude, V. Thiel, M. Blumenberg, K. Knittel, et al. 2002. "Microbial Reefs in the Black Sea Fueled by Anaerobic Oxidation of Methane." *Science* 297 (5583) (August 9): 1013–1015. doi:10.1126/science.1072502.
- Milkov, A. V. 2004. "Global Estimates of Hydrate-bound Gas in Marine Sediments: How Much Is Really Out There?" *Earth-Science Reviews* 66 (3-4) (August): 183–197. doi:10.1016/j.earscirev.2003.11.002.
- Mollenhauer, G., T. I. Eglinton, N. Ohkouchi, R. R. Schneider, P. J. Müller, P. M. Grootes, and J. Rullkötter. 2003. "Asynchronous Alkenone and Foraminifera Records from the Benguela Upwelling System." *Geochimica Et Cosmochimica Acta* 67 (12) (June 15): 2157–2171. doi:10.1016/S0016-7037(03)00168-6.
- Murnick, D. E., O. Dogru, and E. Ilkmen. 2008. "Intracavity Optogalvanic Spectroscopy. An Analytical Technique for 14C Analysis with Subattomole Sensitivity." *Analytical Chemistry* 80 (13) (July 1): 4820–4824. doi:10.1021/ac800751y.
- . 2010. "14C Analysis via Intracavity Optogalvanic Spectroscopy." *Nuclear Instruments and Methods in Physics Research Section B: Beam Interactions with Materials and Atoms* 268 (7-8) (April): 708–711. doi:10.1016/j.nimb.2009.10.010.
- Murnick, D. E., and J. O. Okil. 2005. "Use of the Optogalvanic Effect (OGE) for Isotope Ratio Spectrometry of 13CO2 and 14CO2." *Isotopes in Environmental and Health Studies* 41 (4): 363–371. doi:10.1080/10256010500384440.
- Naraoka, H., and R. Ishiwatari. 2000. "Molecular and Isotopic Abundances of Long-chain N-fatty Acids in Open Marine Sediments of the Western North Pacific." *Chemical Geology* 165 (1–2) (April 4): 23–36. doi:10.1016/S0009-2541(99)00159-X.
- Nauhaus, K., A. Boetius, M. Krüger, and F. Widdel. 2002. "In Vitro Demonstration of Anaerobic Oxidation of Methane Coupled to Sulphate Reduction in Sediment from a Marine Gas Hydrate Area." *Environmental Microbiology* 4 (5) (May): 296–305.
- Niemann, H., and M. Elvert. 2008. "Diagnostic Lipid Biomarker and Stable Carbon Isotope Signatures of Microbial Communities Mediating the Anaerobic Oxidation of Methane with Sulphate." *Organic Geochemistry* 39 (12) (December): 1668–1677. doi:10.1016/j.orggeochem.2007.11.003.

- Niemann, H., T. Lösekann, D. de Beer, M. Elvert, T. Nadalig, K. Knittel, R. Amann, et al. 2006. "Novel Microbial Communities of the Haakon Mosby Mud Volcano and Their Role as a Methane Sink." *Nature* 443 (7113) (October 19): 854–858. doi:10.1038/nature05227.
- Ohkouchi, N., T. I. Eglinton, and J. M. Hayes. 2003. "Radiocarbon Dating of Individual Fatty Acids as a Tool for Refining Antarctic Margin Sediment Chronologies." *Radiocarbon* 45 (1): 17–24. doi:10.2458/azu_js_rc.v45i1.4155.
- Ohkouchi, N., T. I. Eglinton, L. D. Keigwin, and J. M. Hayes. 2002. "Spatial and Temporal Offsets Between Proxy Records in a Sediment Drift." *Science* 298 (5596) (November 8): 1224–1227. doi:10.1126/science.1075287.
- Orcutt, B., A. Boetius, M. Elvert, V. Samarkin, and S. B. Joye. 2005. "Molecular Biogeochemistry of Sulfate Reduction, Methanogenesis and the Anaerobic Oxidation of Methane at Gulf of Mexico Cold Seeps." *Geochimica Et Cosmochimica Acta* 69 (17) (September 1): 4267–4281. doi:10.1016/j.gca.2005.04.012.
- Orphan, V. J., K. U. Hinrichs, W. Ussler, C. K. Paull, L. T. Taylor, S. P. Sylva, J. M. Hayes, and E. F. Delong. 2001. "Comparative Analysis of Methane-Oxidizing Archaea and Sulfate-Reducing Bacteria in Anoxic Marine Sediments." *Applied and Environmental Microbiology* 67 (4) (April 1): 1922–1934. doi:10.1128/AEM.67.4.1922-1934.2001.
- Orphan, V. J., C. H. House, K. U. Hinrichs, K. D. McKeegan, and E. F. DeLong. 2001. "Methane-Consuming Archaea Revealed by Directly Coupled Isotopic and Phylogenetic Analysis." *Science* 293 (5529) (July 20): 484–487. doi:10.1126/science.1061338.
- . 2002. "Multiple Archaeal Groups Mediate Methane Oxidation in Anoxic Cold Seep Sediments." *Proceedings of the National Academy of Sciences of the United States of America* 99 (11) (May 28): 7663–7668. doi:10.1073/pnas.072210299.
- Pancost, R. D., E. C. Hopmans, and J. S. Sinninghe Damsté. 2001. "Archaeal Lipids in Mediterranean Cold Seeps: Molecular Proxies for Anaerobic Methane Oxidation." *Geochimica Et Cosmochimica Acta* 65 (10) (May 15): 1611–1627. doi:10.1016/S0016-7037(00)00562-7.
- Pancost, R. D., J. S. Sinninghe Damsté, S. de Lint, M. J. E. C. van der Maarel, J. C. Gottschal, and The Medinaut Shipboard Scientific Party. 2000. "Biomarker Evidence for Widespread Anaerobic Methane Oxidation in Mediterranean Sediments by a Consortium of Methanogenic Archaea and Bacteria." *Appl. Environ. Microbiol.* 66 (3) (March 1): 1126–1132. doi:10.1128/AEM.66.3.1126-1132.2000.
- Parkes, R. J., B. A. Cragg, N. Banning, F. Brock, G. Webster, J. C. Fry, E. Hornibrook, et al. 2007. "Biogeochemistry and Biodiversity of Methane Cycling in Subsurface Marine Sediments (Skagerrak, Denmark)." *Environmental Microbiology* 9 (5): 1146–1161. doi:10.1111/j.1462-2920.2006.01237.x.
- Paull, C., W. Ussler, T. Lorenson, W. Winters, and J. Dougherty. 2005. "Geochemical Constraints on the Distribution of Gas Hydrates in the Gulf of

- Mexico.” *Geo-Marine Letters* 25 (5): 273–280. doi:10.1007/s00367-005-0001-3.
- Pearson, A. 2000. *Biogeochemical Applications of Compound-Specific Radiocarbon Analysis*.
<http://stinet.dtic.mil/oai/oai?&verb=getRecord&metadataPrefix=html&identifier=ADA380195>.
- Pearson, A., A. P. McNichol, R. J. Schneider, K. F. von Reden, and Y. Zheng. 2006. “Microscale AMS (super 14) C Measurement at NOSAMS.” *Radiocarbon* 40 (1) (March 31): 61–75. doi:10.2458/rc.v40i1.1989.
- Pelletier, B. R. 1975. *Sediment dispersal in the southern Beaufort Sea*. Victoria, B.C.: Beaufort Sea Project, Dept. of the Environment.
- Perry, G. J., J. K. Volkman, R. B. Johns, and H. J. Bavor Jr. 1979. “Fatty Acids of Bacterial Origin in Contemporary Marine Sediments.” *Geochimica Et Cosmochimica Acta* 43 (11) (November): 1715–1725. doi:10.1016/0016-7037(79)90020-6.
- Plummer, R. E., J. W. Pohlman, and R. B. Coffin. 2005. “Compound-Specific Stable Carbon Isotope Analysis of Low-Concentration Complex Hydrocarbon Mixtures from Natural Gas Hydrate Systems.” *AGU Fall Meeting Abstracts* -1 (December): 0608.
- Pohlman, J. W., D. L. Knies, K. S. Grabowski, T. M. DeTurck, D. J. Treacy, and R. B. Coffin. 2000. “Sample Distillation/graphitization System for Carbon Pool Analysis by Accelerator Mass Spectrometry (AMS).” *Nuclear Instruments and Methods in Physics Research Section B: Beam Interactions with Materials and Atoms* 172 (1–4) (October): 428–433. doi:10.1016/S0168-583X(00)00153-1.
- Ratnayake, N. P., N. Suzuki, and M. Matsubara. 2005. “Sources of Long Chain Fatty Acids in Deep Sea Sediments from the Bering Sea and the North Pacific Ocean.” *Organic Geochemistry* 36 (4) (April): 531–541.
doi:10.1016/j.orggeochem.2004.11.004.
- Reeburgh, W. S. 1976. “Methane Consumption in Cariaco Trench Waters and Sediments.” *Earth and Planetary Science Letters* 28 (3) (January): 337–344.
doi:10.1016/0012-821X(76)90195-3.
- . 1980. “Anaerobic Methane Oxidation: Rate Depth Distributions in Skan Bay Sediments.” *Earth and Planetary Science Letters* 47 (3) (May): 345–352.
doi:10.1016/0012-821X(80)90021-7.
- . 2007. “Oceanic Methane Biogeochemistry.” *ChemInform* 38 (20).
doi:10.1002/chin.200720267. <http://dx.doi.org/10.1002/chin.200720267>.
- Roberts, M. L., K. F. Reden, B. X. Han, R. J. Schneider, A. Benthien, and J. M. Hayes. 2003. *Continuous-Flow Accelerator Mass Spectrometry*.
http://scholar.googleusercontent.com/scholar?q=cache:V2C6Yg9y2KMJ:scholar.google.com/&hl=en&as_sdt=0,9&as_vis=1.
- Roberts, M. L., K. F. von Reden, C. P. McIntyre, and J. R. Burton. 2011. “Progress with a Gas-accepting Ion Source for Accelerator Mass Spectrometry.” *Nuclear Instruments and Methods in Physics Research Section B: Beam Interactions with Materials and Atoms* 269 (24) (December 15): 3192–3195.
doi:10.1016/j.nimb.2011.04.017.

- Roberts, M. L., R. J. Schneider, K. F. von Reden, J. S. C. Wills, B. X. Han, J. M. Hayes, B. E. Rosenheim, and W. J. Jenkins. 2007. "Progress on a Gas-accepting Ion Source for Continuous-flow Accelerator Mass Spectrometry." *Nuclear Instruments and Methods in Physics Research Section B: Beam Interactions with Materials and Atoms* 259 (1) (June): 83–87. doi:10.1016/j.nimb.2007.01.189.
- de Rooij, M., J. van der Plicht, and H. J. Meijer. 2011. "Sample Dilution for AMS ¹⁴C Analysis of Small Samples (30–150 Mg C)." *Radiocarbon* 50 (3) (February 12): 413–436. doi:10.2458/rc.v50i3.3223.
- Rose, K., J. E. Johnson, J. P. Smith, R. B. Coffin, W. T. Wood, P. E. Hart, J. Greinert, and T. D. Lorenson. 2009. "The Role of Geology and Shallow Lithostratigraphy in the Distribution of Methane Flux Through Shallow Sediments Across the Beaufort Shelf of Alaska." *AGU Fall Meeting Abstracts* -1 (December): 1179.
- Sachs, J. P., R. R. Schneider, T. I. Eglinton, K. H. Freeman, G. Ganssen, J. F. McManus, and D. W. Oppo. 2000. "Alkenones as Paleoceanographic Proxies." *Geochemistry Geophysics Geosystems* 1 (11) (November 21): 2 PP. doi:2000 10.1029/2000GC000059 [Citation].
- Santos, G. M., J. R. Southon, S. Griffin, S. R. Beaupre, and E. R. M. Druffel. 2007. "Ultra Small-mass AMS ¹⁴C Sample Preparation and Analyses at KCCAMS/UCI Facility." *Nuclear Instruments and Methods in Physics Research Section B: Beam Interactions with Materials and Atoms* 259 (1) (June): 293–302. doi:10.1016/j.nimb.2007.01.172.
- Scott, E. M., D. D. Harkness, and G. T. Cook. 1998. "Interlaboratory Comparisons; Lessons Learned." *Radiocarbon* 40 (1) (January 1): 331–340. doi:10.2458/rc.v40i1.2019.
- Shah, S. R., G. Mollenhauer, N. Ohkouchi, T. I. Eglinton, and A. Pearson. 2008. "Origins of Archaeal Tetraether Lipids in Sediments: Insights from Radiocarbon Analysis." *Geochimica Et Cosmochimica Acta* 72 (18) (September 15): 4577–4594. doi:10.1016/j.gca.2008.06.021.
- Shah, S. R., and A. Pearson. 2007. "Ultra-Microscale (5–25 Mg C) Analysis of Individual Lipids by ¹⁴C AMS: Assessment and Correction for Sample Processing Blanks." *Radiocarbon* 49 (1) (December 20): 69–82. doi:10.2458/rc.v49i1.2900.
- Shakhova, N., and I. Semiletov. 2007. "Methane Release and Coastal Environment in the East Siberian Arctic Shelf." *Journal of Marine Systems* 66 (1–4) (June): 227–243. doi:10.1016/j.jmarsys.2006.06.006.
- Shakhova, N., I. Semiletov, A. Salyuk, V. Yusupov, D. Kosmach, and Ö. Gustafsson. 2010. "Extensive Methane Venting to the Atmosphere from Sediments of the East Siberian Arctic Shelf." *Science* 327 (5970) (March 5): 1246–1250. doi:10.1126/science.1182221.
- Sloan, E. D. 2003. "Fundamental Principles and Applications of Natural Gas Hydrates." *Nature* 426 (6964) (November 20): 353–363. doi:10.1038/nature02135.
- Solomon, S., D. Qin, M. Manning, Z. Chen, M. Marquis, K. B. Averyt, M. Tignor, and H. L. Miller, eds. 2007. *Climate Change 2007: The Physical Science*

- Basis : Contribution of Working Group I to the Fourth Assessment Report of the Intergovernmental Panel on Climate Change*. Cambridge University Press.
- Stein, R., and K. Fahl. 2000. "Holocene Accumulation of Organic Carbon at the Laptev Sea Continental Margin (Arctic Ocean): Sources, Pathways, and Sinks." *Geo-Marine Letters* 20 (1): 27–36. doi:10.1007/s003670000028.
- Taylor, R. E. 2000. "Fifty Years of Radiocarbon Dating: This Widely Applied Technique Has Made Major Strides Since Its Introduction a Half-century Ago at the University of Chicago." *American Scientist* 88 (1) (January 1): 60–67.
- Thiel, V., J. Peckmann, H. H. Richnow, U. Luth, J. Reitner, and W. Michaelis. 2001. "Molecular Signals for Anaerobic Methane Oxidation in Black Sea Seep Carbonates and a Microbial Mat." *Marine Chemistry* 73 (2) (February): 97–112. doi:10.1016/S0304-4203(00)00099-2.
- Thiel, V., J. Peckmann, R. Seifert, P. Wehrung, J. Reitner, and W. Michaelis. 1999. "Highly Isotopically Depleted Isoprenoids: Molecular Markers for Ancient Methane Venting." *Geochimica Et Cosmochimica Acta* 63 (23–24) (December): 3959–3966. doi:10.1016/S0016-7037(99)00177-5.
- Thomas, D. J., J. C. Zachos, T. J. Bralower, E. Thomas, and S. Bohaty. 2002. "Warming the Fuel for the Fire: Evidence for the Thermal Dissociation of Methane Hydrate During the Paleocene-Eocene Thermal Maximum." *Geology* 30 (12) (December 1): 1067–1070. doi:10.1130/0091-7613(2002)030<1067:WTFFTF>2.0.CO;2.
- Treude, T., S. Krause, L. J. Hamdan, J. Schweers, and R. B. Coffin. 2012. "Decoupled Anaerobic Oxidation of Methane and Sulfate Reduction Within the Methanogenic Zone of Arctic Sediments (Beaufort Sea, Alaska)?" In *EGU General Assembly Conference Abstracts*, 14:10644. <http://adsabs.harvard.edu/abs/2012EGUGA..1410644T>.
- U.S. Environmental Protection Agency. 2012. "Inventory of U.S. Greenhouse Gas Emissions and Sinks: 1990 – 2010". Reports & Assessments,. <http://epa.gov/climatechange/ghgemissions/usinventoryreport.html>.
- Uchida, M., Y. Shibata, K. Kawamura, Y. Kumamoto, M. Yoneda, K. Ohkushi, N. Harada, et al. 2001. "Compound-specific Radiocarbon Ages of Fatty Acids in Marine Sediments from the Western North Pacific." *Radiocarbon* 43 (2 PART II): 949–956.
- Uchida, M., Y. Shibata, K. Ohkushi, M. Yoneda, K. Kawamura, and M. Morita. 2005. "Age Discrepancy Between Molecular Biomarkers and Calcareous Foraminifera Isolated from the Same Horizons of Northwest Pacific Sediments." *Chemical Geology* 218 (1–2) (May 16): 73–89. doi:10.1016/j.chemgeo.2005.01.026.
- Valentine, D. L. 2002. "Biogeochemistry and Microbial Ecology of Methane Oxidation in Anoxic Environments: a Review." *Antonie Van Leeuwenhoek* 81 (1): 271–282.
- Valentine, D. L., and W. S. Reeburgh. 2000. "New Perspectives on Anaerobic Methane Oxidation." *Environmental Microbiology* 2 (5): 477–484. doi:10.1046/j.1462-2920.2000.00135.x.

- Volkman, J. K., S. M. Barrett, S. I. Blackburn, M. P. Mansour, E. L. Sikes, and F. Gelin. 1998. "Microalgal Biomarkers: A Review of Recent Research Developments." *Organic Geochemistry* 29 (5–7) (November): 1163–1179. doi:10.1016/S0146-6380(98)00062-X.
- Wakeham, S. G., and T. K. Pearse. 2004. "Lipid Analysis in Marine Particle and Sediment Samples". A Laboratory Handbook. Skidway Institute of Oceanography.
- Wegener, G., H. Niemann, M. Elvert, K. U. Hinrichs, and A. Boetius. 2008. "Assimilation of Methane and Inorganic Carbon by Microbial Communities Mediating the Anaerobic Oxidation of Methane." *Environmental Microbiology* 10 (9) (September): 2287–2298. doi:10.1111/j.1462-2920.2008.01653.x.
- Wuebbles, D. J., and K. Hayhoe. 2002. "Atmospheric Methane and Global Change." *Earth-Science Reviews* 57 (3–4) (May): 177–210. doi:10.1016/S0012-8252(01)00062-9.
- Yunker, M. B., L. L. Belicka, H. R. Harvey, and R. W. Macdonald. 2005. "Tracing the Inputs and Fate of Marine and Terrigenous Organic Matter in Arctic Ocean Sediments: A Multivariate Analysis of Lipid Biomarkers." *Deep Sea Research Part II: Topical Studies in Oceanography* 52 (24–26) (December): 3478–3508. doi:10.1016/j.dsr2.2005.09.008.
- Zencak, Z., C. M. Reddy, E. L. Teuten, L. Xu, A. P. McNichol, and Ö. Gustafsson. 2007. "Evaluation of Gas Chromatographic Isotope Fractionation and Process Contamination by Carbon in Compound-Specific Radiocarbon Analysis." *Anal. Chem.* 79 (5): 2042–2049. doi:10.1021/ac061821a.
- Zhang, C. L., Y. Li, J. D. Wall, L. Larsen, R. Sassen, Y. Huang, Y. Wang, et al. 2002. "Lipid and Carbon Isotopic Evidence of Methane-Oxidizing and Sulfate-Reducing Bacteria in Association with Gas Hydrates from the Gulf of Mexico." *Geology* 30 (3) (March 1): 239–242. doi:10.1130/0091-7613(2002)030<0239:LACIEO>2.0.CO;2.